MODELLING AND ANALYSIS OF COMPOSITE STRUCTURES WITH SEMI-RIGID CONNECTIONS

A DISSERTATION SUBMITTED TO THE DEPARTMENT OF CIVL ENGINEERING AND THE COMMITTEE FOR POSTGRADUATE STUDIES OF THE UNIVERSITY OF STRATHCLYDE, GLASGOW, FOR THE DEGREE OF DOCTOR OF PHILOSOPHY

By

YINGJUN WANG

B.Eng. (Dalian University of Technology, 1987)

M.Eng. (Dalian University of Technology, 1990)

August 2003

Acknowledgements

I would like to give my sincere thanks to my supervisor Professor Howard D. Wright who gave me unstinting encouragement and advice over the past four years. I also would like to thank Professor Wright for his part in my being provided with a University Studentship, without which my research would not be possible.

I would like to give thanks to Mr. Roy Cairns, who was always willing to help whenever I encountered problems.

I would like to give my special thanks to the computing officers Mr. Ron Baron and Mr. John Redgate for their advice regarding computing matters and in particular their efforts in retrieving my valuable files when my computer broke down in the summer of 2002.

I would also like to give my thanks to the department secretary Miss Fiona MacDonald, who was always ready to help and a person people could trust.

I would like to give thanks to my colleagues Dr. Anwar Elbadawy, Mr. Sanjeev Sinha, and Mr. Ian Stewart for their support and help in everyday life.

Finally I would like to give my thanks to every member of my family and relatives, in particular my wife, my parents and my parents-in-law, for their huge support and encouragement during my study.

Abstract

The composite structures studied in this thesis involve concrete slabs with profiled steel sheeting supported by steel beams. The composite interaction is realized by providing shear connectors welded to the top flange of the steel beams. The columns are normally non-composite. The steel beam-to column connections are either designed as pinned or designed as rigid. Recent research has shown that semi-rigid joint behaviour may be achieved in composite joints by considering only a small amount of reinforcement over the connections. However due to the lack of design provisions and a simple and effective analytical method, semi-rigid frame design is rarely adopted by engineers.

In this thesis the behaviour of semi-rigid composite connections, composite beams, and composite frames is investigated. Simple and effective finite element analysis models for composite joints, composite beams and composite frames are proposed. The models are validated against published tests on composite joints and beams. Three composite frames are analyzed and the results are compared with different proposals. Satisfactory agreements are achieved. Design recommendations are promoted for semi-rigid composite frames. Seismic analysis of composite frames is performed using the proposed frame model. The influence of semi-rigid joints on the overall performance of composite frame is investigated. The proposed method is so simple and straightforward that it provides an effective tool for both static and dynamic analysis of composite semi-rigid structures.

Contents

Notation

A area of steel section

A_c area of concrete

A_r area of total reinforcement in the concrete slab within the total effective width

B_e total effective width of concrete slab

D depth of steel section

D_b lever arm of a pair of bolts

D_{eq} equivalent lever arm of reinforcement

D_p overall depth of profile steel sheet

D_r lever arm of reinforcements in concrete slab

or distance from the top of the steel beam to the centroid of the reinforcement

D_s overall depth of slab

D_t transformed depth of composite beam model

d nominal shank diameter of a stud shear connector

d_r design interstorey drift

E Young's modulus of steel

E_c Young's modulus of concrete

f_{cu} characteristic cubic strength of concrete

f_t characteristic strength of concrete in tension

f_y characteristic strength of steel

h overall height of stud

or storey height

I_g second moment of area of uncracked composite section

I_n second moment of area of cracked composite section for negative moments

I_p second moment of area of cracked composite section for positive moments

I_x second moment of area of steel beam about major axis

K degree of shear connection

k reduction factor depending on profile shape

k_1 exponents which influence the shape of the spectrum for a vibration period grater than T_C

k_2 exponents which influence the shape of the spectrum for a vibration period grater than T_D

k_{d1} exponents which influence the shape of the design spectrum for a vibration period grater than T_C

k_{d2} exponents which influence the shape of the design spectrum for a vibration period grater than T_D

L beam span

M moment

M_c moment capacity of composite section with partial shear connection

M_{pc} moment capacity of composite section with full shear connection

M_s moment capacity of steel beam

N number of shear connectors in a group

N_a actual number of shear connectors between intermediate point and the adjacent support

N_n number of shear connectors for negative moments

N_p number of shear connectors for positive moments

Q_k characteristic resistance of shear connector

Q_n capacity of shear connector in negative moment regions

Q_p capacity of shear connector in negative positive regions

P_{tot} total gravity load

p_y design strength of structure steel

q behaviour factor

R_b effective resistance of a pair of bolts in a steel-to-beam connection

R_c resistance of concrete flange

R_f resistance of steel flange

R_q resistance of shear connector

R_r resistance of reinforcement

R_s resistance of steel beam

R_w resistance of overall web depth

R_{yr} yield force of reinforcements

S soil parameter

$S_d(T)$	design response spectrum, normalised by g
$S_e(T)$	elastic response spectrum
T	vibration period of a linear single degree of freedom system
$T_{B,C}$	limits of the constant spectral acceleration branch
T_D	value defining the beginning of the constant displacement range of the spectrum
V_{tot}	total seismic storey shear
a_g	design ground acceleration for the reference return period
s	longitudinal spacing centre-to-centre of groups of shear connectors
t_f	flange thickness
t_w	web thickness
w	uniformly distributed loading on a beam
α	ratio of the design ground acceleration a_g to the acceleration of gravity g ($\alpha = a_g/g$)
α_e	modular ratio
β_0	spectral acceleration amplification factor for 5% viscous damping
δ	Deflection
	or displacement at floor level
δ_c	deflection of steel beam acting alone
δ_s	deflection of composite beam with full shear connection
δ_{sw}	deflection of composite beam subjected to instantaneously applied self weight
ε	strain
η	damping correction factor with reference value $\eta = 1$ for 5% vicous damping
θ	interstorey drift sensitivity coefficient
σ	stress
Δ	interstorey drift index

Chapter 1 Introduction

1.1 Introduction

Studies of the global performance under static loading of steel framed structures date back to as early as the 1920's (Baker, 1980). With the introduction of computer technology in the late 1960's, much progress has been made in various aspects of the overall response of steel frames. Many approaches are now possible in frame analysis. The effects of semi-rigid and partial strength connections have been investigated since the 1980's. The study of steel-concrete composite structures began in the late 1950's. The study of the behaviour of composite frames with semi-rigid beam-to-column connections is fast becoming a major research topic.

In this thesis, the behaviour of semi-rigid composite joints, composite beams and composite frames is investigated. A finite element analytical method for analyzing semi-rigid composite joints is proposed. A finite element analysis composite beam model is also proposed. By incorporating the proposed composite joint model, the behaviour of composite beams with semi-rigid connections can be studied. The proposed composite joint model and beam model are then used in the analysis of composite frames. The limit behaviour of composite frames is investigated and the influence of semi-rigid connections on the overall performance of composite frames is studied.

1.2 Composite frames with semi-rigid connections

A composite frame is a framed structure for a building or similar construction work, in which some or all of the beams and columns are composite members and most of the remaining members are structural steel members (Eurocode 4, Part 1.1, 1994). The composite frames being studied in this thesis include the following members:

- Composite slabs: reinforced concrete slabs with profiled steel sheeting
- Steel beams: with symmetrical sections about their minor axis

- Shear studs: provide shear connection between the composite slabs and steel beams in order that composite behaviour can be achieved
- Composite beams: with combined sections of composite slabs and steel beams connected by shear studs
- Steel columns: with symmetrical sections about their major and minor axis
- Composite connections: the connections between composite beams and steel columns in which reinforcement is intended to contribute to the resistance of the connection

A typical composite beam with profiled steel sheeting is illustrated in Figure 1.1. Composite construction has lots of advantages over traditional reinforced concrete construction, such as lower self-weight, larger beam span, controlled fabrication quality, shorter construction time, etc. Consequently it can significantly reduce the overall construction costs. In the past few decades, this type of construction has been greatly developed and accepted. Now it accounts for over 60% of the UK building market (Dowling & Burgan, 1998).

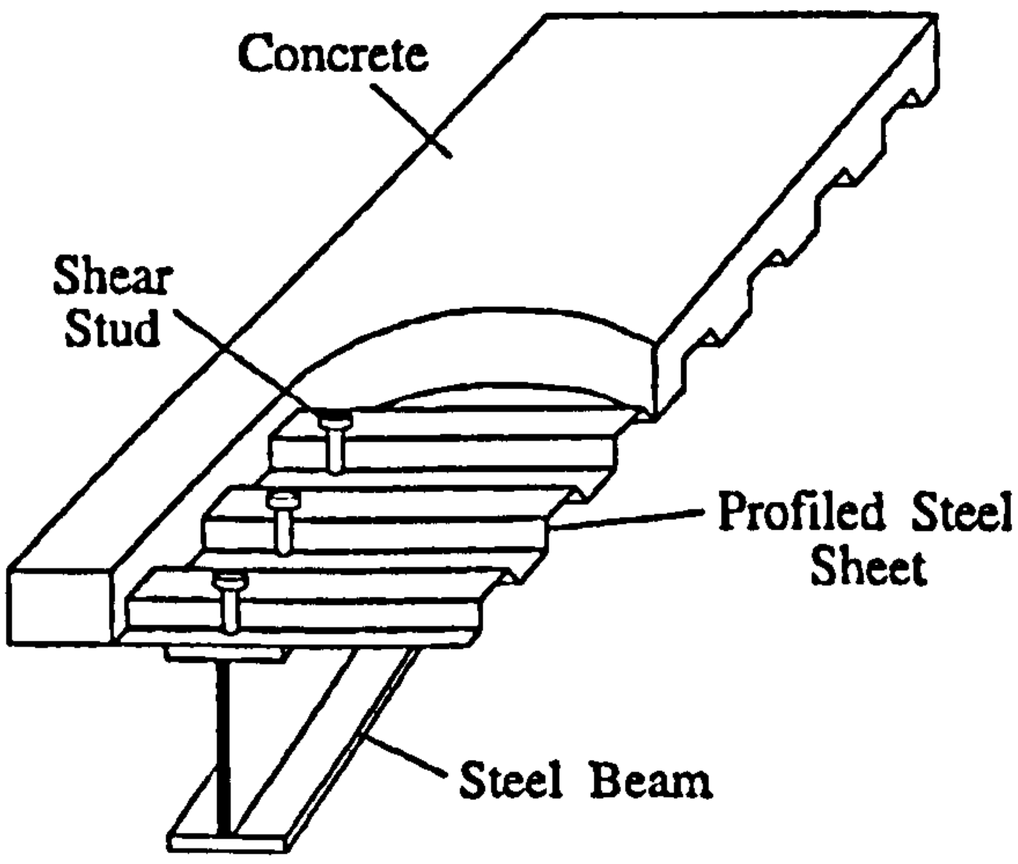

Figure 1.1 Composite beam with profiled steel sheeting

1.2.1 Beam-to-column connections

Generally beam-to-column connections may be classified by rigidity or by strength. By rigidity, beam-to-column connections may be sub-classified as nominally pinned connections, rigid connections and semi-rigid connections.

According to EC 3, Part 1.1 (1992) a nominal pinned connection shall be so designed that it cannot develop significant moments which might affect members of the structure; and it should be capable of transmitting the forces calculated in design and should be capable of accepting the resulting rotations as well. Simple web cleat, fin plate and thin end plate connections are normally assumed as nominally pinned connections.

A rigid connection shall be so designed that its deformation has no significant influence on the distribution of internal forces and moments in the structure, nor on its overall deformation, and it should be capable of transmitting the forces and moments calculated in design. The deformations of rigid connections should not reduce the resistance of the structure by more than 5% (Eurocode 3, Part 1.1, 1992). A typical example of rigid connections is the fully welded connection.

A semi-rigid connection should provide a predictable degree of interaction between members, based on the design moment-rotation characteristics of the joint. It should also be capable of transmitting the forces and moments calculated in design. A typical example of semi-rigid connections is the flush endplate connection.

The moment diagrams of steel frames with nominal pinned, semi-rigid and rigid connections are shown in Figure 1.2. Semi-rigid connection is the optimal choice among the three types of connections under the same loading condition because the mid-span moment is smaller compared to simply supported beams, which leads to possible savings on beam sections. Secondly, the fabrication costs of semi-rigid joints are lower than those required by rigid joint design.

In composite construction, the fabrication and erection costs of structures are estimated to be 30-50% of the total structure costs. The type of connection has great influence on the fabrication and erection costs. In fact, over 60% of the fabrication costs is directly influenced by the fabrication of the connections (Nethercot, 1998). Economic studies in various countries have shown that the possible savings due to semi-rigid design can be 20-25% in case of unbraced frames and of 5-9% in case of braced frames. With the assumption that the costs of the pure steel frames are about 10% of the total costs for office buildings and about 20% for industrial buildings, the reduction of the total building costs could be estimated to 4-5% for unbraced frames and 1-2% for braced frames (Weynand *et al.* 1998).

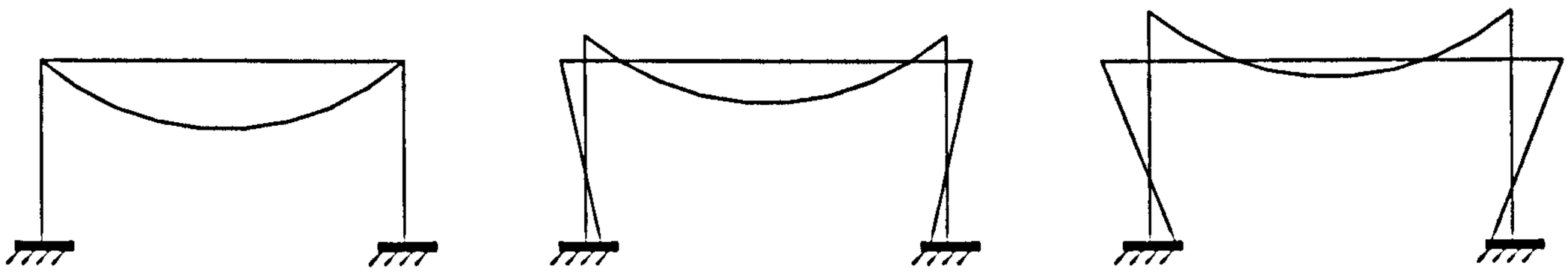

Nominal pinned connection Semi-rigid connection Rigid connection

Figure 1.2 Bending moment diagrams of steel frames

1.2.2 Composite beam to column connections

Composite construction has achieved dominance in the UK because of its overall economy of use of materials and ease of construction relative to alternative reinforced concrete and steel options. Beam to column connections are traditionally considered to be 'simple' with no moment transfer to the columns. However, it has been recognized that even relatively flexible steel connections are stiffer and stronger when used in a

composite frame. This is because of the continuity of reinforcement in the slab and other less quantified effects, such as membrane action of the floor slab.

Composite connections are steel beam to column connections that are designed to act compositely with the floor slab through the reinforcement in the slab. Composite beam to column connections using welded end plate steel connections (Figure1.3) are most accepted. Economies that result from incorporation of composite connections in the design of braced frames may be expressed in terms of

- Reduced beam weights and savings in frame cost
- Reduced beam depths (important for integration of building services, etc.)
- Predictable serviceability performance
- Greater robustness against explosions and fire

These economies increase for multi-bay braced frames, although moments transferred to edge columns have to be considered. It is reported that steel weight savings are of the order of 8% to 12% relative to braced frames. However, the weight and depth saving on the beams may be up to 25%. The corresponding savings are probably in the range of 4% to 6% of the cost of the fabricated work, and 2% to 3% of the cost of the complete structure (Lawson & Gibbons, 1995).

The different forms of fabricated steel beam to column connections that are widely used in the UK are

1. End plate connections, i.e. plate welded to the flange and web of the beam and bolted to the column flange (Figure 1.3 & Figure 1.4). Four types exist:
   (a) Extended end plates with bolt above and below the beam top flange
   (b) Flush end plates with bolts contained within the beam depth
   (c) Partial depth end plates with the plate not directly connected to the complete depth of the web, or both flanges
   (d) Haunched connections with a local deepening of the beam section

2. Cleat connections i.e. using angle cleats (Figure 1.5). They are:
   (a) Web cleats in pairs attached to the web

(b) Web cleats and a seating cleat

(c) Web cleats and top and bottom cleats

3. Fin plate connections i.e. plates welded to the column flange or web and bolted to the beam web (Figure 1.6).

Conventionally, connections of types 1(c), 2(a), 2(b) and 3, listed above, are considered as 'simple', whereas 1(b) and 2(c) are 'semi-rigid' in terms of their behaviour. Only 1(a) and 1(d) can be designed effectively as 'rigid', and 1(d) can also be treated as full strength. The only connections currently covered by design rules for partial strength in Eurocode 3 are 1(a) and 1(b).

1.3 Aim of the research

The aim of this research is to produce a finite element analytical model for the nonlinear three-dimensional analysis of composite structures with semi-rigid connections.

The objectives of the research are:

- Propose a finite element model of shear connectors so that each shear connector can be directly modelled by a finite element.
- Propose a finite element model for the analysis of semi-rigid composite joints.
- Investigate the nonlinear behaviour of semi-rigid composite joints.
- Validate the semi-rigid composite joint model against tests from published papers.
- Propose a finite element model for the analysis of composite beams.
- Investigate the nonlinear behaviour of composite beams regarding partial shear connection and semi-rigid joints.
- Validate the proposed composite beam model against current design code method and tests from published papers.
- Propose an analytical method for the analysis of composite frames.
- Investigate the limit behaviour of semi-rigid composite frames and the influence of semi-rigid connections on the overall behaviour of composite frames.

- Validate the proposed analytical method of composite frames against different approaches from published papers.
- Perform seismic analysis of composite frames.

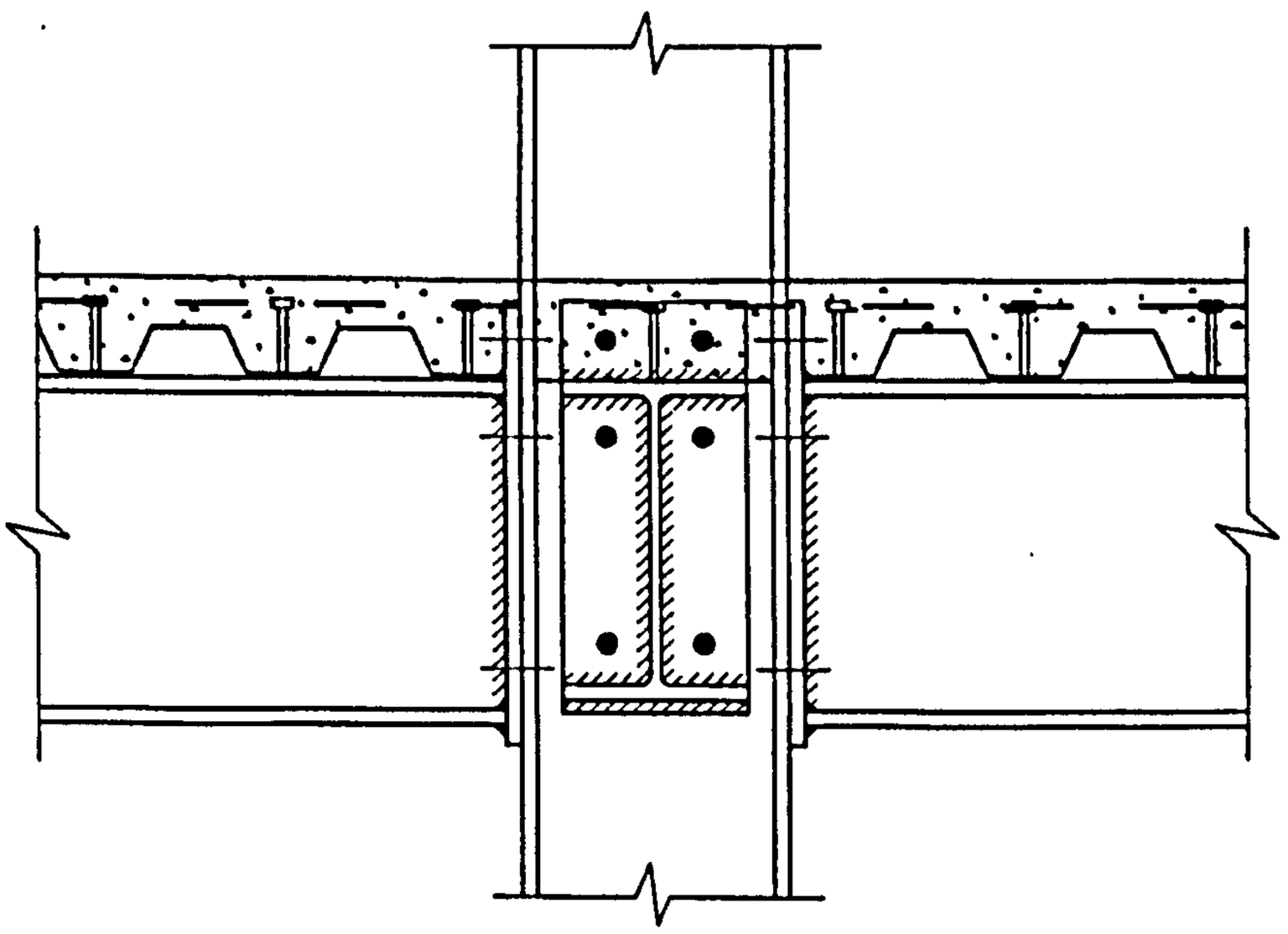

Extended End Plate Connection

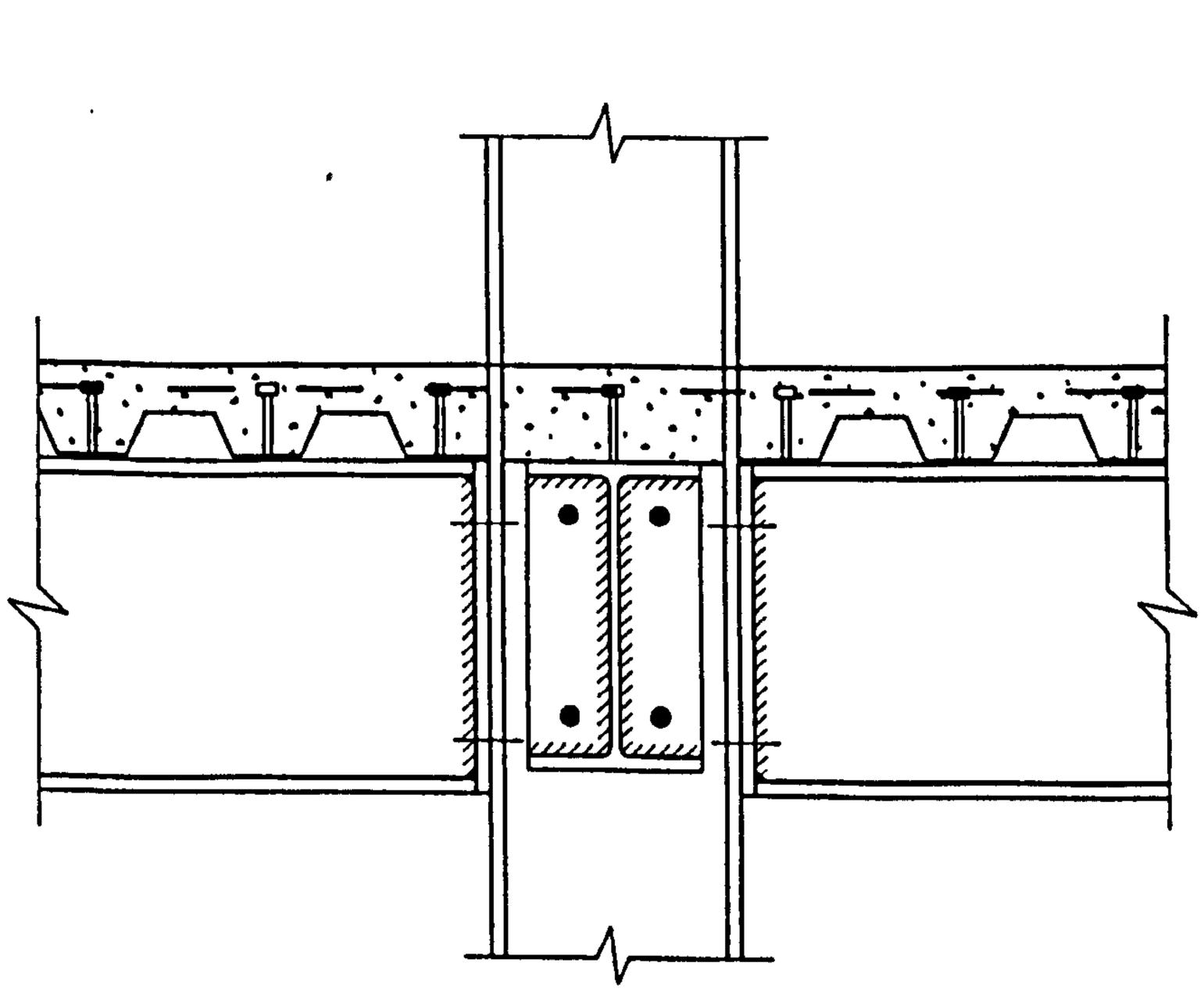

Flush End Plate Connection

Figure1.3 Extended end plate and flush end plate connections

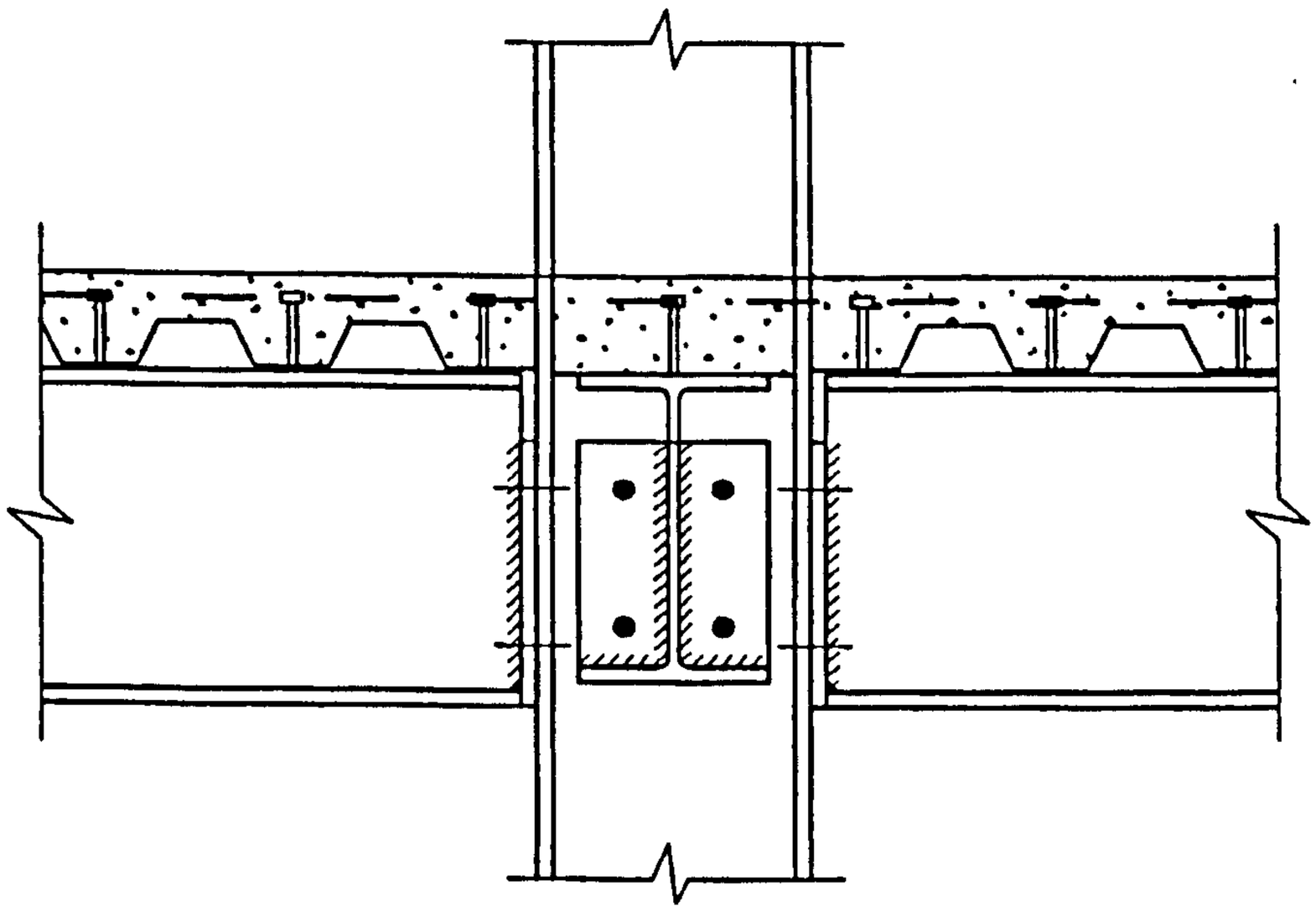

Partial Depth End Plate Connection

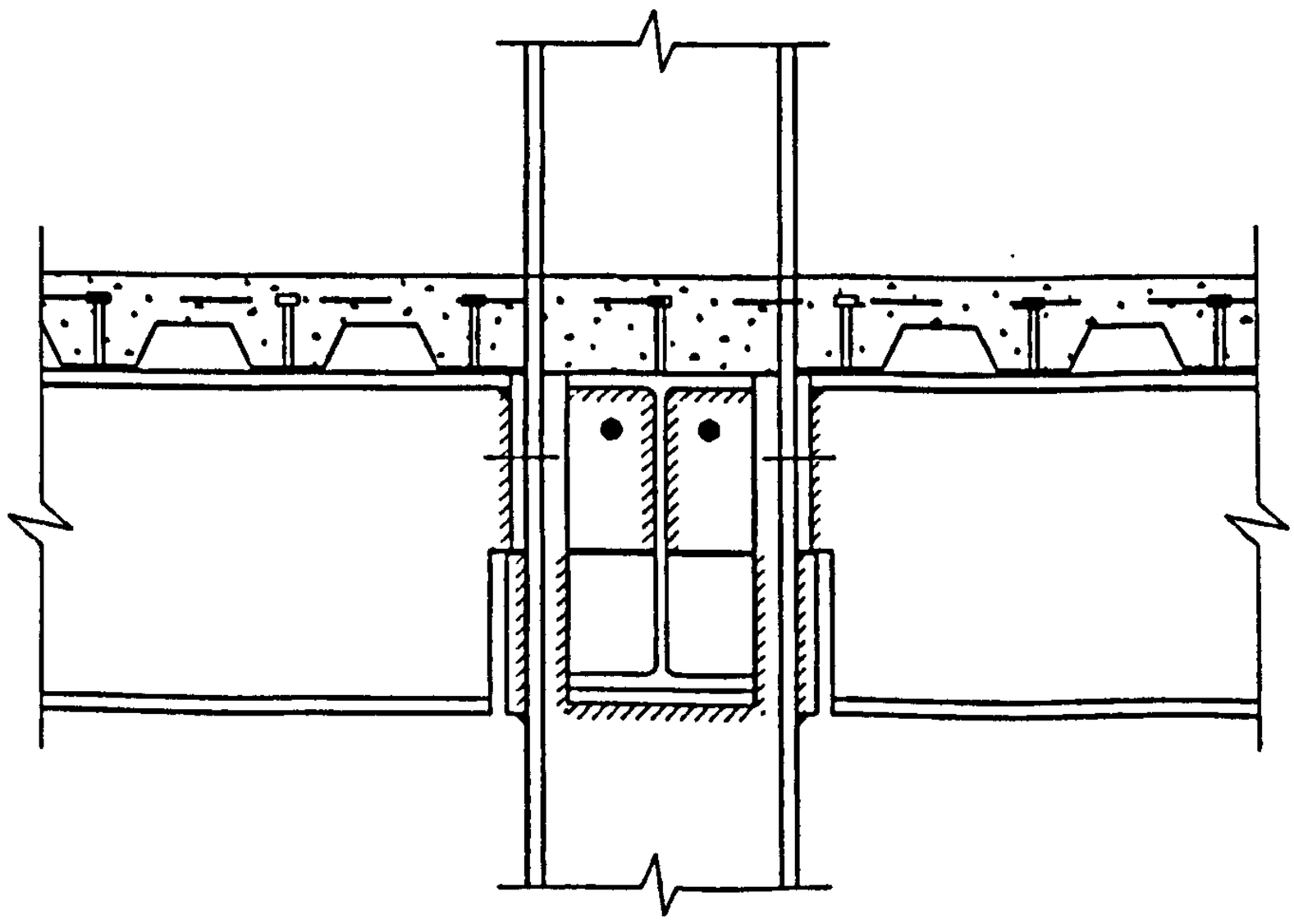

Partial Depth End Plate with Welded Shear Block

Figure1.4 Partial depth end plate connections

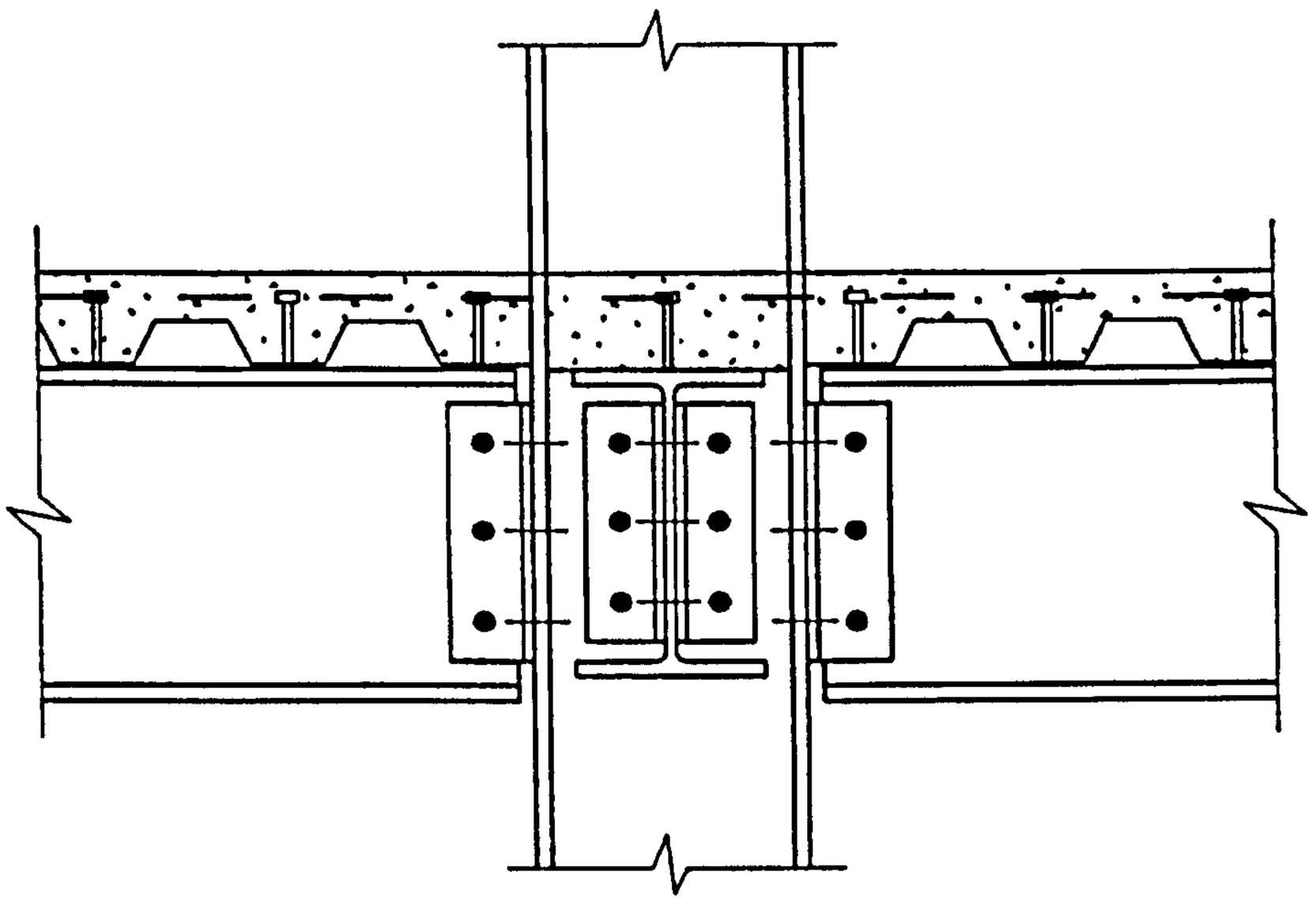

Web Cleats (on both sides of web)

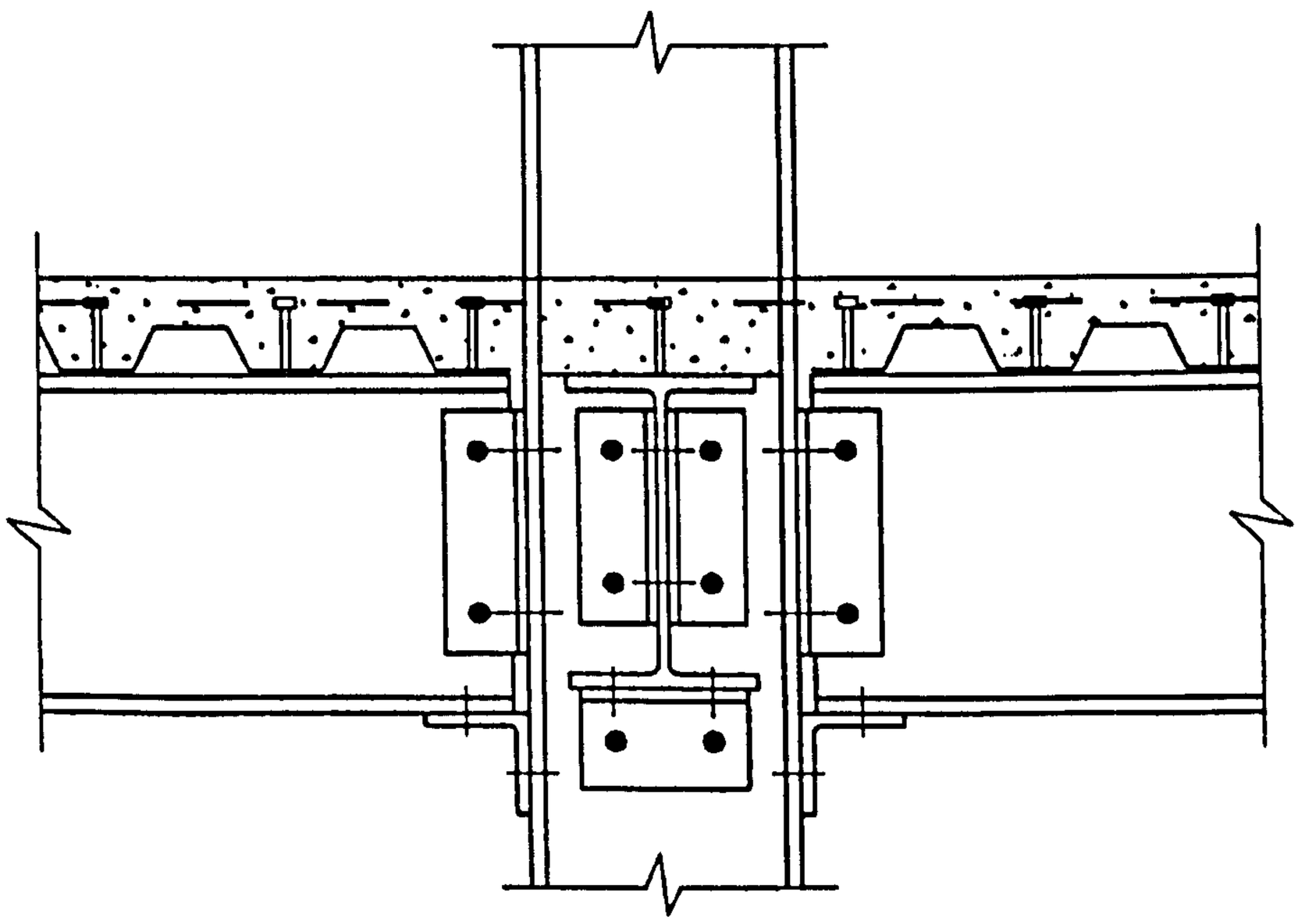

Web Cleat (single or double) and Seating Cleat

Figure1.5 Web cleat connections

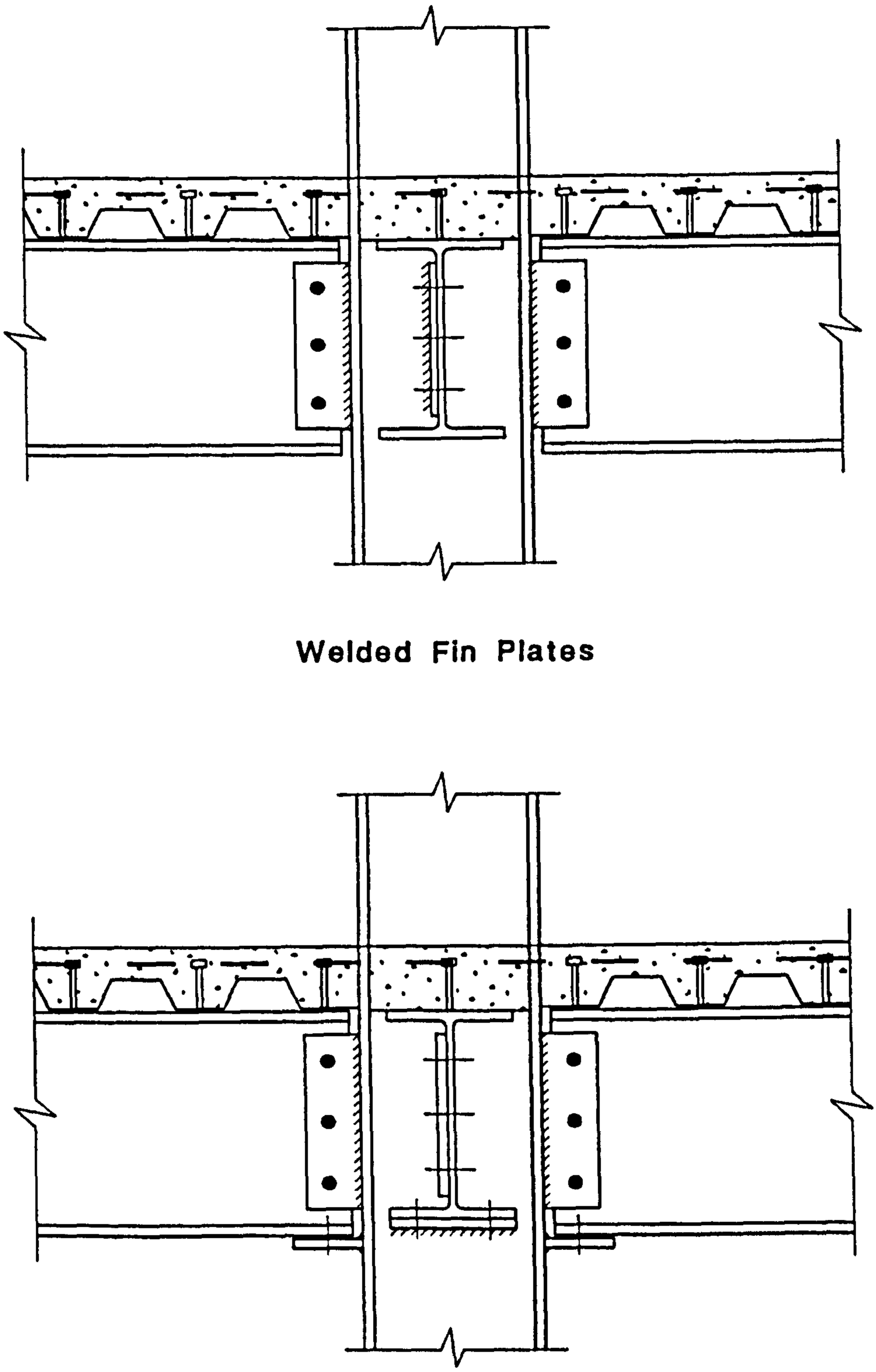

Welded Fin Plates

Welded Fin Plate and Bottom Plate

Figure1.6 Fin plate connections

1.4 Outline of the thesis

There are nine chapters in this thesis. A brief introduction to composite construction and semi-rigid beam-to-column connections has been given in Chapter 1.

In Chapter 2, the current design code method for steel beam-to-column connections is reviewed. Current research effort on the theoretical analysis of composite beam-to-column connections is also reviewed.

The research on the analysis of composite beams is reviewed in Chapter 3 and the current design code method for simple support composite beams is outlined. The design recommendations for continuous composite beams are also outlined.

In Chapter 4, the basic concept of finite element method and stiffness matrix method is reviewed. The LUSAS structural analysis program is introduced and the procedure of seismic analysis using time domain method is described.

In Chapter 5, recent finite element models of semi-rigid composite joints are discussed and a simple composite joint model is proposed (including a shear connector model). The proposed composite joint model is validated against published joint tests and the non-linear behaviour of semi-rigid composite joints is investigated.

In Chapter 6, the history of finite element modelling of composite beams is reviewed and a simple composite beam model is proposed. By incorporating the proposed composite joint model, composite beams with semi-rigid joints can be analysed. The proposed beam model is validated against the current British design code method and published composite beam tests. The behaviour of composite beams with partial shear connection and semi-rigid joints is investigated.

In Chapter 7, the design recommendations on composite frames are reviewed and recent analytical proposals of composite frames are investigated. A simple finite element method for the nonlinear analysis of composite frames is proposed by incorporating the

proposed composite joint model and beam model. The proposed composite fame model is validated against different proposals through the analysis of three composite frames. The limit behaviour of composite frames is investigated and the influence of semi-rigid connections on the overall behaviour of composite frames is discussed.

In Chapter 8, recent research on the seismic analysis of composite structures is reviewed. The proposed composite frame model is used to analyse a six-storey sample composite frame. The influence of composite joint stiffness on the overall behaviour of composite frames is investigated.

In Chapter 9, the conclusions on the modelling of composite structures are outlined and design recommendations for semi-rigid composite frames are made. Future research work on improving the modelling and dynamic analysis of composite structures is indicated.

Chapter2 Semi-rigid beam-to-column connections

2.1 Introduction

The advantages and benefits of semi-rigid construction have been generally accepted but because of the lack of design provisions, semi-rigid design is rarely adopted in the current building industry. The main reason for this is because of the complexity of semi-rigid beam-to-column connections, especially in a composite joint design. The current European design code EC3 (DD ENV 1993-1-1) introduces a design method for the endplate type of steel beam-to-column connections. Research is still under way on the design of composite beam-to-column connections.

In this chapter, the classifications of semi-rigid beam-to-column connections are introduced and the current design code method of endplate beam-to-column connections is reviewed. Recent design recommendations on composite beam-to-column connections are outlined.

2.1.1 Moment-rotation relationship

Generally speaking the moment-rotation relationship of a beam-to-column connection is non-linear. An approximate design moment-rotation relationship could be obtained from a more precise curve by an appropriate linearised approximation (e.g. bi-linear or tri-linear), provided that the approximate curve is below the more precise relationship (Figure 2.1).

The design of the moment-rotation relationship should define three main properties:

- Moment of resistance
- Rotational stiffness
- Rotation capacity

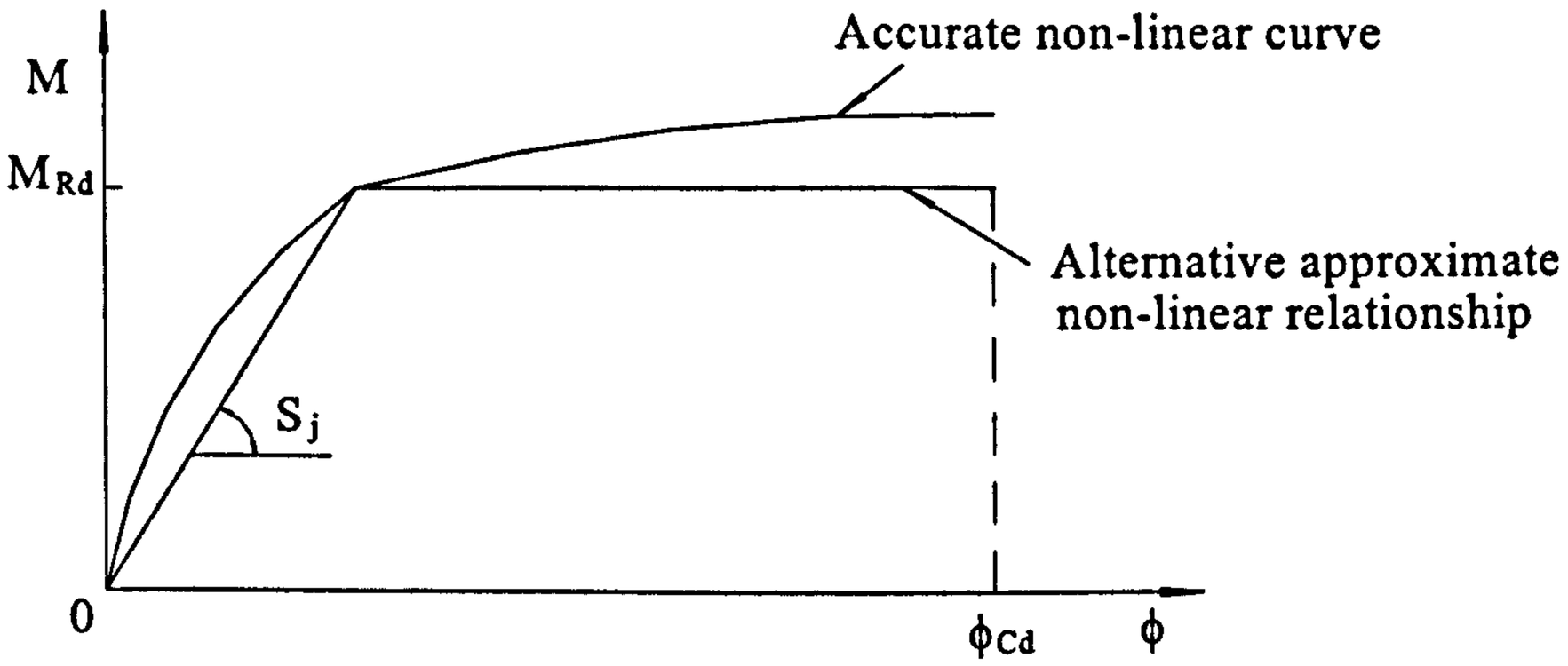

M_{Rd} --- Design moment resistance

S_j --- Rotational stiffness

ϕ_{Cd} --- Design rotation capacity

Figure 2.1 Bi-linear relationship of beam-to-column connections

2.1.2 Classification of beam-to-column connections according to EC3

Generally beam-to-column connections may be classified by rotational stiffness or by moment of resistance. By rotational stiffness, beam-to-column connections may be sub-classified as nominally pinned connections, rigid connections and semi-rigid connections. By moment of resistance, beam-to-column connections may be sub-classified as nominally pinned connections, full-strength connections and partial-strength connections.

2.1.2.1 Classification by rotational stiffness

According to EC3 a beam-to-column connection may be classified as nominally pinned if its rotational stiffness S_j satisfied the condition:

$$S_j \leq 0.5EI_b / L_b \qquad (2.1)$$

where S_j is the secant rotational stiffness of the connection

I_b is the second moment of area of the connected beam

L_b is the length of the connected beam

A beam-to-column connection in a braced frame or an unbraced frame may be considered to be rigid compared to the connected beam, if the rising portion of its moment-rotation curve lies above the solid line on the diagram in Figure 2.2.

However, for an unbraced frame every storey should satisfy:

$$K_b / K_c \geq 0.1 \qquad (2.2)$$

in which K_b is the mean value of I_b/L for all the beam members at the top of that storey

and K_c is the mean value of I_c/L_c for all the columns in that storey

where I_b is the second moment of area of a beam

L is the span of a beam (centre-to-centre of columns)

I_c is the second moment of area of a column

L_c is the storey height for a column

If the rising portion of its moment-rotation curve lies below the solid line in Figure 2.2, a beam-to-column connection is classified as semi-rigid, unless it also satisfies the requirements for a nominal pinned connection.

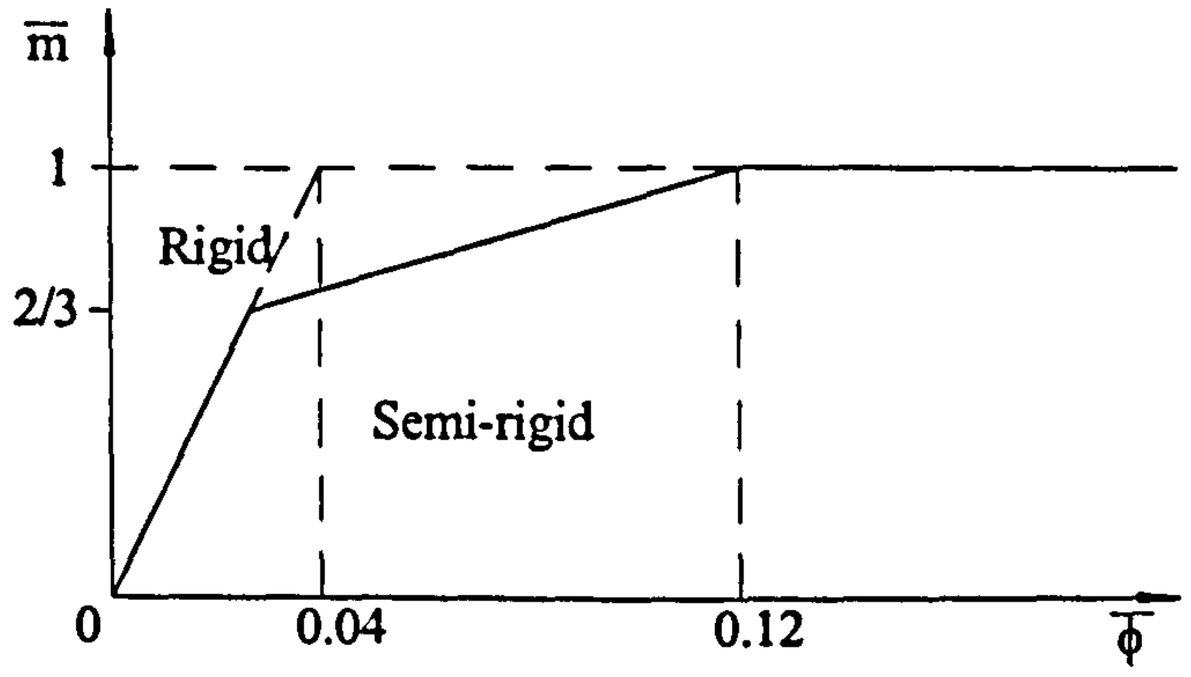

(a) Unbraced frames

when $\bar{m} \leq 2/3$: $\bar{m} = 25\bar{\phi}$

when $2/3 < \bar{m} \leq 1.0$: $\bar{m} = (25\bar{\phi}+4)/7$

$$\bar{m} = \frac{M}{M_{Rd}}$$

$$\bar{\phi} = \frac{E I_b \phi}{L_b M_{pl,Rd}}$$

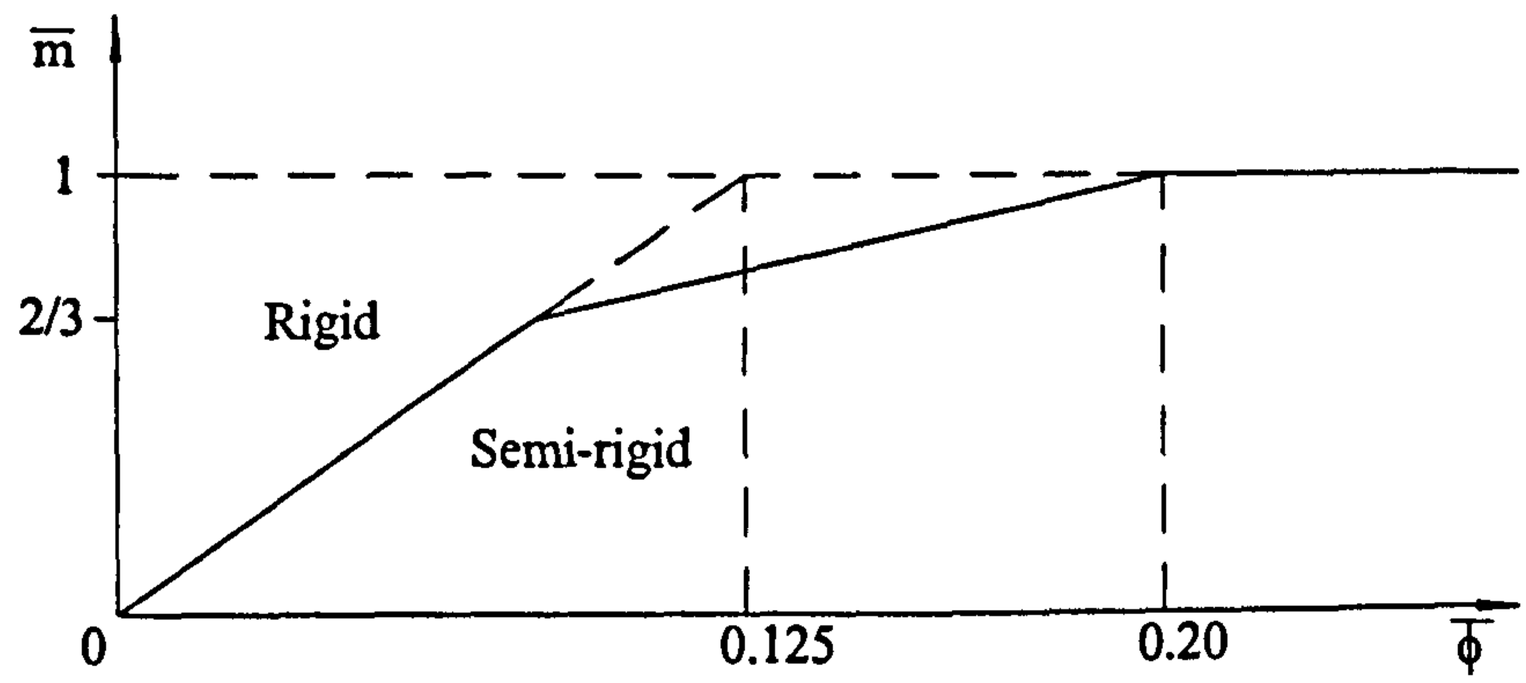

(a) Braced frames

when $\bar{m} \leq 2/3$: $\bar{m} = 8\bar{\phi}$

when $2/3 < \bar{m} \leq 1.0$: $\bar{m} = (20\bar{\phi}+3)/7$

Figure 2.2 Classification boundaries for rigid beam-to-column connections from EC3

2.1.2.2 Classification by moment of resistance

According to EC3, a beam-to-column connection may be classified as nominally pinned if its design moment of resistance M_{Rd} is not greater than 0.25 times the design plastic moment of resistance of the connected beam $M_{pl,\,Rd}$, provided that it also has sufficient rotation capacity.

A beam-to-column connection may be classified as full strength if its design moment of resistance M_{Rd} is at least equal to the design plastic moment of resistance of the connected beam $M_{pl,\,Rd}$, provided that it also has sufficient rotation capacity.

A beam-to-column connection should be classified as partial-strength if design moment of resistance M_{Rd} is less than $M_{pl,\,Rd}$.

The classification of typical moment-rotation relationships for beam-to-column connections with respect to both rotational stiffness and moment of resistance is illustrated in Figure 2.3.

2.1.3 Design criteria

In EC3 the design criteria of the moment of resistance, rotation capacity and the rotational stiffness of a beam-to-column connection is promoted by considering three critical zones as shown in Figure 2.4. They are:

- Tension zone (in column & beam web)
- Compression zone (in column web)
- Shear zone (in column web)

2.1.3.1 Moment of resistance

The design moment of resistance should be determined by taking account of the following criteria:

(a) Tension zone

- Yielding of the column web
- Yielding of the beam web
- Yielding of the column flange
- Yielding of the connection material (e.g. end plate)
- Weld failure
- Bolt failure

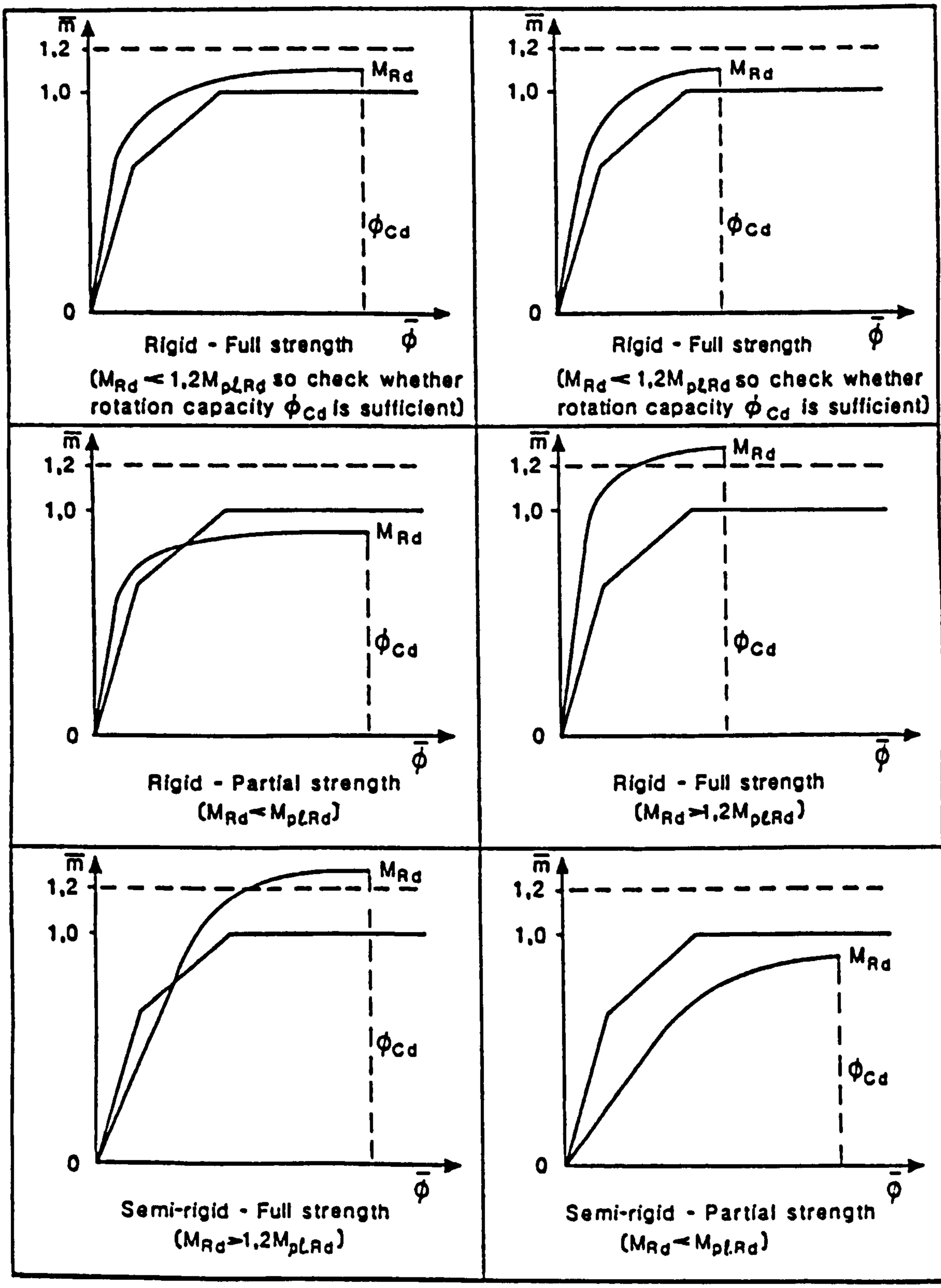

Figure 2.3 Examples of classification of moment-rotation relationships for beam-to-column connections from EC3 (DD ENV 1993-1-1)

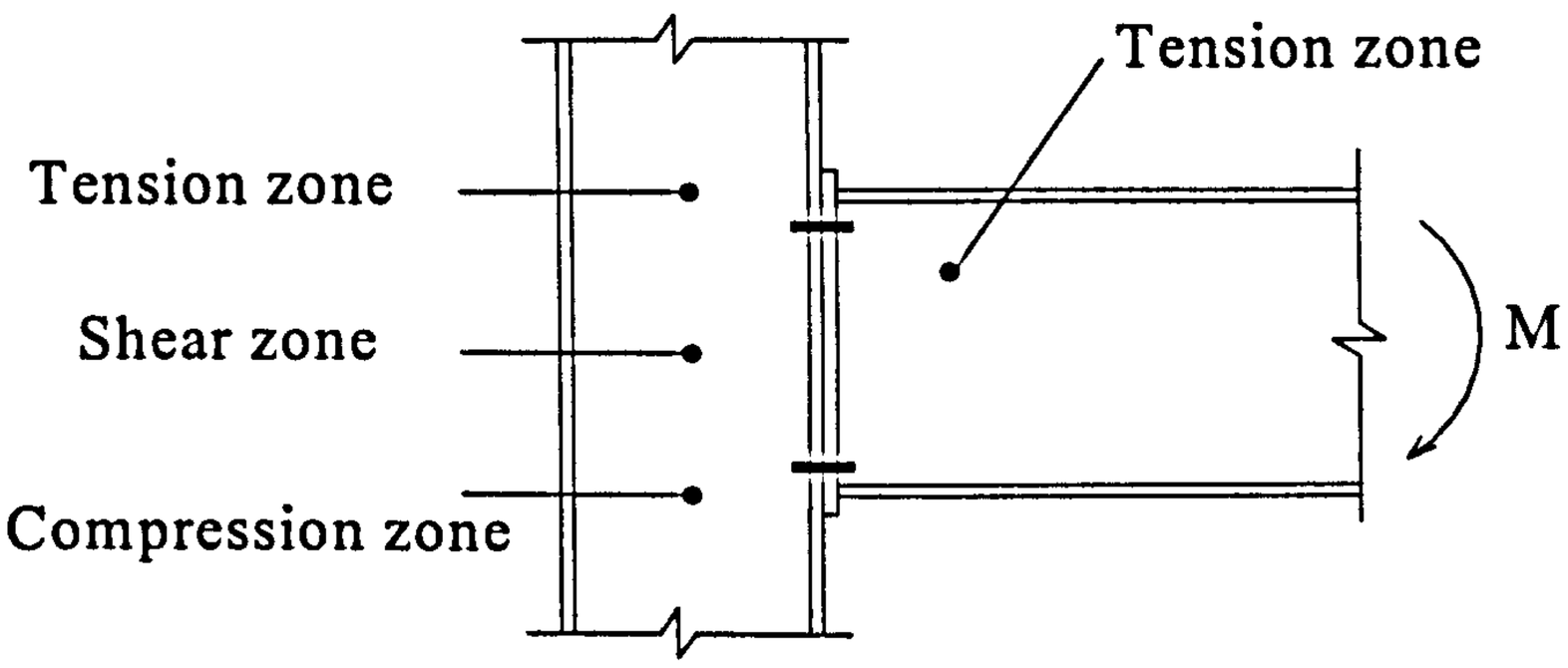

Figure 2.4 Critical zones in beam-to-column connections

(b) Compression zone

- Crushing of the column web
- Buckling of the column web

(c) Shear zone

- Shear failure of the column web panel

The design moment of resistance of a beam-to-column connection is taken as the smaller of the resistance of the tension zone and the compression zone, multiplied by the distance between their centers of resistance.

2.1.3.2 Rotational stiffness

It is suggested in EC3 that the calculated rotational stiffness of a beam-to-column connection should be based on the flexibilities of the components of the critical zones.

2.1.3.3 Rotation capacity

It is suggested in EC3 (DD ENV 1993-1-1) that the calculated rotation capacity of a beam-to-column connection should be determined from the plastic deformation

capacity of the same critical zone which governs in the calculation of the design moment of resistance of the connection.

2.2 Design of semi-rigid beam-to-column connections according EC3

Bolted endplate connections are typical semi-rigid connections. In the connection, the column web may be un-stiffened or stiffened in line with one or both flanges of the beam. Some types of endplate connections are shown in Figure 2.4. In Annex J of EC3, Part 1.1 (1992), the design method of endplate connections is provided.

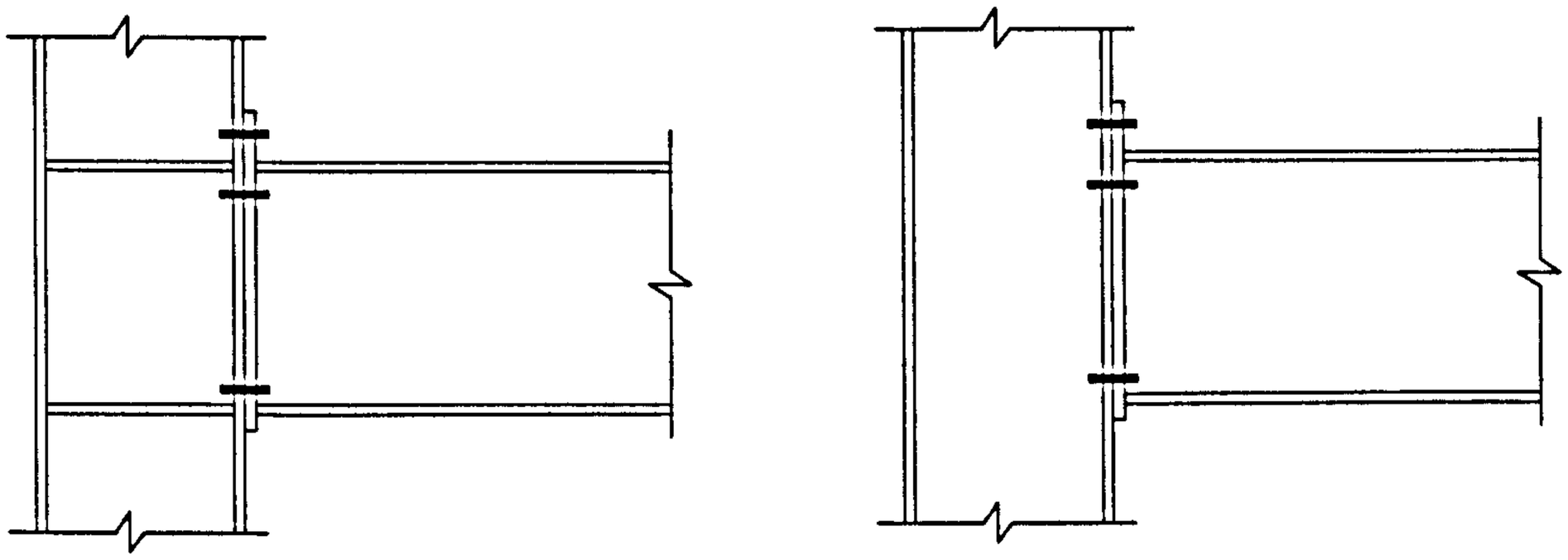

(a) Bolted connections with extended end plates

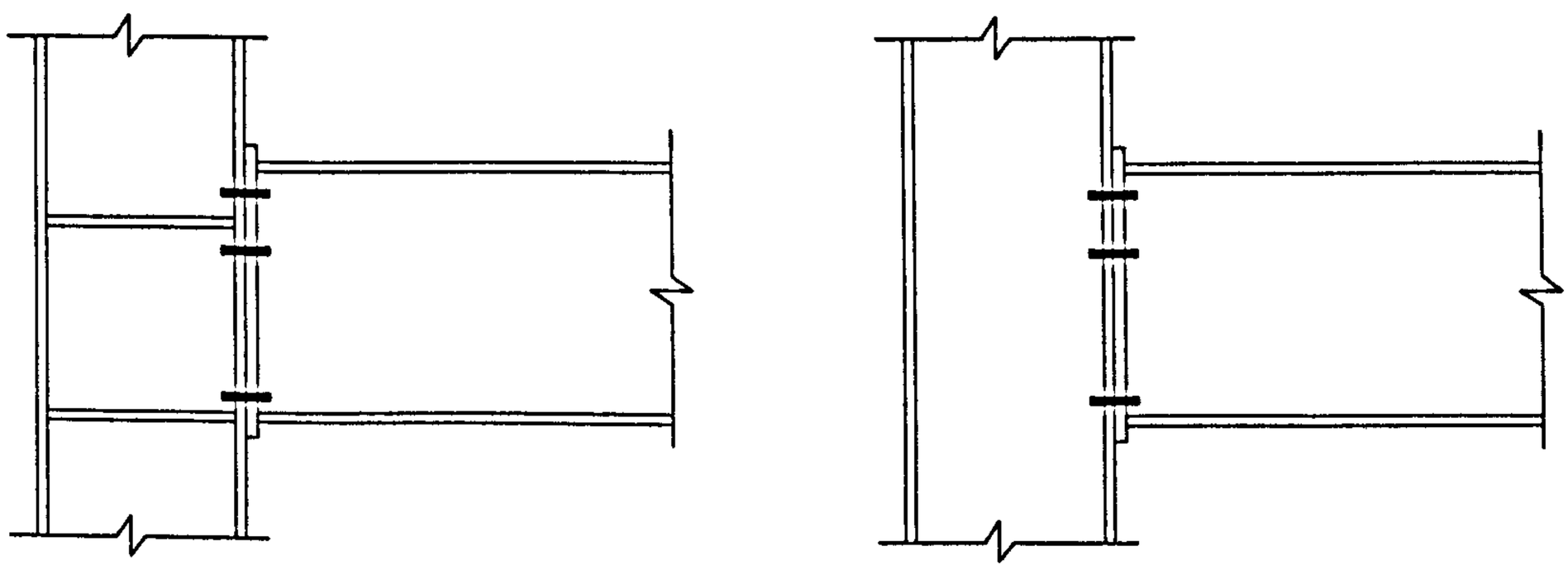

(b) Bolted connections with flush end plates

Figure 2.4 Bolted endplate beam-to-column connections

2.2.1 Moment of resistance

In EC3 the design value of the moment of resistance of a bolted beam-to-column connection is given by

$$M_{Rd} = \sum [F_{ti,Rd} \cdot h_i] \qquad (2.3)$$

where $F_{ti,Rd}$ is the design value of the effective resistance of an individual row of bolts

h_i is the distance from that bolt-row to the centre of resistance of the compression zone

2.2.2 Rotational stiffness

In EC3 the rotational stiffness of a bolted end-plate beam-to-column connection is given by:

$$S_j = \frac{E h_1^2 t_{wc}}{\sum \frac{\mu_1}{k_i} [\frac{F_i}{F_{i,Rd}}]^2} \qquad (2.4)$$

where

S_j is the secant stiffness with respect to a particular moment M in the connection ($M \leq M_{Rd}$)

M_{Rd} is the design moment of resistance of the connection

h_1 is the distance from the first bolt-row below the tension flange of the beam, to the centre of resistance of the compression zone

μ_1 is the modification factor. For i = 1, 2 or 3, μ_1 = 1. For i = 4, 5 or 6,

$$\mu_1 = \frac{h_1 F_{1,Rd}}{M_{Rd}}$$

k_i is the stiffness factor for component i.

F_i is the force in component i of the connection due to moment M.

$F_{i, Rd}$ is the design resistance of component i of the connection

The definition of the stiffness factor (k_i) can be found in Annex J of Eurocode3, Part1.1.

2.2.3 Rotation capacity

The rotation capacity of a bolted end-plate beam-to-column connection is given in EC3 from

$$\Phi_{Cd} = \frac{10.6 - 4\beta_{cr}}{1.3h_1} \tag{2.5}$$

where

h_1 is the distance (in mm) from the first bolt-row below the tension flange of the beam to the centre of resistance of the compression zone.

β_{cr} is the value of β for the component with the lower value of $F_{t,Rd}/\Sigma B_{t, Rd}$

$\Sigma B_{t, Rd}$ is the total design resistance of all bolt-plate assemblies

The definition of β, $\Sigma B_{t, Rd}$ can also be found in Annex J, Eurocode3, Part1.1 (1992).

2.3 Design recommendations of composite semi-rigid connections

A composite connection is defined in Eurocode 4, Part 1.1 (1994) as 'a connection between a composite member and any other member in which reinforcement is intended to contribute to the resistance of the connection'. Endplate connections are a commonly used form of connection for frames in the UK. A considerable amount of research has been carried out on their performance, both as steel and composite connections. Early studies have shown that endplate connections possess good rotation capacity and can achieve effective transfer of compression at the beam bottom flange. They can provide 'robustness' as required in BS 5950: Part 1 (2000). And design guidance is only available for endplate type of composite connections.

The force transfer at a typical composite end plate connection is shown in Figure 2.5. The moment of resistance of composite connections may be evaluated by plastic analysis or 'stress block' principles, provided:

- There is an effective compression transfer to and through the column
- The amount of reinforcement is above a certain minimum, so that cracking of the concrete develops in a controlled manner
- There are sufficient shear connectors to develop the tensile forces in the reinforcement
- The reinforcement is effectively anchored on both sides of the connection
- The bolts provide sufficient shear resistance

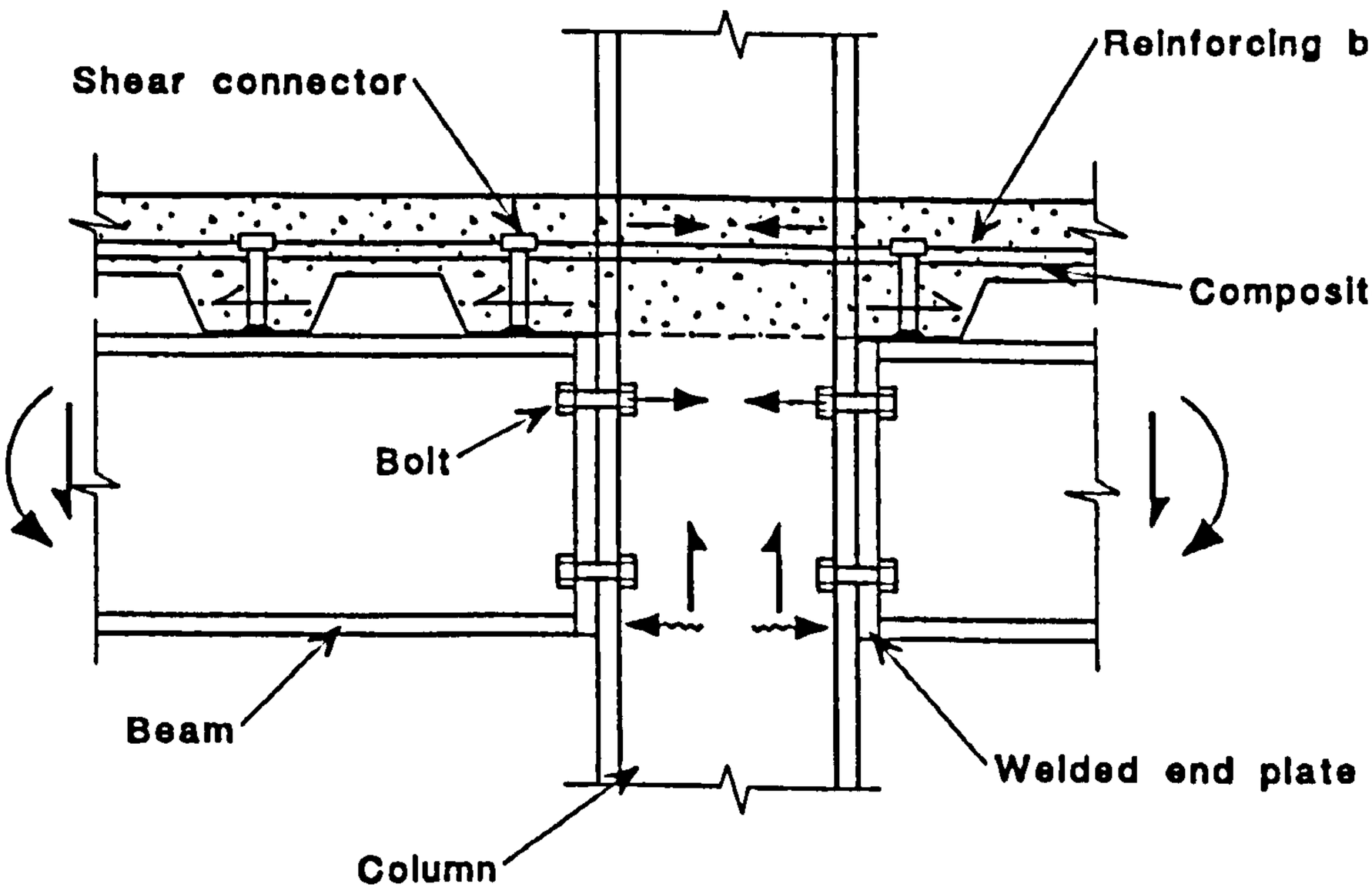

Figure 2.5 Force transfer at a typical composite end plate connection

2.3.1 Tensile force in the reinforcement

The effective breadth of slab over which the reinforcement may be considered to act in tension in the negative region is given in Clause4.6 of BS 5950: Part 3. This effective breadth is equivalent to 1/8 of the average of the adjacent beam spans,

which is half of the value for a simple supported beam. Reinforcement outside this zone is neglected.

The minimum percentage of bar reinforcement (expressed as a proportion of the slab cross-sectional area) should be sufficient to control the cracking of the concrete (0.5% is a recommended practical minimum for crack control at the connections). Additionally, the rotation capacity of the connection increases with the amount of reinforcement placed in the slab and therefore a higher percentage of reinforcement may be required. The maximum percentage of reinforcement is dependent either on the ability of the shear connectors placed in the negative moment region to transfer the required force to the reinforcement, or on the compression resistance of the beam or the column web. It is suggested that for typical shear connector spacing and beam sizes the sensible maximum percentage of reinforcement is about 2% (Lawson, 1995). Mesh reinforcement is ignored in moment of resistance calculations because of its possible lack of ductility.

2.3.2 Tensile force in the bolts

In the joint design the upper bolts may be considered as part of the tensile resistance of the composite connection, provided the steel to steel connection is classified as 'full' or 'partial' strength according to Eurocode 3 Annex J. Mode 1 failure, defined in Annex J of EC3, corresponds to development of the necessary yield line mechanism in the end plate before bolt failure. If Mode 1 failure does not occur, the connection may not have guaranteed ductility compatible with the extension of the reinforcement at the required rotation of the connection.

2.3.3 Compression in the bottom flange

The transfer of the compression force through the connection relies on direct bearing of the bottom flange of the beam. It is possible to argue that the bottom flange can resist stress of up to $1.2p_y$, due to strain hardening, as in the conventional design of steel connections to resist moments. In heavily reinforced connections, the neutral

axis may extend into the beam web. The maximum depth of beam web adjacent to each flange that can resist compression is $19t_w\varepsilon$, before onset of local buckling. Class 3 (semi-compact) webs may be analysed by ignoring the ineffective portions of the web in compression when the depth in compression exceeds $38t_w\varepsilon$. (t_w is the web thickness and $\varepsilon = \sqrt{(p_y / 275)}$ for steel of design strength, p_y)

Checks also have to be made on the adequacy of the connected parts i.e. plates and welds, and on the local resistance of the column in compression. The buckling or bearing resistance of the column web may limit the maximum compression force that can be transferred. Web stiffeners may be required for composite connections with a high percentage of slab reinforcement, leading to a greater compression transfer at the bottom flange.

2.3.4 Shear force in the bolts

The shear resistance of the connection relies on the connecting parts. It is considered inappropriate to include the shear resistance of the concrete or reinforcement because of the influence of cracking in this zone. Conventionally, the bottom pair of bolts in a steel connection is often assumed to resist the total shear force on the beam. However, the top bolts that are highly stressed in tension may resist a proportion of their design shear resistance without affecting their tensile resistance (BS 5950: Part 1, 2000).

2.3.5 Longitudinal shear force

The development of the tensile force in the reinforcement depends on the longitudinal shear forces between the slab and beam being transferred by the shear connectors. It is normal practice to adopt a standard spacing of the shear connectors throughout the beam span. BS 5950: Part 3 (1990) requires that full shear connection is developed in the negative moment region, and this may lead to the use of shear connectors at the minimum spacing for highly reinforced slabs. The reinforcement

should extend over the negative moment region and be anchored into the compression zone of the slab, as required by BS 8110 (1997).

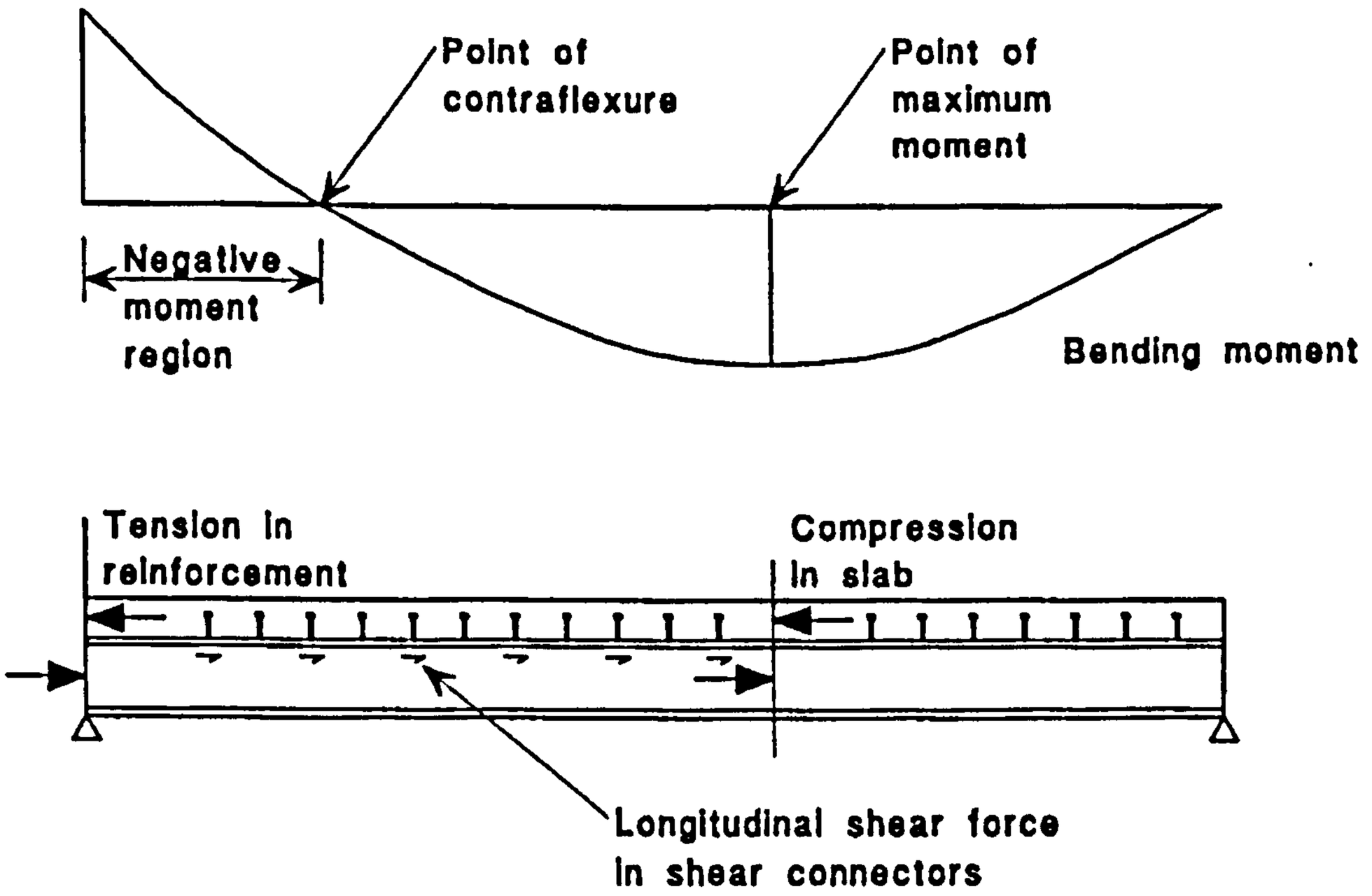

Figure 2.6 Transfer of longitudinal shear forces in a composite beam

2.3.6 Moment of resistance of composite connections

Several methods have been proposed to predict the moment of resistance of composite end plate connections (Anderson & Najafi, 1994; Lawson & Gibbons, 1995; Xiao et al, 1996; Brown & Anderson, 2001, etc.). In these proposals, the moment of resistance of composite end plate connections is determined from plastic analysis principles in terms of the following parameters:

R_r tensile resistance of the reinforcement placed within the effective breadth of the slab.

R_b effective tensile resistance of a pair of bolts, determined by the yield line pattern in the end plate or column flange (achieve mode 1 failure, according to EC3 Annex J)

R_f compression resistance of the beam bottom flange, or alternatively, the resistance of the column web in buckling or bearing if this is smaller.

The method described by Lawson & Gibbons is introduced in detail below.

2.3.6.1 Flush end plate connections

In flush end plate connections, it is considered that only the upper pair of bolts is effective in tension, provided also that the steel connection is classified as 'partial strength'. This limitation is made due to the potentially low strains in the bolts relative to the reinforcement, and the possibility that both elements may not reach their tensile resistance simultaneously. The moment of resistance of the composite connection is evaluated using the stress block analysis and symbols shown in Figure 2.7.

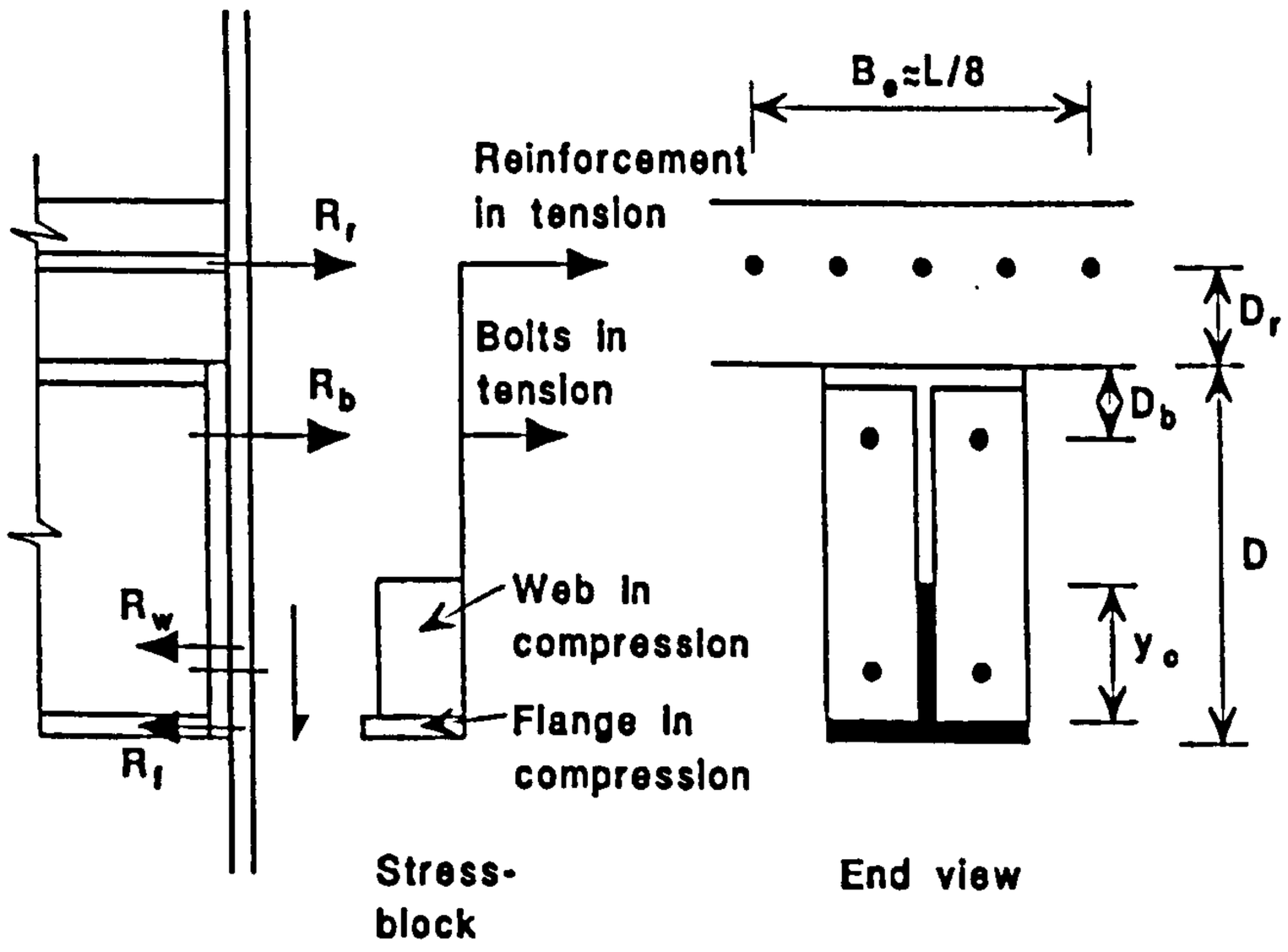

Figure 2.7 Stress block analysis of the moment of resistance of a composite connection using a flush end plate (Lawson, 1995)

(a) The plastic neutral axis of the composite section subject to negative moment lies in the beam bottom flange, when

$$R_f > R_b + R_r \tag{2.6}$$

In this case, the moment of resistance of the composite connection, M_{Rd}, is determined by taking moments about the centre of the beam bottom flange, and is given by:

$$M_{Rd} = R_r (D + D_r - 0.5\, t_f) + R_b(D - D_b - 0.5\, t_f) \tag{2.7}$$

where D is the beam depth

D_b is the distance of the first row of bolts below the top of the beam

D_r is the distance of the reinforcement above the top of the beam

t_f is the flange thickness

(b) The plastic neutral axis of the composite section lies in the beam web, when

$$R_f \leq R_b + R_r \tag{2.8}$$

The neutral axis depth, y_c, above the bottom flange is given by:

$$y_c = \frac{R_r + R_b - R_f}{t_w p_y} \tag{2.9}$$

The web is fully effective in compression provided $y_c \leq 38 t_w \varepsilon$. If not, the analysis may be continued by considering only an effective portion of the web of depth $19 t_w \varepsilon$ adjacent to both the bottom flange and the neutral axis.

The moment of resistance of the composite connection with a fully effective web is determined by taking moments about the centre of the beam bottom flange, and is given by:

$$M_{Rd} = R_r (D + D_r - 0.5\, t_f) + R_b(D - D_b - 0.5\, t_f) - R_w (y_c + t_f)/2 \quad (2.10)$$

where $R_w = y_c\, t_w p_y$

As the amount of reinforcement is increased, the plastic neutral axis rises into the upper portion of the web. When $y_c > 0.5D$ it is proposed that the tensile resistance of the bolts should be neglected due to their low strains relative to the reinforcement. The moment of resistance of the connection with ineffective bolts and web can be calculated from the first principles. However, this design case indicates that the slab is heavily reinforced and it is unlikely that full shear connection in the negative moment region can be achieved. In practice, therefore, the above equations should be sufficient for design purpose.

2.3.6.2 Extended end plate connections

In extended end plate connections, the upper pairs of bolts above and below the upper beam flange are considered to be effective in tension. The moment of resistance is evaluated using the same basic expressions as in flush end plate connections assuming that the tension bolts are equally spaced about the upper flange. The effective resistance of the four tension bolts is $2R_b$. And the compression stress of $1.2p_y$ is also assumed in calculating R_f. However, it is often necessary to stiffen the column web in extended end plate connection in order to develop this compression resistance. Otherwise, the maximum value of R_f would be limited to a maximum value given by buckling or bearing of the column web.

(c) The plastic neutral axis of the composite section lies in the beam bottom flange, when

$$R_f > R_b + R_r \quad (2.11)$$

The moment of resistance of the composite connection, M_{Rd}, is determined by taking moments about the centre of the beam bottom flange, and is given by:

$$M_{Rd} = R_r (D + D_r - 0.5\, t_f) + 2R_b(D - 0.5\, t_f) \qquad (2.12)$$

(d) The plastic neutral axis of the composite section lies in the beam web, when

$$R_f \leq 2R_b + R_r \qquad (2.13)$$

The neutral axis depth, y_c, above the bottom flange is given by:

$$y_c = \frac{R_r + 2R_b - R_f}{t_w p_y} \qquad (2.14)$$

As for flush end plate connections, when the depth of the web in compression exceeds $38t_w\varepsilon$, the ineffective portion of the web is neglected in the moment of resistance calculations.

The moment of resistance of the composite connection with a fully effective web is given by:

$$M_{Rd} = R_r (D + D_r - 0.5\, t_f) + 2R_b(D - 0.5\, t_f) - R_w (y_c + t_f)/2 \qquad (2.15)$$

where $R_w = y_c\, t_w p_y$

As the amount of reinforcement is increased, the plastic neutral axis rises into the upper portion of the web. When $y_c > 0.5D$, the tensile resistance of the bolts below the top beam flange is neglected, and only the upper pair of bolts is considered, until $y_c = 0.5D$ when these bolts are also neglected. The above equations should be modified accordingly.

2.3.7 Initial stiffness and rotation capacity of composite connections

2.3.7.1 Anderson & Najafi's model

Anderson & Najafi (1994) proposed a simplified spring model of composite connections with steel end plate joints to predict the joint stiffness and the joint rotation. In their model, each spring simulates the stiffness of a component of the connection and in principle is assumed to be elastic or elasto-plastic. Assuming full interaction, no slip occurring at the interface of the steel beam and concrete slab and the concrete to be cracked, the rotational stiffness of the composite connection is converted to the following springs as shown in Figure 2.8.

- K_a the compression spring
- K_b the tension spring. $K_b = \infty$ when the column we is stiffened
- K_r the spring corresponds to the reinforcement

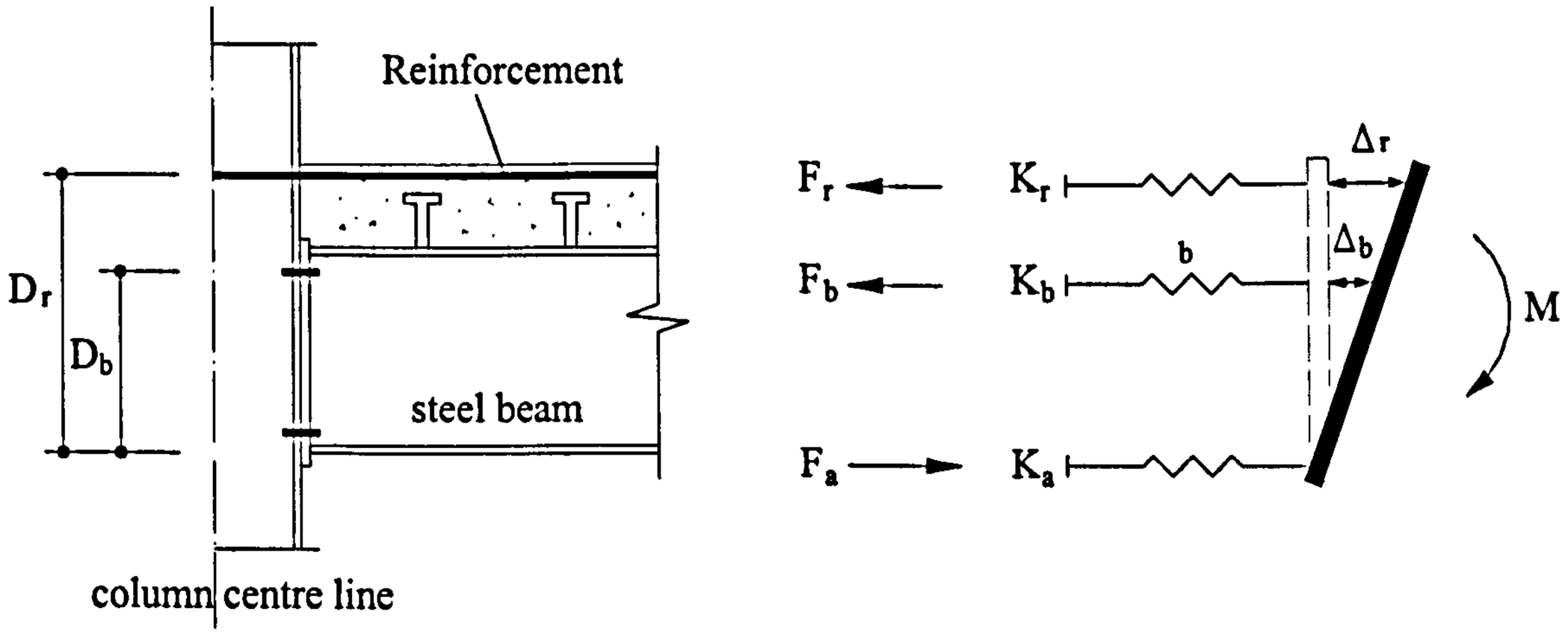

Figure 2.8 Anderson & Najafi's simplified model including steelwork joint and reinforcement

The rotational stiffness of the steelwork connection is:

$$C_s = \frac{M_s}{\phi_s} = \frac{F_b D_b}{\phi_s} \tag{2.16}$$

The joint rotation ϕ_s can be written as:

$$\phi_s = \frac{\Delta_b}{D_b} = \frac{\Delta_r}{D_r} \tag{2.17}$$

where Δ_b is the extension of spring b, i.e. the displacement at the level of the top bolt row. From the above two equations, the stiffness of spring b can be written as:

$$K_b = \frac{F_b}{\Delta_b} = \frac{C_s}{D_b^2} \tag{2.18}$$

The stiffness C_s can be calculated for steel end plate joints from EC3. Assuming that the reinforcement obeys Hooke's law:

$$\Delta_r = \frac{F_r}{K_r} = \frac{F_r l}{E_r A_r} \tag{2.19}$$

where l is the assumed length of reinforcing bars having extension Δ_r , $l = D_c/2$. where D_c is the depth of the column section. Hence:

$$K_r = \frac{E_r A_r}{l} \tag{2.20}$$

Assuming rotation about the bottom flange, the overall equilibrium and compatibility equations for the connection are:

$$M = F_r D_r + F_b D_b \tag{2.21}$$

Using the above equations to eliminate F_r and F_b,

$$M = (K_b D_b^2 + K_r D_r^2)\phi \tag{2.22}$$

Hence for a given moment, the corresponding rotation is given by:

$$\phi = \frac{M}{K_b D_b^2 + K_r D_r^2} \tag{2.23}$$

However, the predicted joint rotations at half the moment of resistance of the composite joint are much less than the experimental values. The authors concluded that the flexibility of shear connectors cannot be excluded from the derivation of connection stiffness. It is assumed that the slip at the connection depends initially on the nearest stud to the column. Under increasing load this stud provides resistance to slip, until it becomes plastic. Its force then remains constant and equal to its maximum resistance. Additional load is then assumed to be resisted by the next stud deforming elastically until the plastic resistance of that stud is reached also. Further load will then be carried by the next stud and so forth. The spring model representing the deformation of both the reinforcement and the shear connection is shown in Figure 2.9.

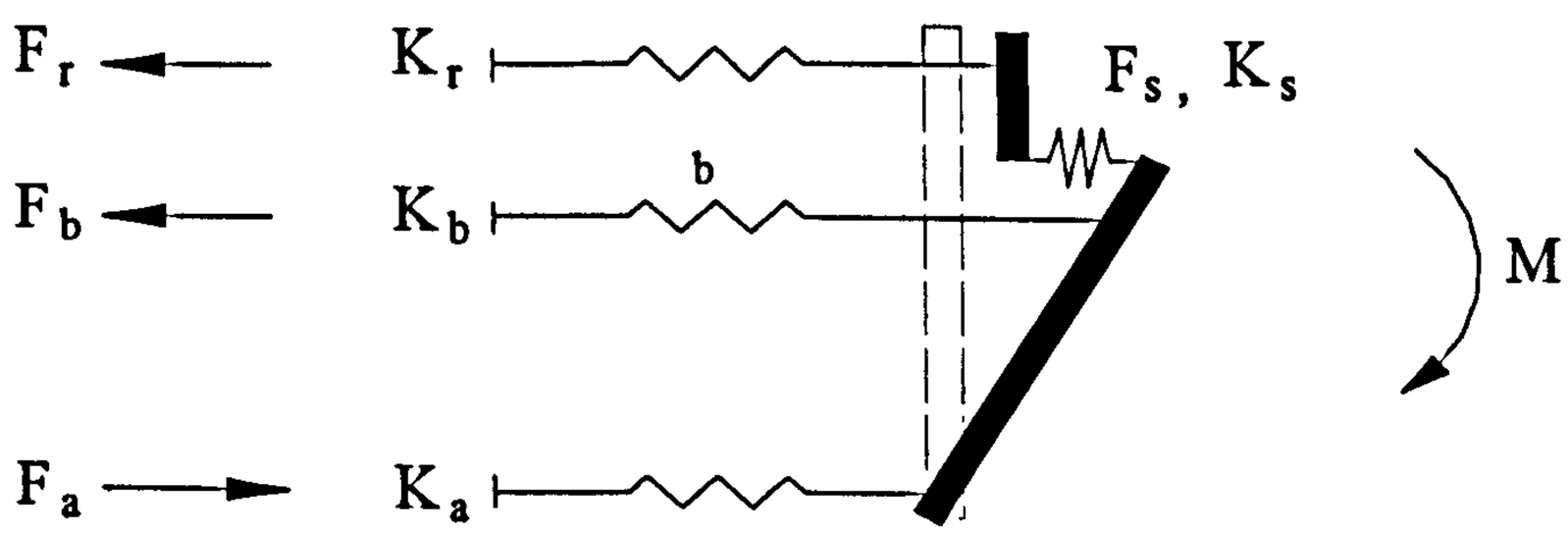

Figure 2.9 Anderson & Najafi's proposed model including steelwork joint, shear connectors and reinforcement

The joint rotation is:

$$\phi = \frac{\Delta_b}{D_b} = \frac{\Delta_r + \Delta_s}{D} \tag{2.24}$$

where D is the depth of the steel beam to the centre of the bottom flange. And the deformation Δ_s due to shear connection is given by:

$$\Delta_s = \frac{F_s}{K_s} \tag{2.25}$$

where the stiffness of the stud K_s can be obtained from push-off tests. And the force in the shear connection F_s equals to that in the reinforcement F_r. Proceeding in a similar manner to previously it can be obtained that for a particular bending moment M, the rotation ϕ is given by:

$$\phi = \frac{M}{[\frac{K_r K_s D_r D}{K_r + K_s} + K_b D_b^2]} \tag{2.26}$$

The force F_r in the reinforcement is given by:

$$F_r = (\frac{K_r K_s D}{K_r + K_s})\phi \tag{2.27}$$

For the reinforcement to yield, $F_r = A_r f_{ry}$, where f_{ry} is the yield strength of the bars. It is found that when yield occurs:

$$\phi = \frac{f_{ry}(A_r + \frac{K_s l}{E})}{K_s D} \tag{2.28}$$

As account is taken of deformation of the shear connection, the authors suggest that it is appropriate to increase the length l of the reinforcement having extension Δ_r to be the distance between the centre line of the column and the first stud.

2.3.7.2 Brown & Anderson's method

Brown and Anderson (2001) proposed a method to predict the connection stiffness and the rotation capacity of composite end plate beam-to-column connections. Their approach was justified by their tests and earlier tests and the agreement was good.

- **Initial stiffness**

In Eurocode 3 for steel joints, the initial stiffness $S_{j,ini}$ is summed to be applicable for moments up to $0.67M_{Rd}$. For steel end plate connections it is recommended that the secant stiffness at M_{Rd} should be taken as one-third of the initial value. This proposal has been shown to be appropriate also for composite joints with steel end plate connections.

According the component approach of EC3 to calculate $S_{j,ini}$, Brown and Anderson assumed that the active components are the bolt row in tension and the reinforced concrete slab. The deflections due to the column web stiffener in compression and the column web panel in shear are neglected.

In Brown and Anderson's model, each bolt row in tension comprises the column web in tension, the column flange in bending, the end plate in bending and the bolts in tension. These individual components are shown by separate springs in Figure 2.10. For each of these components, Eurocode3 gives a stiffness coefficient denoted by the author as k_1-k_4. The components in the row are then combined to give an effective stiffness, as shown in Figure 2.10 (b). For composite joints, the reinforced concrete slab in tension acts in a similar manner to a bolt row, but it is represented by a single component. The assembly of the components is then simplified by replacing the

tension springs by an equivalent single stiffness k_{eq} and the rotational stiffness is given by:

$$S_{j,\,ini} = Ek_{eq}z^2 \tag{2.29}$$

To determine the stiffness coefficient for the slab, Anderson assumed the concrete to be fully cracked. The rotational stiffness at the beam-to-column interface is then dependent on the extension of the reinforcement over half the depth of the column section $h_c/2$, and the total slip at the end of the beam due to deformation of the shear connection.

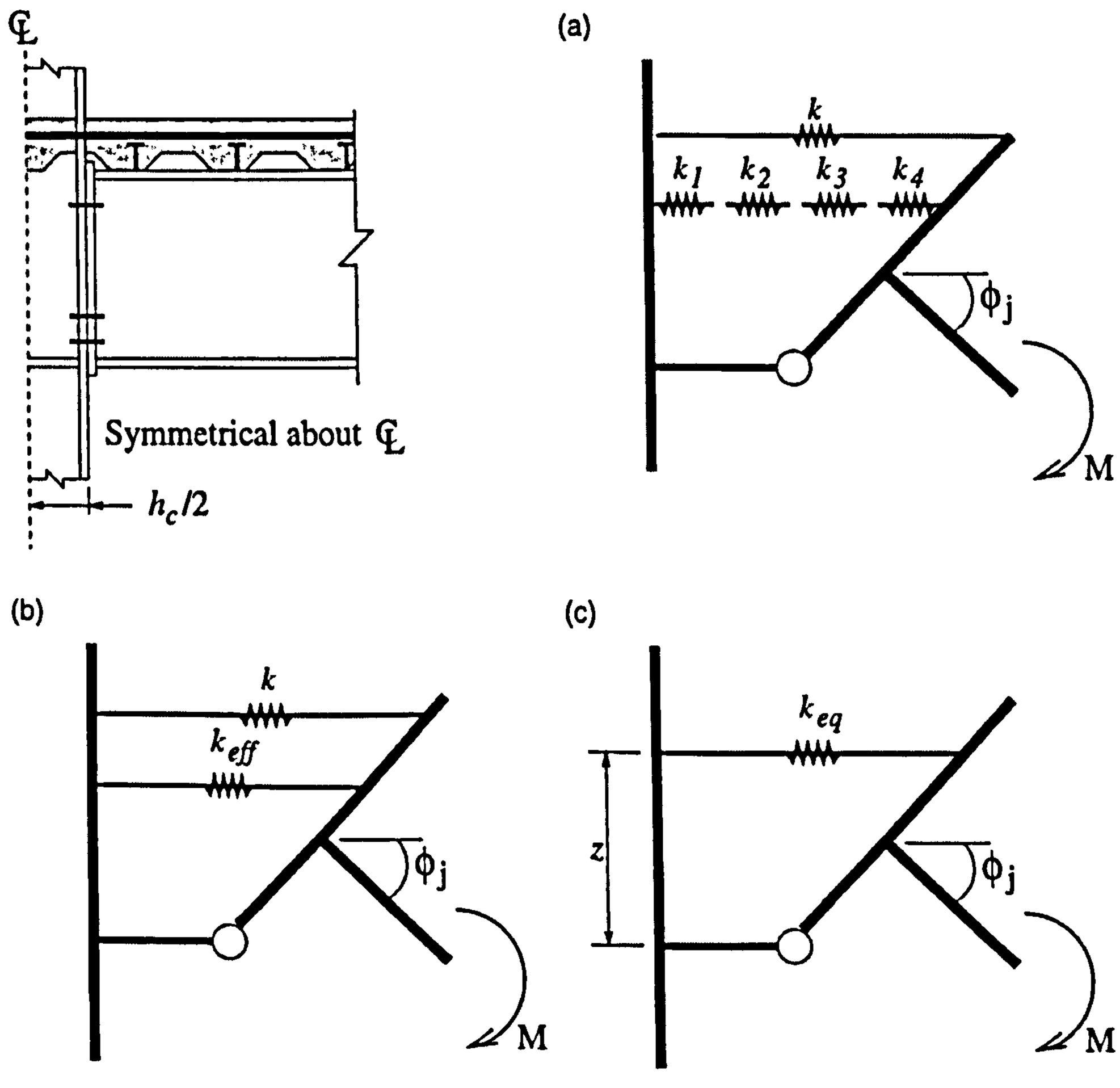

Figure 2.10 Brown & Anderson's stiffness prediction model

- **Connection rotation capacity**

Generally the moment of resistance of a composite joint is less than that of the adjacent composite beam section. The yielding therefore occurs within the composite joint. Yielding of the reinforcement is the main source of dependable rotation capacity of the composite joint. Brown & Anderson take this as the rotation capacity of the joint because the M-ϕ relationships of their tests show that the joints sustain values of moment greater than the calculated resistance up to the point of fracture. They assume that for a slab in tension the maximum strain in the reinforcement occurs only at crack locations, elsewhere the strain is lower. To predict the deformation capacity of a length of reinforcement $\Delta_{u,s}$ the average strain $\varepsilon_{s,m}$ should be calculated from the ultimate value which will arise at the crack. In their method, the length of reinforcement is calculated from the column depth h_c , the distance to the first shear connector, and the 'transmission' length L_t over which the bond between the concrete and the reinforcement has broken down (Figure 2.11).

In Brown & Anderson's method, the slip deformation s due to shear connectors and the compression deformation in the beam flange Δ_a immediately adjacent to the joint are also considered. To assess plastic compression of the beam flange, they assume that at ultimate moment the strain in the compression flange is eight times the yield value, at which the strain hardening is assumed to commence. This strain is assumed over the distance from the face of the connection to the inclinometer used to measure rotation in their tests. And the inclinometers are positioned 85mm to the surface of the end plates in test specimens. The rotation capacity ϕ_c is finally calculated as:

$$\phi_c = \frac{\Delta_{u,s}}{D_r} + \frac{[s + \Delta_a]}{D} \tag{2.30}$$

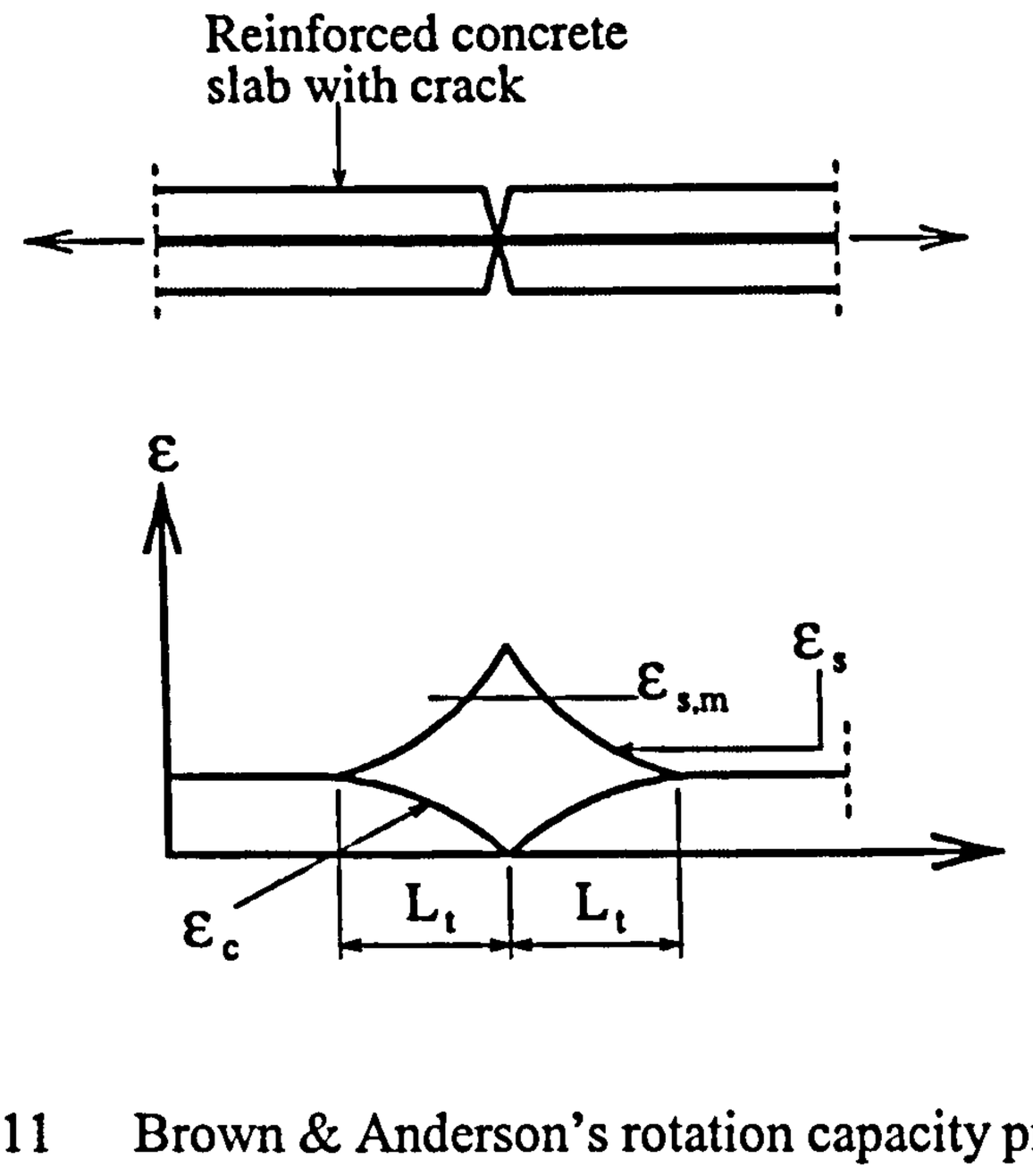

Figure 2.11 Brown & Anderson's rotation capacity prediction model

2.4 Summary

For the design of steel beam-to-column connections, the detailed design method can be found in current European design code Eurocode 3 (1992) for welded connections and bolted connections with flush or extended end plates. For other types of beam-to-column connections, the design methods are not clearly defined.

For the design of composite beam-to-column connections, the design method is not available in current design codes. Extensive research has been made to investigate the characteristics of composite beam-to-column connections. Since the design method of the steel bolted end plate connections is available, composite connections contained this type of steel connections are mostly studied.

There are two approaches for the design of composite connections: the stress block analysis developed by Lawson (1995) and the spring model analysis developed by Anderson & Najafi (1994) and Brown & Anderson (2001). Lawson (1995) proposed a method to predict the moment resistance of composite connections. However the

calculations of the initial stiffness and the rotation capacity were not mentioned. Anderson & Najafi (1994) proposed a spring model of the composite joint and gave the method to calculate the moment resistance and the joint rotation of the composite joint until the yield of the rebars. Brown & Anderson (2001) used the same method as Lawson (1995) to predict the moment resistance of the composite joint, but considered three approaches of defining the compression resistance of the bottom flange of the steel beam. The prediction of the initial stiffness of the composite joint was given according to a revised spring model derived from the spring model of Anderson & Najafi (1994). The rotation capacity of the composite joint was defined as the rotation at which the fracture of the reinforcement occurred and a formula was given to calculate the rotation capacity.

Chapter 3 Design of composite beams

3.1 Introduction

In traditional steel construction concrete slabs are supported by steel beams in a non-composite manner. Under working load the concrete slab and steel beam deform separately and slip occurs between the concrete and steel beam interface. If the slab and steel beam act together in a composite state, the slip may be eliminated or considerably reduced, and the strength and stiffness will also increase compared to a non-composite beam. Composite construction has been increasingly used since it has a number of advantages over non-composite construction. Firstly the savings in steel weight are reported to reach 30% to 50% over non-composite beams (Lawson, 1989). Composite beams are shallower for the same span, leading to lower storey height and savings in cladding, etc. Since steel profiled sheeting or precast slabs are often used in the composite slab design, no props are needed during the construction. The construction period and the cost are significantly reduced. Typical composite beam sections with profile steel decking are illustrated in Figure 3.1.

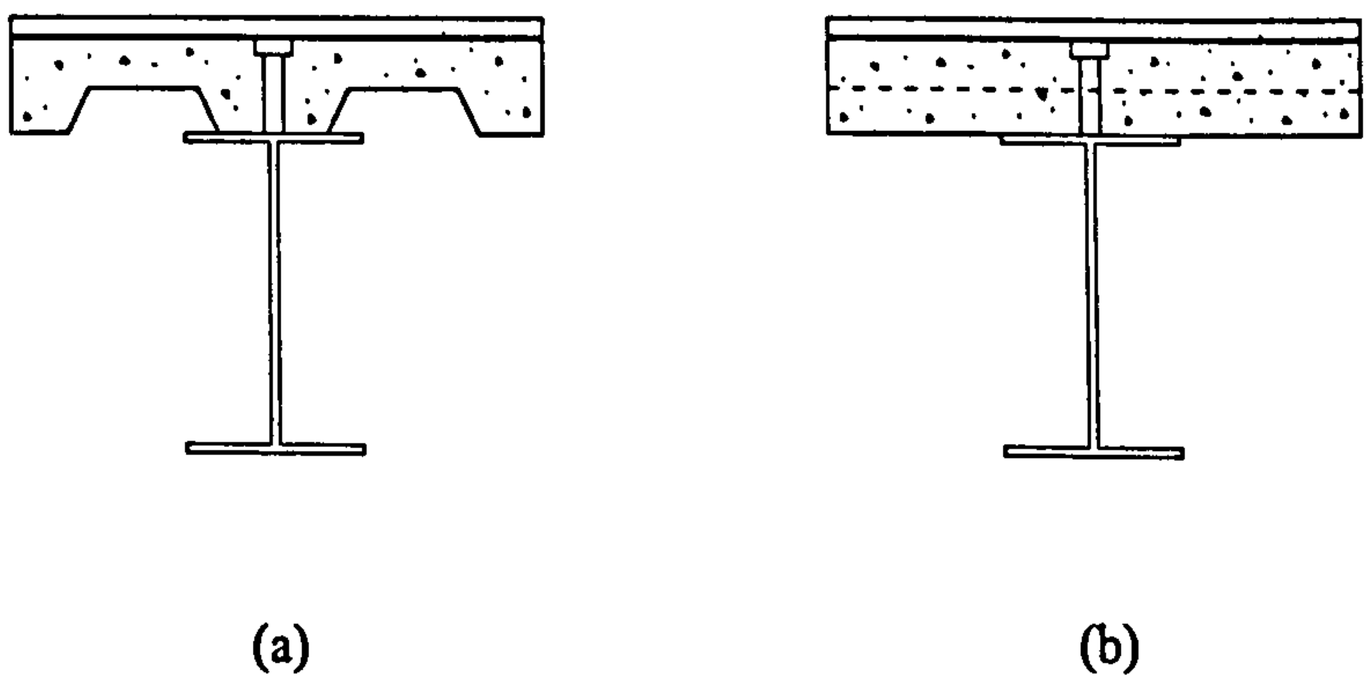

Figure 3.1 Composite beam sections with profile steel decking: (a) deck parallel to steel beam, (b) deck perpendicular to steel beam

In order that the composite state is formed, shear connectors should be designed to bear the longitudinal shear force on the steel-concrete interface. The most commonly used type of shear connector is the welded headed stud. The normal size of welded headed studs ranging from 13-25 mm in diameter and 65-125 mm in height as suggested in BS 5950, Part 3 (1990). The shear studs are often welded through the steel deck. Other types of welded shear connectors, such bars with hoops, and channels, are mainly used in bridge construction. The research on headed stud shear connector began in the 1950's (Viest, 1955). In the 1960's, a number of pushoff tests were carried out to study the ultimate shear capacity of stud shear connectors, and different empirical equations were proposed to predict the ultimate shear capacity of the studs relating to the height and diameter of studs and the concrete strength (Chapman 1964, Chapman & Balakrishnan 1964, Slutter & Driscoll 1965). The strength of shear connectors in hogging moment region of composite beam was also studied (Johnson, et al. 1969). In the 1970's, the research on shear connectors flourished with the increasing use of profiled steel sheeting and lightweight concrete in concrete floor construction. Menzies (1971) and Ollgaard et al. (1971) studied the strength of shear connectors in normal weight and lightweight concrete. The behaviour of shear studs in composite beams with profiled steel sheeting was also studied (Fisher 1970 & Grant et al. 1977). The influence of the metal deck shape on the strength of shear studs was investigated, and empirical stud strength reduction formulae were proposed. In the 1980's and early 1990's, many pushoff tests were performed on studs with various types of steel decking (Jayas & Hosain 1988, Robinson 1988, Lawson 1989, Lloyd & Wright 1990, Rakib 1991). Improved stud strength reduction formulae were proposed. The shear cone failure mode was studied and an empirical expression of the resistance of shear studs was proposed. The current British design code adopted the strength reduction idea and suggests the expression of calculating the reduction factor take the same form as proposed by Grant et al. (1977) but with revised parameters. More recently Johnson & Yuan (1998[1]) reviewed 269 previous pushoff tests with profile steel sheeting and performed 34 new push tests to study existing design rules for the static shear resistance of stud connectors. It was found that existing design rules were of limited scope and low accuracy, especially for studs

placed off-centre in the steel troughs. They established seven distinctive failure modes. Theoretical models, calibrations, and new design rules for these modes were proposed (Johnson & Yuan 1998[2]).

In a composite beam if sufficient shear connectors are provided that the full plastic capacity of the section may be developed, the composite beam is considered to be designed with full shear connection. But it is not always necessary or possible to design a composite beam with full shear connection. Especially when the concrete slab with steel profile sheeting is used, the spacing of shear connectors is restricted to the spacing of the troughs. In such cases, limited amount of shear connectors is needed, and the composite beams should be designed with partial shear connection. Though the strength and stiffness of beams with partial shear connection are lower than beams with full shear connection, the overall beam costs may be economic.

The study of the behaviour of composite beams with partial shear connection began in the late 1960's. Yam & Chapman (1968) reported three beam tests with degrees of shear connection of 43%, 60% and 80%. Stud shear failure occurred when the degree of shear connection was less than 43% and concrete crunching failure was observed for the degree of shear connection above 43%. McGarraugh & Baldwin (1971) proposed a linear interaction method to predict the moment of resistance of composite beams with partial shear connection and a minimum of 50% shear connection was suggested. Wright (1989) performed two groups of four beam tests to investigate simple supported composite beams with relatively low degrees of shear connection from 20% to 50%. Two types of simple supports were used in the tests: idealized roller support and web cleat connection. BS 5950: Part 3 (1990) gives the formulae of the plastic capacity of composite beams derived from the stress block method. The lower limit of shear connection is suggested 0.4. In this chapter the current composite beam design method of BS 5950 is introduced.

3.2 Analysis of composite beams

There are two design criteria for composite beams: elastic analysis and plastic analysis. Elastic analysis will result in larger beam size because the full plastic capacity of the section is not developed. Elastic analysis is used for serviceability analysis of composite beams, or the strength of beams subject to the effect of instability, for example, in continuous construction, or in beams where the ductility of shear connection is not adequate. Plastic analysis, however, is used in most cases.

3.2.1 Elastic analysis

For elastic analysis, the extreme fibre stresses are assumed to be not greater than the designed yield values of steel and concrete. The concrete is assumed to be uncracked under positive moment, and the concrete within troughs is neglected. This is conservative because the strength of this part of concrete is neglected. The elastic section properties can than be calculated from the transformed section as shown in Figure 3.2.

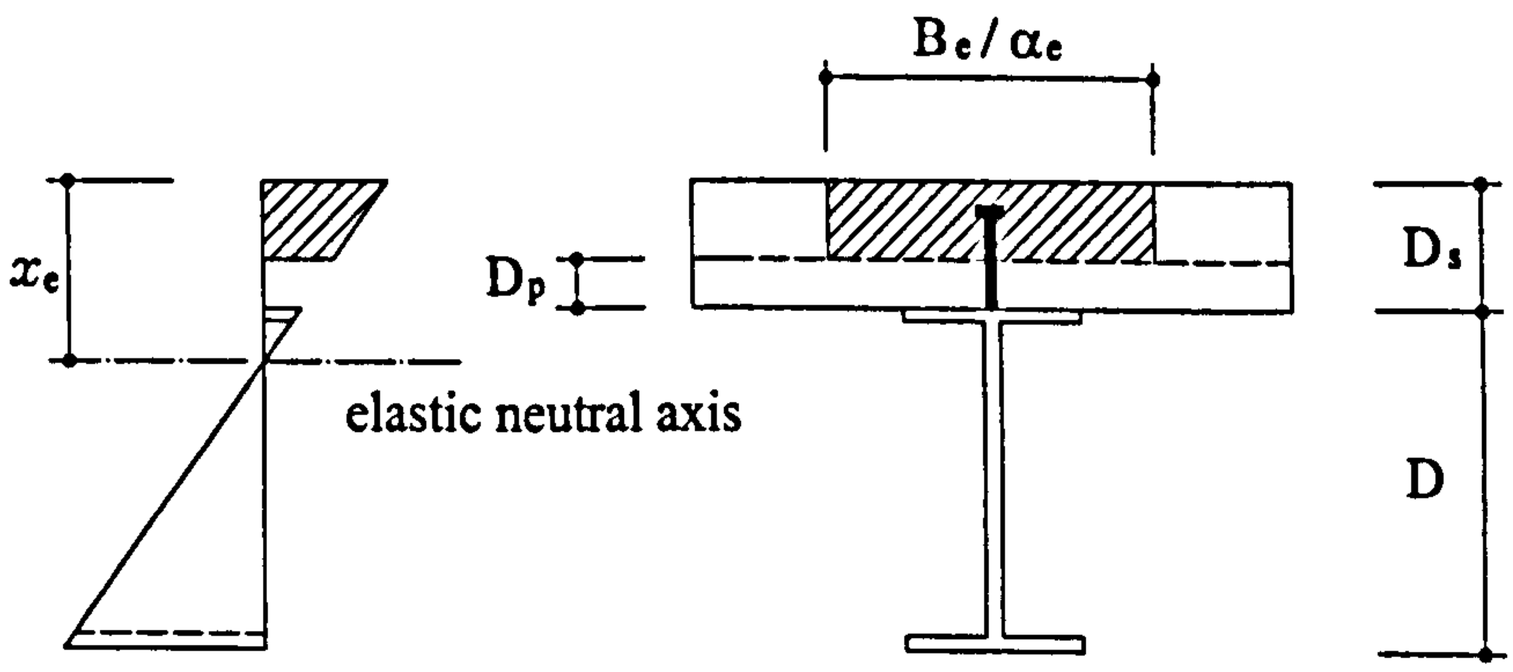

Figure 3.2 Elastic analysis of composite beam

The elastic neutral axis depth, x_e, below the upper surface of the slab is determined from the following formula:

$$x_e = \frac{\frac{D_s - D_p}{2} + \alpha_e r(\frac{D}{2} + D_s)}{1 + \alpha_e r} \tag{3.2}$$

where

$$r = \frac{A}{(D_s - D_p)B_e} \tag{3.3}$$

The second moment of area of the uncracked composite section is:

$$I_g = \frac{4(D + D_s + D_p)^2}{4(1 + \alpha_e r)} + \frac{B_e(D_s - D_p)^3}{12\alpha_e} + I_x \tag{3.4}$$

The section modulus for the steel in tension is:

$$Z_t = \frac{I_c}{D + D_s - x_e} \tag{3.5}$$

The section modulus for the concrete in compression is:

$$Z_c = \frac{I_c \alpha_e}{x_e} \tag{3.6}$$

3.2.2 Plastic analysis of composite beams with full shear connection

Tests by Slutter & Driscoll (1965) show that the full flexural capacity of the composite section may be achieved if the design is for full shear connection, the ultimate strength of a composite beam is independent of loading history and of propped or unpropped construction. For the analysis, Slutter & Driscoll (1965) used the stress block method to calculate the plastic capacity of a composite section. Two cases of plastic neutral axis (PNA) were considered: PNA in the slab and PNA in the steel beam. Lawson (1989) used the same method but three cases of plastic neutral axis were considered: PNA in the slab, PNA in the steel flange and PNA in the web. The method introduced here complies with the method proposed by BS 5950: Part 1.

The ultimate strength of a composite section is determined from its plastic capacity. It is assumed that the strains across the section are sufficiently great that the stress of the whole steel section reaches its yield value, and the concrete stress is at its design strength. The concrete is assumed to have no tensile strength. The plastic stress blocks are rectangular as shown in Figure 3.3. The stress in the steel is p_y, and $0.45f_{cu}$ in the concrete. The tensile capacity of the steel section is

$$R_s = p_y A \tag{3.7}$$

Assuming the deck perpendicular to the steel beam, the resistance of concrete in compression is

$$R_c = 0.45 f_{cu} (D_s - D_p) B_e \tag{3.8}$$

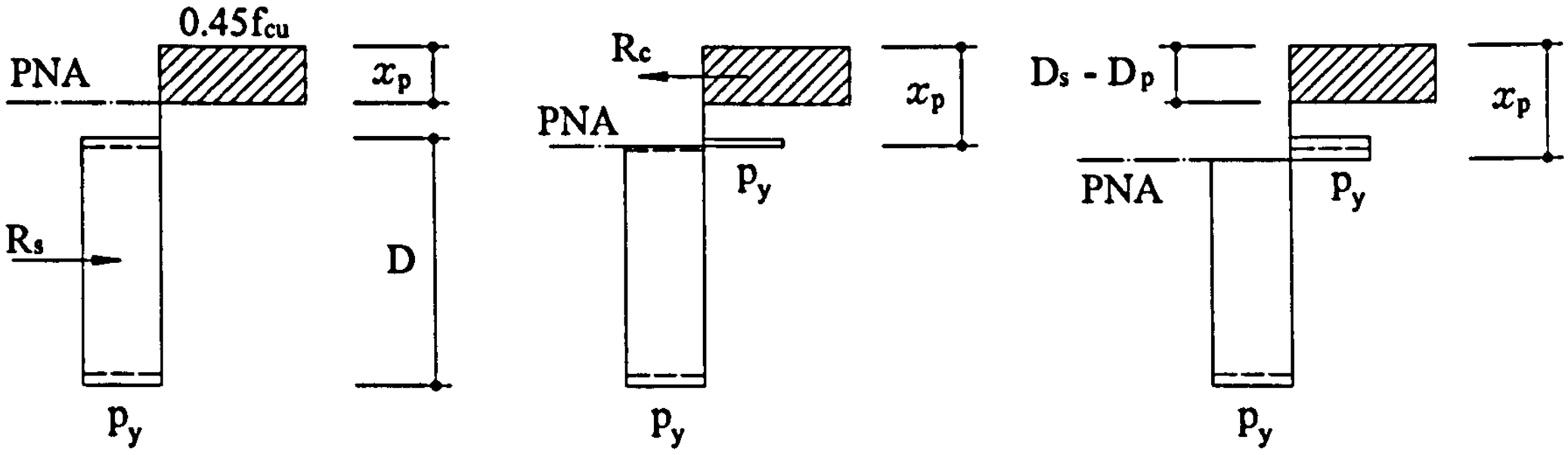

Figure 3.3 Plastic analysis of composite beam under positive bending

Three cases of neutral axis should be considered when calculating the plastic capacity of a composite section. Assuming the steel top flange is fully restrained by the concrete slab, and the web is compact, i.e. not subject to local buckling, the plastic moment capacity of a composite beam is given by:

Case 1: $R_c > R_s$ (plastic neutral axis lies in concrete slab)

$$M_{pc} = R_s[\frac{D}{2} + D_s - \frac{R_s}{R_C}(\frac{D_S - D_P}{2})] \tag{3.9}$$

Case 2: $R_s > R_c > R_w$ (plastic neutral axis lies in steel flange)

$$M_{pc} = R_s \frac{D}{2} + R_C(\frac{D_S + D_P}{2}) - \frac{(R_S - R_C)^2}{R_f}\frac{t_f}{4} \tag{3.10}$$

Case 3: $R_c < R_w$ (plastic neutral axis lies in steel web)

$$M_{pc} = M_s + R_C\left(\frac{D_S + D_P + D}{2}\right) - \frac{R_C^{\,2}}{R_w}\frac{D}{4} \qquad (3.11)$$

where M_s is the plastic capacity of the steel section alone. R_w is the plastic capacity of steel web, $R_w = p_y t_w D$.

3.2.3 Plastic analysis of composite beams with partial shear connection

For full plastic capacity of a composite section to be achieved, the total capacity of shear connectors between the points of zero and maximum moment (R_q) is greater than the smaller of R_s and R_c. If R_q is less than the smaller of R_s and R_c, the full plastic capacity of the composite section cannot develop. In such cases, the composite beam is designed with partial shear connection. The degree of shear connection is hence defined as

$$K = R_q / R_s \quad for\ R_s < R_c$$
$$\text{or} \quad K = R_q / R_c \quad for\ R_c < R_s \qquad (3.12)$$

Using the stress block method, the moment capacity of a composite beam with partial shear connection can be calculated from following equations

Case 4: $R_q > R_w$ (plastic neutral axis lies in flange)

$$M_c = R_s\frac{D}{2} + R_q[D_s - \frac{R_q}{R_c}(\frac{D_S - D_P}{2})] - \frac{(R_S - R_q)^2}{R_f}\frac{t_f}{4} \qquad (3.13)$$

Case 5: $R_q < R_w$ (plastic neutral axis lies in web)

$$M_c = M_s + R_q[\frac{D}{2} + D_s - (\frac{D_S - D_P}{2})] - \frac{R_q^{\,2}}{R_w}\frac{D}{4} \qquad (3.14)$$

An alternative approach, which mentioned before, is the linear interaction method proposed by McGarraugh & Baldwin (1971). The plastic moment capacity of composite beams with partial shear connection is given by:

$$M_c = M_s + K(M_{pc} - M_s) \tag{3.14}$$

McGarraugh & Baldwin suggested a lower limit of $K = 0.5$ for partial shear connection to avoid 'shear failure'. In Eurocode 4: Part 1.1 (1994) and BS 5950: Part 3 (1990), a lower limit of $K = 0.4$ is given. The stress block method and the linear interaction method is illustrated in Figure 3.4. It can be seen that the stress block method shows a significant benefit in the range of $K = 0.5$ to 0.7.

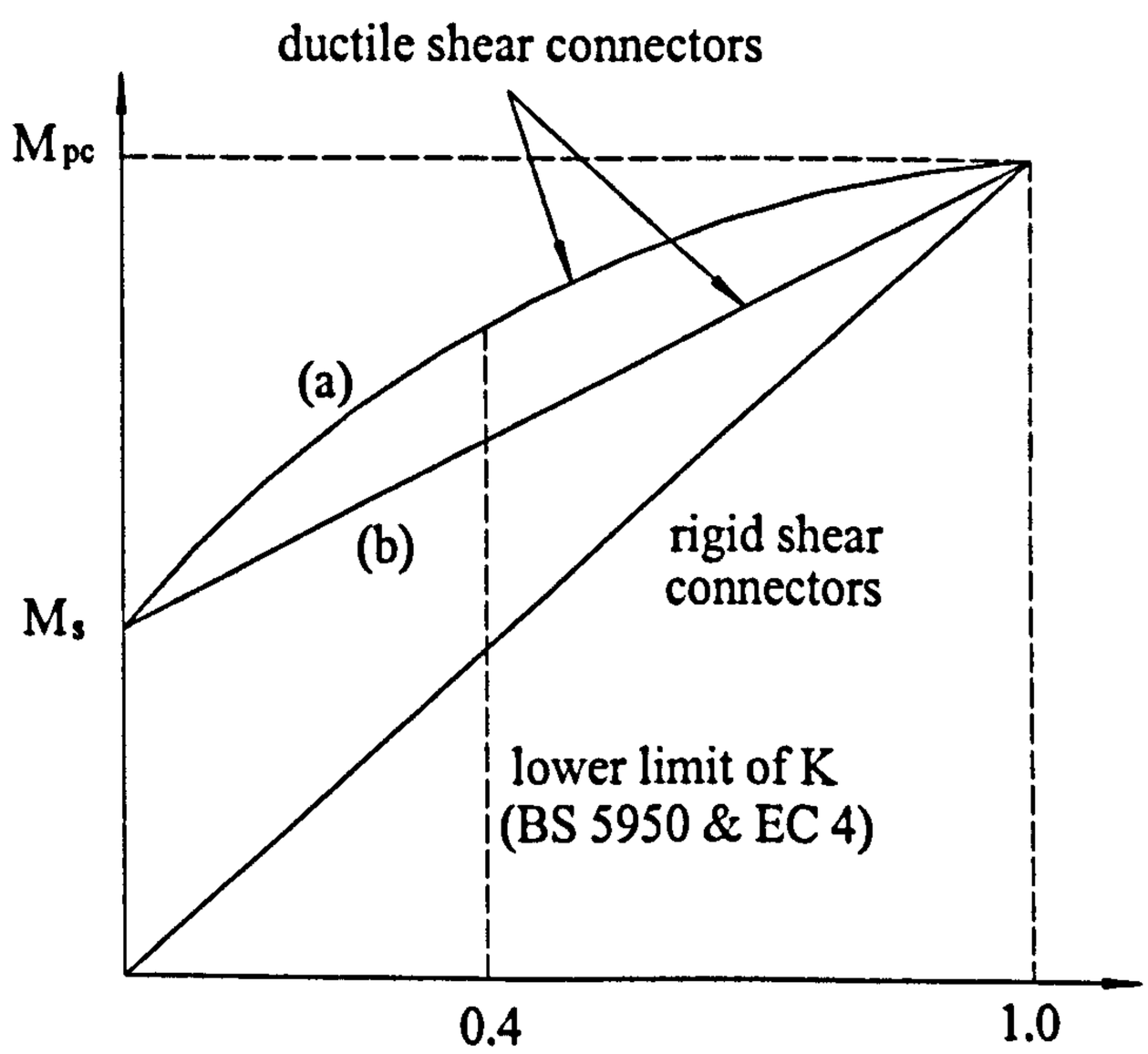

Figure 3.4 The relationship between moment capacity and degree of shear connection. (a) stress block method, (b) linear interaction method.

3.2.4 Deflections

For composite beams with full shear connection, the deflections may be calculated using the section properties from elastic analysis (see **3.2.1**). For composite beams with partial shear connection, Johnson & May (1975) argued that it was accurate enough to use linear partial –interaction theory when analysing the deflections. A non-dimension parameter $(\delta-\delta c)/(\delta_s-\delta_c)$ was used to measure the influence of the degree of shear connection. Analysis gave a curve similar to ABC in Figure 3.5. Johnson & May used a straight line DE to simplify the curve. The deflection can therefore be calculated from

$$\delta = \delta_c + \alpha(1-K)(\delta_s - \delta_c) \qquad (3.15)$$

where δ_c is the deflection of steel beam acting alone; δ_s is the deflection of composite beam with full shear connection for the same loading. For propped construction the parameter α was given as 0.5. For unpropped construction BS 5950: Part1 suggests α taken as 0.3. Hence, the deflections of composite beam with partial shear connection may be calculated from the following expressions:

For propped construction $\delta = \delta_c + 0.5(1-K)(\delta_s - \delta_c)$ (3.16a)

For unpropped construction $\delta = \delta_c + 0.3(1-K)(\delta_s - \delta_c)$ (3.16b)

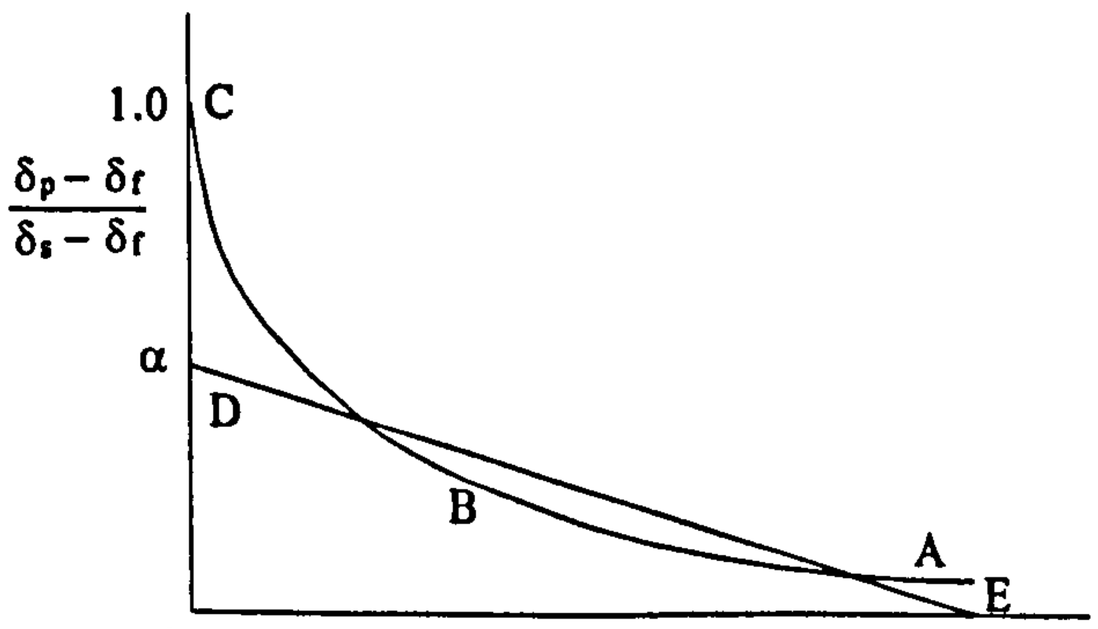

Figure 3.5 Influence of degree of shear connection on the deflection of composite beams (Johnson & May, 1975)

3.3 Analysis of continuous composite beams

A continuous composite beam is defined in Eurocode 4, Part 1.1 (1994) as 'a beam with three or more supports, in which the steel section is either continuous over internal supports or is jointed by full-strength and rigid connections, with connections between the beam and each support such that it can be assumed that the support does not transfer significant bending moment to the beam. At the internal supports the beam may have either effective reinforcement or only nominal reinforcement'. For the design of continuous composite beams both Eurocode 4, Part 1.1 (1994) and BS 5950, Part3.1 (1990) suggest that the positive moment capacity of a continuous composite beam may be determined as for a simply supported beam and the negative moment capacity may be determined as for a cantilever. In this section, the design recommendations of BS 5950, Part3.1 (1990) are introduced.

3.3.1 Effective breadth of concrete flange

According to BS 5950, Part3.1 (1990), the total effective breadth B_e of concrete flange is calculated from

$$B_e = L_z / 4 \tag{3.17}$$

Where L_z is the distance between points of zero moment. For a simply supported beam L_z is equal to the effective beam span. For an internal support of a continuous beam,

$$L_z = 0.25\ (L_1 + L_2) \tag{3.18}$$

Substitute L_z in equation (3.17) with equation (3.18), we have

$$B_e = (L_1 + L_2) / 16 \tag{3.19}$$

Where L_1 and L_2 are the effective beam spans on both sides of the support respectively. But the calculated effective breadth of concrete flange should not exceed the actual breadth of the concrete slab when the slab span is perpendicular to the beam. And the calculated B_e should not exceed 80% of actual breadth of the concrete slab when the slab span is parallel to the beam.

3.3.2 Simplified method

A simplified method is given by BS 5950, Part3.1 (1990) to calculate the moments of continuous composite beams subjected to uniformly distributed loading. Firstly the beams are assumed to be simply supported, and moments are calculated by *wL/8*, where *w* is the uniformly distributed loading. Then the moments at different locations of the continuous beam are calculated by the moment coefficients multiplied by *wL/8*. The moment coefficients are provided in Table 3 of BS 5950, Part3.1 (1990).

Table 3 of BS 5950, Part3.1 (1990)

Simplified table of moment coefficients (to be multiplied by *wL/8*)

Location	Number of spans	Classification of compression flange in negative moment region				
		Class 4 Slender	Class 3 Semi-compact	Class 2 compact	Class 1 Plastic	
					Generally	Non-reinforced (see 5.2.1.2)
Middle of end span	2	0.71	0.71	0.71	0.75	0.79
	3 or more	0.80	0.80	0.80	0.80	0.82
First internal support	2	0.91	0.81	0.71	0.61	0.50
	3 or more	0.86	0.76	0.67	0.57	0.48
Middle of internal spans	3	0.51	0.51	0.52	0.56	0.63
	4 or more	0.65	0.65	0.65	0.65	0.67
Internal supports except the first	4 or more	0.75	0.67	0.58	0.50	0.42

3.3.3 Elastic analysis

For general continuous beams analysis, the stress block method may be used in the cross section analysis. For beam sections under positive bending, the method for analyzing

simply supported composite beams described in section 3.2 can be used. For beam sections under negative bending, different design equations must be developed.

Under negative moment if the stresses of the extreme fibres of the concrete slab and the steel beam are below the design yield values, the uncracked section properties can be used in the elastic analysis. The transformed method can be used in the analysis, as shown in Figure 3.2. And the concrete slab is regarded as un-reinforced. The moments at supports can be redistributed to the mid-span and the adjacent span to maintain the equilibrium. Table 4 of BS 5950, Part3.1 (1990) gives the maximum moment redistribution percentage.

Table 4 of BS 5950, Part3.1 (1990)

Maximum redistribution of support moments for elastic global analysis, using properties of gross uncracked section

Classification of compression flange at support				
Class 4 Slender	Class 3 Semi-compact	Class 2 Compact	Class 1 Plastic	
			Generally	Non-reinforced
10%	20%	30%	40%	50%

If the stresses of the extreme fibres of the concrete slab exceed the design tensile stress, the cracked section properties must be used in the elastic analysis. The cracked region is assumed within a length of 15% of the span on each side of the support. The section properties are calculated considering the steel beam and the main reinforcement within the effective breadth of the concrete slab at the support. The second moment of area I_n of the cracked section for negative moment is given by

$$I_n = I_x + \frac{A \cdot A_r (D + D_r)_2}{4(A + A_r)} \qquad (3.20)$$

The depth y_r of the elastic neutral axis below the centroid of the reinforcement is given by

$$y_r = \frac{A(D+2D_r)}{2(A+A_r)} \tag{3.21}$$

The elastic section modulus for the stress in the reinforcement can be calculated from

$$Z_r = I_n / y_r \tag{3.22}$$

The elastic section modulus for the stress in the bottom flange of the steel beam can be calculated from

$$Z_s = I_n /(D+D_r - y_r) \tag{3.23}$$

The support moments from the analysis using the cracked section can also be redistributed. Table 6 of BS 5950, Part3.1 (1990) gives the maximum moment redistribution percentage.

Table 6 of BS 5950, Part3.1 (1990)

Maximum redistribution of support moments for elastic global analysis, using properties of cracked section

Classification of compression flange at support				
Class 4 Slender	Class 3 Semi-compact	Class 2 Compact	Class 1 Plastic	
			Generally	Non-reinforced
0%	10%	20%	30%	40%

3.3.4 Plastic analysis

The ultimate moment capacity of composite beams is obtained from the plastic analysis. The negative moment capacity of continuous beams is calculated when the reinforcement and the whole depth of the steel section reach the design yield stresses. But under negative moment, the steel bottom flange and the lower part of the web are in compression, it is possible that the capacity of the steel section may be limited by the local buckling of the web and the bottom flange. Therefore, the moment capacity of the beam should be calculated based on the effective cross section.

BS 5950, Part3.1 (1990) classified steel sections as four classes: class 1 plastic, class 2 compact, class 3 semi-compact, and class 4 slender. The classification of steel sections is given in Table 2 of the design code. When the steel section is class 1 plastic or class 2 compact, the whole steel section can be used in the plastic analysis. When the steel section is class 3 semi-compact, the effective section should be used as shown in Figure 3.6.

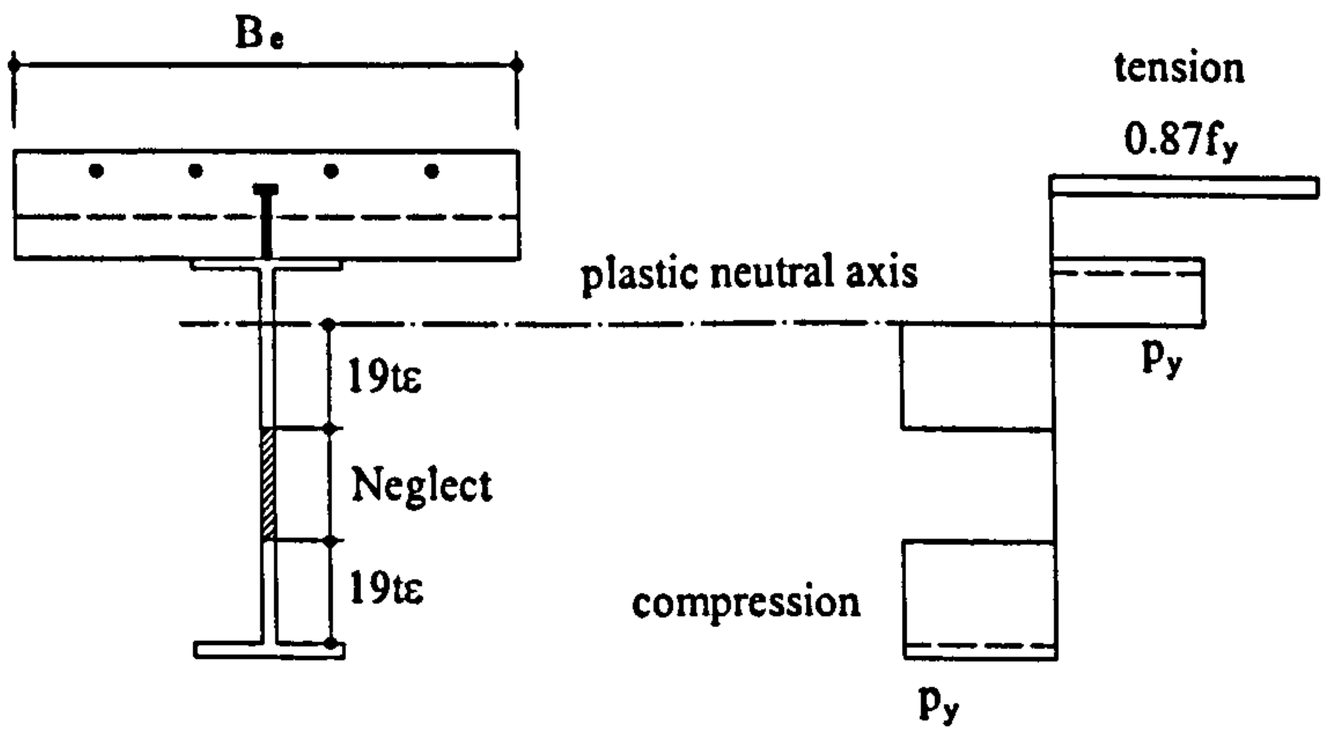

Figure 3.6 Effective section for plastic analysis

Table 2 of BS 5950, Part3.1 (1990), Limiting width to thickness ratios for webs

(Elements which exceed these limits are to be taken as class 4 slender)

Type of element	Class of section		
	Class 1 Plastic	Class 2 Compact	Class 3 Semi-compact
Web, with neutral axis at mid-depth	$\frac{d}{t} \leq 64\epsilon$	$\frac{d}{t} \leq 76\epsilon$	$\frac{d}{t} \leq 114\epsilon$
Web, generally	$\frac{d}{t} \leq \frac{64\epsilon}{1+r}$	$\frac{d}{t} \leq \frac{76\epsilon}{1+r}$	when r ≥ 0.66: for rolled sections: $\frac{d}{t} \leq \frac{114\epsilon}{1+2r}$ for welded sections: $\frac{d}{t} \leq \left(\frac{41}{r} - 13\right)\epsilon$ when $0.66 > r \geq 0$: $\frac{d}{t} \leq \frac{114\epsilon}{1+2r}$ when $r < 0$: $\frac{d}{t} \leq \frac{114\epsilon(1+r)}{(1+2r)\frac{3}{2}}$

NOTE 1 These ratios apply to the composite section. During construction the classification in BS 5950-1 applies.
NOTE 2 Check webs for shear buckling in accordance with BS 5950-1 when $d/t \geq 63\epsilon$.
NOTE 3 The values in this table do not apply to T-sections.
NOTE 4 $\epsilon = [275/p_y]^{1/2}$

3.4 Summary

The design method of simply supported composite beams with full or partial shear connections has been fully developed and can be found in current British design code BS 5950 (1990). For the design of continuous composite beams, it is assumed that the steel section is either continuous over internal supports or is jointed by full-strength and rigid connections. The internal joint moment can therefore be calculated and redistributed to the beam spans. For continuous beams with semi-rigid joints, however, the design method is not available.

Chapter 4 Finite element method and stiffness matrix method

4.1 Introduction

In this chapter, the basic concepts of the finite element method and the stiffness matrix method are presented. A finite element analysis program LUSAS 13 and a stiffness matrix analysis program QSE are introduced. In addition the procedure of seismic analysis of multi-degree of freedom systems is described.

The finite element method is a numerical procedure for solving the ordinary and partial differential equations that arise in engineering and mathematical physics (Mohr, 1992). It is the most commonly used numerical analysis method in modern engineering. The stiffness matrix method may be considered as a 'simplified' form of finite element method, which is used for the elastic analysis of frame structures.

4.2 Finite element method

Consider a general three-dimensional body subject to forces, the body will be displaced from its original configuration by an amount u, which give rise to strains ε and corresponding stresses σ. The governing equations of equilibrium may be formed by utilizing the principle of virtual work. That is, for any small, virtual displacements imposed on the body, the total internal work must equal the total external work for equilibrium to be maintained. The total potential energy of a linearly elastic solid in three-dimensional Cartesian coordinates (x, y, x) is given by

$$\Pi = \frac{1}{2}\int \{\varepsilon\}^t \{\sigma\} dV - \int \{\bar{u}\}^t \{T\} dS \tag{4.1}$$

where

$$\{\varepsilon\} = \{\varepsilon_x, \varepsilon_y, \varepsilon_z, \varepsilon_{xy}, \varepsilon_{yz}, \varepsilon_{zx}\}$$

$$\{\sigma\} = \{\sigma_x, \sigma_y, \sigma_z, \sigma_{xy}, \sigma_{yz}, \sigma_{zx}\}$$

$$\{\bar{u}\} = \{u, v, w\}$$

$$\{T\} = \{t_x, t_y, t_z\}$$

They are respectively the strains referred to the *x,y,z*-axes, the stress referred to the *x,y,z*-axes, the displacements parallel to these axes, and the surface tractions (with dimensions of force per unit area) parallel to these axes. dS and dV are infinitesimal increments of the surface area and volume of the solid. It is assumed that the stresses and strains are related by

$$\{\sigma\} = D\,\{\varepsilon\} \tag{4.2}$$

where D is the modulus matrix. In the finite element method the strain energy is computed for a number of subdomains or finite elements, and the total potential energy of the complete domain is given by summation of the element energies. In finite element analysis, the body is approximated as an assemblage of discrete elements interconnected at nodal points. The displacements within any element are thought of relatively small in relation to the complete domain. It is then assumed that the displacements can be represented with sufficient accuracy by the interpolation from the displacements at the nodal points corresponding to that element, i.e.,

$$\{\bar{u}\} = F^t\,\{d\} \tag{4.3}$$

where F is the displacement interpolation or shape function matrix and $\{d\}$ is the vector of nodal displacements of the element. The strains within an element may be related to the displacements by

$$\{\varepsilon\} = B\,\{d\} \tag{4.4}$$

where B is the strain-interpolation or strain-displacement matrix.

Once the matrices D, B and F have been defined we can determine the stresses, strains, and displacements at any point in an element. And the strain energy can then be obtained. Substitute equations (4.2), (4.3) and (4.4) into equation (4.1), we have

$$\Pi_e = \frac{1}{2}\{d\}' \int B' DBdV\{d\} - \{d\}' \int F\{T\}dS \tag{4.5}$$

Minimizing equation (4.5) with respect to each of the nodal displacements in turn, denoted as $\partial\Pi_e / \partial\{d\}$, we have

$$\frac{\partial\Pi_e}{\partial\{d\}} = \int B' DBdV\{d\} - \int F\{T\}dS = k\{d\} - \{q_t\} = \{0\} \tag{4.6}$$

where k is the element stiffness matrix and $\{q_t\}$ is the vector of consistent loads corresponding to the surface tractions. Then summing over all elements and including and loads directly applied at the nodes in a vector $\{Q_n\}$, we obtain

$$\sum k\{D\} = \sum \{q_t\} + \{Q_n\}$$

or

$$K\{D\} = \{Q_t\} + \{Q_n\} = \{Q\} \tag{4.7}$$

where K is the system stiffness matrix and $\{Q\}$ is the system load vector. Equation (4.7) is the governing equation of linear static analysis of a general three-dimensional body by finite element method.

4.3 Nonlinear analysis

Nonlinear problems related to the study of this thesis arise in the nonlinear material properties, i.e., nonlinear stress-strain relationships. With nonlinear materials Hooke's

law is no longer valid, but it is generally possible to obtain a relationship between small increments of stress and strain in the form

$$d\{\sigma\} = D_T d\{\varepsilon\} \tag{4.8}$$

where D_T is called the tangent modulus matrix. Once the appropriate relationship has been found finite element method can be used to solve such problems.

For the formulation of problems involving material nonlinear effects, the principle of virtual work may still be used, i.e.,

$$\int \{\delta\varepsilon\}^t \{\sigma\} dV - \int \{\delta\bar{u}\}^t \{T\} dS = 0 \tag{4.9}$$

Introducing the finite element interpolations, after summation and re-arranging, we get

$$\Sigma \int B^t \{\sigma\} dV = \Sigma \int F\{T\} dS = \Sigma\{q_t\} \tag{4.10}$$

On the other hand, if the system is not in equilibrium, then

$$\Sigma \int B^t \{\sigma\} dV - \Sigma\{q_t\} = \{R\} \tag{4.11}$$

where *{R}* is an out of balance force factor (the residual loads), and the matrix B and stresses $\{\sigma\}$ are nonlinear functions of the displacements and strains. Then nonlinear finite element problems can be exactly solved by evaluating $\int B^t \{\sigma\} dV$, the element reactions, at each step of an iterative procedure until the residual loads *{R}* vanish and equation (4.10) is satisfied. This process is called equilibrium iteration.

Take Newton's method (Mohr, 1992) for example, the total load is first applied and an initial solution $\{D\}_1 = K_0^{-1}\{Q\}$ obtained. Then equation (4.11) is used to calculate the residual loads *{R}*. Corrections of the solution are calculated iteratively from

$$\{D\}_{i+1} = \{D\}_i + K_T^{-1}\{R\} \tag{4.12}$$

where K_T and *{R}* are calculated using the displacement $\{D\}_i$. The iteration finishes until convergence is obtained. This procedure is employed in the LUSAS program.

4.4 LUSAS program

LUSAS is a finite element analysis software capable of solving all types of linear and nonlinear stress, dynamics, composite and thermal engineering analysis problems. It is developed by Finite Element Analysis (FEA) Ltd., UK. The present version of LUSAS Modeller is version 13.3-2 released in November 2000. Three types of elements are used in the nonlinear analysis of composite structures described in this thesis: 3D bar element, 3D nonlinear thick beam element, and 3D nonlinear thick beam element with quadrilateral cross-section.

4.4.1 3D bar element

This is an isotropic three-dimensional bar element provided by LUSAS Modeller as shown in Figure 4.1. It can be straight (named as BRS2) or curved (named as BRS3), and can accommodate varying cross section area. Two nodes are required for BRS2 and three nodes are required for BRS3. Each node has three degrees of freedom: *u*, *v*, and *w*. The required geometric properties are the cross section area at each node. For nonlinear analysis a strain hardening curve can be input.

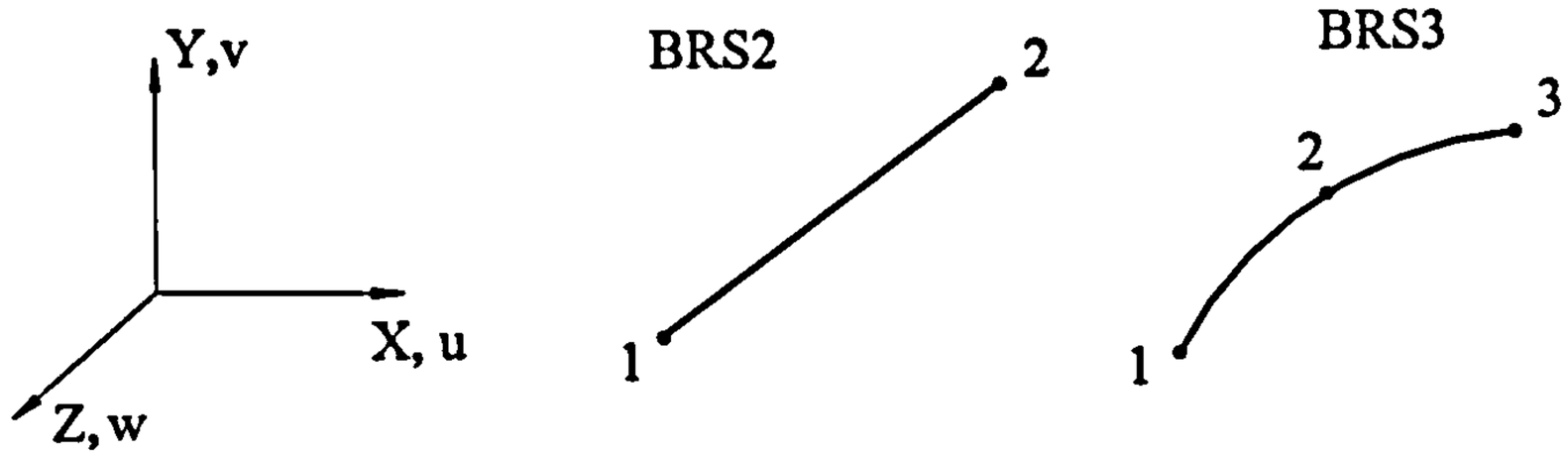

Figure 4.1 3D bar element

4.4.2 3D nonlinear thick beam element

This is a straight beam element in 3D for which shear deformations are included (Figure 4.2). The geometric properties are constant along the length. Three nodes are needed to define the beam. The third node is used to define the local *xy*-plane. There are six degrees of freedom at each node. They are: u, v, w, θ_x, θ_y, θ_z. For plastic material properties, two options are available: circular hollow section and rectangular solid section. Universal beams and columns with I-section are considered as rectangular solid section group.

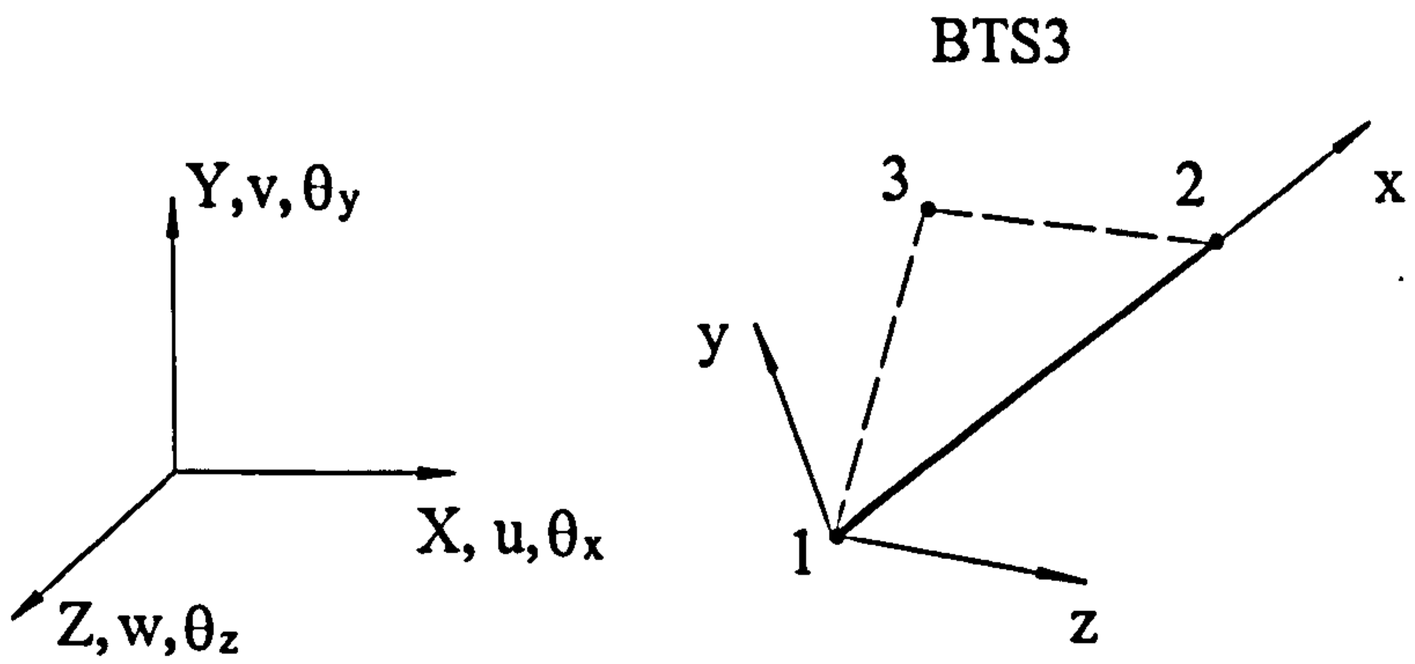

Figure 4.2 3D nonlinear thick beam element

4.4.3 3D nonlinear thick beam element with quadrilateral cross-section

The properties of this element are mostly the same as the 3D nonlinear thick beam element except that the geometric properties are different. This is also a straight beam element in 3D for which shear deformations are included (Figure 4.3). The element has a cross-section which is constant along the length. Three nodes are needed to define the beam. The third node is used to define the local *xy*-plane. There are six degrees of freedom at each node. They are: u, v, w, θ_x, θ_y, θ_z. In order to define the geometric properties, the local coordinate pairs at each corner of the cross section are required (Figure 4.3b). The coordinates of the cross section are numbered clockwise around the local *x*-axis (the beam nodal line). For plastic material properties, two options are available: circular hollow section and rectangular solid section. The proper choice should be rectangular solid section for this type of element.

BTX3

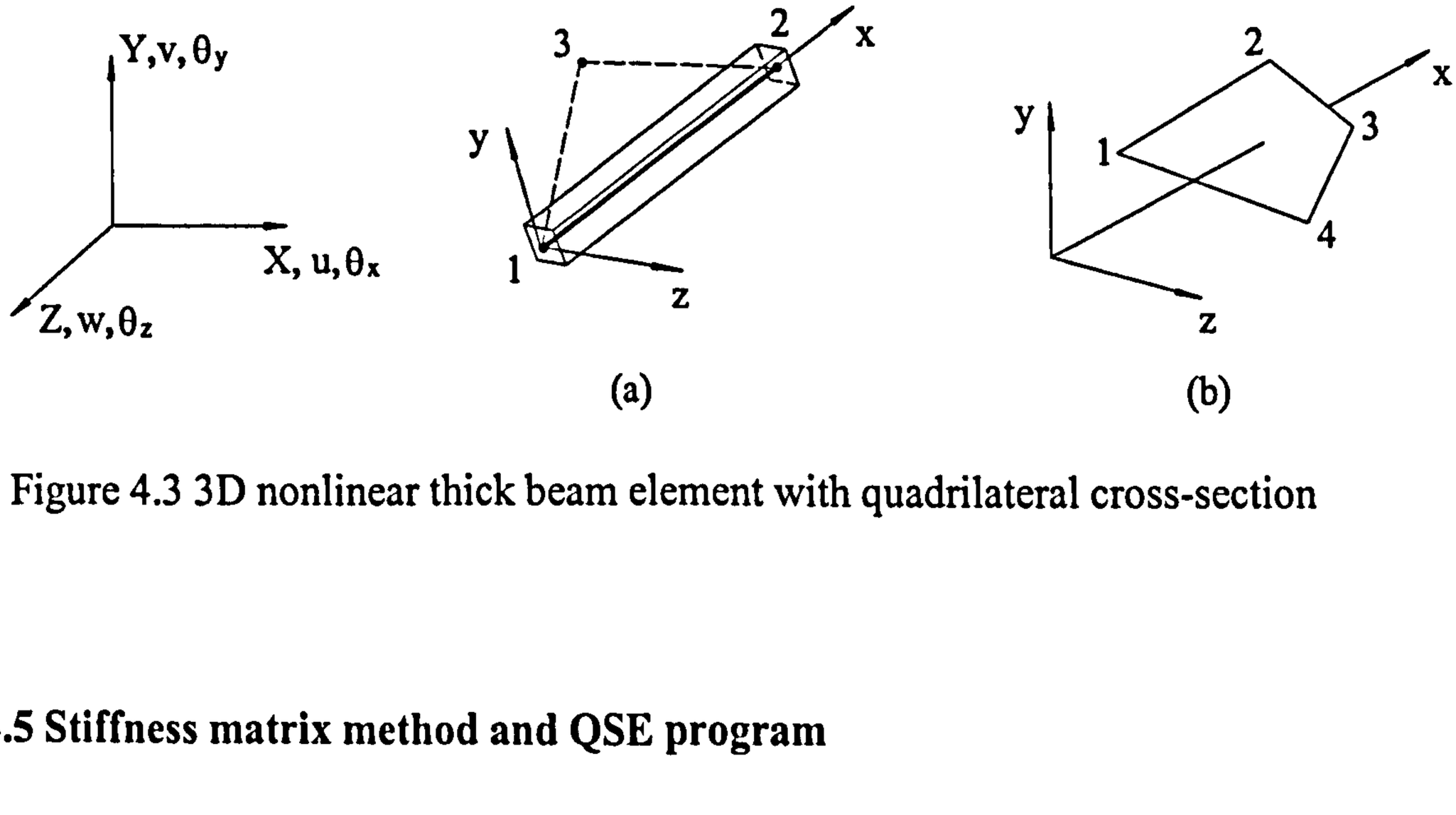

Figure 4.3 3D nonlinear thick beam element with quadrilateral cross-section

4.5 Stiffness matrix method and QSE program

4.5.1 Stiffness matrix method

The stiffness matrix method is used for elastic analysis of frame structures composed of only beam elements. It may be regard as a simplified form of finite element method. The

governing equation of finite element analysis $K\{D\}=\{Q\}$ still applies to stiffness matrix method. In stead of using the principle of virtual work, the stiffness matrix of a beam element may be obtained through the analysis of the differential equation of the beam. Summing the matrices of all beam elements corresponding to the node numbers, the stiffness matrix for the whole system can be formed. And then the unknown nodal freedoms or the displacements can be found by standard matrix solution techniques.

Take the example of a two-dimensional beam as shown in Figure 4.4, the differential equation governing the shape of the neutral axis of a bent beam is

$$\frac{EId^4v}{dx^4} = p(x) \tag{4.13}$$

where v is the transverse deflection of the beam and $p(x)$ is the intensity of distributed loading upon the beam.

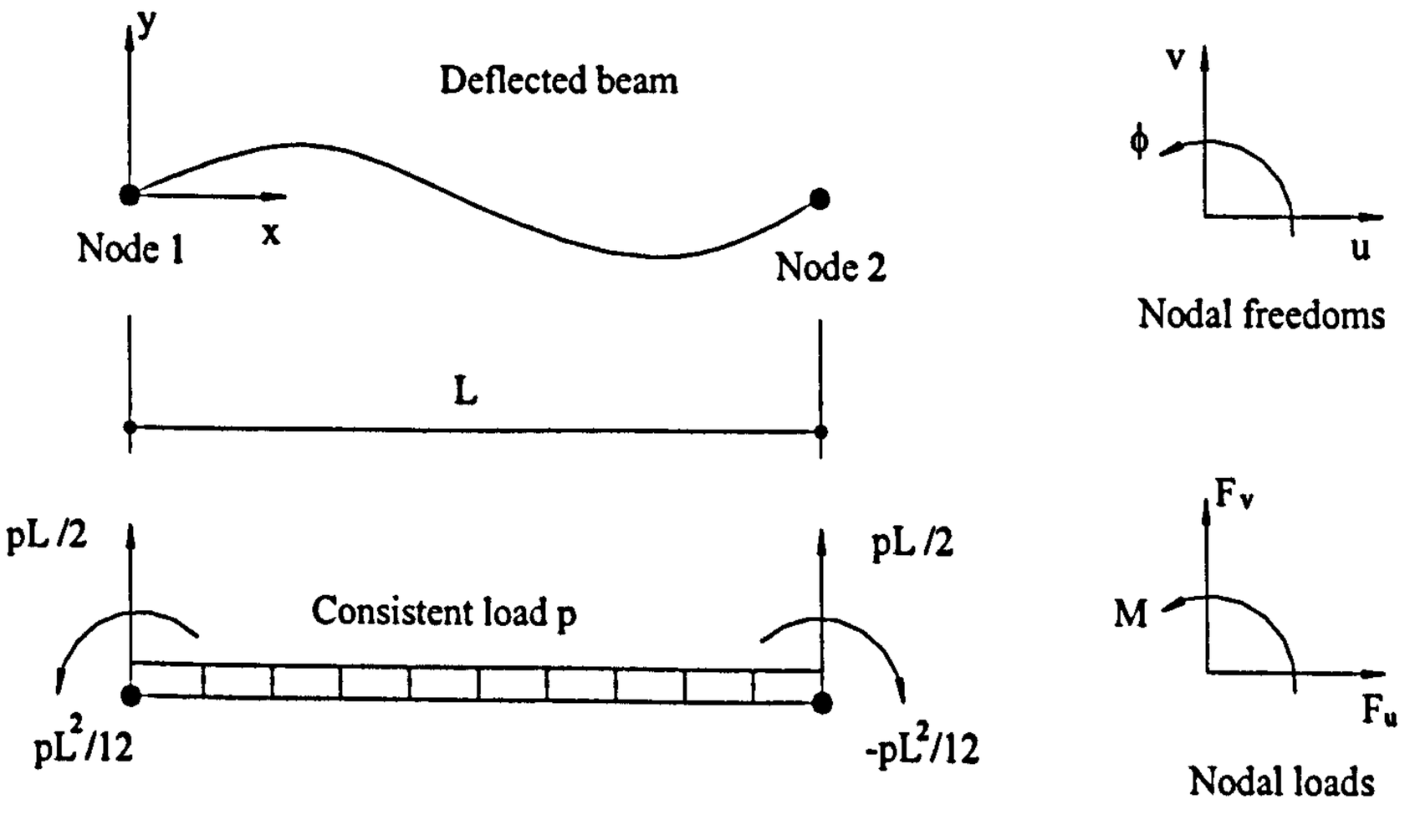

Figure 4.4 A two-dimensional beam element

There are three freedoms at each node: u, v, and ϕ. Assuming the internal loading is uniformly distributed, i.e., $p(x)=p$, equation (4.13) can be integrated four times with respect to the coordinate x, yielding the four equations

$$\frac{EId^3v}{dx^3} = px + c_1 \tag{4.14a}$$

$$\frac{EId^2v}{dx^2} = \frac{px^2}{2} + c_1x + c_2 \tag{4.14b}$$

$$\frac{EIdv}{dx} = \frac{px^3}{6} + \frac{c_1x^2}{2} + c_2x + c_3 \tag{4.14c}$$

$$EIv = \frac{px^4}{24} + \frac{c_1x^3}{6} + \frac{c_2x^2}{2} + c_3x + c_4 \tag{4.14d}$$

Put $x=0$ in equations (4.14c) and (4.14d), we get $c_3=EI\phi_1$ and $c_4=EIv_1$. And put $x=L$, we get

$$EI\phi_2 = \frac{pL^3}{6} + \frac{c_1L^2}{2} + c_2L + EI\phi_1 \tag{4.15}$$

$$EIv_2 = \frac{pL^4}{24} + \frac{c_1L^3}{6} + \frac{c_2L^2}{2} + EIL\phi_1 + EIv_2 \tag{4.16}$$

c_1 and c_2 can then be solved. Let $x=0$ and $x=L$ in equations (4.14a) and (4.14b) respectively, the shear forces and moments at both nodes of the beam element can be obtained. Writing the results in matrix form, we have

$$\begin{Bmatrix} F_{v1} + pl/2 \\ M_1 + pl^2/12 \\ F_{v2} + pl/2 \\ M_2 - pl^2/12 \end{Bmatrix} = \frac{EI}{L^3} \begin{bmatrix} 12 & 6L & -12 & 6L \\ 6L & 4L^2 & -6L & 2L^2 \\ -12 & -6L & 12 & -6L \\ 6L & 2L^2 & -6L & 4L^2 \end{bmatrix} \begin{Bmatrix} v_1 \\ \phi_1 \\ v_2 \\ \phi_2 \end{Bmatrix} \tag{4.17}$$

The axial force in the beam may be written as

$$T = \sigma A = EA\varepsilon = \frac{EA\delta L}{L} = \frac{EA(u_2 - u_1)}{L} \tag{4.18}$$

Hence the axial forces at both nodes can be obtained: $F_{u1}=T$ and $F_{u2}=-T$. Combining them with equation (4.17), the element stiffness matrix for a six-freedom beam is

$$\begin{bmatrix} F_{u1} \\ F_{v1} \\ M_1 \\ F_{u2} \\ F_{v2} \\ M_2 \end{bmatrix} + \begin{bmatrix} 0 \\ pL/2 \\ pL^2/12 \\ 0 \\ pL/2 \\ -pL^2/12 \end{bmatrix} = \begin{bmatrix} k_1 & 0 & 0 & -k_1 & 0 & 0 \\ 0 & k_2 & k_3 & 0 & -k_2 & k_3 \\ 0 & k_3 & k_4 & 0 & -k_3 & k_5 \\ -k_1 & 0 & 0 & k_1 & 0 & 0 \\ 0 & -k_2 & -k_3 & 0 & k_2 & -k_3 \\ 0 & k_3 & k_5 & 0 & -k_3 & k_4 \end{bmatrix} \begin{bmatrix} u_1 \\ v_1 \\ \phi_1 \\ u_2 \\ v_2 \\ \phi_2 \end{bmatrix}$$

or

$$\{q_r\} + \{q_l\} = k\{d\} \tag{4.19}$$

where $k_1=EA/L$, $k_2=12EI/L^3$, $k_3=6EI/L^2$, $k_4=4EI/L$, *and* $k_5=2EI/L$. The vector $\{q_l\}$ contains the consistent loads corresponding to the uniformly distributed load p. And the vector $\{q_r\}$ contains the interelement reactions. In element assembly process these forces and moments must cancel between elements, i.e. $\Sigma\{q_r\}=\{0\}$. Therefore we have

$$\{Q\} = \Sigma\{q_r\} + \Sigma\{q_l\} = \Sigma\{q_l\} \tag{4.20}$$

Note all forces applied to the whole structure should be included in the load vector $\{Q\}$. After assembling all the element stiffness matrices, the same form of equation as equation (4.7) can be obtained.

4.5.2 QSE program

QSE Space is a 2D and 3D frame analysis program. The analysis is performed using the stiffness matrix method based on the elastic behaviour of the structure. It is assumed that the displacements of beams do not affect the geometry of the structure. This is to ensure that the non-linearity due to large displacements would not happen. Elements are assumed to be long compared to their cross sections, hence deflection due to shear forces is ignored. Secondary factors such as buckling are also ignored.

4.6 Dynamic analysis

There are basically two approaches for predicting the dynamic response of structures: time domain method and frequency domain method. The time domain method is used to construct time histories of such variables as forces, moments and displacements by calculating the response at the end of a succession of very small time steps. It can be used to calculate the dynamic response of both linear and nonlinear structures and requires that time histories for the dynamic forces be available or can be generated. The frequency domain method is used to predict the maximum value of the same quantities by adding the response in each mode in which the structure vibrates. It is limited to linear structures, since the natural frequencies of nonlinear structures vary with the amplitude of response. Despite its limitations, frequency domain analysis is commonly used by engineers because it permits the use of response spectra which are more easily available than time histories. In Chapter 8 of this thesis, the frequent domain method is used in the earthquake analysis of sample frames with the response spectra recommended by current design code. In this section of the thesis, the theory of frequency domain analysis is described.

4.6.1 Eigenvalue analysis

In general structures have an infinite number of degrees of freedom (DOF). By replacing the distributed mass of structures with an equivalent system of lumped masses, and assuming the elastic member to be weightless, the structure can be approximated to N DOF systems. This lumped mass idealization provides a simple means of limiting the number of DOF that must be considered in a dynamic analysis.

The equations of dynamic equilibrium of an N DOF system can be written in matrix form as:

$$M \cdot \ddot{x} + C \cdot \dot{x} + K \cdot x = P(t) \tag{4.21}$$

For natural frequency analysis, the damping matrix and the external force vector are both zero. And each freedom is assumed to excite harmonic motion in phase with all other freedoms, which may be expressed as

$$x(t) = x \sin(\omega t + \theta) \tag{4.22}$$

and the second time derivative of equation (4.22) gives the acceleration as

$$\ddot{x} = -\omega^2 x \sin(\omega t + \theta) \tag{4.23}$$

Substituting equations (4.22) and (4.23) into equation (4.21), yields

$$(K - \omega^2 M)x = 0 \tag{4.24}$$

This is equivalent to a generalised eigenvalue problem. The quantities of ω^2 are the eigenvalues or characteristic values indicating the square of the free-vibration

frequencies, while the corresponding displacement vectors x express the corresponding eigenvectors or mode shapes.

4.6.2 Response spectra

A response spectrum is a curve that shows how the maximum response, velocity or acceleration of oscillators with the same damping ratio, but with different natural frequencies, responds to a specific earthquake (Buchholdt, 1997). Considering a one DOF system subjected to a ground acceleration $\ddot{x}_g(t)$, the equation of motion can be written as

$$M \cdot \ddot{x} + C \cdot \dot{x} + K \cdot x = M \cdot \ddot{x}_g(t) \qquad (4.25)$$

By calculating the maximum response of oscillators with different frequencies, but with the same damping, it is possible to construct a response spectrum in the frequency domain for oscillators with the same damping ratio. By repeating the process for oscillators with different damping ratios, it is possible to construct a number of response spectra for the same record.

Since the obtained response spectra are usually raw, they need to be smoothened for design purpose. And in design it is usual to employ consolidated response spectra normalized to a peak acceleration of 1.0g with corresponding maximum values for ground displacement and velocity. Such design response spectrum is recommended in Eurocode 8, Part 1.1 (1994).

4.6.3 Seismic analysis using response spectra

For a linear multi-degree of freedom system subjected to a support motion $x_g(t) = x_g$ with acceleration $\alpha\ddot{x}_g(t)$, the general form for the equation of motion is

$$M \cdot \ddot{x} + C \cdot \dot{x} + K \cdot x = M \cdot \alpha \ddot{x}_g(t) \tag{4.26}$$

Let

$$\begin{aligned} x &= Zq \\ \dot{x} &= Z\dot{q} \\ \ddot{x} &= Z\ddot{q} \end{aligned} \tag{4.27}$$

where

$$Z = [Z_1, Z_2, \ldots, Z_I, \ldots, Z_N]$$

is the normalized modeshape matrix associated with equation (4.26). Substitute equation (4.27) into (4.26) and postmultiplication of each term in the equation by Z^T yield

$$Z^T M Z\ddot{q} + Z^T C Z\dot{q} + Z^T K Z q = Z^T M \alpha \ddot{x}_g(t) \tag{4.28}$$

From the orthogonal properties of normalized eigenvectors, we have

$$\begin{aligned} Z^T M Z &= I \\ Z^T C Z &= 2\xi\omega \\ Z^T K Z &= \omega^2 \end{aligned} \tag{4.29}$$

Substitute these expressions for the matrix products into equation (4.28) will uncouple the equations of motion and yield

$$\ddot{q} + 2\xi\omega\dot{q} + \omega^2 q = Z^T M \alpha \ddot{x}_g(t) \tag{4.30}$$

where $2\xi\omega$ and ω^2 are diagonal matrices. Equation (4.30) may also be written as

$$\ddot{q}_1 + 2\xi_1\omega_1\dot{q}_1 + \omega_1^2 q_1 = Z_1^T M \alpha \ddot{x}_g(t)$$

$$\ddot{q}_2 + 2\xi_2\omega_2\dot{q}_2 + \omega_2^2 q_2 = Z_2^T M \alpha \ddot{x}_g(t)$$

.....

.....

$$\ddot{q}_i + 2\xi_i\omega_i\dot{q}_i + \omega_i^2 q_i = Z_i^T M\alpha\ddot{x}_g(t) \tag{4.31}$$

.....

.....

$$\ddot{q}_N + 2\xi_N\omega_N\dot{q}_N + \omega_N^2 q_N = Z_N^T M\alpha\ddot{x}_g(t)$$

where the product $Z_i^T M$ is referred to as the i-th participation vector. Since the mass in each of the above equivalent one DOF systems is unity, it follows that the equivalent ground acceleration in the generalized coordinate system is $\ddot{q}_{g_i}(t) = Z_i^T M\alpha\ddot{x}_g(t)$. The maximum value of $\ddot{q}_{g_i}(t)$ occurs when $\ddot{x}_g(t)$ is equal to 1.0g, i.e.,

$$\ddot{q}_{g_i,\max} = Z_i^T M\alpha g \tag{4.32}$$

From a response spectrum based on a damping ratio, the response $\tilde{q}_{i,\max}$ corresponding to the frequency ω_i can be obtained. And the maximum response of the system can therefore be found. As the response spectrum is normalized to a peak acceleration of 1.0g, it follows that

$$q_{i,\max} = Z_i^T M\alpha\tilde{q}_{i,\max} \tag{4.33}$$

Thus

$$q_{\max} = Z_i^T M\alpha\tilde{q}_{\max} \tag{4.34}$$

And therefore

$$x_{\max} = Zq_{\max} = ZZ_i^T M\alpha\tilde{q}_{\max} \tag{4.35}$$

This procedure assumes that the maximum response in each of the modes will occur simultaneously and relative to each other as in the modeshape matrix. Since this is highly unlikely to occur, for design purpose each element in the maximum response vector x_{max} is modified as the square root of the sum of the squares of the contribution from each mode, i.e.,

$$x_r = \{(Z_{r1}\, q_1)^2 + (Z_{r2}\, q_2)^2 + \ldots + (Z_{rN}\, q_N)^2\}^{1/2} \tag{4.36}$$

or

$$x_r = \sqrt{\left[\sum_{i=1}^{N} (Z_{ri} q_i)^2\right]} \tag{4.37}$$

4.7 Summary

In this chapter, a two-dimensional beam is used as an example to explain the formation of the stiffness matrix and the procedure of the finite element analysis. The LUSAS analysis program and the QSE program are briefly introduced. The basic concept of the Eigenvalue analysis are introduced and the procedure of the seismic analysis using response spectra is described for the future dynamic analysis of composite frames.

Chapter 5 Modelling of composite semi-rigid connections

5.1 Introduction

Studies of the global performance under static loading of steel framed structures date back to as early as the 1920's. With the introduction of computer technology in the late 1960's, much progress has been made in various aspects of the overall response of steel frames. And various approaches are possible in frame analysis. The effects of semi-rigid and partial strength connections have been investigated since the 1980's. The study of steel-concrete composite structure began in late 1950's as reported by Johnson (1975). The study of the behaviour of composite frames with semi-rigid beam-to-column connections remains a vibrant research topic.

In the modelling of semi-rigid composite frames, the first problem is to establish an effective composite beam-to-column joint model. Eurocode3 Part1.1 suggests 'a rotational spring model' which resides between the centreline of the column and the connected beam at the point of interaction. This spring model has been generally accepted in the analysis of steel frames with semi-rigid joints in recent years.

5.1.1 Fang et al. (1999)

Composite joints were modelled as spring elements by Fang et al. (1999) in their finite elements analysis of composite frames. A 'curve-fitting' method was used to model the nonlinear behaviour of composite joints. In view of the plastic plateau in the M-ϕ curve of composite connections under hogging moments, the simple form of exponential expression proposed by Shi et al. (1996) was used.

$$|M_c| = |M_{cu}|(1 - e^{-\alpha\phi}) \tag{5.1}$$

where M_c is the moment at rotation ϕ and M_{cu} is the ultimate moment of resistance. This formula can accurately simulate the M-ϕ characteristics of a composite connection, but test data are required to determine the parameters M_{cu} and α for curve-fitting. This may not be available for certain types of joints due to limited tests on composite connections. To overcome this, Fang et al. proposed a method to calculate M_{cu} and α based on the spring model of composite connections proposed by Anderson & Najafi (1994).

For composite joints under a sagging moment, due to the uncertainty on the contact between concrete slab and column flange and lack of experiment data, three M-ϕ models were proposed. The first model, termed as model 'A', takes the same form as equation (5.1). In the second model, model 'B', a lower value of ultimate moment of resistance is assumed, i.e.,

$$|M_c| = 0.66|M_{cu}|(1-e^{-1.5\alpha|\phi|}) \tag{5.2}$$

The third model 'C' is a simple linear model, i.e.,

$$|M_c| = \alpha|M_{cu}\phi| \tag{5.3}$$

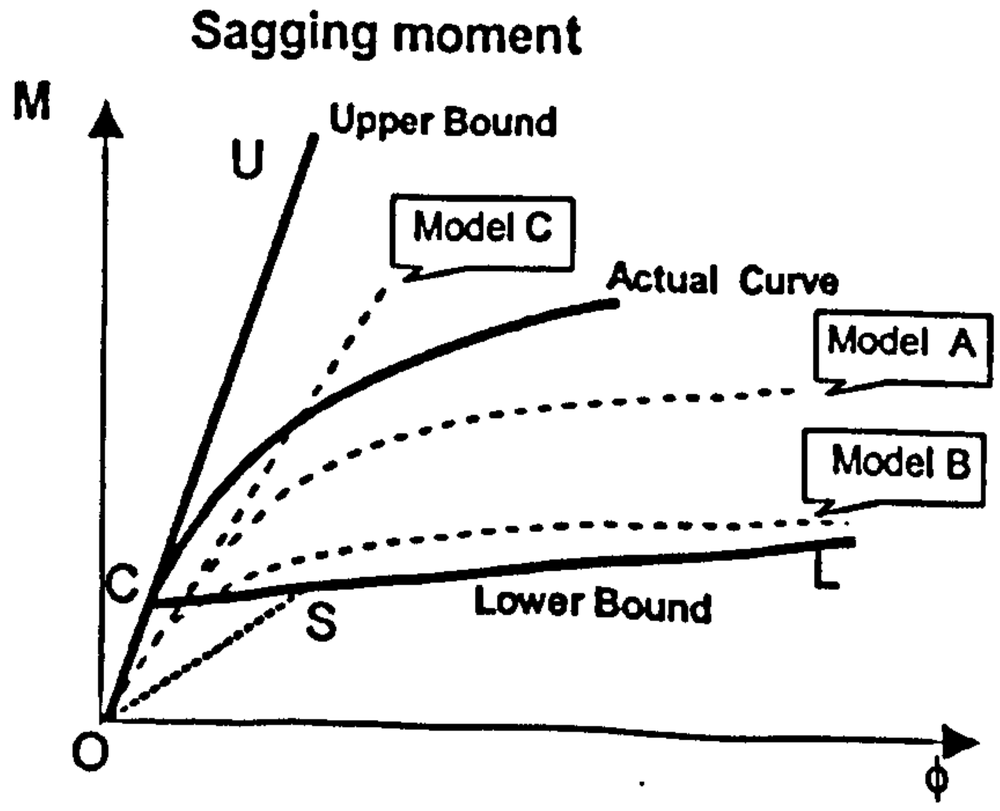

Figure 5.1 Moment-rotation relationship of composite joint in sagging moments proposed by Fang et al. (1999)

The advantage of this semi-empirical joint model proposed by Fang et al. (1999) is that the nonlinear behaviour of composite joints can be simulated both under positive bending and negative bending with sufficient accuracy. The disadvantage is that the model relies on test data of the steel joint.

5.1.2 Dissanayake et al. (2000)

Dissanayake et al. (2000) proposed a composite beam model with semi-rigid joints for the nonlinear analysis of composite frames. The beam model contains two parts: a composite beam element allowing for partial shear interaction, and a macro composite joint element as shown in Figure 5.2. The composite beam element used the same element proposed by Oven et al. (1997). And the proposed macro joint model contains three elements. A two-noded spring element of zero length with six degrees of freedom is used to model the semi-rigid behaviour of the steelwork connection. A stiff beam element is used to model the column web. The reinforced concrete slab is modelled as an ordinary beam element. And it is connected to the stiff beam element with very low translation interaction to allow for the continuity of the concrete slab over the support.

The modelling of edge connections depends on the detailing of the slab reinforcement at the edge columns. A fully connected arrangement is shown in Figure 5.2 (a). However, it is not always practical to achieve sufficient anchorage for slab reinforcement. In such cases, it is suggested that for a conservative modelling only the steel-to-steel connection be used at edge columns.

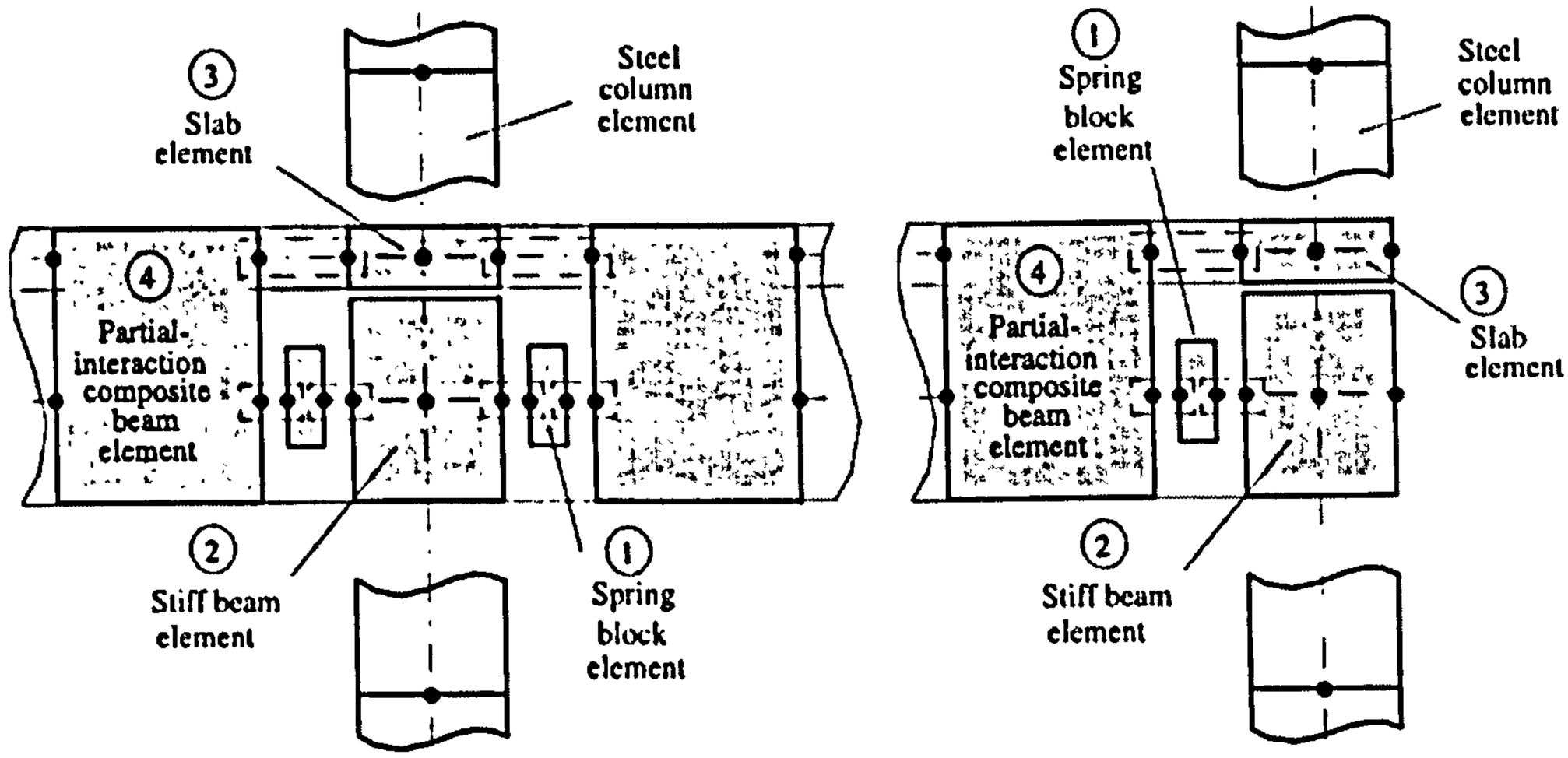

(a) Macro-element model

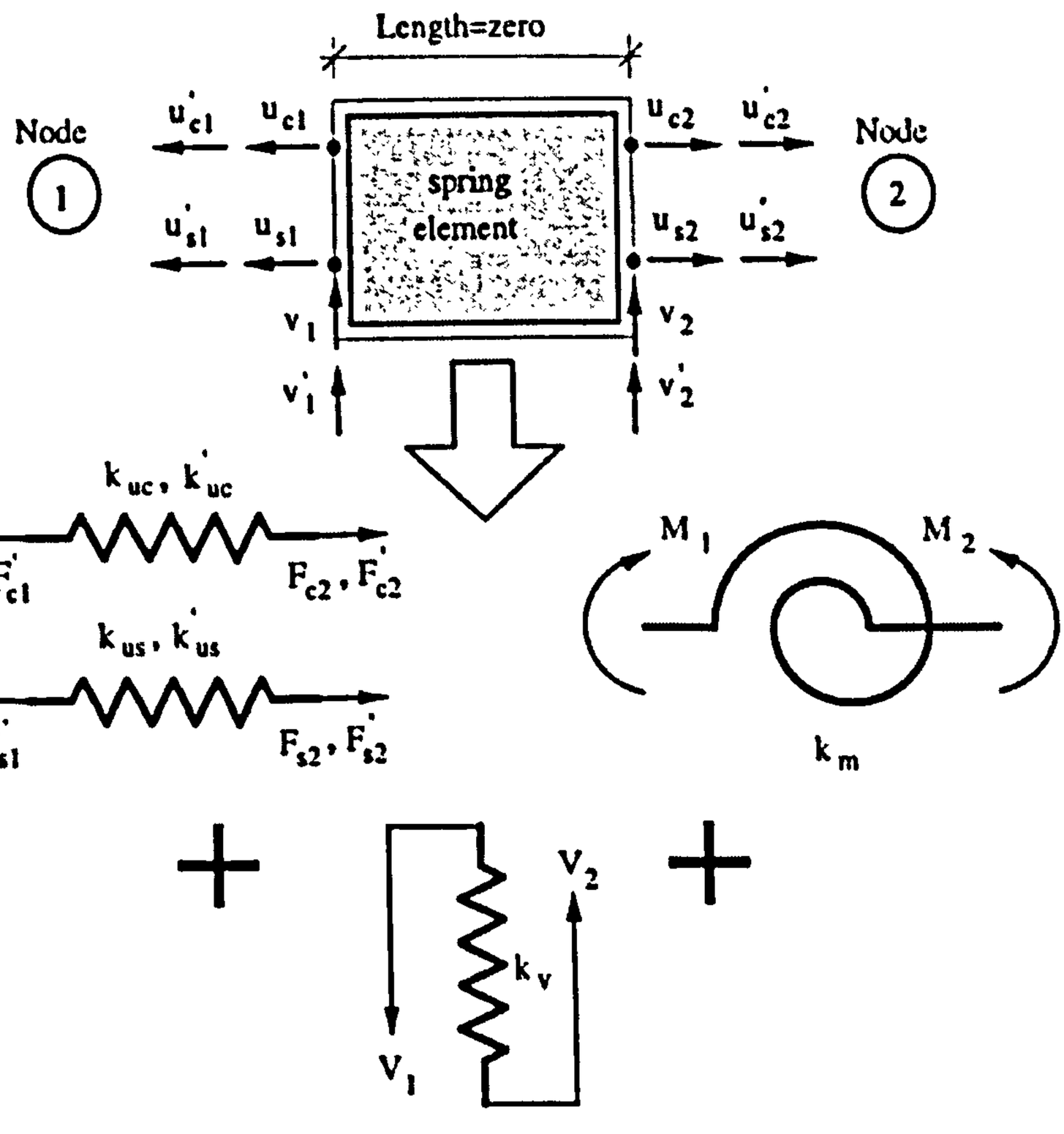

(b) Degrees of freedom of the spring element

Figure 5.2 Composite joint model proposed by Dissanayake et al. (2000)

5.1.3 Kattner & Crisinel (2000)

In 1993 a research project with the object to study theoretically and experimentally the behaviour of composite semirigid beam-to-column connections was started at the Institute ICOM-Steel Structures at the Swiss Federal Institute of Technology Lausanne (EPFL). A numerical model to analyse non-linear composite joints was developed and integrated in a composite beam analysis program in 1996. Based on previous research, Kattner & Crisinel (2000) proposed a refined and more efficient finite element model of composite joints.

A general two-dimensional composite joint model is shown in Figure 5.3. In the model, the steel beam and concrete slab are modelled as beam elements, located at the same geometric level as the steel-concrete interface. The element axes do not coincide with the geometric center of the steel beam and concrete slab cross sections. Hence an eccentricity is defined for each section. The steel beam and concrete slab elements are connected by horizontal translational springs representing the shear connectors. Empirical load-slip relationships from known push-out tests are assigned to those springs.

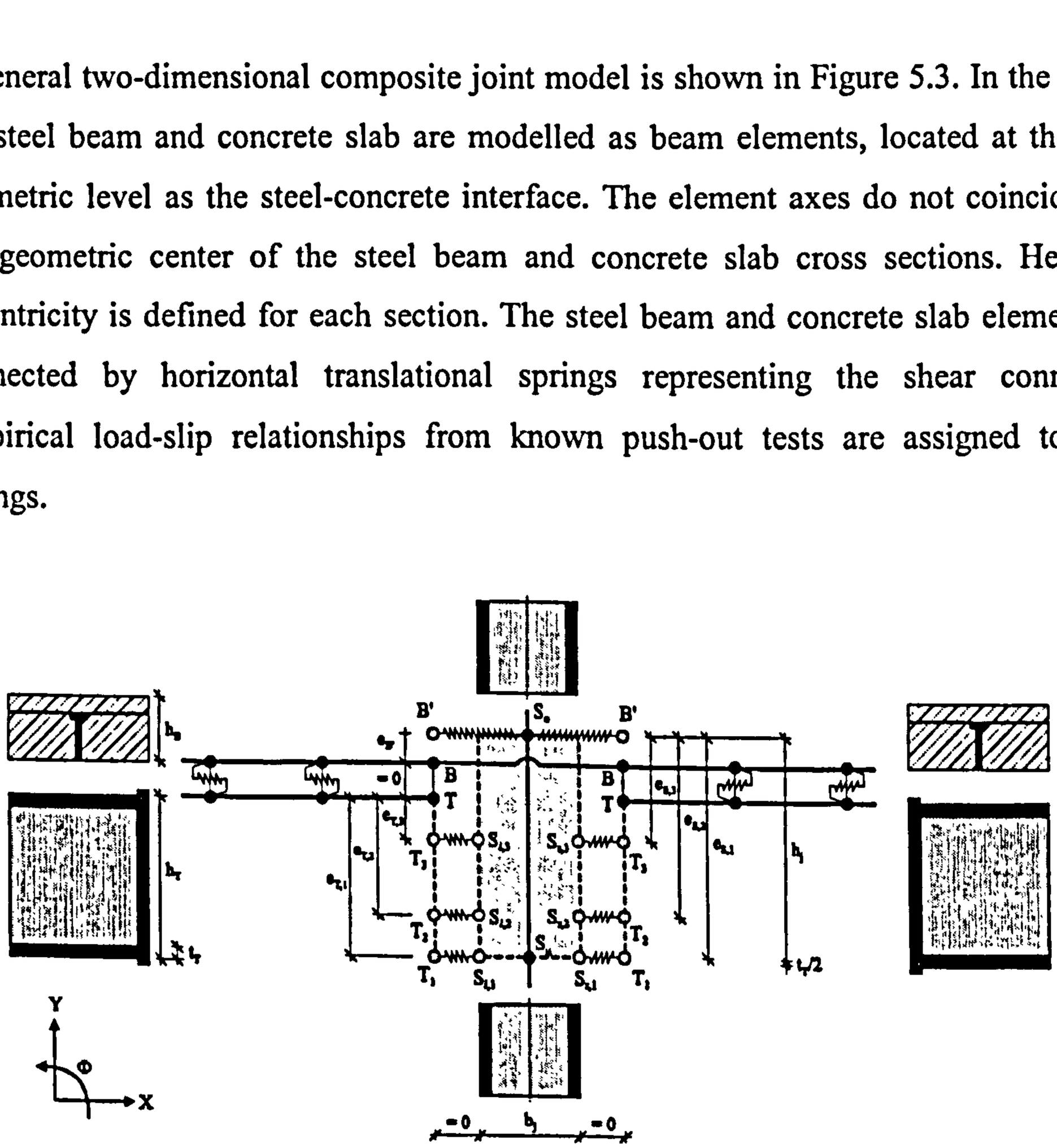

Figure 5.3 Composite joint model of Kattner & Crisinel (2000)

The steel connection is modelled as translational spring elements. The number and geometric positions of the translational springs depend on the type of the steel connection. For a joint with flush endplate connection in Figure 5.3, four translational springs are needed representing the following: lower beam flange in compression, lower steel beam web in compression, upper bolts in tension/compression, and concrete slab-steel column flange interaction.

Considering an unbalanced moment transmitted to the joint, contact forces between the concrete slab and the column flange may develop on one side of column. This slab-column interaction is allowed for in the model by introducing horizontal spring elements on each side of the column. Only compression forces activate the springs.

The steel column is modelled by vertical beam elements coincident with the geometric center of the cross sections. Linear constraint conditions called 'Tyings' are used to link the composite beam and the steel column. 'Tyings' are specified linear dependencies between degrees of freedom of the system of equations (displacements and rotations). These dependencies are specified according to the geometry of the joint. The flexibility of the composite beam and joint are taken into account by using nonlinear constitutive laws for the translational springs.

In order to take into account the non-linear behaviour of materials, strain hardening is allowed for steel members. And for concrete a non-linear model allowing for the contribution of the concrete between cracks (tension stiffening effect) are used. A bilinear stress-strain relationship for reinforcement and a linearised load-slip relationship for shear connectors is assumed. A bilinear load-displacement behaviour for the translational springs representing the steel connection is also assumed.

There are quite a few advantages in Kattner & Crisinel's composite joint model. Firstly all components of the steel joint may be modelled in their real geometric positions. The dimensions of the joint are respected. Different types of steel joints can be modelled by

modifying the number, location and property of the springs representing the different components of the joint, and the joint model can be analysed by existing finite element programs without additional programming. The disadvantages of the model result from the complexity of the load-displacement behaviour of the translational spring elements and the difficulties in defining the 'Tyings'.

The advantage of spring model is obvious. It greatly simplified the complexity of composite semi-rigid joint behaviour and made it possible for the concept of semi-rigid joint to be applied in practical design. But so far all the proposals for nonlinear analysis of composite joints are not quite suitable for practical design purpose. The proposal of Fang et al. (1999) needs test data of steel connections, and its application is therefore limited. The model of Dissanayake et al. (2000) is complicated and needs additional programming. The model proposed by Kattner & Crisinel (2000) does not need additional programming, but the nonlinear behaviour of every component of the composite joint should be obtained, which is difficult for most composite joints. This also increases the complexity of the model.

In this chapter a simplified composite joint model based on previous models is proposed. In this model, once the design parameters of the composite joint are established, the characteristics of the joint can be obtained through structural analysis programs without additional programming and reliance on tests. This composite joint model is simple to use and very little computer effort is needed. For further studies, the proposed composite joint model may be used in the analysis of composite beams and frames with semirigid beam-to-column connections.

5.2 Modelling of composite joints

5.2.1 Proposed composite joint model

A typical composite endplate beam-to-column joint is shown in Figure 5.4. There are five components considered in the joint: the steel column, the steel beam-to-column connection, the steel beam, the concrete slab, and the main reinforcement in the slab. Among them, the steel column acts as support. In order that the full plastic behaviour is developed, the concrete slab is assumed to be fully cracked. To simplify the procedure, the contribution of the concrete slab to the moment of resistance and rotation capacity of the composite joint is neglected. Consequently, only three components are to be considered in the nonlinear analysis of the composite joint, i.e., the steel beam-to-column connection, the steel beam, and the main reinforcement in the slab. In previous composite joint models (Dissanayake et al. 2000, and Kattner & Crisinel 2000) the components within the steel beam-to-column connection are treated separately as a group of spring elements. But in present modelling, the steel beam-to-column connection is taken as one component of the composite joint, and the overall behaviour of the steel connection is considered. This will greatly simplify the whole procedure of the composite joint modelling. Furthermore, in modelling of the composite joint, instead of using spring models for the joint, the idea of line element model is proposed, i.e., all the components in the joint are modelled as beam/bar elements.

Previous studies have shown that in the plastic analysis of composite joints the yielding of the reinforcement is recognized as the main source of dependable deformation, and the resulting joint rotation may be taken as the rotation capacity of the joint (Brown & Anderson 2001). It follows that the contribution of the steel connection to the rotation capacity of the composite joint may be neglected. However, the moment of resistance of the steel connection must be taken into account when calculating the moment capacity of the composite joint.

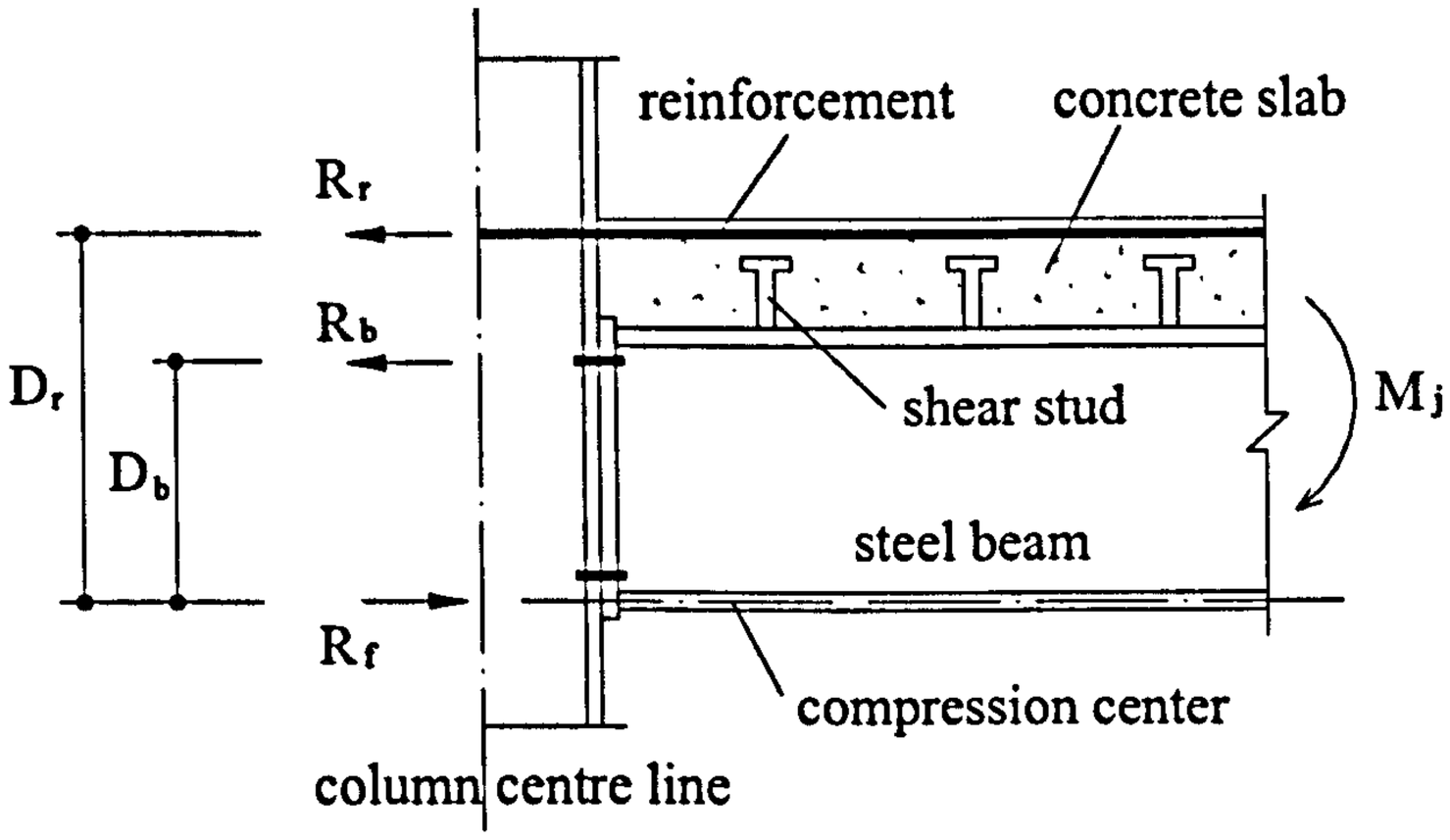

Figure 5.4 Typical endplate composite beam-to-column joint

In frame design the 'strong column, weak beam' principle is normally adopted. In composite joint analysis, it is therefore reasonable to assume that the premature buckling of the column flange and web are prevented. This is to ensure that the ultimate capacity of the composite joint could develop during the loading procedure. Since the deformations of column flange and web in compression are very limited, they are neglected in the joint analysis. The cross section of the steel beam is assumed to be compact, i.e., the local buckling of the beam web would not occur. Assuming balanced load on both sides of the joint, using the analytical model of composite joints proposed by Anderson & Najafi (1994), and assuming the compression center lies at the center of the steel beam bottom flange, the moment capacity of a composite joint (M_j) may be obtained from the following equation,

$$M_j = R_r \cdot D_r + \sum R_b \cdot D_b \qquad (5.4)$$

where R_r is the effective tensile resistance of the reinforcement

R_b is the effective resistance of a pair of bolts, which can be determined according to EC3 Annex J (1993)

D_r is the lever arm of R_r

D_b is the lever arm of R_b

In order to determine the effective tensile resistance of the reinforcement R_r two failure modes of the composite joint may be considered.

- Failure mode 1: Fracture of the reinforcement bars in concrete slab

In this case $R_f \geq R_{yr} + R_b$, where R_{yr} is the yield force of the reinforcement bars, $R_{yr} = f_y A_r$, and f_y and A_r are the yield stress and total area of the reinforcement bars, respectively; and R_f is the compressive resistance of the beam bottom flange. In plastic analysis R_f may be taken as $1.2 p_y\, b_f\, t_f$ considering strain hardening (EC 3, Part 1.1), where p_y is the yield stress of steel bottom flange, b_f and t_f are the breadth and thickness of the flange, respectively. The effective tensile resistance of the reinforcement R_r is

$$R_r = R_{yr} = f_y A_r \tag{5.5}$$

- Failure mode 2: Local buckling of steel bottom flange

In this case $R_f < R_{yr} + R_b$, since R_f is always greater than R_b in a composite connection, the effective tensile resistance of the reinforcement R_r can be calculated from

$$R_r = R_f - R_b \tag{5.6}$$

In order to eliminate R_b and D_b from equation (5.4), assuming that the moment of resistance of the composite joint is achieved through the resistance of the reinforcement over an equivalent lever arm (D_{eq}), i.e.,

$$M_j = R_{yr} \cdot D_{eq} \tag{5.7}$$

Equilibrating (5.4) and (5.7), and rearrange, we obtain

$$D_{eq} = \frac{R_r}{R_{yr}} D_r + \frac{\sum R_b D_b}{R_{yr}} \tag{5.8}$$

In this way the steel joint is eliminated from the composite joint model and the characteristics of the composite joint is assumed to be dependent on the reinforcement working together with the steel beam and shear studs over a hypothetical lever arm of D_{eq}. From the above derivation it can be seen that the moment of resistance of the composite joint model will remain the same. But the rotation capacity of the joint will mainly depend on the deformation of the reinforcement in the concrete slab.

In order to satisfactorily predict the rotation capacity of the composite joint, the effective length of the reinforcement should be properly chosen. Anderson & Najafi (1994) and Kemp & Nethercot (2001) take the length as half the depth of the steel column. Brown & Anderson (2001) suggests that the length of reinforcement be calculated from the column depth, the distance to the first shear connector and the 'transmission' length over which the bond between concrete and reinforcement is broken down. In the model described here, the length of the reinforcement element is taken as the distance from the column centreline to the first shear connector.

The proposed composite joint model is described as the following. The reinforcement in the concrete is modelled as a bar element. The length of the bar element is defined from the column centreline to the first shear stud. From the first shear stud and beyond, beam elements are used to model the concrete in tension. The bar element and concrete beam elements are located at the same level as the reinforcement. Each shear stud is modelled as a vertical beam element. The length of these elements is taken as the length of shear studs after welding. The steel beam is also modelled as beam elements which are placed horizontally in line with the compression center of the composite joint. The gaps between the shear stud elements and the steel beam elements are filled with vertical

'rigid links' with high stiffness. The function of the rigid links is to transfer the forces between the beam elements and shear stud elements. The high stiffness is to ensure that deformations due shear and bending are small so that the model behaves closely to real cases. This is achieved by assuming the value of Young's modulus of the links as 1000 times that of steel. Trial analyses have shown that this value (E_{link}=1000E_{steel}) is high enough in force transfer and values greater than that may lead to an 'ill-conditioned' stiffness matrix. The steel column is regarded as support for the elements in the composite joint model. A simple support is assigned to the bar element. And the bottom beam element is fixed at one end because it is assumed that there are no relative displacements and rotations between the steel beam and the column. The proposed composite joint model is therefore obtained as in Figure 5.5.

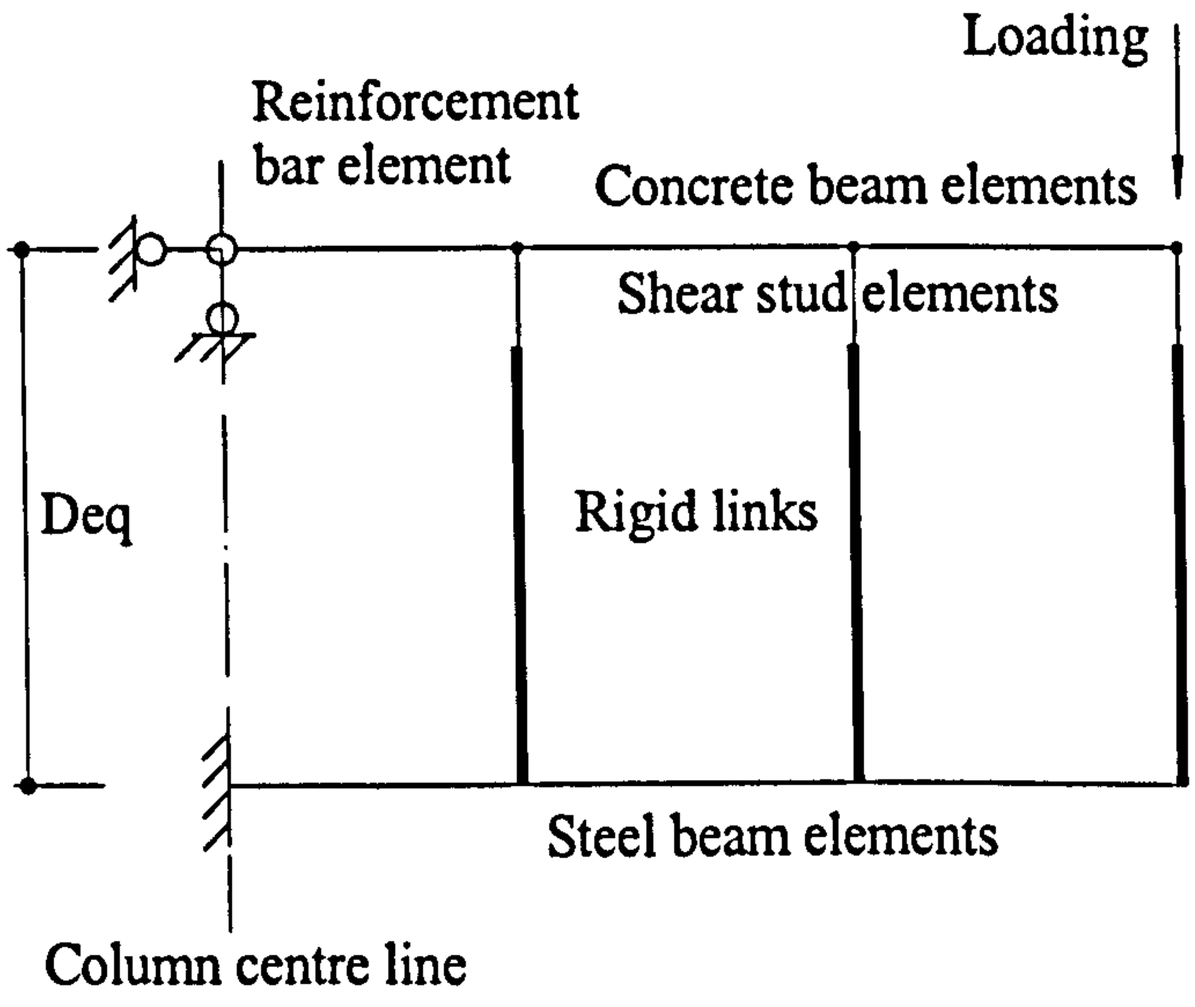

Figure 5.5 Proposed model of composite joint

In order to model the nonlinear material properties of the joint, idealized bi-linear stress-strain relationships may be assumed for bar element and steel beam elements if the strain hardening is considered. And elastic-perfect plastic relationships may be assumed for

concrete elements, shear stud elements, and rigid link elements. The stress-strain relationships are illustrated in Figure 5.6.

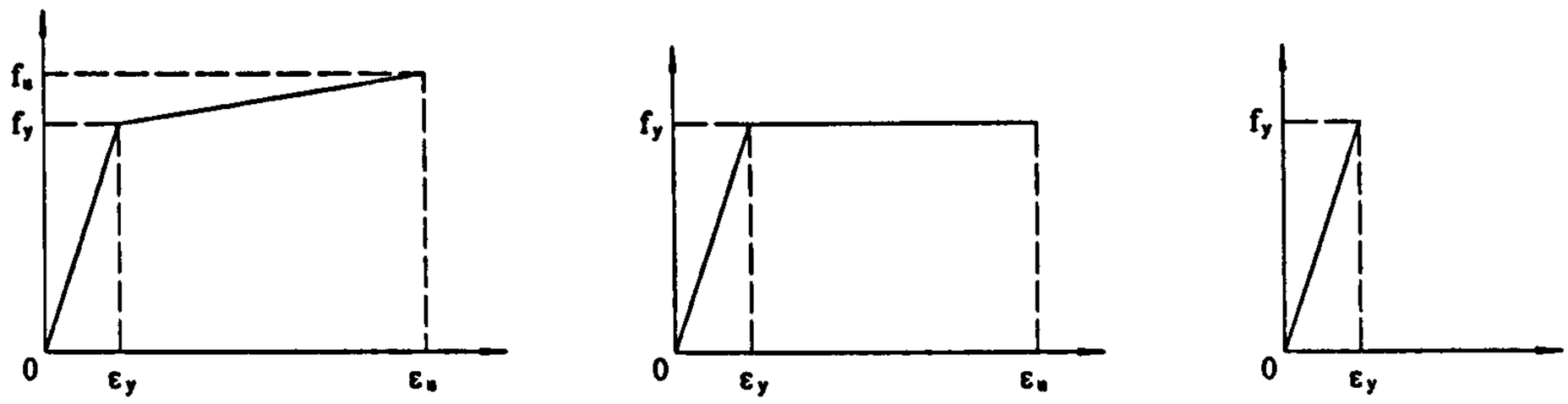

(a) For bar and steel beam elements (b) For stud elements (c) For concrete and rigid link elements

Figure 5.6 Stress-strain relationships for the proposed composite joint model

5.2.2 Shear stud model

In order that the composite joint model may simulate the 'real' composite behaviour of the joint, the shear connection between the steel beam and the concrete slab should be properly accounted for. If an effective and explicit shear stud model were established, the analysis of composite joints and beams would be much easier. But such a model can hardly be achieved because the behaviour of shear studs in a profiled concrete slab is so complicated that it is almost impossible for a stud model to accommodate all the parameters that affect its strength and deformation.

In early composite construction, the steel beam-concrete slab type of composite beams was mainly used in highway bridge design. Efforts have been made in the finite element analysis and modelling of such beams since 1970's. Wegmuller & Amer (1975) modelled composite beams by dividing the beam into a layered system. Full shear connection was assumed and the modelling of shear studs was therefore avoided. Arizumi et al. (1981) proposed a simpler method to model composite beams with incomplete (or partial) shear connection, in which the steel beam and the concrete slab

were each modelled as a single element, and the shear connectors were assumed to act as continuous media along the interface of the steel beam and the concrete slab. Compared to the 'layer model' of Wegmuller & Amer (1975), this method is simpler, and the behaviour of partial shear connection may be taken into account. The first direct modelling of shear connectors was established by Razaqper & Nofal (1990). A general three-dimensional composite beam model was proposed, in which the concrete slab and the steel beam were modelled as thin plate elements, and shear connectors were modelled as specialised bar elements with three translational degrees of freedom at each end. The composite beam and shear stud model are shown in Figure 5.7. For shear connectors, the authors assumed that the load is transferred primarily by shear and the flexural and torsional stiffness are neglected. The stiffness of shear connectors was calculated from an exponential empirical shear force-slip relationship proposed by Yam & Chapman (1968). In this proposal, the stud model is simple and easy to use, but test load-slip curves for different shear connectors are needed to determine the parameters of the empirical expression. Additional programming is also needed.

In recent years the modelling of the shear connection or the shear connectors is mostly found in finite element analysis of composite beams. Instead of establishing a model for each stud, the shear connection between the steel beam and the concrete slab is taken into account by the overall performance of all shear connectors within the composite beam. In the Oven et al. (1997) beam model, as with Arizumi et al. (1981), the shear connectors are assumed to act as a continuous shearing media along the length of the beam between the steel beam and the concrete slab. The same assumption is also adopted by Salari et al. (1998) and Fang et al. (2000). Fabbrocino et al. (1999), however, consider the shear connectors in their actual positions and their action is assumed to consist of an interaction force applied at a discrete number of sections. The total interaction force is simply obtained by the summation of the force carried by every stud.

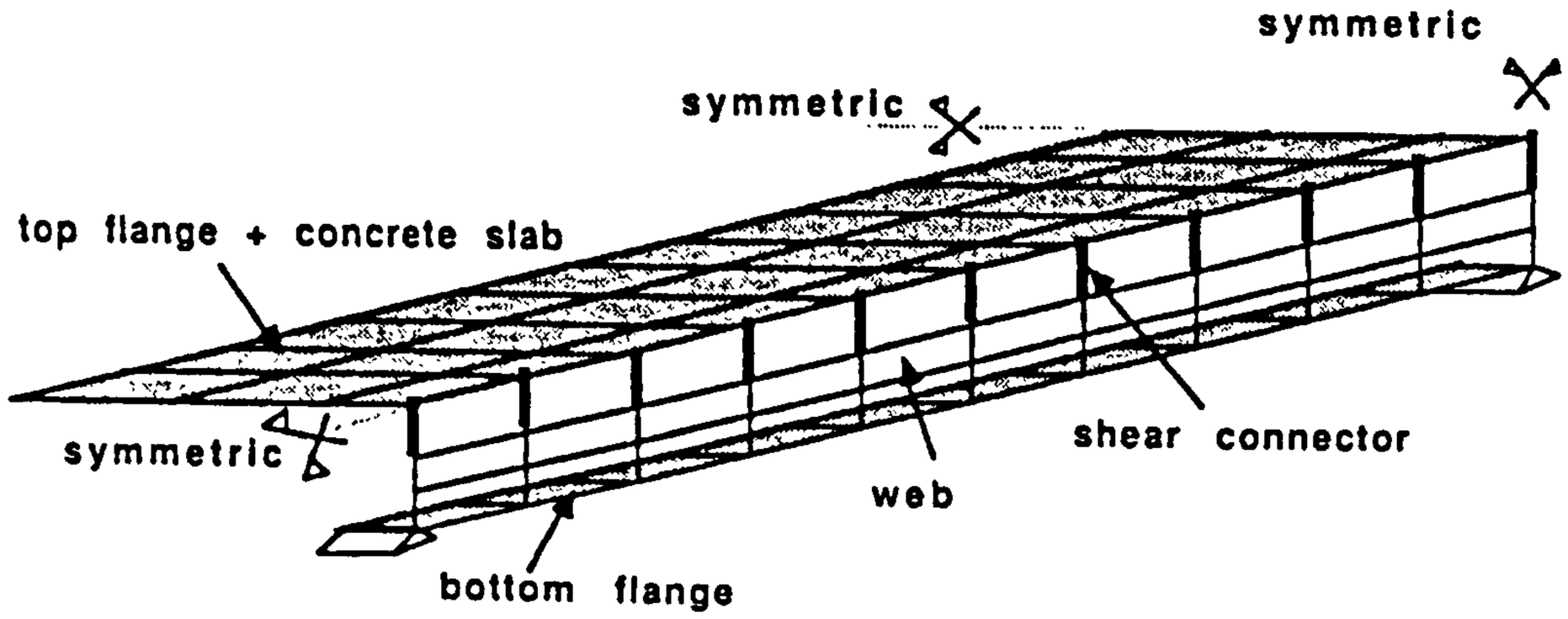

(a)

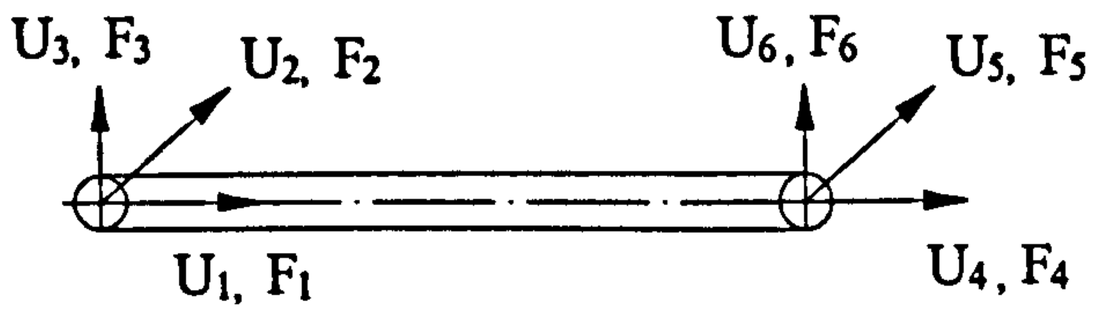

(b)

Figure 5.7 Composite beam and shear stud model proposed by Razaqper & Nofal (1990). (a) composite beam model; (b) shear stud model

Another angle to model the shear connection is to investigate the degree of shear connection. Gattesco (1999) proposed a composite beam model by regarding the moment capacity of the beam section as a function of the degree of shear connection. Liew et al. (2001) related the stiffness of the composite section to the degree of shear connection to calculate the curvature of composite beams with partial shear connection. A direct way of modelling shear connectors is to use the spring model. In Sebastian & McConnel's (2000) composite beam model, the shear connector action is modelled by a novel concrete slab-steel beam interface element consisting of axial and rotational springs. In Kattner & Crisinel's (2000) composite joint model, shear connectors are modelled as translational springs that connect the horizontal concrete slab and steel beam elements.

Having reviewed all the available proposals of shear connector models, a simple shear connector model is proposed by modelling the shear stud as a nonlinear cross-section beam element. The proposed shear stud model is shown in Figure 5.8. The behaviour of shear studs in composite beams is so complicated that seven modes of failure are established by Johnson & Yuan (1998). Since it is not possible and practical for one beam element to model all the possible cases, only Mode 1 failure is assumed in the stud model. In Mode 1 failure, shear studs fail by shank shear. A plastic zone develops just above the weld collar, and the stud shears off with little damage to the surrounding concrete. The axial tension in the stud is very low.

The purpose of the stud model is to produce an acceptable load-slip curve compared to those from push-off tests. Normally the geometric and material properties of shear connectors are defined by composite beam designs. But not all the values are appropriate to be used by the stud model because the behaviour of shear studs in a concrete slab has huge difference to the studs acting alone. Therefore, suitable geometric and material properties should be defined for the stud beam element. In order to satisfactorily model the behaviour of a shear stud in the concrete slab, the following factors should be taken into account:

- Weld connection between steel beam flange and shear studs
- Effect of concrete confinement to stud shanks
- Effect of concrete confinement to stud heads
- Deck shape
- Number of studs per trough

In push-off tests or composite beams, shear studs are welded on the steel beam flange. The premature weld failure is usually avoided. There are no relative displacements and rotations between the stud bottom and the steel flange. In the analysis of the stud beam model, the beam model may be assumed to be fixed at the bottom. The length of the model is taken as the same as the shear stud after welding. For the stud head, because of

the effect of concrete confinement to stud heads, it is reported that the rotations of the stud heads are very limited at the end of push-off tests (Lloyd & Wright, 1990). Since the longitudinal deformation of the shear stud is also very limited, the top vertical displacement and rotation of the analytical stud beam model in Figure 5.8(b) are therefore assumed to be restrained. Considering the confinement of the concrete to the stud shank, a large cross section area of the stud is assumed. This is to ensure that the length-to-diameter of the stud is small and the beam element fails by shear. And also the stress due to bending is kept small and P-δ effect does not occur. An elastic-perfect plastic stress-strain relationship is assumed for the stud steel. Under horizontal load (P), the lateral displacement of the beam model is taken as the slip (s).

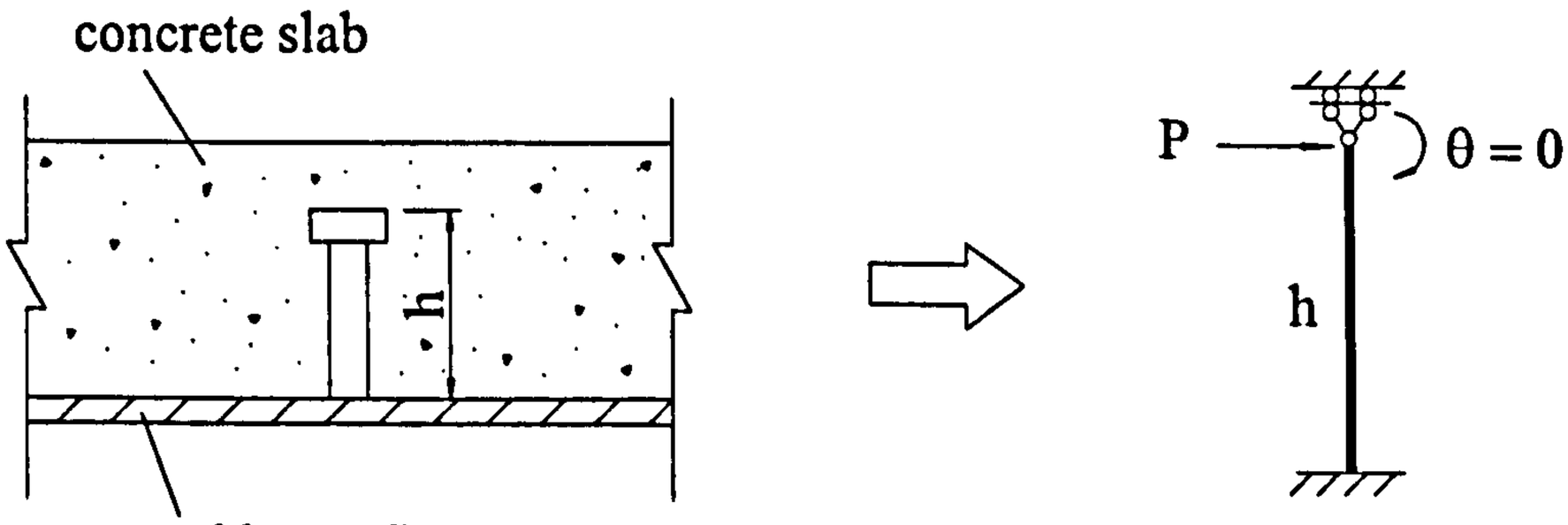

(a) a stud in slab (b) a stud model

Figure 5.8 Proposed shear stud model

The bearing stress on the shank of a stud connector in a plane concrete slab is shown in Figure 5.9. By comparing the two diagrams, it can be seen that the triangular diagram of the model is slightly conservative in predicting the strength of the shear stud compared to the parabolic curve of actual situation (Johnson, 1975).

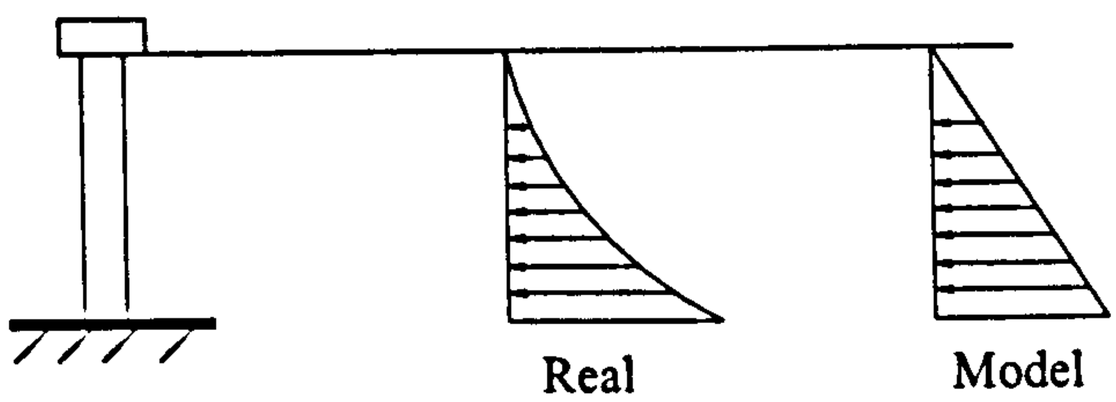

(Johnson, 1975)

Figure 5.9 Bearing stress on the shank of a stud connector in plane slab

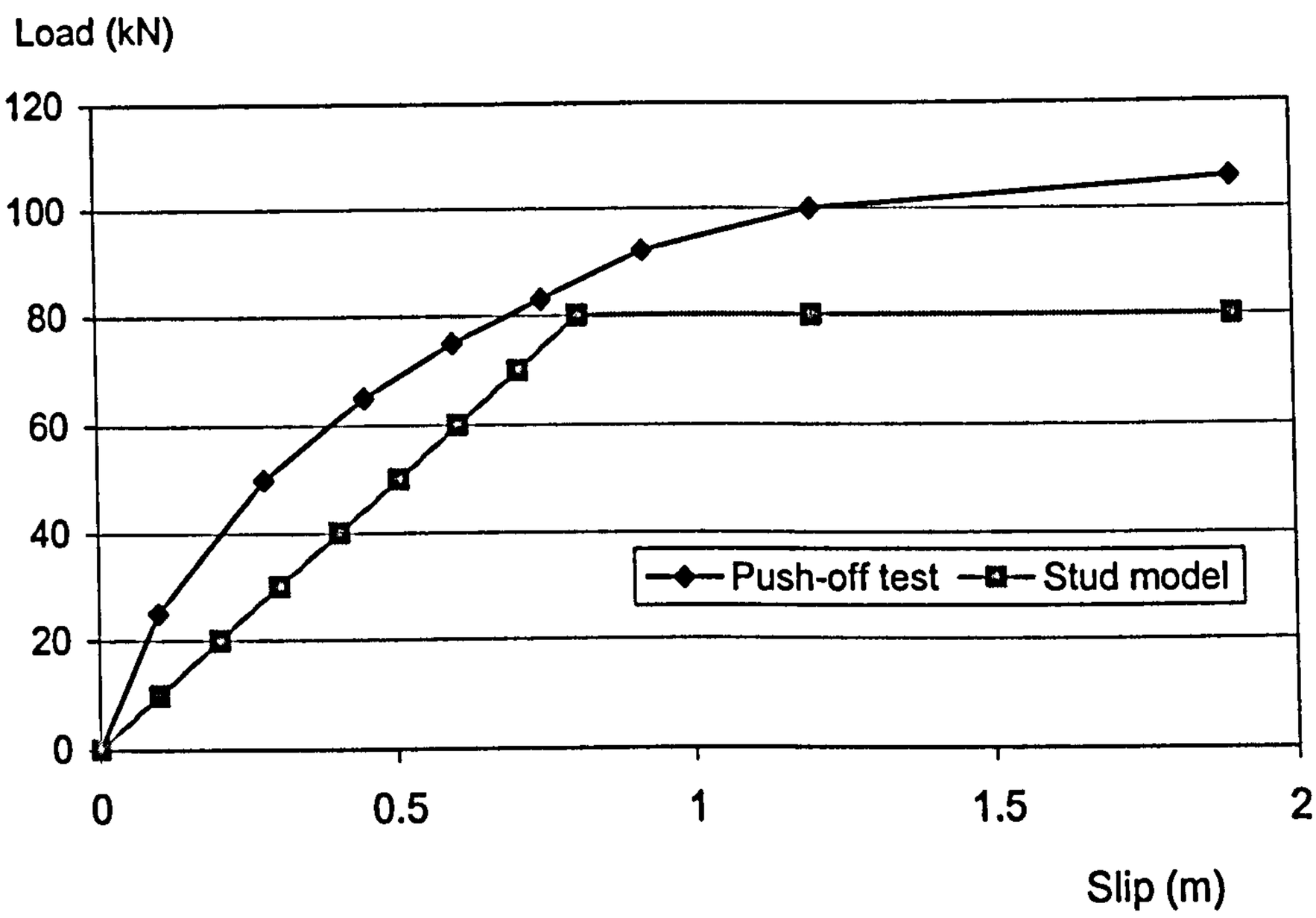

Figure 5.10 Load-slip curve of 19-mm shear stud model

In this study, the model of the 19mm-diameter stud with the length of 95mm after welding is produced. A bi-linear load-slip curve is obtained and is shown in Figure 5.10. The test curve is taken from Lloyd & Wright's (1990) push-off tests. The bi-linear load-slip curve of the stud model shows conservative agreement to the test curve. It should be

noted that for different shear studs different stud models should be worked out to match the test load-slip curves.

From Figure 5.10 it can be seen that the shear capacity of the stud model is 80kN. This is because that according to BS5950, Part 3.1 (1990), the characteristic resistance Q_k of such studs is 100kN in concrete slabs with the strength of 30 N/mm^2. And the design capacities of shear connectors in a solid slab should be taken as $0.8Q_k$, i.e., 80kN.

In fact, by changing the geometric and material properties of the stud model, different stiffness and values of design resistance of shear connectors can be obtained. Once the shear stud model is established, the proposed composite joint model can be utilized in composite joint analysis.

5.3 Validation of composite joint model

In order to validate the proposed composite joint model, two groups of composite joint samples are modelled and analysed. These composite joints are taken from the experiments performed by Brown & Anderson (2001) and Anderson & Najafi (1994). The advantage for this is that the analytical results can be directly compared to tests.

5.3.1 Model vs. Brown & Anderson's tests

Five end-plate joint tests were reported by Brown & Anderson in 2001. All tests presented major axis, internal beam-to-column connections and were configured in a cruciform arrangement, providing two connections in each specimen. The first test, named Test 1, is a steel only joint to provide a control for the following composite joint tests. The others, named Test 2, Test 3, Test 4 and Test 5, are composite joints. For all joints 12 mm stiffeners were provided to prevent failure of column web and flange in compression.

These composite joint tests were designed to investigate the influence of the spacing of the main reinforcement in the slab, the end-plate thickness, bolt size, and larger sizes of beam and column on the behaviour composite joints. The changes of the design parameters of the joints are listed in Table 5.1. And the test arrangements and joint details are shown in Figure 5.11.

The proposed composite joint model is used to model all four composite joints and the LUSAS 13 program is employed for the analysis. A snapshot of LUSAS Modeller window is shown in Figure 5.12, in which Test 2 is being modelled and the node numbers are made visible.

To explain the procedure of joint modelling by LUSAS Modeller, the model of Test 2 is taken as an example. Considering the symmetry of the joints about the column center, only half the joint is modelled. The global *x*-axis is taken as the center of the steel beam elements, and the column centreline is taken as the global *y*-axis.

- Steel beam

The steel beam section is modelled as thick beam elements with shear deformation included. All the elements are on *x*-axis and each element is divided into four divisions. The geometric properties of generally used structural sections have bean grouped in the 'Section Library' of LUSAS Modeller and are ready to use. The beam sizes are input according to Table 5.1 for each joint. The material properties are taken as the average values of web and flange from material tests. They can be found in Table 5.2 (a). Elastic-perfect plastic stress-strain relationship is assumed for steel beam elements.

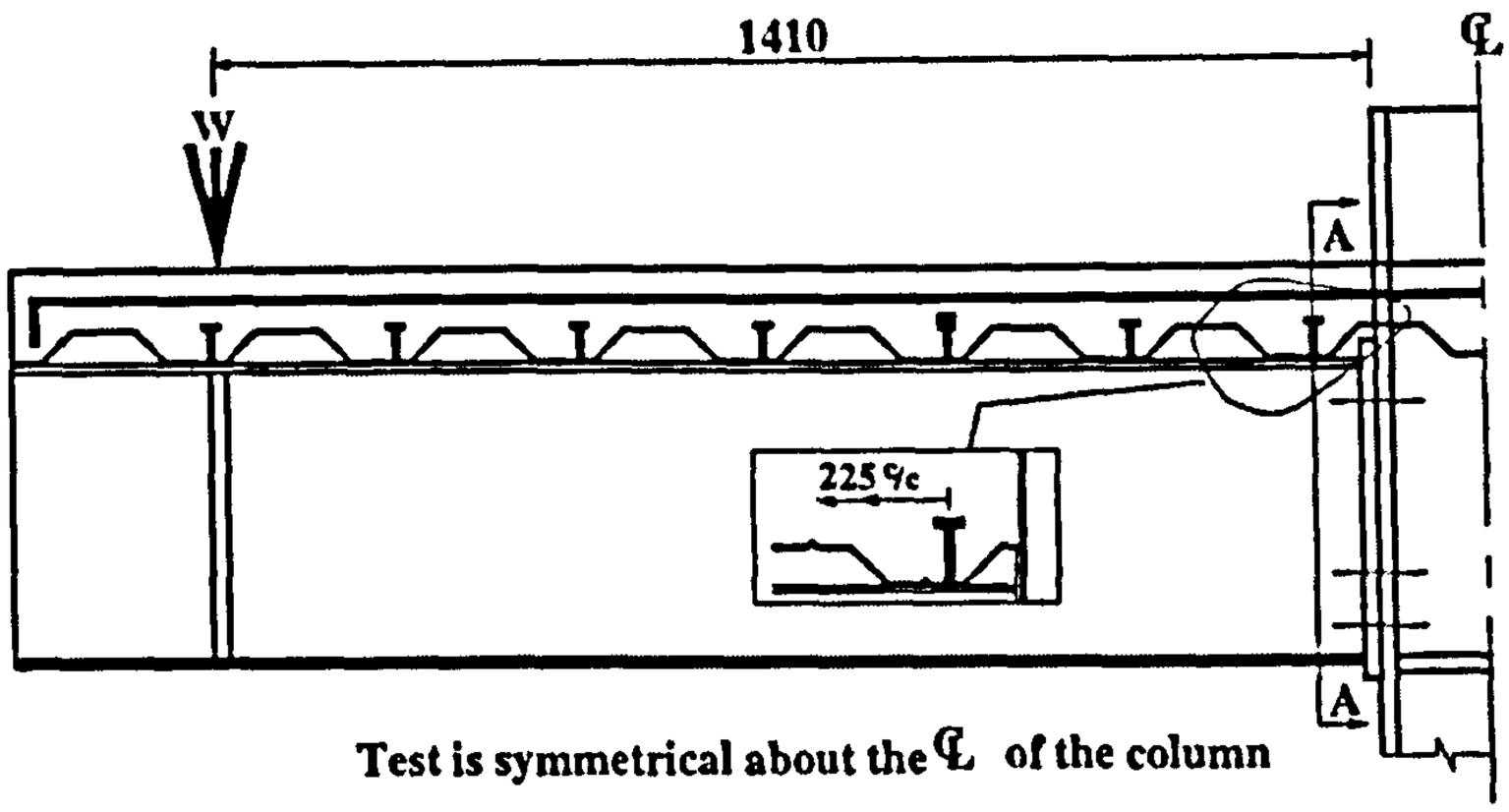

Test is symmetrical about the ℄ of the column

test	a	b
1	-	-
2	270	100
3	270	220
4	270	220
5	315	220

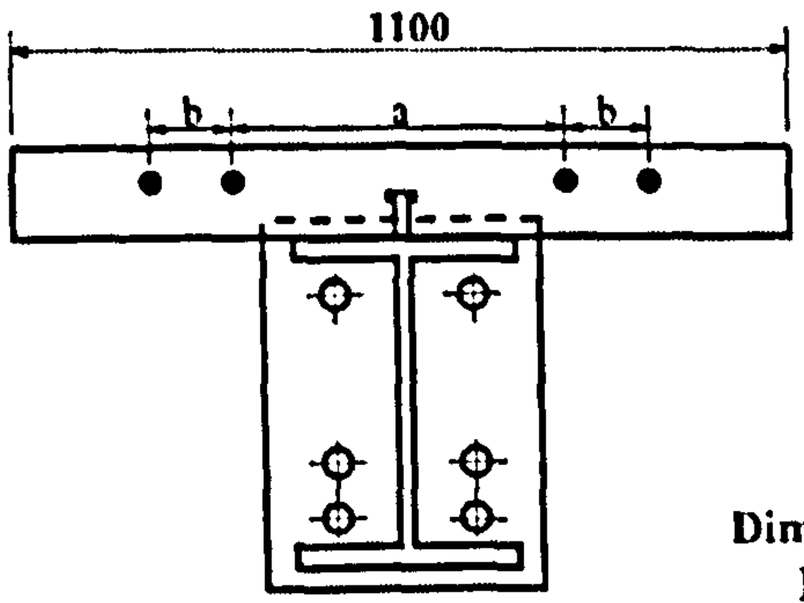

Section A-A

Dimensions in mm
Not to scale

Decking..... **PMF46** - orientated transversely with respect to the beam direction

Effective breadth of slab..... **1100mm**

Overall slab depth **120mm**

Shear connection..... **7 no. 19mm diameter studs by 100mm long on each beam**

Main longitudinal reinforcement..... **4 no. T16 bars**

Secondary reinforcement..... **A142 mesh**

Cover to reinforcement..... **25mm**

Concrete compressive strength..... **Nominally 30 N/mm^2- cube strength**

(a)

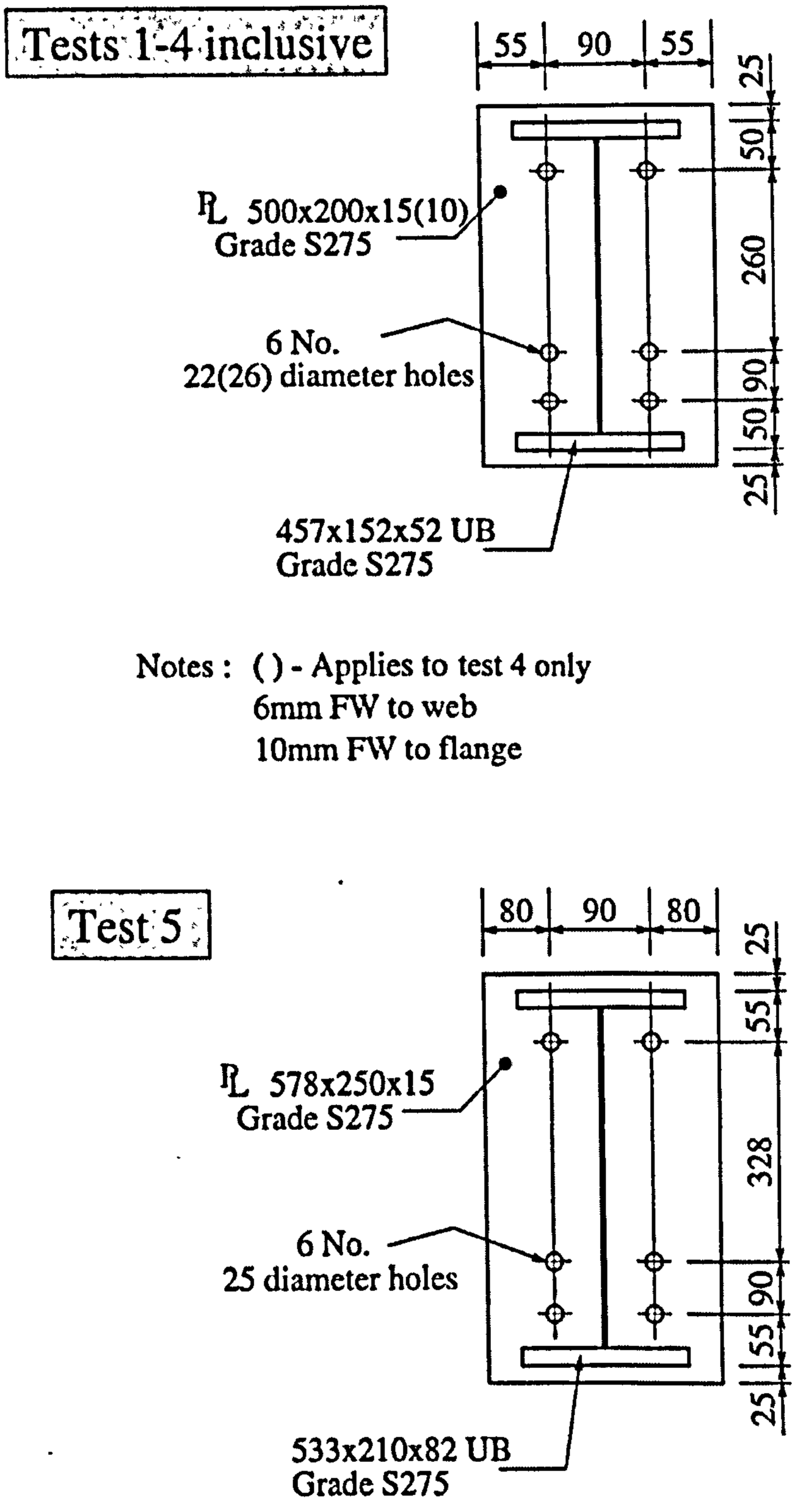

Notes : ( ) - Applies to test 4 only
6mm FW to web
10mm FW to flange

Notes : 6mm FW to web
10mm FW to flange

(b)

Figure 5.11 Parameters of composite joints from Brown & Anderson (2001)

Table 5.1 Changes of composite joint parameters of Brown & Anderson (2001)

	Column (UC)	Beam (UB)	End-plate thickness (mm)	Bolt size (grade 8.8) (mm)
Test 2	203×203×52	457×152×52	15	M20
Test 3	203×203×52	457×152×52	15	M20
Test 4	203×203×52	457×152×52	10	M24
Test 5	254×254×73	533×210×82	15	M24

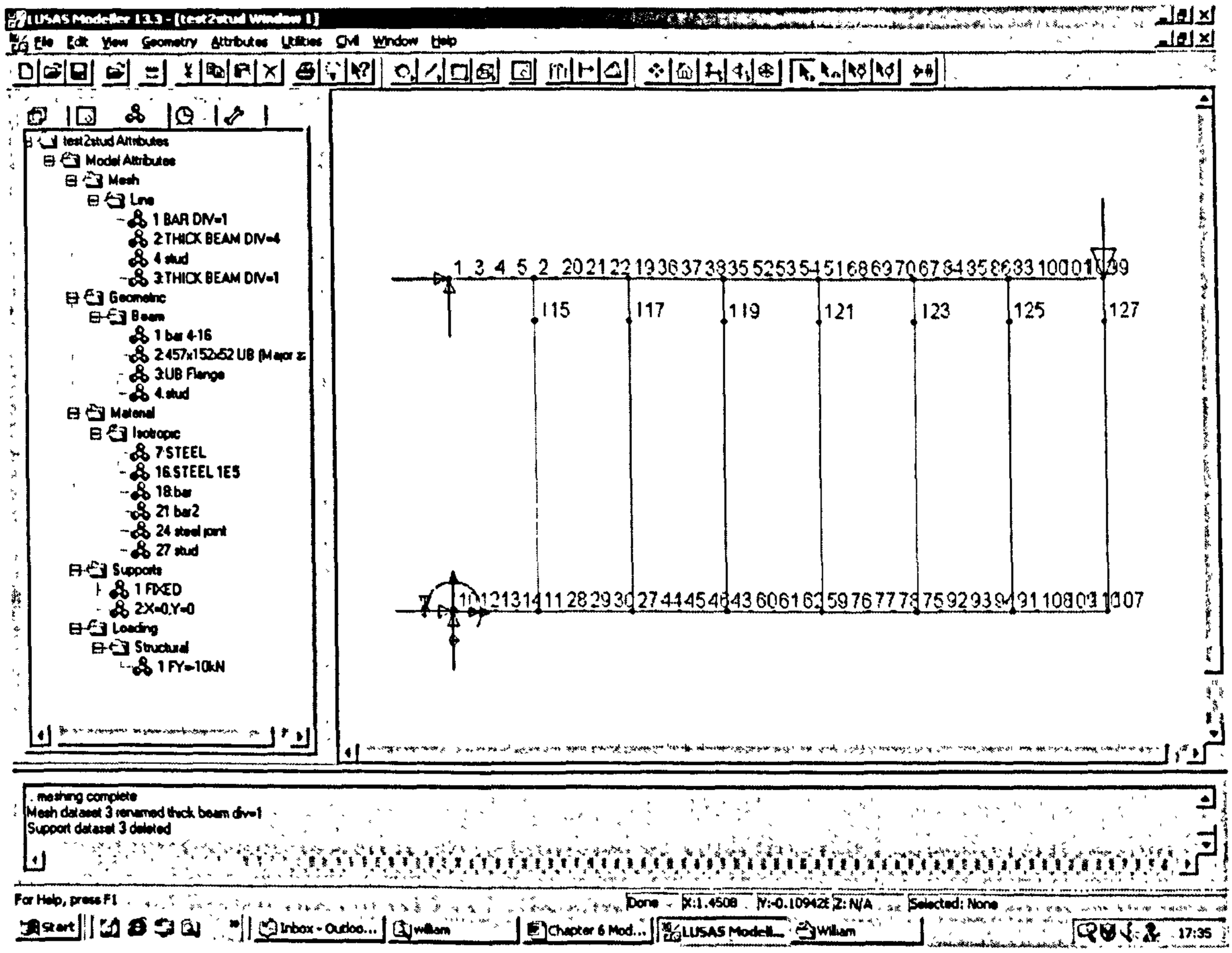

Figure 5.12 Snapshot of Test 2 model in LUSAS Modeller

- Main reinforcement in the slab

  The main reinforcement in the concrete slab (4T16) is combined together and modelled as one bar element. The total area is assigned to the bar element. The two nodes are Node 1 and 2 in Figure 5.12 and four divisions are assigned to the element. The length of the element is calculated from the column centreline to the first shear stud. The element lies at the geometric center of the reinforcement. The material properties are taken from the average values of material tests. The Young's modulus is 200kN/mm^2, the yield stress is 504 N/mm^2, and the ultimate stress is 611 N/mm^2. The elongation of the bar steel at maximum stress is 13%. This is used in the model analysis as the threshold value to terminate the nonlinear iteration procedure. A bi-linear stress-strain relationship is assumed for the bar element.

- Concrete slab

  The concrete slab is modelled as non-linear cross section elements. The overall thickness and breadth of the slab are used for the section input data. These elements lie in line with the bar element. The number of the elements is determined by the number of shear studs. The tensile strength of concrete can be found in Table 5.2 (a). In the model analysis, once a concrete element is found to yield, it is replaced by the aforementioned bar element. Elastic-perfect plastic stress-strain relationship is assumed for concrete beam elements.

- Shear studs

  The shear studs are modelled as non-linear cross section elements. There are seven studs at a spacing of 225 mm. The number of shear studs determines the numbers of concrete beam elements, rigid link elements and steel beam elements. The geometric and material are determined as such that the load-slip relationship of the model match the actual load-slip curve. Since the studs are 19mm in diameter and 95mm height after welding, and the concrete in the tests was designed to achieve a characteristic strength of 30 N/mm^2, the bi-linear load-slip relationship of the stud

model is used in all joint models. The length of the stud model is therefore 95 mm. The cross section area of the stud model is input as ten times of the original stud section to mimic the concrete confinement effects. The Young's modulus is assumed as 200 kN/mm^2, and the strength is assumed as 800 N/mm^2.

- Rigid links

  Rigid links are elements with high stiffness linking steel beam elements and shear stud elements. These elements are the same as the steel beam elements except that the Young's modulus is assumed to 1000 times higher. This will ensure their deformations due to shear and bending are small.

- Equivalent lever arm of the bar element, D_{eq}

  The equivalent lever arm of the bar element (D_{eq}) is used to determine the position of the bar element. Once this value is obtained, the overall geometry of the joint model can be defined. Prior to calculating the equivalent lever arm, the moment of resistance of the steel joint should be calculated. The equivalent lever arm can then be obtained from equation (5.8). For all the models, this value is listed in Table 5.2 (b).

- Support

  The joint model is assumed to be supported along the column centreline, i.e., the *y*-axis. Due to symmetry, for nodes on the *y*-axis, all displacements in *x*-direction must be zero. Neglecting the shear deformations of column web, the vertical displacements of nodes on the *y*-axis are also zero. Assuming no relative displacements and rotations between the steel bottom flange and column web, the rotation of the first node of the steel beam element (Node 10 in Figure 5.12) is also restrained.

- Loading

  A vertical point load is applied to the models at the position of the last shear stud, which is the same as the tests. The initial value of the load is 10 kN, and the load factor for each iteration step is set as 5, i.e., for the first load increment, the load is 50 kN; for the second increment, the load is 100 kN; for the third increment, the load is 150 kN, and so on. For plastic analysis, the increment of the load is reduced according to the secant stiffness of the stress-strain relationship until the convergence is reached. The whole iteration will stop when the termination criterion is met.

Table 5.2 Design data of joint models of Brown & Anderson (2001)

(a) Material properties

	Test 2	Test 3	Test 4	Test 5
Average Young's modulus of steel beam (kN/mm^2)	197	197.5	203.5	203.8
Average yield stress of steel beam (N/mm^2)	321.3	314.8	315	367.5
Tensile stress of concrete (N/mm^2)	3.85	3.4	3.6	3.5

(b) Length of bar elements and the equivalent lever arm, D_{eq}

	Test 2	Test 3	Test 4	Test 5
L_0 (m)	0.206	0.206	0.206	0.254
D_{eq} (m)	0.77	0.78	0.74	1.056

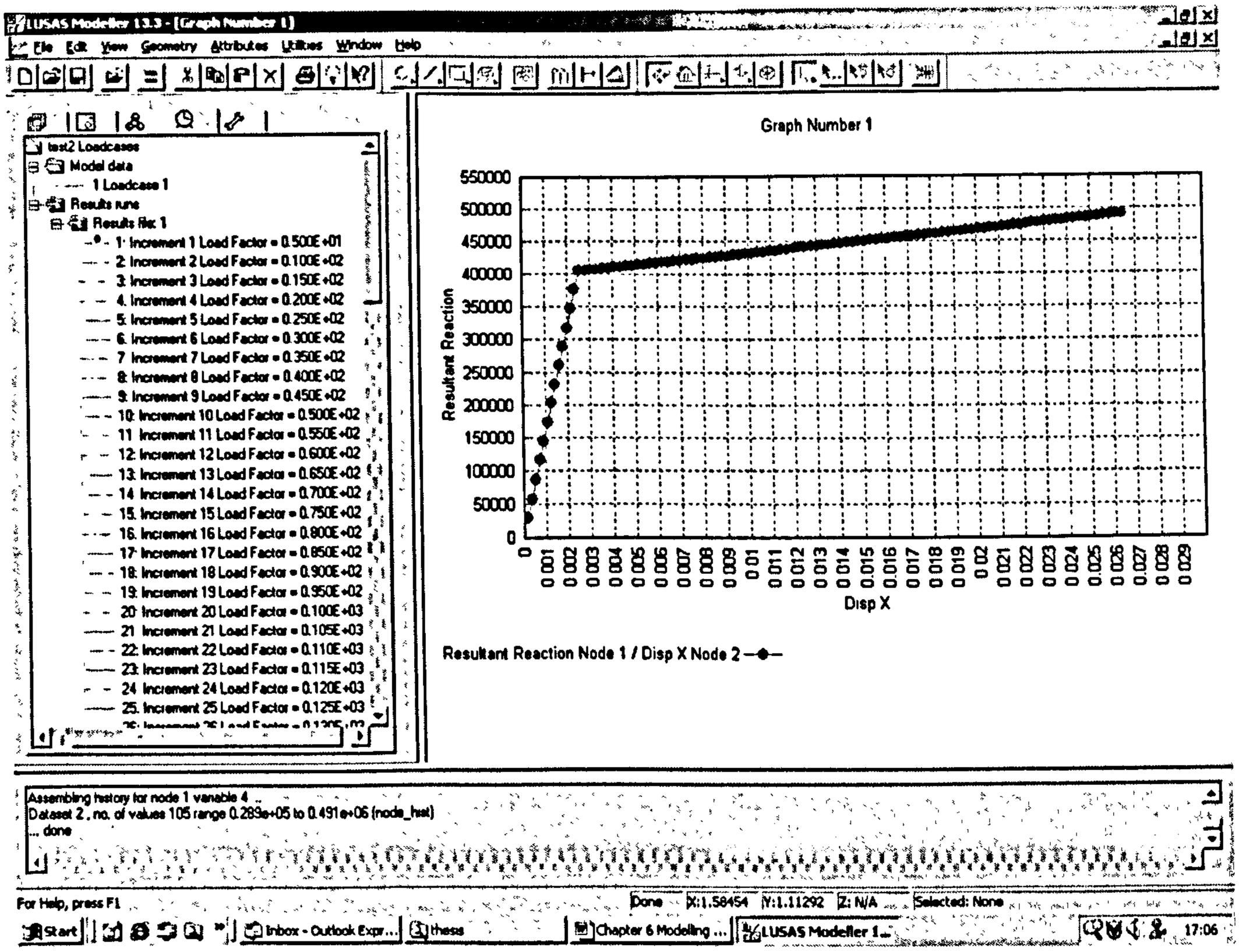

Figure 5.13 Snapshot of the Graph Wizard window of LUSAS Modeller

Once the joint models are formed, they are can be analysed by the LUSAS Solver. Note that the characteristics of the joint model cannot be directly obtained from the output data of LUSAS Solver. But they can be calculated from the reaction forces and the nodal

displacements of the bar element. The relationship between the horizontal reaction forces of Node 1 (Figure 5.12) and the horizontal displacements of the bar element at Node 2 (Figure 5.12) can be easily found by the Graph Wizard of LUSAS Modeller. A snapshot of the Graph Wizard window is shown in Figure 5.13. The units used throughout this work are N, m, kg.

Assuming the reaction force of the bar element is R_{bar} and the corresponding total extension of the bar element, i.e., the horizontal displacement of Node 2 in Figure 5.12, is Δ_{bar}, the joint moment, M_j and the joint rotation, ϕ_j can be calculated in relating to the equivalent lever arm, D_{eq}.

$$M_j = R_{bar} \times D_{eq}$$
$$\phi_j = \Delta_{bar} / D_{eq} \qquad (5.9)$$

For the moment capacity and rotation capacity of the joint models, the results of the last iteration step are used. While for the calculation of the initial stiffness of the joint model, $S_{j,ini}$, the results of the first iteration step are used.

$$S_{j,ini} = M_{j1} / \phi_{j1} \qquad (5.10)$$

where M_{j1} and ϕ_{j1} are the joint moment and rotation after the first load increment, respectively.

All four composite joints, Test 2, Test 3, Test 4, and Test 5 are modelled and analysed. The joint characteristics are calculated according to equations (5.9) and (5.10), and the results are listed in Table 5.3. By calculating the groups of data at different loading steps, the moment rotation curves of the four joint models can be obtained. They are illustrated in Figure 5.13 a, b, c, d, respectively, along with the curves from the joint tests.

Table 5.3 Characteristics of the composite joints of Brown & Anderson (2001)

		Test 2	Test 3	Test 4	Test 5
Moment of resistance (kNm)	Model	383	377	357	510
	Test	380	390	370	493
Rotation capacity (mrad)	Model	33.8	33.8	34.8	22
	Test	>33	48	35	20
Initial stiffness (kNm/mrad)	Model	98.1	98.3	90.5	175.7
	Test	142	144	136	211

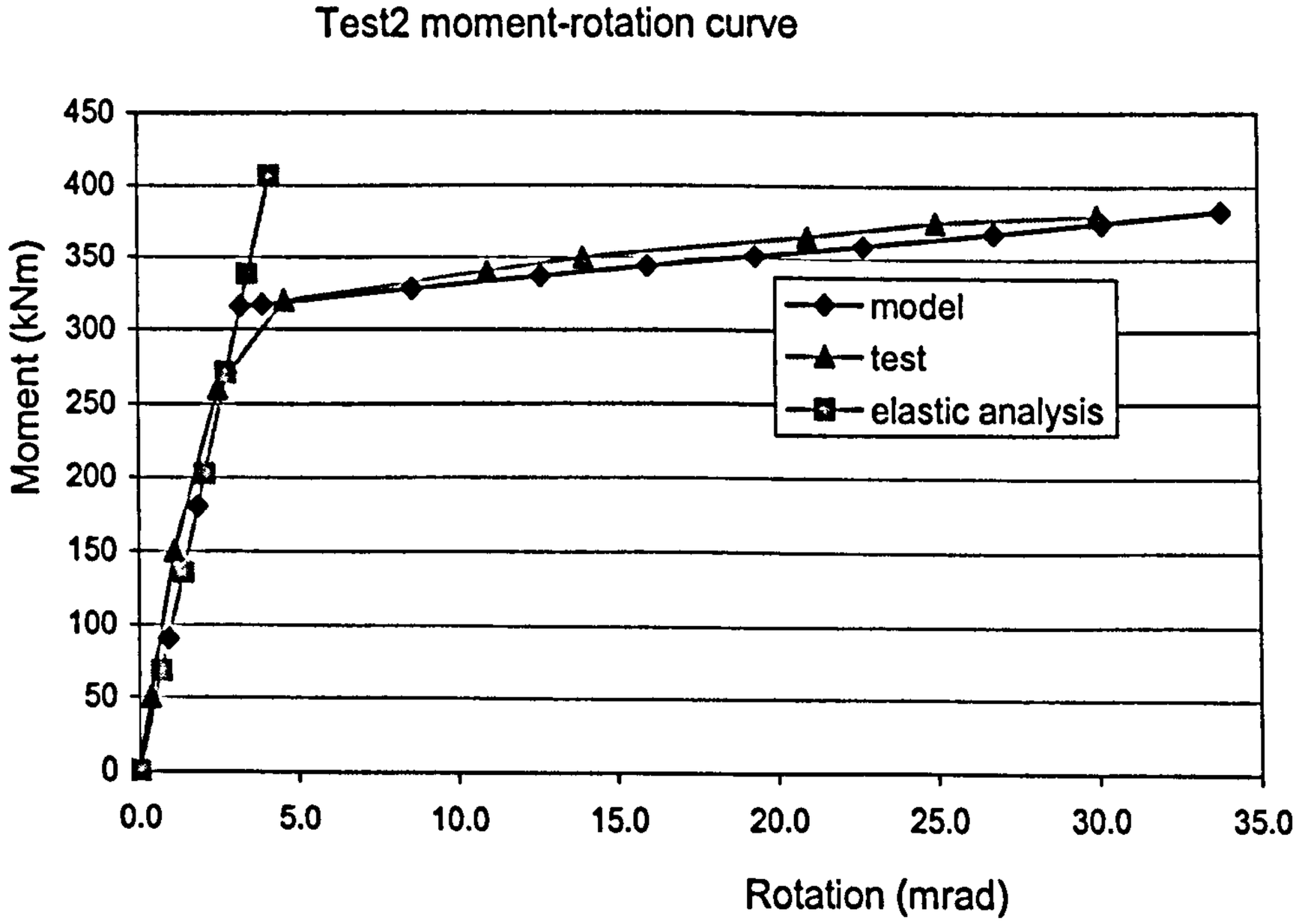

Figure 5.13a Moment-rotation curve of Test2 model

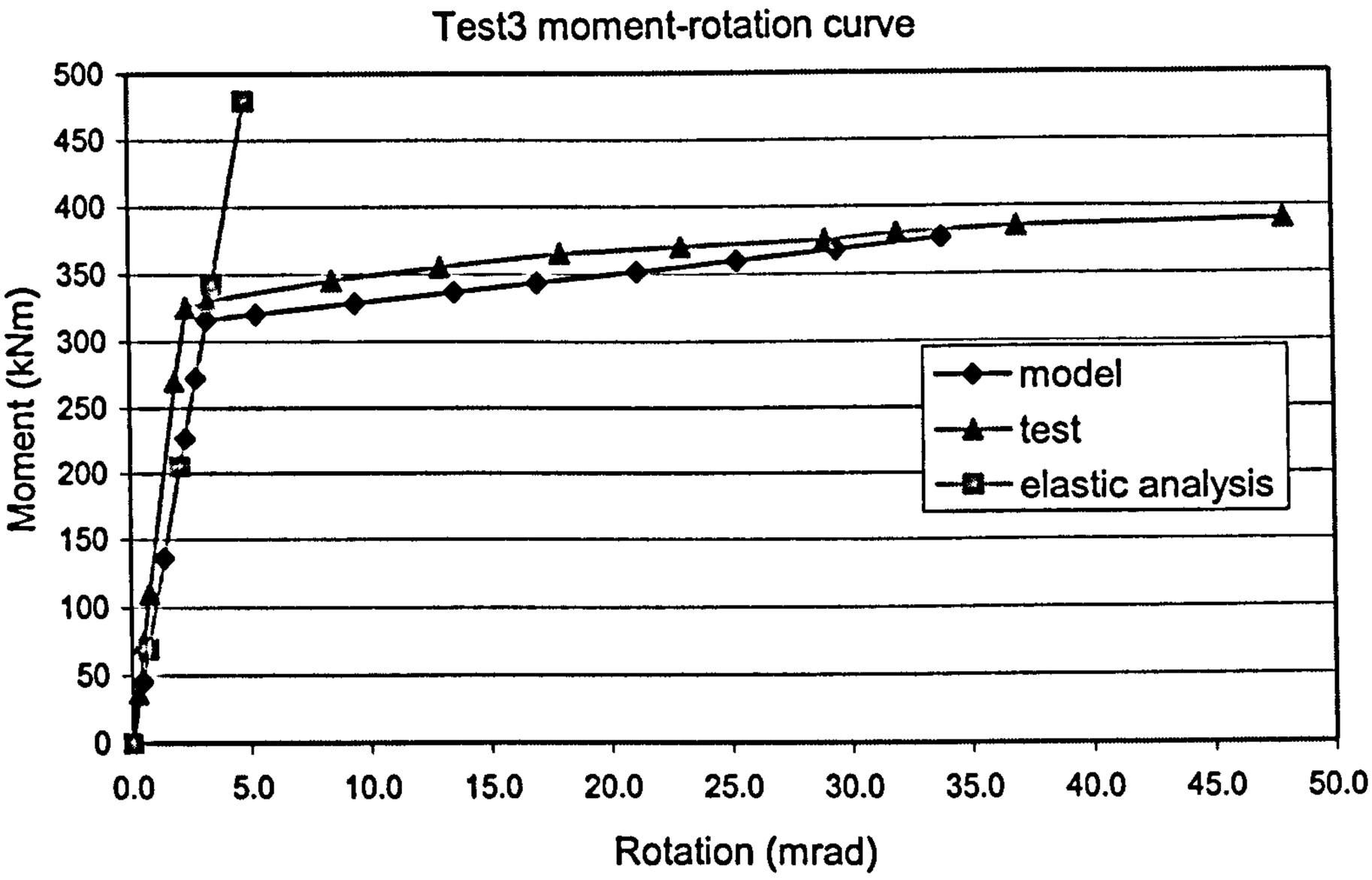

Figure 5.13b Moment-rotation curve of Test3 model

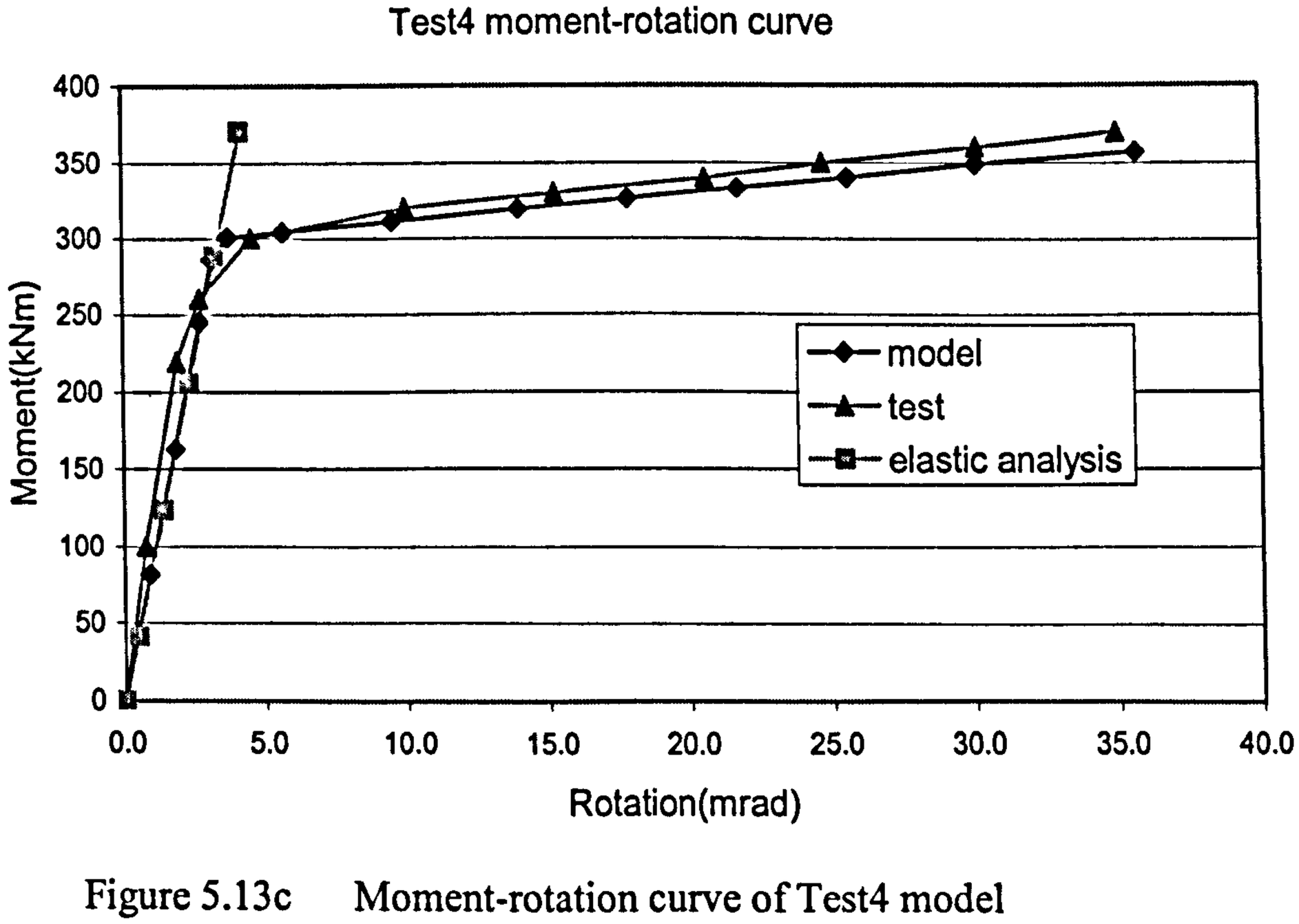

Figure 5.13c Moment-rotation curve of Test4 model

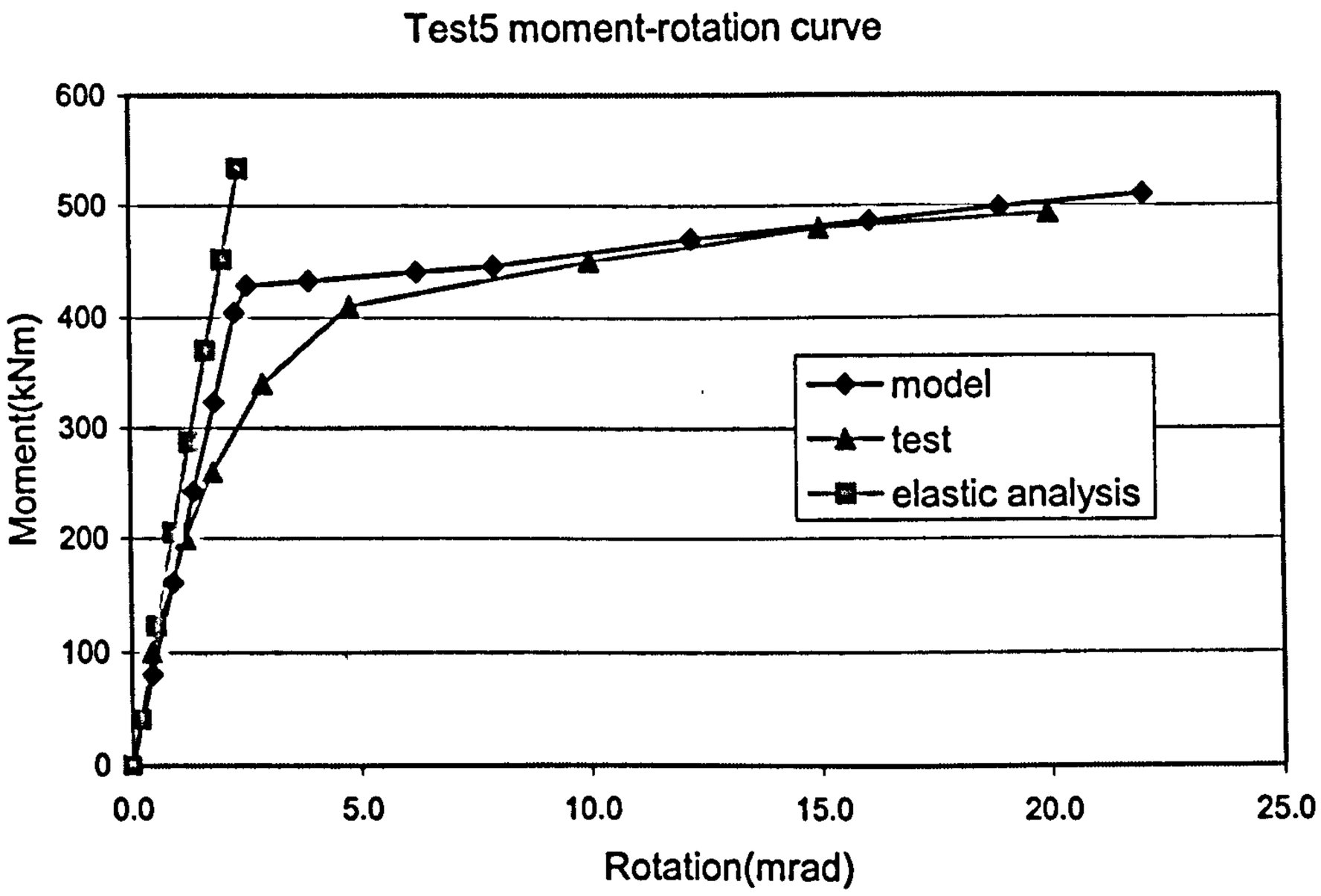

Figure 5.13d Moment-rotation curve of Test5 model

Generally speaking, good agreement is obtained between model analysis and tests. From Figures 5.13a to 5.13d, it can be seen that the moment-rotation curves of the composite joint models agree well with tests at elastic stage and at plastic stage as well. At the elastic stage, though, the initial stiffness of the joint model is slightly lower than that of tests. Direct comparison of the initial stiffness between model and tests can be found in Table 5.3. The ratio between model and tests ranges from 0.65 to 0.83. The reason is probably because that the stiffness of the steel joint at the early stage of the composite joint deformation is not accounted for in the proposed model. Secondly, this may also be a result of the conservative load-slip relationship of the shear stud model. From Table 5.3 it can be seen that the analytical results of the moment of resistance and the rotation capacity are quite satisfactory compared to tests.

The analytical results of Test 2 and Test 3 are very close. This is true because these two tests are identical except that the transverse spacing between the main reinforcement is

changed. The difference is mainly caused by the minor changes of the material properties of the joint components. The proposed model, however, cannot model the changes of the spacing of the reinforcement, because only one bar element contains the total cross section area of the reinforcement is used in the model. All the reinforcement is assumed to yield and fail simultaneously.

Test 4 is identical to Test 3 except that the endplate thickness is reduced from 15 mm to 10 mm, and the bolt size is increased from M20 to M24. The change in endplate thickness will result in a lower moment of resistance of the steel joint, and a consequent lower moment of resistance of the composite joint. The initial stiffness of the composite joint may also decrease. In the joint model, the equivalent level arm D_{eq} of Test 4 is therefore smaller than that of the Test 3 model. The predicted moment of resistance and initial stiffness by model analysis are less than those of Test 3. These results are in compliance with the expectations and are proved by the test results.

The rotation capacity of Test 4 model, however, is larger than Test 3 model. This is because the same length and extension capacity of the bar element are assumed for both models. According to equation (5.9), smaller equivalent lever arm D_{eq} will result in larger value of joint rotation. Tests show that the rotation capacity of Test 3 (48mrad) is larger than Test 4 (35mrad). The predicted rotation capacity of Test 3 is 30% lower than the tests. Very close results are obtained between Test 4 analysis (34.8mrad) and tests (35mrad).

In Test 5, large beam and column sizes are used, but the amount of reinforcement is not changed. As we know, the moment of resistance of a steel joint will increase with the increase of beam size if the mode 1 failure of the endplate occurs. According to equation (5.4), the moment of resistance of the composite joint will increase and consequently, the equivalent lever arm of reinforcement (D_{eq}) of the joint model will also increase according to equation (5.8). Assuming the same extension capacity of the reinforcement,

the rotation capacity of the composite joint will decrease according to equation (5.9). But the initial stiffness of the composite joint will increase according to equation (5.10).

In the Test 5 model, the equivalent lever arm of reinforcement (D_{eq}) is much larger than other models due to the increase of the steel beam size. The length of the bar element is also increased as a result of the increase of the column size since this value is taken as the distance between the column centreline and the first shear stud. As expected, through the analysis of Test 5 model, there is a significant increase in the moment of resistance and initial stiffness. But the rotation capacity of the composite joint reduced remarkably at the same time. The results of model analysis and the test agree very well in this case.

5.3.2 Model vs. Anderson & Najafi's tests

Five composite joint tests, identified as S4F, S8F S12F, S8E and S8FD, were reported by Anderson & Najafi in 1994. The endplate type of connection was used for all joints, in which an endplate was welded to the steel beam and bolted to the column flange. All the tests were carried out on cruciform specimens with two cantilevers on each side to model internal joints in a braced frame. The arrangement of specimens and the details of the steel joints are shown in Figure 5.14.

The design parameters of the joints are as the following:

Structural steel	Grade 43
Beam	305 × 165 UB40, except in S8FD which is 457 × 152 UB52
Column	203 × 203 UC52
End plate	15 mm thick
Bolts	20mm diameter, Grade 8.8
Deck	PMF CF46 0.9mm thick
Slab	1100mm wide, 120mm deep overall
Concrete	normal weight, Grade 30
Reinforcement	A142 mesh plus T12 longitudinal bars

Shear connectors 19 mm stud, 100 mm long before welding

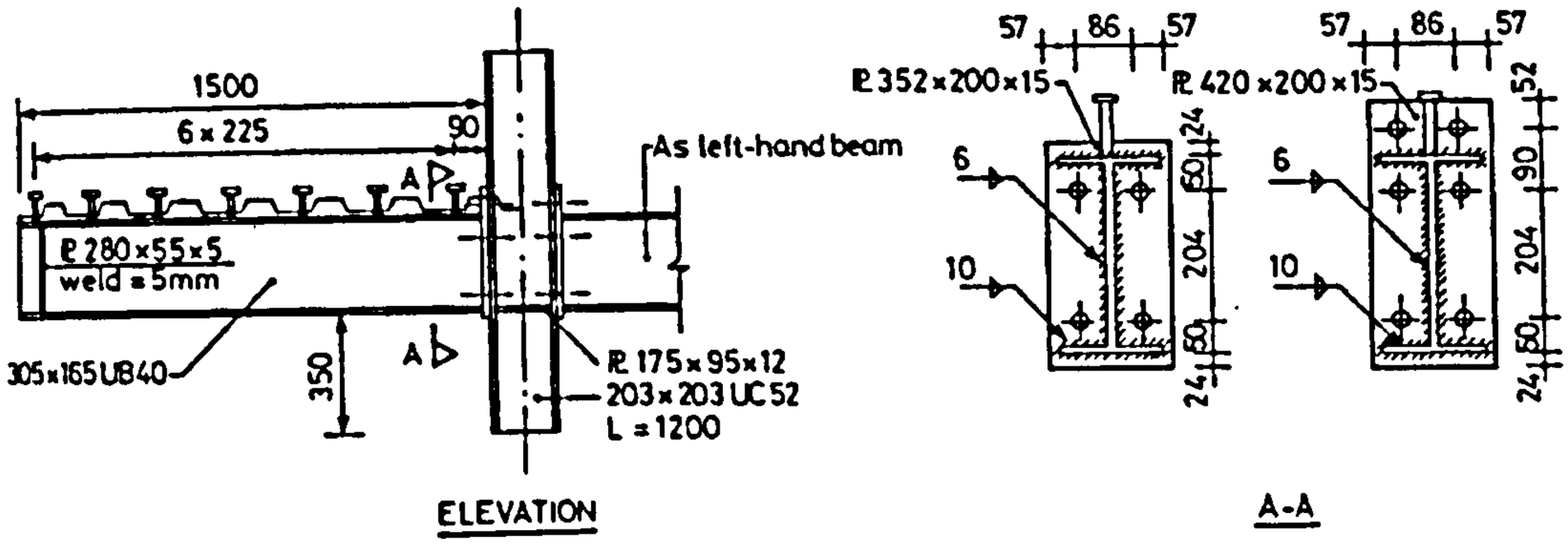

Figure 5.14 Arrangement of test specimens from Anderson & Najafi (1994)

Among the five joints, the amount of tensile reinforcement, the depth of the steel section and the type of end plate were varied. The changes of the parameters of the specimens are listed in Table 5.4.

Table 5.4 Changes of design parameters of the tests from Anderson & Najafi (1994)

	Type of end plate connection	Beam (UB)	Main reinforcement	Equivalent lever arm, D_{eq} (mm)
S4F	Flush end plate	305 × 165 UB40	4-T12	699
S8F	Flush end plate	305 × 165 UB40	8-T12	549
S12F	Flush end plate	305 × 165 UB40	12-T12	499
S8E	Extended end plate	305 × 165 UB40	8-T12	786
S8FD	Flush end plate	457 × 152 UB52	8-T12	814

These five joints are modelled by using the proposed composite joint model through the LUSAS 13 program. A snapshot of the LUSAS Modeller window with S4F being modelled is shown in Figure 5.15. Again the node numbers are made visible.

For these five joints, the procedure of modelling in LUSAS Modeller is the same as that of the joint models of Brown & Anderson (2001). Considering the symmetry of the joints about the column centreline, half the joint is modelled. The global *x*-axis is set to coincide with the center of the steel beam elements, and the column centreline is taken as the global *y*-axis.

- Steel beam

  The steel beam section is modelled as thick beam elements with shear deformation included. All the elements are on *x*-axis and each element is divided into four divisions. The beam sizes are input according to Table 5.4 for each joint. Since the results of material tests are not provided in the reference, the material properties are taken from the values suggested by EC 3, Part 1.1 (1992). The Young's modulus is taken as 210 kN/mm^2, the Poisson's ratio is 0.3, and the yield stress is 275 N/mm^2. An elastic-perfect plastic stress-strain relationship is assumed for steel beam elements.

- Main reinforcement in slab

  The main reinforcement in the concrete slab (T12 bars) are combined together and modelled as one bar element. The two nodes are Node 1 and 2 in Figure 5.15 and four divisions are assigned to the element. The length of the element is calculated from the column centreline to the first shear stud. Since the size of column section is not changed, this value is the same for all joints. The element is positioned at the geometric center of the rebars. The Young's modulus is taken as 200 kN/mm^2 according to EC 2 Part 1.1 (1992), and the yield stress is taken as 486 N/mm^2. The elongation of the bar steel at maximum stress is 17% from material tests. This

value is used to set the termination point of the nonlinear iteration procedure. An elastic-perfect plastic stress-strain relationship is assumed for the bar element.

- Concrete slab

  The concrete slab is modelled as non-linear cross-section beam elements. The overall thickness and breadth of the slab are used to define the cross section. These elements lie in line with the bar element. The number of the element is determined by the number of shear studs. According to EC 2 Part 1.1 (1992), the Young's modulus concrete is taken as 32 kN/mm^2. The tensile strength of concrete is taken as 2.9 N/mm^2. In the model analysis, once a concrete element is found to yield, it is replaced by the aforementioned bar element. An elastic-perfect plastic stress-strain relationship is assumed for concrete beam elements.

- Shear studs

  There are seven studs at a spacing of 225 mm on each side. The proposed shear stud model is used to model each stud. The number of shear studs determines the numbers of concrete beam elements, rigid link elements and steel beam elements. The length of the stud model is taken as 95 mm, which is the length after welding. The cross section area of the stud model is input as ten times of the original stud section to mimic the concrete confinement effects. The Young's modulus is assumed as 20 N/mm^2, and the strength is assumed as 800 N/mm^2.

- Rigid links

  Rigid links are elements with high stiffness linking steel beam elements and shear stud elements. The material properties of these elements are the same as the steel beam elements except that the Young's modulus is assumed to 1000 times higher. This is to ensure their deformations due to shear and bending are small.

- Equivalent lever arm of the bar element, D_{eq}

  The equivalent lever arm of the bar element (D_{eq}) is used to determine the coordinates of the bar element, and hence the geometry of the joint model can be obtained. The equivalent lever arm is calculated from equation (5.8). For all the models, this value is listed in Table 5.4 (b).

- Support

  Due to symmetry, for nodes on the *y*-axis, the displacements in *x*-direction must be zero. Neglecting the shear deformations of column web, the vertical displacements of nodes on the *y*-axis are also zero. Assuming no relative displacements and rotations between the steel bottom flange and column web, the rotation of the first node of the steel beam element (Node 10 in Figure 5.12) is also restrained.

- Loading

  A vertical point load is applied to the models at the position of the last shear stud, which is the same as the tests. The initial value of the load is 10 kN, and the load factor for each iteration step is set as 10, i.e., for the first load increment, the load is 100 kN; for the second increment, the load is 200 kN; for the third increment, the load is 300 kN, and so on. For plastic analysis, the increment of the load is reduced according to the second stiffness of the stress-strain relationship until the convergence is reached. The whole iteration will stop until the termination criterion is met.

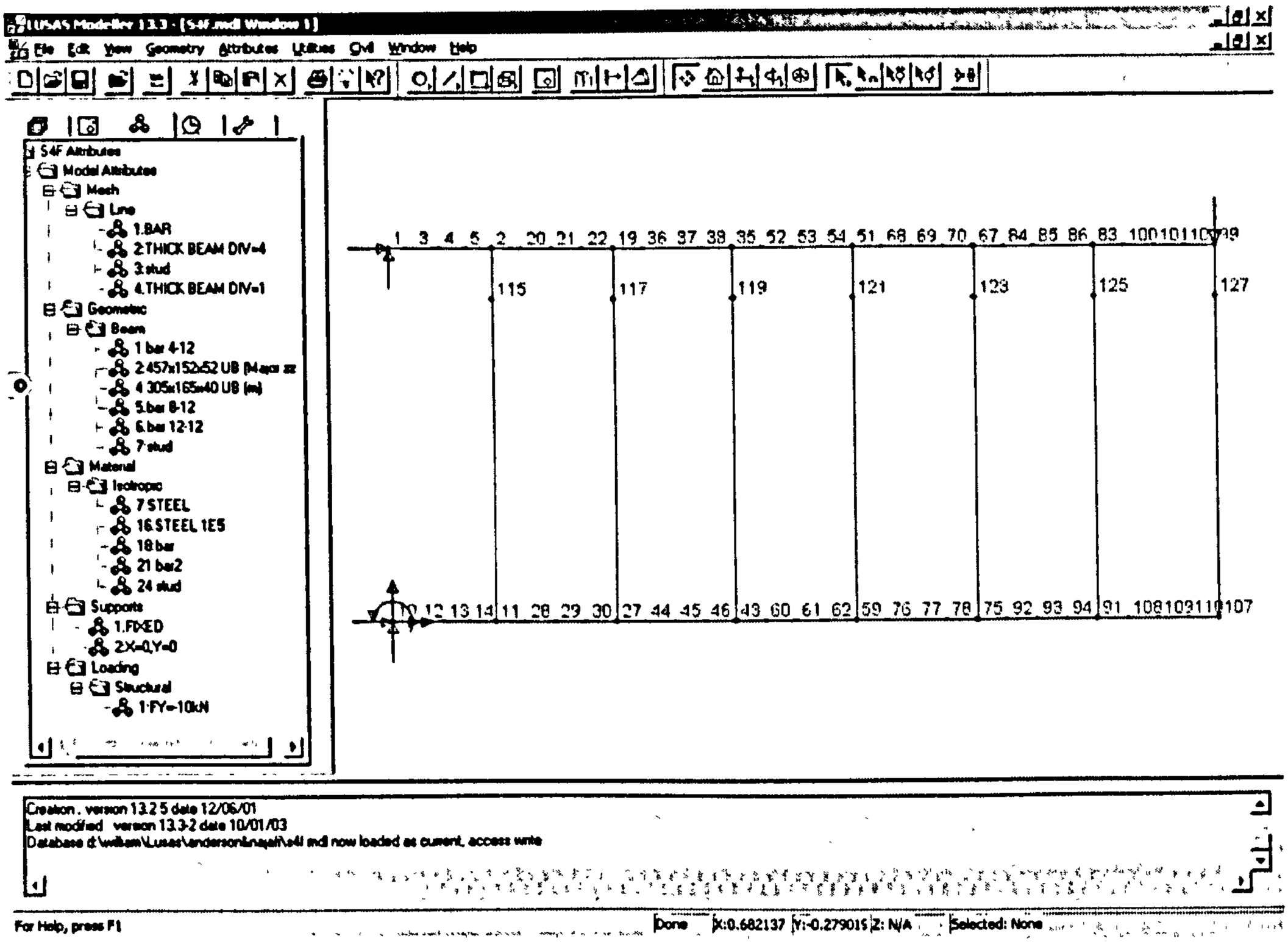

Figure 5.15 Snapshot of S4F model in the LUSAS Modeller

All five composite joint models are obtained through the above procedure and then analysed by the LUSAS Solver. Again the characteristics of the joint model cannot be directly obtained from the output data of LUSAS Solver. But they can be calculated from the reaction forces and the nodal displacements of the bat element in association with the equivalent lever arm. The relationship between the horizontal reaction forces of Node 1 (Figure 5.15) and the horizontal displacements of the bar element at Node 2 (Figure 5.15) can be easily found by the Graph Wizard of LUSAS Modeller. Figure 5.16 shows the results of S4F model.

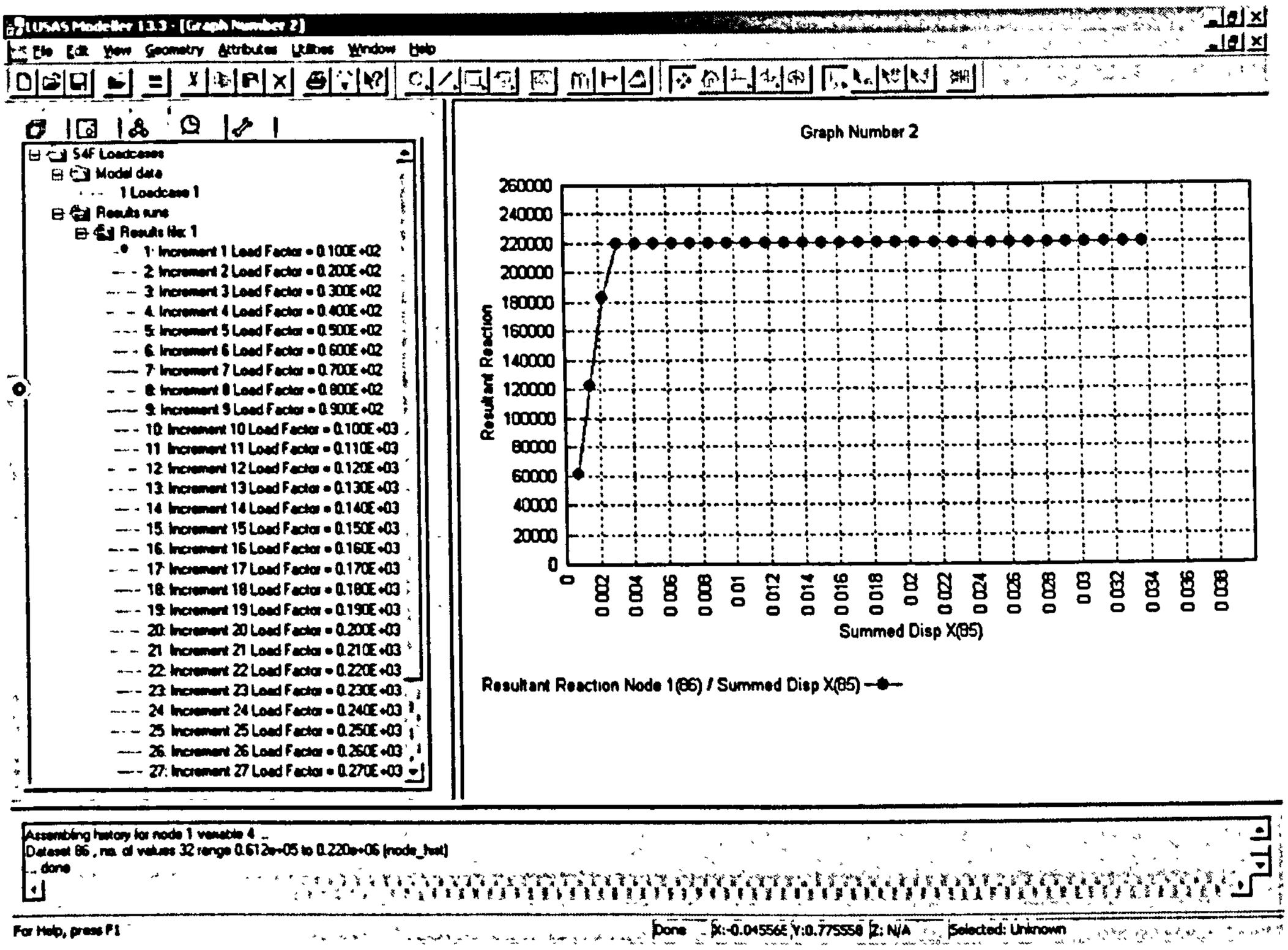

Figure 5.16 A screen shot of LUSAS post-process window of S4F model analysis

The joint moment of resistance and rotation capacity are found by equation (5.9), and the initial stiffness can be found from equation (5.10). For all five joints these values are shown in Table 5.5. The relationship between joint moment and rotation can therefore be found by calculating the pair of values at each load increment. For each joint, the moment-rotation relationship is shown in Figure 5.17a, b, c, d, e.

Table 5.5 Analytical results joint models from Anderson & Najafi (1994) tests

		S4F	S8F	S12F	S8E	S8FD
Moment of resistance (kNm)	Model	154	241	298	283	345
	Test	179	262	302	291	416
Rotation capacity (mrad)	Model	25.7	32.7	42.7	30	22.6
	Test	26.6	35.8	55.7	40	14
Initial stiffness (kNm/mrad)	Model	40	50	51	69.2	102.7
	Test	55	65	85	145	140

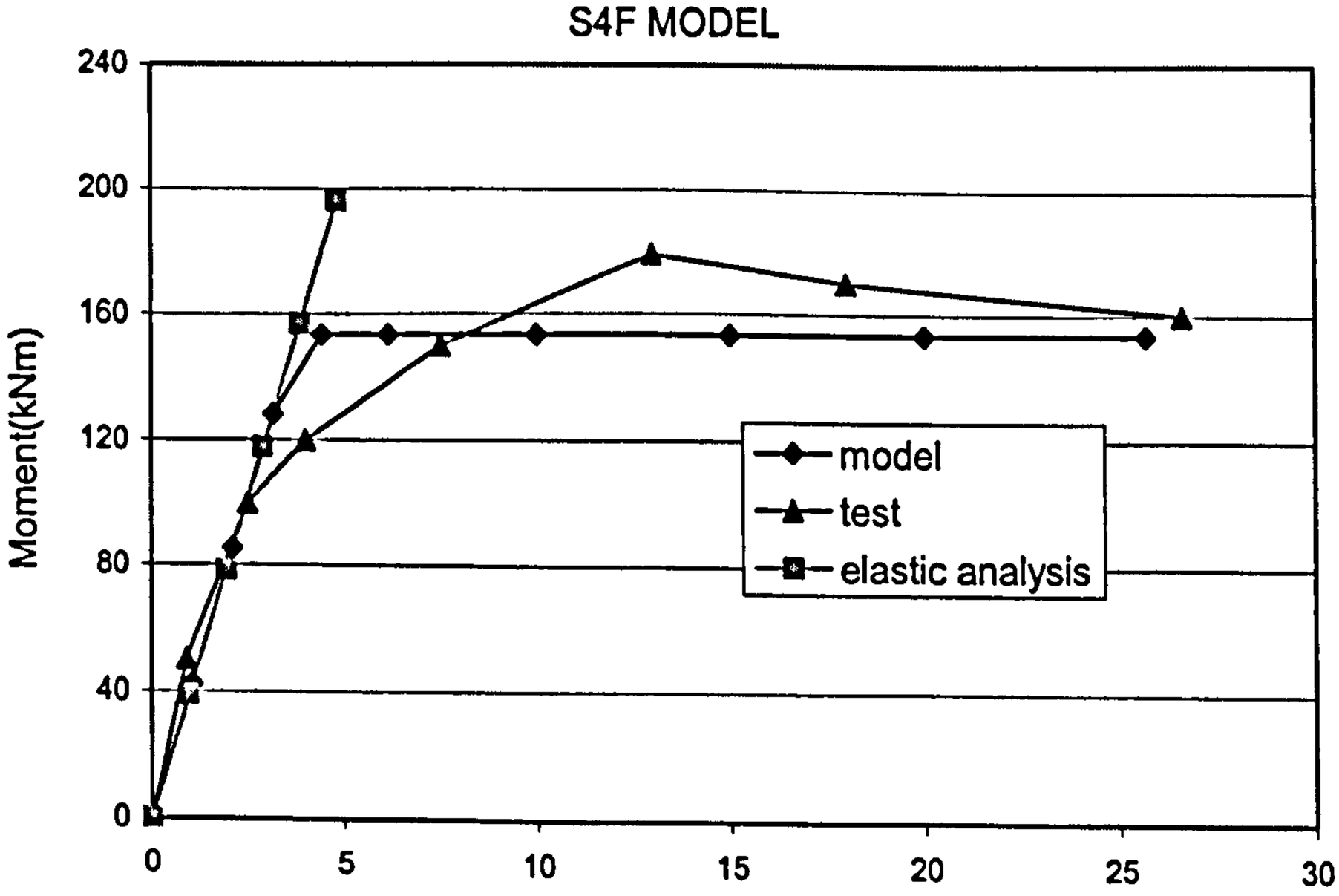

Figure 5.17a Moment-rotation curve of S4F model

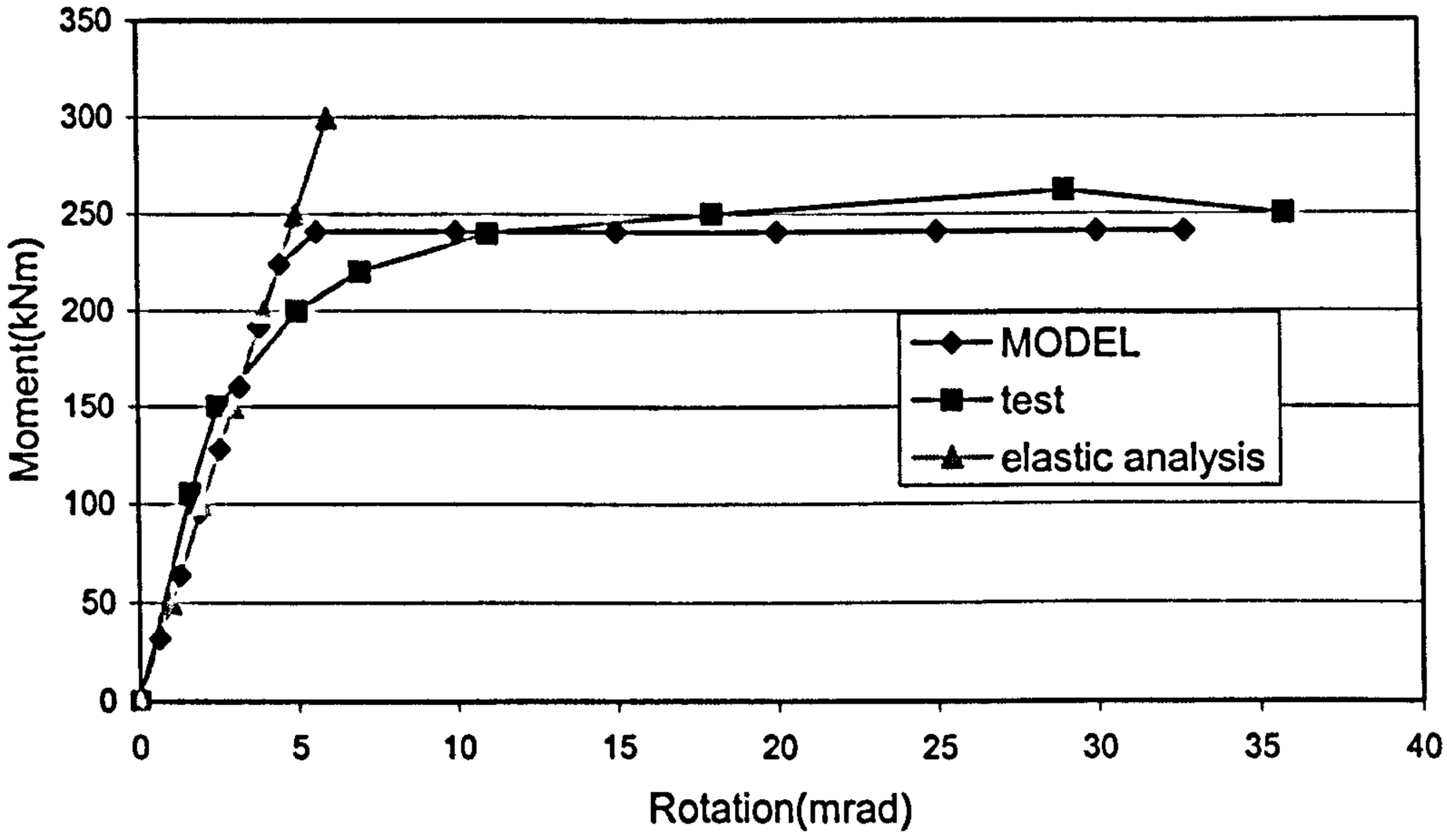

Figure 5.17b Moment-rotation curve of S8F model

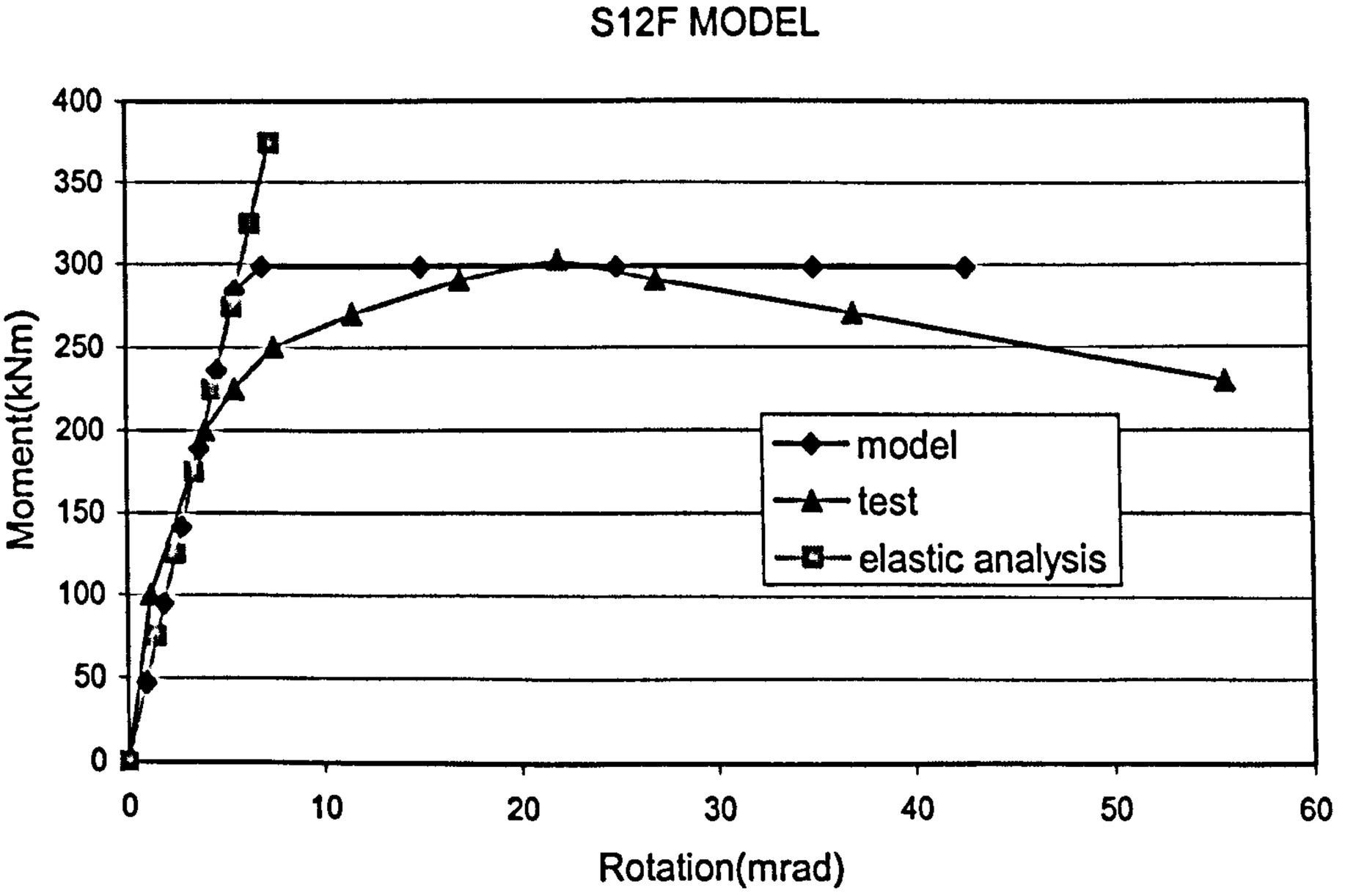

Figure 5.17c Moment-rotation curve of S12F model

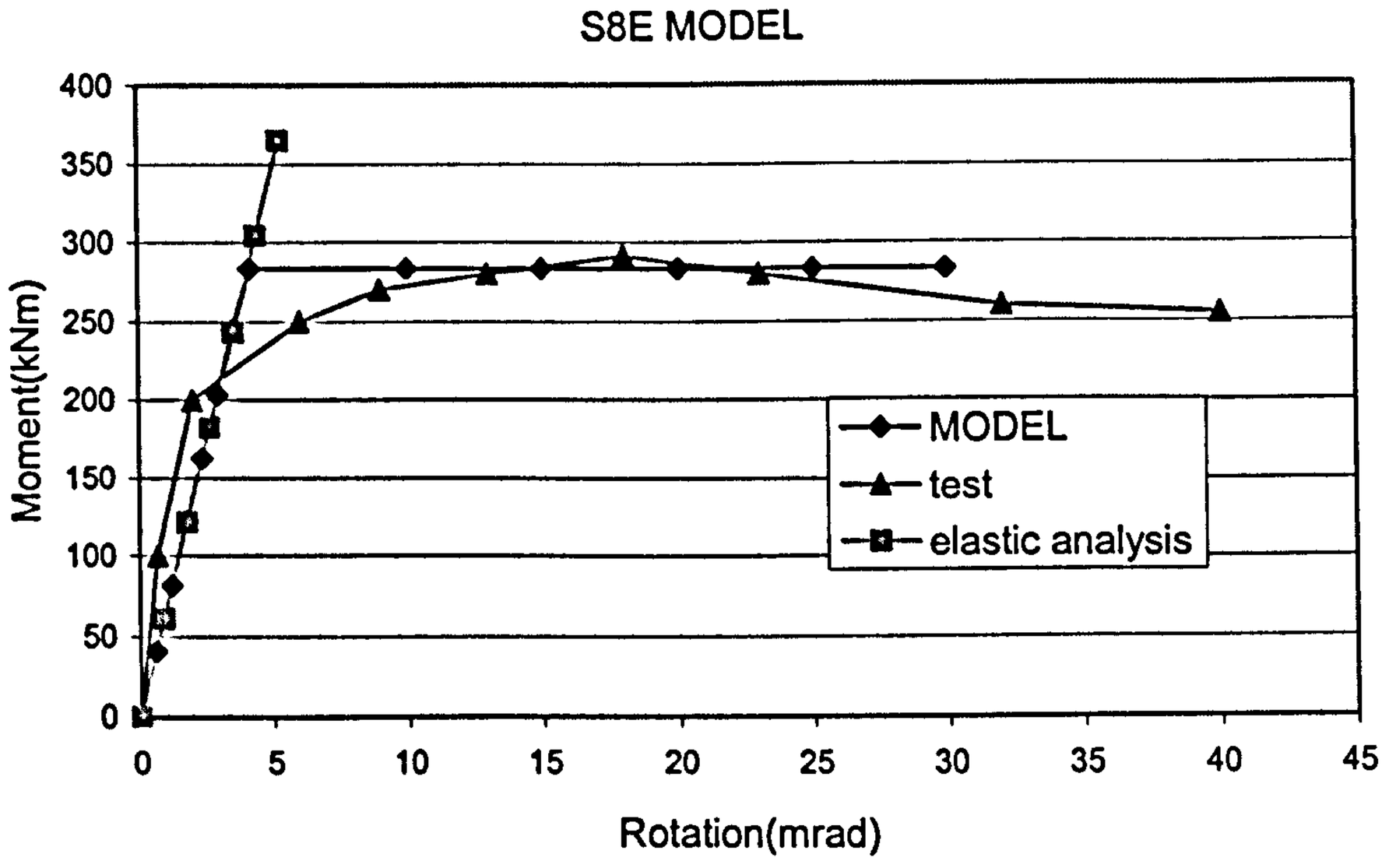

Figure 5.17d Moment-rotation curve of S8E model

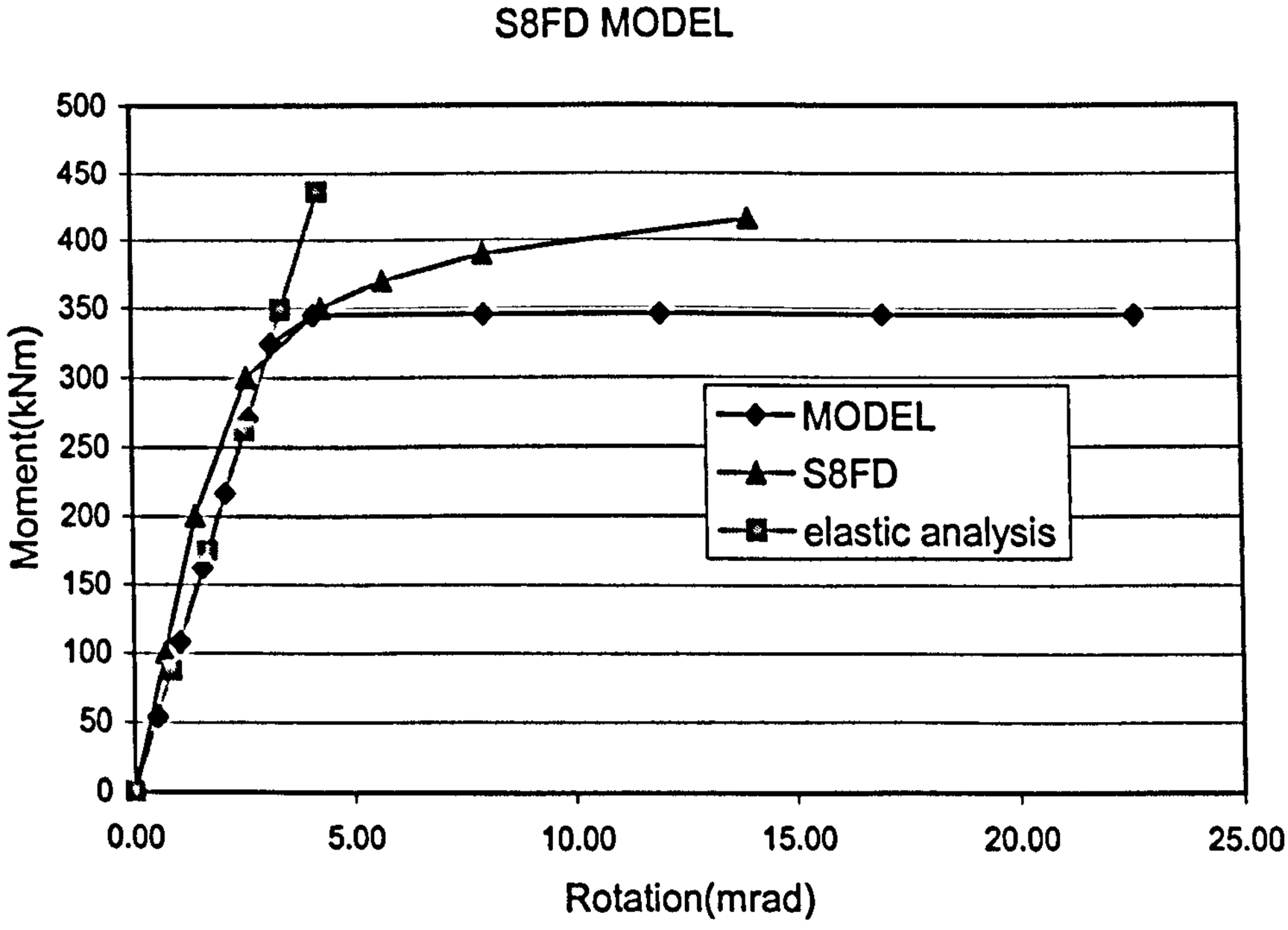

Figure 5.17e Moment-rotation curve of S8FD model

Through the finite element analysis of these five composite joint models – S4F, S8F, S12F, S8E, S8FD – we can see that good agreement is achieved compared with the joint tests. From the moment-rotation curves of the joint models, it can be seen that the joint moment remains constant until failure. The yield moment is taken as equal to the moment of resistance of the joint. The reason for this is that for all materials, an elastic-perfect plastic stress-strain relationship is assumed. As a result, the predicted yield moment of the joint is higher than the tests. The yield joint moment from tests is about 60-70% of the joint model and the predicted moment of resistance is conservative compared to the tests. The initial stiffness of the joint is calculated from joint moment and rotation of the first load increment and the rotation capacity is taken as the value where the iteration stops. Except for the rotation capacity of S8FD model, all predicted values are on the safer side and in a close range to the test results.

In the first three tests - S4F, S8F, and S12F, the amount of reinforcement is changed. The numbers 4, 8 and 12 are the numbers of T12 bars are placed in the slab. By comparing the analytical results of joint models with tests through Figures 5.17a, b, c, it can be observed that with the increase of the reinforcement in the concrete slab, the moment of resistance, rotation capacity and the initial stiffness of the composite joint are all increased. For tests of S4F and S8F which fail by rebar fracture, the joint model predicted the moment-rotation curves satisfactorily. For S12F which fails by the local buckling of beam bottom flange, the model predicted the moment of resistance and initial stiffness well but underestimated the rotation capacity.

In the S8E test, an extended end plate is used compared to S8F. Both test and model analysis have shown that the moment of resistance and initial stiffness increased. Since S8E failed by the local buckling of beam bottom flange in the test, the rotation capacity the two tests cannot be compared. The joint model, however, again underestimated the rotation capacity of S8E.

In the S8FD test a large steel beam section is used compared to S8F. The model analysis shows that there is a significant increase in the moment of resistance and initial stiffness, but a significant decrease in the rotation capacity. S8FD fails by the fracture of the rebars. And in this case the model overestimated the rotation capacity of the joint compared to the tests. It should be noted that in the test S8FD was unloaded twice: at about 60% of the failure load and at about 90% of the failure load. The first unload-reloading procedure would not affect the joint properties much because the joint is mostly in elastic stage. In the second unloading-reloading procedure, however, when the whole joint is plastic and near failure, the plasticity of the materials, especially the rebars would decrease. And the brittle fracture of the rebars would occur. In such a case, the joint fails when the moment reaches its maximum value. Unlike the other three tests, the descending stage of the moment-rotation curve would not occur. In the joint model the elongation of the rebars at failure is taken as 17% for all joints. This may not be true for S8FD.

In the proposed model, it is assumed that the joints fail by the fracture of the rebars. For joints falling into the assumption, the proposed model predicts the characteristics of the joints quite well. For joints failing by local buckling of beam bottom flange, this assumption has little influence on the prediction of the moment of resistance and initial stiffness, but the proposed model tends to underestimate the rotation capacity.

By studying the moment-rotation curves from joint tests, except for S8FD, it can be found that they are very similar to normal material tests on steel members, i.e., the curve may be roughly divided into three stages: elastic stage, hardening stage, and post-hardening stage. Due to the complexity of composite joint deformations, the yield moment of the joint is not clearly distinguished. The value of $0.67M_{Rd}$ may be used as the yield moment (Brown & Anderson, 2001). After yield, a hardening plateau can be observed. The peak value of the joint moment is taken as the moment of resistance of the composite joint by Anderson & Najafi (1994). The moment-rotation curve then declines

until failure. The joint rotation just before failure is taken as the rotation capacity in the tests.

According to the test curves of the moment-rotation relationship, a more accurate tri-linear moment-rotation relationship may be recommended for future composite joint design. In Figure 5.18, three straight lines are used to simulate the three stages of the moment-rotation curve. Point A is the elastic limit; point B simulates the peak point of the hardening stage when the joint rotation reaches 50% of the rotation capacity, and point C represents the point of failure. The yield moment is assumed to be $0.67M_{rd}$. It can be seen that the recommended tri-linear moment-rotation relationship is a more accurate simulation of the real composite joint behaviour.

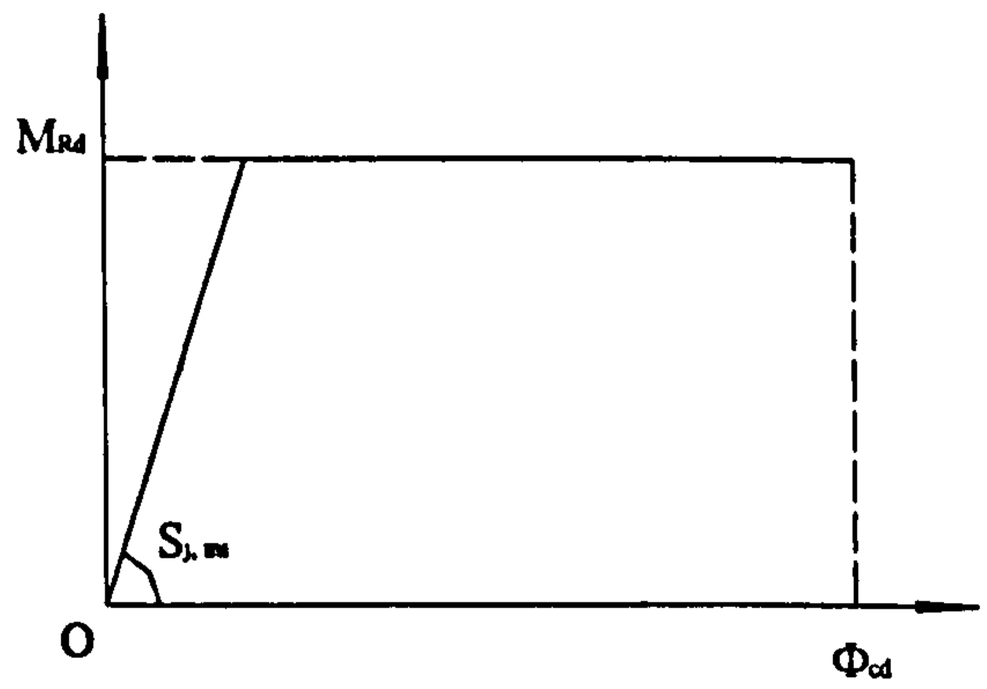

(a) Predicted bi-linear relationship from the proposed model

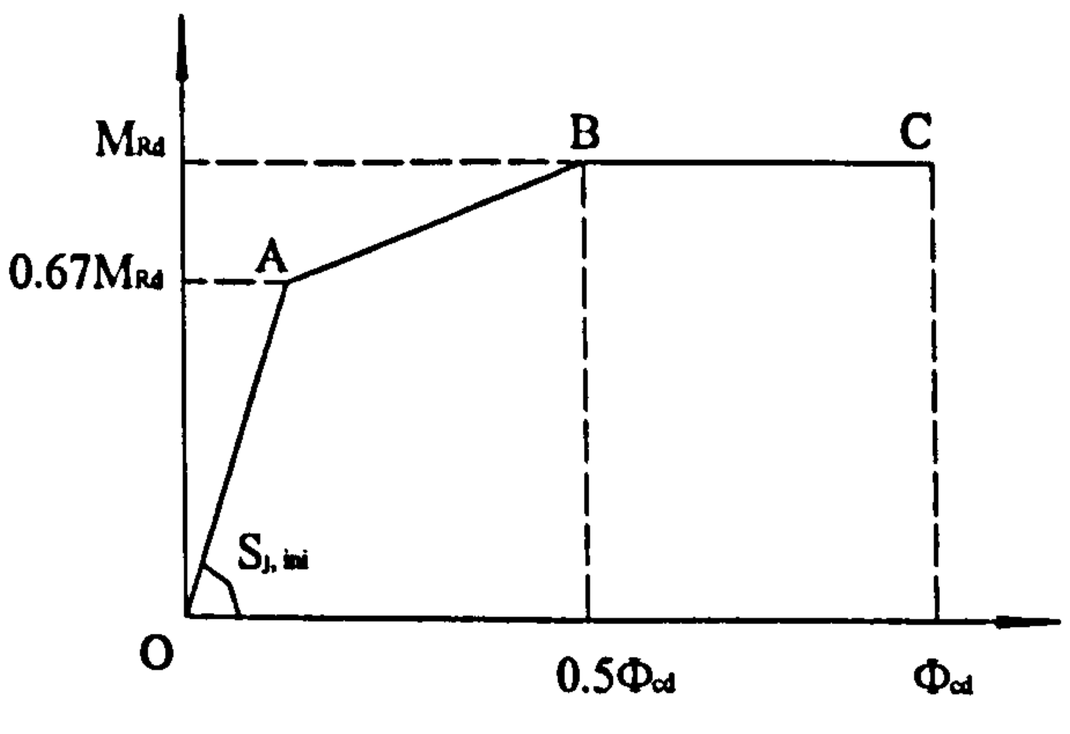

(b) Recommended tri-linear relationship

Figure 5.18 Proposed tri-linear moment-rotation relationship

5.3.3 Elastic analysis of composite joints

Since the proposed composite joint model is so simple that it uses only bar and beam elements, it is possible that such problems may be solved by small structural analysis packages, such as QSE, rather that employing big finite element analysis programs. Packages like QSE program are widely available at much lower price but they normally provide limited functions as linear elastic analysis only. Through linear elastic analysis, only the initial stiffness of composite joints can be predicted. The moment capacity and rotation capacity of the joint cannot be found. EC 3 provides a method to predict the moment capacity and rotation capacity of composite joints. By combining the linear elastic analysis and EC 3 method, the characteristics of composite joints can be obtained.

Linear elastic analysis is performed on the previously reported two series of composite joint specimens from the tests of Brown & Anderson (2001) and Anderson & Najafi (1994). Linear elastic analysis can be performed by using either QSE program or LUSAS program. Since plastic analysis has been performed on the composite joints previously, it is easy to do linear elastic analysis on the same model just by replacing the plastic material properties with elastic ones. Note that the shear deformations of beam elements are excluded when performing linear elastic analysis.

The results of the elastic analysis of the composite joint specimens are shown in Figures 5.13a, b, c, d and Figures 5.17a, b, c, d, and e. From the figures it can be observed that the moment rotation relationship from linear elastic analysis is the same as that of the elastic stage from plastic analysis of the joints, except for the Test 5 model. That follows that except for the Test 5 model, the initial stiffness is the same when using linear elastic analysis or plastic analysis. In other words, the predicted initial stiffness of linear elastic analysis has the same accuracy as the plastic analysis.

In Test 5, a deeper steel beam section ($533 \times 210 \times 82$) is used than other specimens ($457 \times 152 \times 52$) of the same joint series. From Figure 5.13d, it can be observed that the

joint rotations predicted by linear elastic analysis is slightly smaller that those from plastic analysis. The initial stiffness of Test 5 model from elastic analysis is therefore larger that that from plastic analysis. Note that in the joint test, Test 5 specimen failed by the local buckling of the lower flange of the steel beam. The decrease in the initial stiffness of the joint is probably caused by the early yield of the lower beam flange, which cannot be perceived by linear elastic analysis.

Considering all the above, linear elastic analysis can be performed on small structural analysis programs and give the same accuracy as plastic analysis carried out using a big finite element analysis programs in terms of the initial stiffness of composite joints. Together with EC 3, the characteristics of composite joints can be obtained with limited effort. In cases when early yield of joint members occur, linear elastic analysis may overestimate the initial stiffness of the joint.

5.4 Conclusions

A simple analytical composite joint model is proposed along with a shear stud model. It gives satisfactory predictions of the characteristics of composite joints in general. The proposed joint model is based on previous analytical models. The moment of resistance of the steel joint should be calculated according to Annex J of EC4 (1994) before the composite joint model can be established. A shear stud model is also proposed in order that the influence of the deformation of shear studs can be accounted for. The shear stud model is established according to its load-slip behaviour. For different shear studs, a different stud model should be established. The advantages of the proposed joint model are that a finite element model can be easily established once the moment of resistance of the steel joint is calculated, and the proposed model is simple to use and does not need further programming. To establish the shear model, however, the load-slip curve is needed.

The following assumptions are proposed in the formation of the composite joint model:

1. The composite joint is subject to negative bending.
2. The compression center coincides with the center of the bottom flange of the steel beam, and the whole composite joint rotates about the compression center.
3. Failing or buckling of the column web and flange in compression do not occur, and the deformations of the column web and flange in compression are neglected.
4. The shear deformation of column web in shear zone is neglected.
5. The deformations of the column web and flange in tension zone are neglected.
6. The rotation capacity of the composite joint is measured by the extension of the bar element in connection with the equivalent lever arm.
7. The full shear strength of the shear studs may develop before failing.

From the model analysis the following conclusions may be drawn:

1. The proposed model may be used in the predictions of the characteristics of composite joints subject to negative bending.
2. The deformations of the shear connectors are considered in the proposed model.
3. For composite joints failing by the fracture of the rebars, the predictions of the moment of resistance, rotation capacity, and initial stiffness are satisfactory. For composite joints failing by the local buckling of the bottom flange of the steel beam, the predictions of the moment of resistance and initial stiffness are satisfactory but the proposed model tends to underestimate the rotation capacity.
4. A tri-linear moment-rotation relationship is recommended for the future design of composite joints.

5. Linear elastic analysis of composite joints shows that it can provide the same accuracy in predicting the initial stiffness of composite joints provided that the early yield of the joint components does not occur. Together with EC 3, the characteristics of composite joints can be obtained without employing big finite element analysis programs. Due to the limitations of linear elastic analysis, elasto-plastic analysis needs to be performed to capture the whole history of the moment-rotation relationship of composite joints.

To conclude, the proposed semi-rigid composite joint model shows good agreement with tests and can effectively predict the moment of resistance, rotation capacity and initial stiffness of semi-rigid composite joints. It can be applied for the further studies of composite beams and frames.

Chapter 6 Modelling of composite beams with semi-rigid connections

6.1 Introduction

Research on composite steel and concrete beams dates back as early as the 1940's, and extensive research has been carried out on composite beams since then. Many tests have been done and the behaviour of simple supported composite beams under various loading conditions and different degrees of shear connections has been made relatively clear. More recently, research on composite beams with semi-rigid joint connections has taken place with several experiments having been carried out on such beams. Some analytical approaches have been proposed by different researchers. In this chapter, previous studies on composite beams are reviewed. The types of composite beam include: simple supported beams, two-span continuous beams, continuous beams with a cantilever beam. The types of support or joint connection include: roller support, web cleat joint and endplate joint. Several analytical composite beam models are reviewed. Finally, a simple and effective composite beam model is proposed by the author. The proposed beam model may be used for the analysis of simple supported beams, continuous beams, and beams with semirigid connections. The proposed beam model is validated against tests and published papers and satisfactory agreements are achieved.

6.1.1 Barnard & Johnson, 1965[1,2]

Barnard & Johnson (1965[1]) proposed a method of predicting the ultimate moment of resistance of composite beams. At the time of the study, it was accepted that welded-stud shear connectors could be designed by an ultimate strength method which assumes that connectors may be spaced uniformly in the region between adjacent cross sections of maximum and zero bending moment, and each connector is loaded to its ultimate capacity when the collapse load of the beam as a whole is reached. The number of connectors required in such a region is found by dividing the longitudinal force in the

steel at maximum moment by the capacity of one connector. It was also accepted that when the slab-width/span ratio is properly chosen, the distribution of strain across the slab would be uniform right to ultimate moment. Based on the above theory, it was assumed no slip occurred and the strain distributions in steel and concrete are both linear. A method of predicting the ultimate moment of resistance of composite beams was proposed by assuming both structural steel and reinforcement behave in a perfect elastic-plastic manner in both tension and compression. The method was validated by the results of six simple-supported beam tests performed by the authors and a computer programme developed by the authors. It was claimed that the theory predicted very accurately the value of maximum moment, when comparing with the results of both the actual and the computer tests.

A study on the plastic behaviour of continuous beams then followed (Barnard & Johnson 1965[2]). Four tests on three-span continuous beam were reported. Through studying the continuous beam test the authors indicated that shear connectors and appreciable slab reinforcement are desirable in negative moment regions. It was concluded that the simple plastic theory of simple supported composite beam may be used to predict the maximum moment of resistance of continuous composite beams where the concrete section is in compression.

6.1.2 Slutter & Driscoll, 1965

Slutter & Driscoll (1965) conducted a series of tests to investigate the ultimate strength properties of composite steel and concrete beams. The experimental work of the investigation consisted of twelve simple span composite beams of 15-feet span and one two-span continuous beam of the same span. The spacing of the shear connectors was varied among the beams and several different loading conditions were used in the tests. Based on the test results the authors proposed a criterion for minimum shear connector requirements for composite beams. And it was reported that when this criterion is satisfied, the ultimate strength of beams in which the neutral axis at ultimate moment

lies within the slab is not reduced by slip between slab and beam. A method of determining the ultimate bending capacity of beams with partial shear connection was proposed. The proposal was validated by test results and good correlation was obtained. Based on their tests, the authors suggested that the redistribution of load on shear connectors prior to failure makes it unnecessary to space the shear connectors in accordance with the shear diagram for the case of uniform loading. Regarding the test of the continuous beam, the authors suggested that not only the ultimate strength theory but, in a limited way, plastic analysis also may be applied to composite beams.

6.1.3 Ansourian, 1975

A three-dimensional elastic finite element analysis of composite beams was first reported by Ansourian (1975). The author firstly modelled the concrete slab as 8/16 node solid elements. And the steel beam was modelled as plane stress elements. Each flange was modelled as one element and the web as two elements. The top flange was connected to the lower surface of the slab elements. Satisfactory convergence was obtained with this method, but the data preparation for the solid elements was 'cumbersome'. A simplified simulation was then put forward.

In the second method, instead of solid elements the concrete slab was represented by a network of thin plate elements. And the steel beam was represented by conventional beam elements. In the assembly of the composite system, the plate elements were at the mid-surface of the slab, and the beam elements were at the centreline of the steel beam. The plate elements and the beam elements were connected by 'rigid links'. These were not actual physical members, but their function was simulated numerically by making the displacements along the beam axis depend on the displacements of the slab nodes located vertically above. The displacements at the nodes along the beam axis were therefore fully determined by the corresponding slab displacements. The proposed composite beam model proved to be effective in elastic analysis. The author then extended the same model for the plastic analysis of composite beams (Ansourian &

Roderick, 1978), in which the yielding of the steel, the nonlinearity in the concrete, and even the effects of the interface slip of shear connectors were included. The stiffness of shear connectors was determined by the load-slip curve obtained from push-out tests and simulated by an initial linear section followed by a polynomial. The plastic analysis proved to be successful compared with the results of six full-scale composite beam tests.

6.1.4 Kristek & Studnicka, 1982

Kristek & Studnicka (1982) used finite element method to investigate the influence of deformable connecters on the stress and deflections of composite beams. In their method, the concrete slab, steel beam flanges and web were idealized as an assembly of rectangular elements, called 'folded plates', connected along the longitudinal joints. The connection of the concrete deck to the top flange was made by a 'special element' to model as truthfully as possible the action of the connection. Due to the complexity of the 'special element', it was replaced by the 'rigid dummy links' between the centroidal axis of the concrete deck and the top flange of the steel beam. The stiffness of shear connectors was measured by 'the deformability characteristic of the connection' K, defined by the author.

The accuracy and convergence of the analytical model was tested through a simple supported composite beam carrying a harmonic loading of unit value at midspan. Then three types of composite beams were studied of the influence of deformable connections, and finally conclusions were made.

6.1.5 Razaqpur & Nofal, 1990

Razaqpur & Nofal (1990) developed a finite element program for the nonlinear analysis of general three-dimensional composite steel-concrete structures. Two composite beams and a bridge were analysed and compared with the corresponding experimental results. Good agreement was achieved. It is reported that the nonlinear finite element method

can used to reliably evaluate the inelastic behaviour and ultimate strength of composite beams and bridges.

In the analysis of composite beams, three parts of the structure must be properly modelled, i.e., the concrete slab, steel beam and shear connectors. In the program developed by the authors, the concrete slab was divided into several layers and each layer modelled as a quadrilateral membrane element called RQUAD4. And the top and bottom flanges and the web of the steel beam were each modelled as an improved discrete Kirchhoff quadrilateral plate bending element called IDKQ. The reinforcement in the slab was smeared and also modelled as an IDKQ element. A combined element was formed by combining the concrete layers, the smeared steel layer and the top flange layer. Each shear connector was modelled as a specialized bar element with three translational degrees of freedom at each end. The stiffness of the shear stud element was obtained from an empirical load-slip relationship:

$$F = a\,(1 - e^{-b\lambda})$$

Where F = shear force in a given direction acting on the connector; λ = slip in the direction of F; a and b = experimental constants, depending on the connector geometry and strength as well as the surrounding concrete strength; and e = base of natural logarithm. The shear connector element was capable of modelling of full, partial, and no interaction at the interface of the concrete and the steel beam.

6.1.6 Wright, 1990

A series of full-scale beam tests were carried out to investigate the behaviour of composite beams with discrete flexible connection. The folded plate method of Kristek & Studnicka (1982) was used to simulate the composite beams. In Kristek & Studnicka's (1982) method, the concrete slab and the steel beam were modelled as plates and jointed by 'dummy' elements. By adjusting the material properties of the dummy

element, the shear stiffness may be simulated. This method is suitable for linear shear connection. Wright (1990) extended the folded plate method to account for discrete non-linear connection by disconnecting the dummy element from the beam, and introduced longitudinal forces along the surface to represent the stud connections. By adjusting the forces, it is possible to match the load-slip relationship found from push-off tests. As each stud load and resulting slip is applied individually to the analysis, non-linear effects are automatically included.

6.1.7 Oven et al., 1997

In composite construction, composite action is achieved by means of shear connection, typically in the form of headed studs welded to the steel flange and embedded in the concrete slab. The design capacity of composite beams is based on the assumption of full interaction, and the number of shear connectors required to achieve this can be calculated. However it is not always practical to accommodate this number of studs, particularly when profiled decking is used as part of a composite slab. The connectors can only be fitted at the profiled troughs, and this limits the spacing of studs. Under these circumstances modified calculation methods must be used to take into account the partial interaction that develops. Thus the advantages of composite interaction can be realised, but in a reduced manner. Oven et al. (1997) proposed an analytical model for investigating the behaviour of such composite beams.

The model is based on a two-dimensional non-linear finite element analysis program INSTAF, developed originally for steel frames. And it is extended to include the reinforced concrete slab and the slip at its interface with the steel in composite construction. The steel I-section is modelled by line elements with four degrees of freedom at each node, namely the axial displacement, axial strain, vertical displacement and rotation. The program considers material non-linearity of the steel, geometrical non-linearity due to large displacements, and a non-linear strain-displacement relationship. In the proposed model the additional effects of material non-linearity in the concrete and

shear connectors, and the effect of slip on large displacements are also incorporated. The concrete slab and slip at the interface are taken into account by introducing two parallel line elements representing the beam and slab. The model includes two additional degrees of freedom, allowing the concrete and steel to have independent axial displacements and strains. In the case of partial interaction the axial deformations of the slab and the bean are different and two line elements representing these two components are used, with axes positioned at the centroids of the concrete slab and steel I-section. The assumptions made by the author are:

- The distributions of axial strain in the concrete slab and the steel I-section are assumed to be linear but different from one another;
- The shear connectors are assumed to be act as a continuous shearing medium along the length of the beam, between the concrete slab and steel I-section;
- The vertical displacement, rotation and curvature of the concrete slab and the steel I-section are identical at the end of an element.

Nonlinear stress-strain relationship of steel and concrete is used. And a tri-linear stress-strain relationship is adopted for shear connectors.

In order to define the transformed section the composite cross-section is divided into 11 segments. The variation in strain is assumed to be linear across each segment. The width of each region is modified by multiplying by the current tangent modulus divided by the initial elastic modulus. Once the transformed thickness of each region has been determined, the first and second moments of area of the total cross section can easily be calculated.

In order to validate the program, some comparisons were made with test results published previously for composite beams with partial interaction. Both simple supported and continuous beam were included in the validation. The comparison shows that the analysis gives consistent results. It is reported that the analysis appears to predict the deflection and slip behaviour at various load levels quite well. The program is

believed to be very effective in predicting slip behaviour, and could lead to more economical design of composite beams with partial interaction.

6.1.8 Salari, *et al.*, 1998

In a steel-concrete composite beam, the strength and stiffness of a composite section depend on the degree of composite action between the steel and concrete components. The degree of composite action is related to the geometrical and mechanical properties of the shear connectors. Therefore in a realistic analytical model the actual strength and stiffness of the mechanical connectors must be accounted for. Based on previous research, a force-based composite beam element was proposed for the analysis of composite beams under small displacements. This element is believed to be more accurate and computational efficient than previous approaches by modelling the internal forces in a more precise and consistence manner. In order to establish the element, the basic equations that govern the behaviour of a composite beam with deformable shear connectors are derived. The equations are then used to develop a composite beam element in a force-based finite-element framework. The element consists of two beam components, i.e., the concrete and the steel beam, and an interface. The interface model represents the shear connectors because it is accepted that a distributed interface with equivalent strength and stiffness properties can be used to simplify the discrete distribution of shear connectors. The interface shear in the force-based element is approximated with a cubic polynomial. The proposed composite beam model by Salari, *et al.* (1998) is illustrated in Figure 6.1.

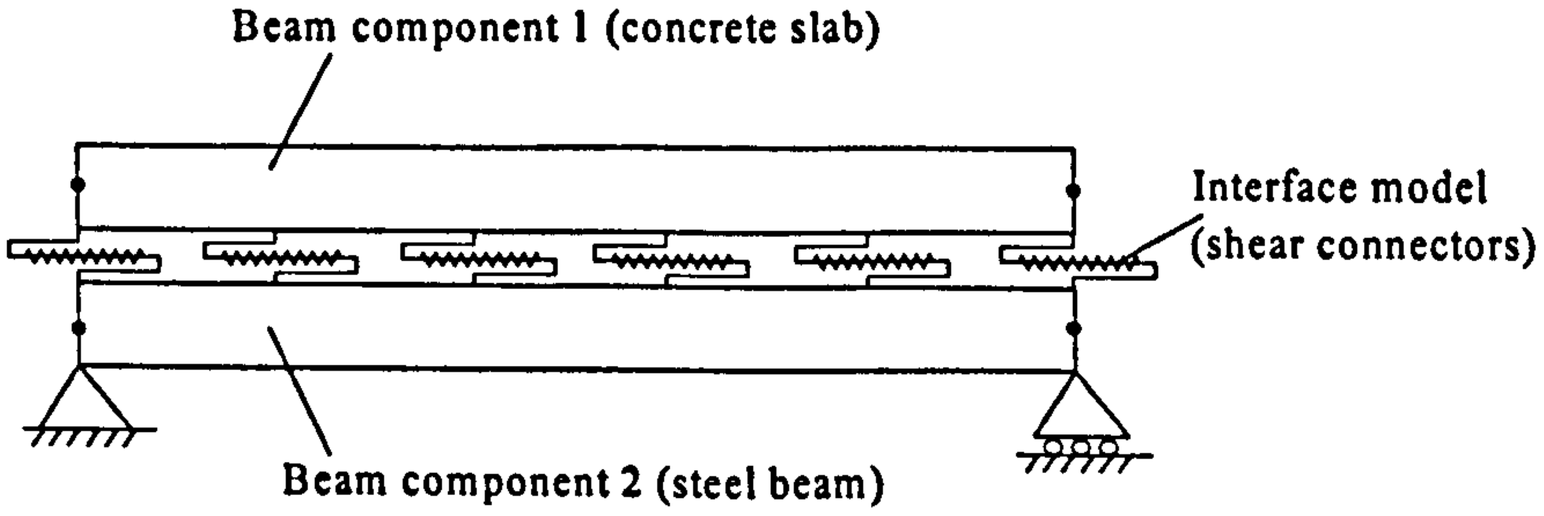

Figure 6.1 Proposed composite beam model by Salari, *et al.* (1998)

6.1.9 Wang, Y. C., 1998

As we know, it may not always be possible or necessary to design a composite beam with full shear connection because the number of shear connectors may be too large to be accommodated in a composite beam especially when the profiled steel sheeting is used, and secondly the applied load could be safely sustained with less shear connectors than required by full shear connection. Therefore it is necessary to study the deflection of composite beams with partial shear connection. A number of design equations have been available for calculating the maximum deflection of a composite beam with partial shear connection in design codes, i.e., BS 5950 Part 3, Eurocode 4 Part 1.1, and the American Institute of Steel Construction (AISC) design guidance (1993). By studying the relationship between the composite beam deflection and the stiffness of shear connectors, Wang (1998) proposed a new simple method for calculating the maximum deflection of composite beams with partial shear connection based on existing solutions.

In the study, the analytical solution for a simple supported beam with uniformly distributed load was used, and the following assumptions were made:

- Shear connection stiffness is uniform along the length of the composite beam
- The curvature and vertical deflection of both the steel and concrete components are the same as those of the beam
- The beam behaviour is linear elastic
- Deflection is small and shear deformation in the steel and concrete components is neglected
- Only shear connectors provide composite action between the steel and concrete components

An equation relating to the stiffness of shear connectors for calculating the deflection of composite beams with partial shear connection was obtained. It is noted that the proposed equation can be used for composite beams with other types of loading and boundary conditions.

For the validation of the proposed method, a finite element analysis is used. In the finite element modelling, a composite beam is divided into a number of line elements. Four degrees of freedom are assigned to each node. They are the axial displacement of the steel component (U_s), the axial displacement of the concrete component (U_c), the vertical deflection (V), and the rotation of the beam (θ). This finite element analysis beam model is shown in Figure 6.2. The two axial displacements at each node are related via the shear connector stiffness. For composite beams under various loading conditions and support conditions with shear connector stiffness ranging from providing no shear interaction to nearly complete shear interaction, the differences between the finite element predictions and the proposed equations are reported to be less than 5%. Comparisons are also made among a few available tests, design codes, and the proposed equations. The proposed method is reported to be effective.

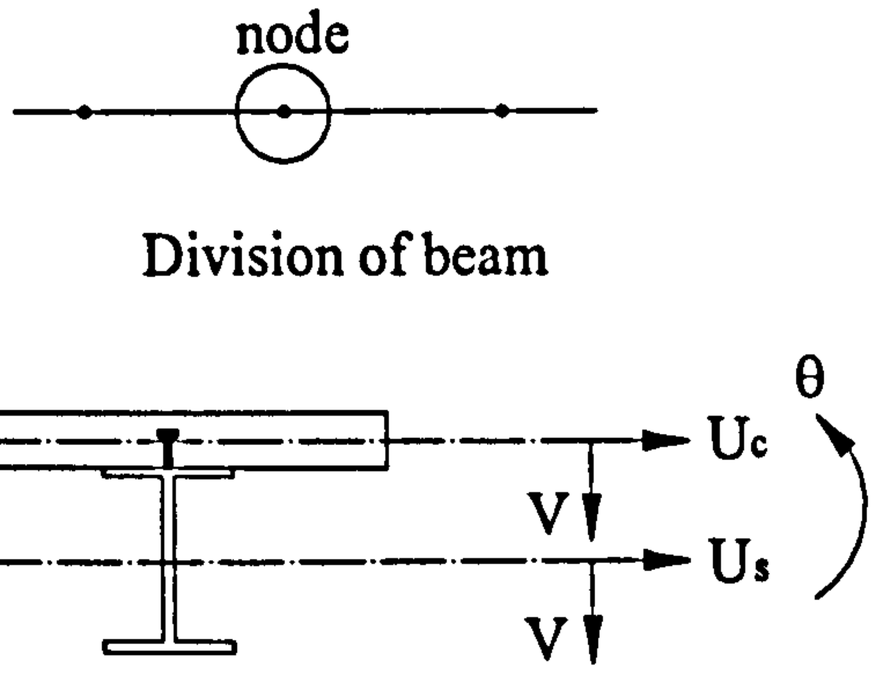

Figure 6.2 Finite element composite beam model used by Wang (1998)

6.1.10 Kim, 1999

Kim (1999) studied a continuous stem girder system comprising two cantilevers and a interspan composite beam. Experimental work and finite element analysis method were

employed in the study. For the finite element analysis, the push-out specimen was simulated. And then the whole beam system was analysed. The LUSAS program was used for the analysis.

- Push-out specimen

The push-out specimen was modelled by 2-dimensional finite elements. The steel beam, concrete slab and studs were modelled as plane stress elements, and the profiled steel sheeting as bar elements. The stud was assumed as a rectangular section. The properties of the circular stud section were transferred to an equivalent rectangular cross-section. The analysis shows that the load-slip curve is little changed if the profiled steel sheeting is neglected. Comparing the load-slip curves from test and analysis, it can be seen that the 2D modelling was not completely successful. A 3D linear elastic modelling of the push-out specimen was then preformed, in which the steel beam and the profiled sheeting were modelled as shell elements, the studs as beam elements, and the concrete as volume elements. The 3D analysis showed a better agreement to the test curve especially in the early stage of loading. The author believed that a 3D non-linear analysis might give a good agreement to the test curve. But it could not be realized because of the limitation of 3D elements of the LUSAS program and the time taken for the analysis.

- The continuous stem girder system

Kim (1999) performed linear-elastic two-dimensional finite element analysis of the continuous stem girder system. The steel beam and concrete slab were represented by beam elements at their mid-surface and connected by 'rigid links'. The profiled steel sheeting and the concrete in troughs were not taken into account. The rigid links were connected together using joint elements at the location of the top flange of the steel beam. The joint elements represented the shear studs, and the elastic connection stiffness from push-out tests was given the joint stiffness. Two beams were analysed and it was believed that the model was 'reasonably correct'.

6.1.11 Sebastian & McConnel, 2000

Sebastian & McConnel (2000) developed an advanced nonlinear finite element program for the analysis of general composite structures of steel and reinforced concrete. For composite beams, a four-noded layered thin-plate bending-membrane (2D) element was used to model the concrete slab, with nodes located at the base of the slab to enable connection of shear stud element. A two-noded layered bending-membrane (1D) element was used to model the steel beam, with nodes located along the concrete slab-steel beam juncture line. Each shear connector was modelled by a novel concrete slab-steel beam interface (stub) element of zero length consisting of axial and rotation springs. The stiffness of the axial springs was determined by an empirical shear force-slip relationship, and partial shear interaction was enabled. The stiffness of the vertical springs and rotational springs was assumed as 'very high'. The composite beam model is shown in Figure 6.3.

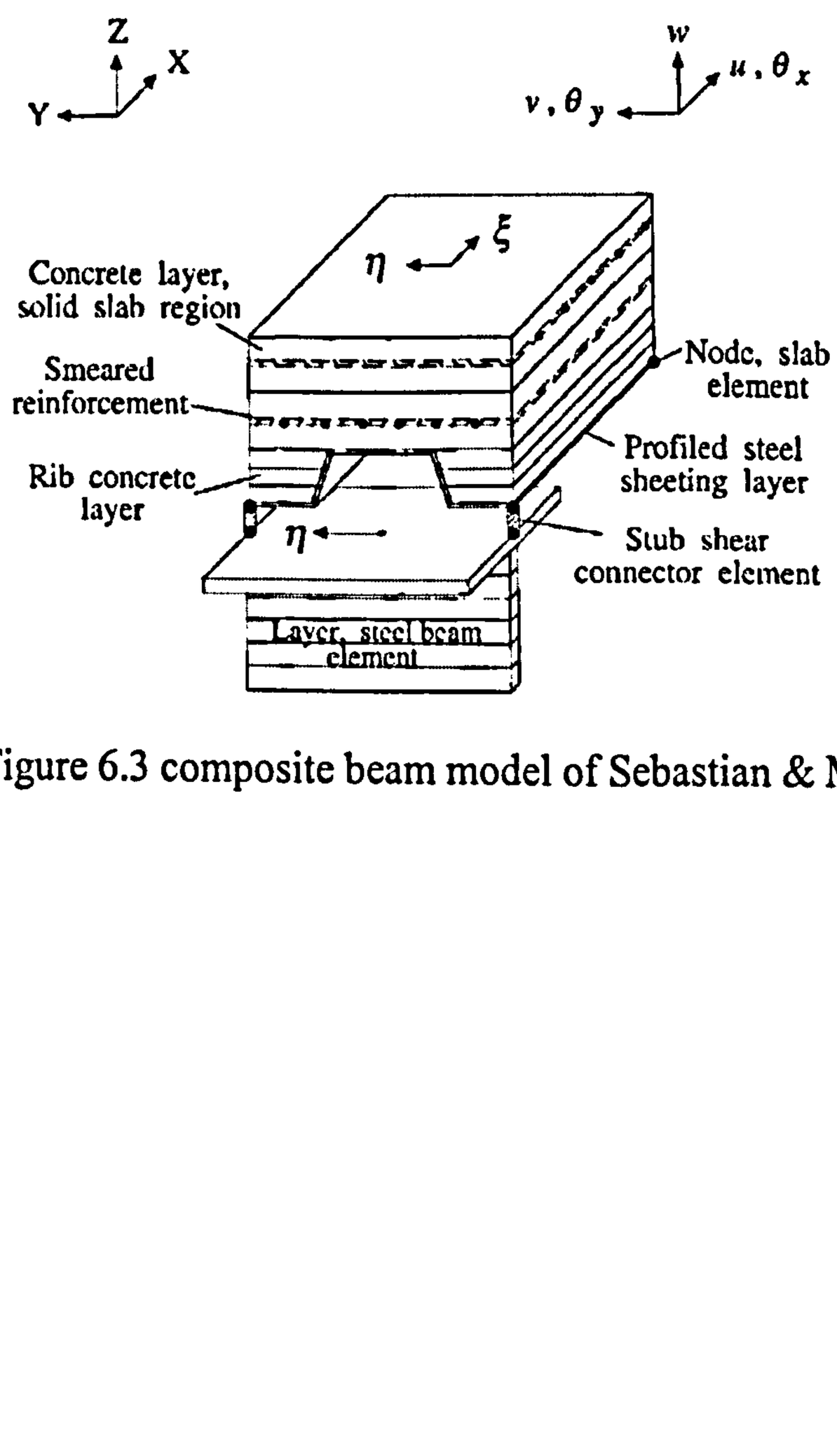

Figure 6.3 composite beam model of Sebastian & McConnel (2000)

6.1.12 Summary of literature review

In reviewing previous finite element analysis of composite beams, it can be found that the finite element method is an effective and economical way to analysis composite beams. Both three-dimensional and two-dimensional models may be used in the analysis. 3D analysis generally achieved more accurate results than 2D analysis. 2D analysis, on the other hand, is much simpler and acceptable accuracy may be achieved if the elements are properly designed. Nonlinear analysis must be included if a satisfactory analytical model is expected. With the development of finite element techniques and modern computer technology, the cost of nonlinear analysis has been greatly reduced. In a composite beam model, the modelling of shear connectors plays a key role. Various shear connector elements have been suggested by different researchers. The stiffness of shear connector elements is either determined from test load-slip curves or simulated by empirical load-slip curves. By incorporating shear connector elements, the behaviour of composite beams with different degrees of shear connection can be analysed.

In this chapter, a very simple composite beam model is proposed by incorporating the proposed composite joint model reported in Chapter 5. The elements of the beam model are all selected from LUSAS program, therefore no extra programming is needed. The proposed model is capable of analyzing composite beams with different degrees of shear connection, various loading conditions, and different types of joint support conditions.

6.2 Proposed model of composite beams

Since the composite joint model has been proposed, the idea is consequently used and extended to the modelling of composite beams. For a composite beam, the concrete slab, steel beam and shear connectors are modelled. For composite beams with semirigid joint connections, the composite joints are also modelled according to the proposed joint model of Chapter 5. When profiled steel sheeting is used in a composite beam, the steel

profile sheeting and the concrete in each trough are omitted. Also the reinforcement in concrete slab is neglected as well. The selection of elements is based on the element library of the LUSAS program. The proposed composite beam model is illustrated in Figure 6.4.

In the proposed model each component of the composite beam is described as the following

- Steel beam

  The steel beam is modelled as conventional beam elements in line with the geometric centre of the steel beam cross-section. For elasto-plastic analysis, idealized elastic-perfect plastic of bi-linear stress-strain relationship is assumed for steel beam elements.

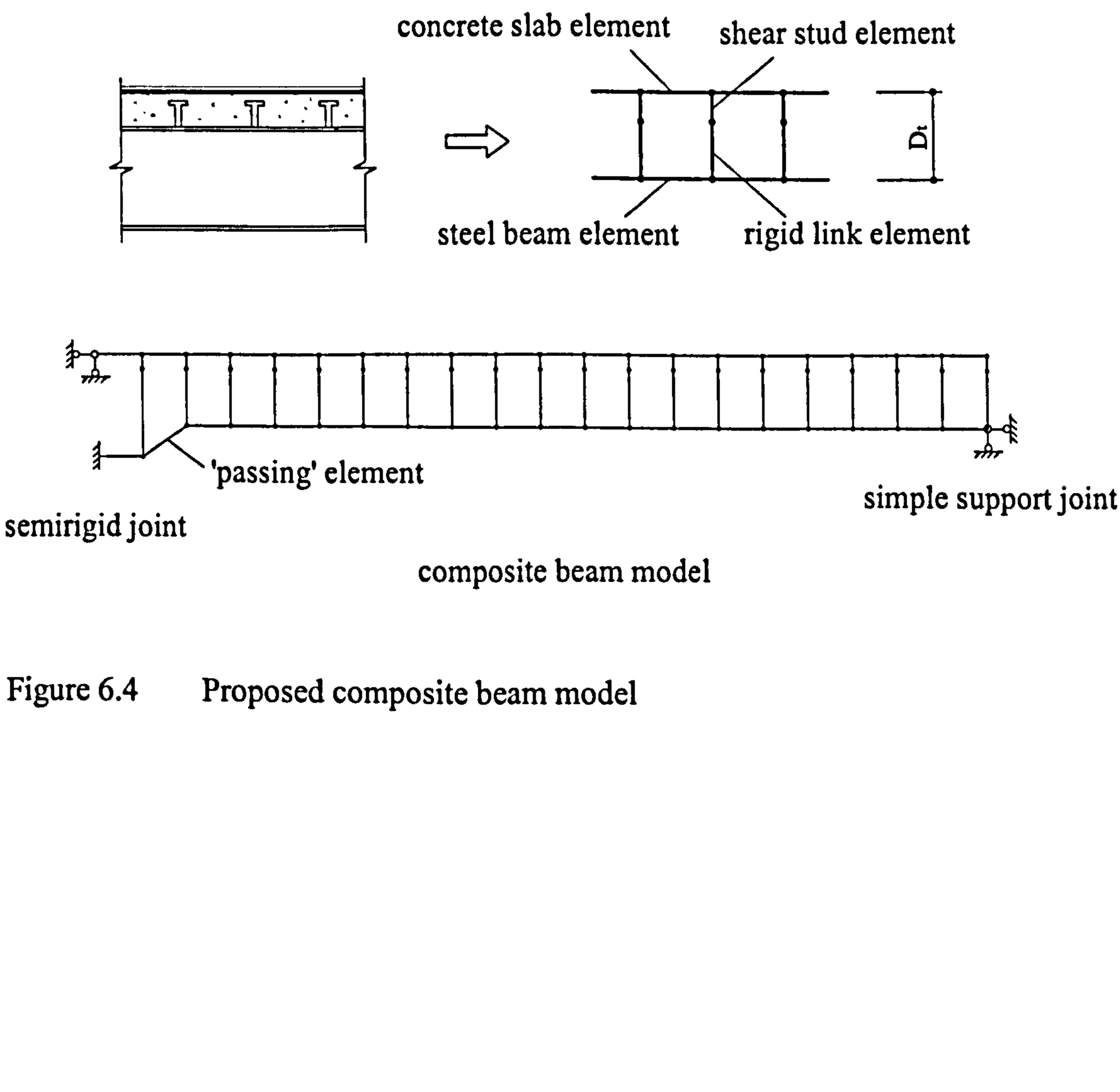

composite beam model

Figure 6.4 Proposed composite beam model

- Concrete slab

  The concrete slab is modelled as nonlinear cross-section elements in line with the center of the main reinforcing bars. Normally, the concrete slab elements should be placed at the geometric centre of the cross-section neglecting the troughs. For simple supported beam, where joint moments are assumed zero, this method should be adopted. For beams with semirigid joints, where the proposed joint model is incorporated, an eccentricity would occur if the concrete slab elements are placed at its geometric centre of the cross-section. To avoid this eccentricity, the centre of the concrete slab elements is shifted up to coincide with the centre of the rebar elements. Trial analysis on simple supported beams has shown that very little difference is observed because of the shift of the concrete slab elements, since the eccentricity is usually small (within 5cm) compared to the overall depth of the composite cross-section.

- Shear connectors

  The shear connector model derived for the composite joint model is used in the beam model. The length of the shear stud elements is taken as the after weld length of the shear studs. They provide vertical links between concrete slab elements and rigid link elements

- Rigid links

  Vertical beam elements are placed between the shear stud and steel beam elements. They have very high stiffness, i.e., $E_{link}=10^3 E_{steel}$. The geometric properties are assumed to be the same as the steel beam elements. The high stiffness is to ensure little energy loss in force transfer between the shear studs and the steel beam.

- Composite beam-to-column joints

  For beams with semirigid joints, the proposed composite joint model of Chapter 5 is used. The equivalent lever arm (D_{eq}) is calculated according to the geometric

and material properties of the joint. Since the equivalent lever arm (D_{eq}) is always greater than the 'transformed beam depth' (D_t) (Figure 6.4), an eccentricity will occur between the centres of the steel beam elements to the beam element in line with the compression center of the joint. A slanted 'passing' steel beam element is therefore needed to complete the beam model. It should be noted that more 'passing' elements are need to avoid sudden change of beam element center if the eccentricity is too large. For simple supported beams, there is no need to calculate the equivalent lever arm (D_{eq}) because the joint moment is zero. And the transformed beam depth (D_t) is used along the whole beam span.

6.3 Validation of the proposed composite beam model

Firstly two composite beam examples from 'Steel Designer's Manual' (Owens *et al.*, 1994) are analysed: a simple supported beam, and a two-span continuous beam with same beam design data. This is to compare the FEM analytical results with the design code, i.e., BS5950, Part 3 (1990). Secondly, the composite beam model is used to analyse four composite beams with different degrees of shear connections. And the results are compared with the beam tests (Wright, 1989). Lastly a continuous beam with a cantilever beam is analysed, and the results are compared with the test by Rakib (1991).

6.3.1 Beam model vs. BS5950, Part 3

Two composite beam design examples can be found in '*Steel Designer's Manual*' (Owens *et al.*, 1994). One is a simple supported beam, and the other is a two-span continuous beam with same beam design data. They are designed according to present composite beam design code - BS5950, Part 3 (1990). Both beams are modelled and analysed in LUSAS. The mid-span or maximum deflections under imposed loading and the natural frequencies are obtained through the analysis.

6.3.1.1 Modelling of 12m-span simple support composite beam

This is a 12-meter-span composite beam with a total imposed loading of 18kN/m. The composite slab is 130mm deep with the profile height of 50mm. The effective breadth of concrete slab is taken as 3m. The trough spacing and average width are 300mm and 150mm, respectively. The cube strength of concrete f_{cu} is 30N/mm^2, and the density of the lightweight concrete is taken as 1800kg/cm^3. For the steel beam a UB457x191x67 grade 50 (p_y=300N/mm^2) is chosen. Shear connectors are 19mm diameter and 95mm as-welded length. Two shear connectors are placed per trough providing the 0.76 degree of shear connection. The modelling of this composite beam is shown in Figure 6.5.

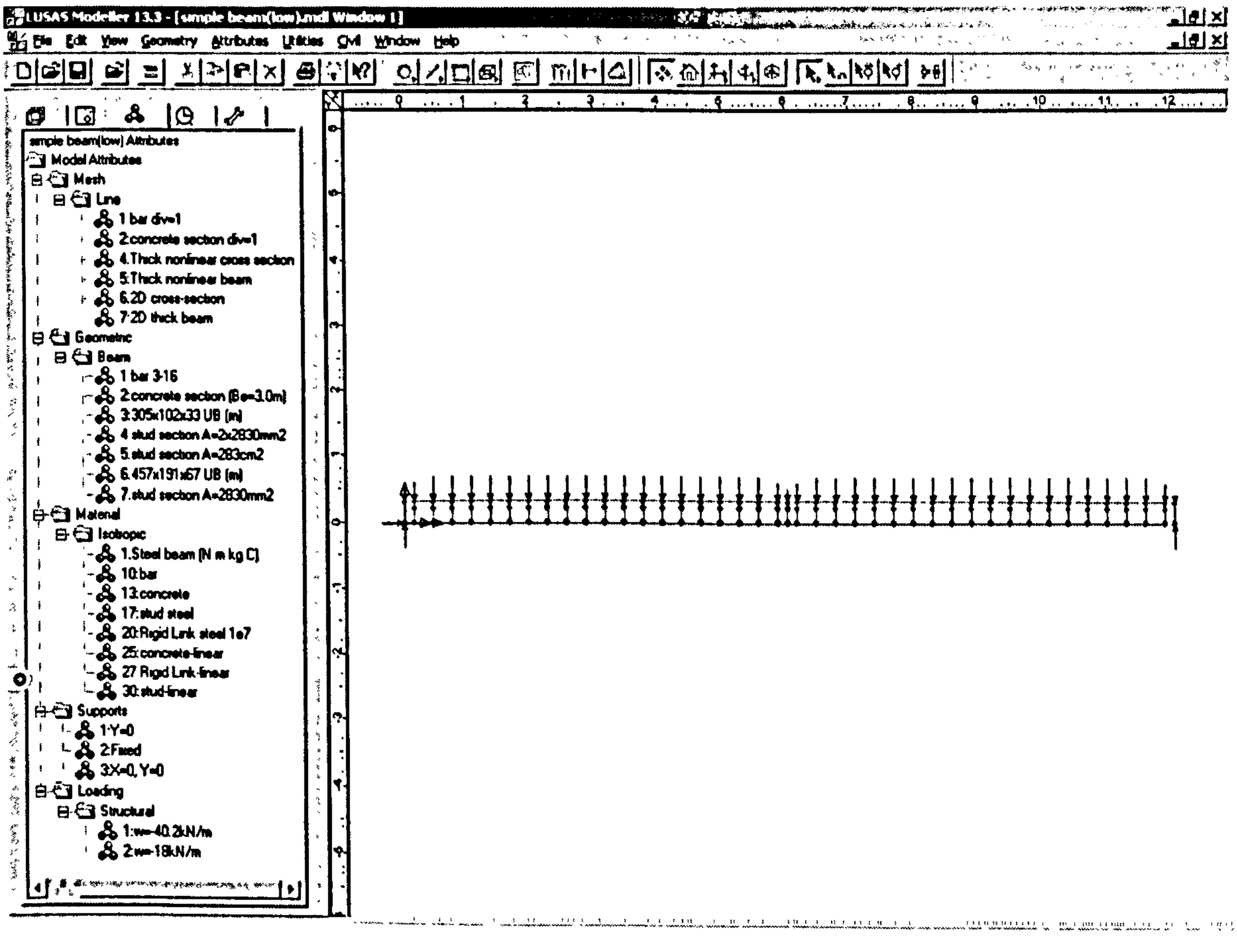

Figure 6.5 12m-span simple support composite beam model in LUSAS Modeller

In order to get the mid-span deflection, one extra pair of shear stud element and rigid link is placed at beam mid-span in the model. This will not affect the analytical results and the degree of shear connection of the composite beam because the shear force at mid-span is zero under uniformly distributed loading, and hence no shear force is transferred through the shear studs at mid-span. At both supports since the joint moments are zero, there is no need to calculate the equivalent lever arm, and the depth of the beam model is the 'transformed depth' (D_t) throughout the beam. In order to exclude the extra self-weight caused by the rigid link elements, the mass density of these elements is set zero when performing the eigenvalue analysis. Through the model analysis the mid-span deflection and natural frequency of the beam are obtained. And they are shown in Table 6.1.

Table 6.1 Analytical results of 12m-span simple support composite beam

	Mid-span deflection (mm)	Natural frequency (Hz)
Owens *et al.*, 1994	31.3	4.91
Beam model	28.8	5.95

From Table 6.1, it is can be seen that the prediction of the mid-span deflection is satisfactory with the error of 8% between the model analysis and BS5950. For the prediction of the natural frequency, the proposed model produced 21% higher value than the empirical method used by Owens *et al.* (1994). It should be noted that in computer program the lump mass method is used when calculating the natural frequencies of structures, in which the mass of the element is lumped at the nodes. This lump mass method has been generally accepted in the dynamic analysis of multi-freedom structures, and great accuracy may be obtained if enough elements are used in the finite element model. In *Steel Designer's Manual,* an simplified equation was used to predict the natural frequency of the beam.

$$f \approx \frac{18}{\sqrt{\delta_{sw}}} \tag{6.1}$$

where f is the natural frequency, and δ_{sw} is the deflection of composite beam subjected to instantaneously applied self weight. The instantaneously applied self weight includes the self weight of slab and beam, 10% imposed load, and ceiling load but excluding partitions. This empirical method is conservative and underestimates the natural frequency of the composite beam compared to the finite element analysis.

6.3.1.2 Modelling of two-12m-span continuous composite beam

The same design data is used as the simple support beam except that the effective breadth of the concrete slab is reduced to 2.1m and a smaller size (UB406x178x60) is chosen for the steel beam. The degree of shear connection is 0.86. In the reference 40% support moment redistribution is assumed when calculating the beam deflection. The natural frequency is calculated as if it were a 12m-span simple support beam.

The modelling of this continuous beam is shown in Figure 6.6. At both end supports the proposed joint model is not applicable because the joint moments are zero. As with the simply supported beam in Figure 6.5, the beam depth at both end supports is taken as the 'transformed depth' (D_t). At the middle support, however, a certain degree of continuity is maintained by the steel connections and the reinforcement over the support. The depth of the beam model at the middle support should be determined in accordance with the joint moment capacity. The proposed joint model is used at the middle support, and the depth of the joint is taken as the calculated equivalent lever arm D_{eq}. As with the simply supported beam, zero mass density is assigned to the rigid link elements in Eigenvalue analysis. Through the LUSAS analysis, the mid-span deflection, the natural frequency, and the negative moment at the mid-support are obtained. They are listed in Table 6.2.

From Table 6.2, it can be seen that the mid-span deflection of the continuous beam from the model analysis is 21% lower than the result of Owens *et al.* (1994), while the predicted joint moment is 17% higher than that of Owens *et al.* In '*Steel Designer's Manual*', the mid-span deflection is calculated by assuming that 40% of the maximum theoretical negative moment ($wL^2/8$) is carried out by the joint. Through the model analysis, the actual negative moment undertaken by the joint can be obtained, which is equivalent to 47% of the maximum theoretical support moment. Since the value of the negative moment has significant effect on the prediction of the mid-span deflection, there is no doubt that beams with higher joint moments will result in smaller mid-span deflections, and vice versa.

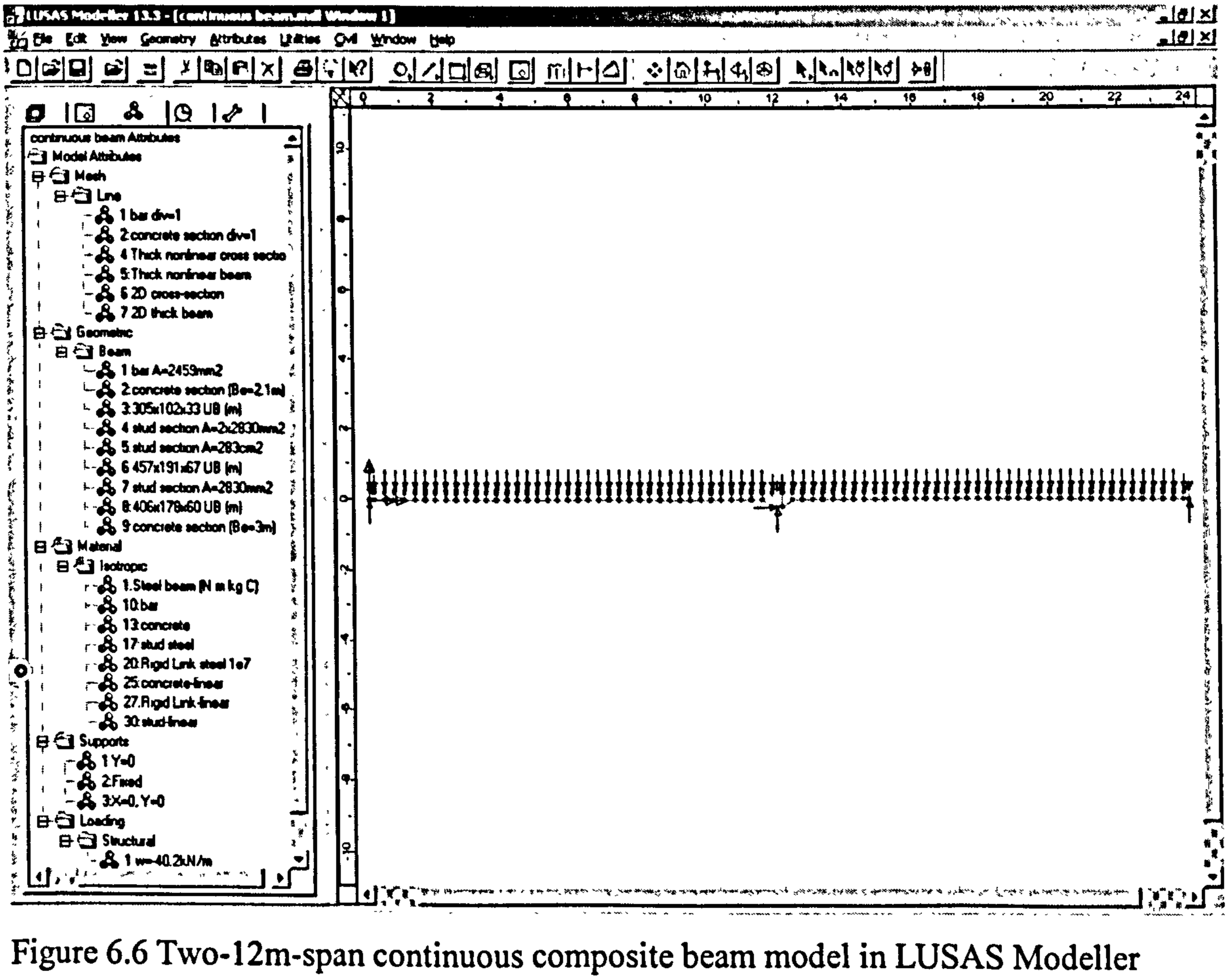

Figure 6.6 Two-12m-span continuous composite beam model in LUSAS Modeller

Table 6.2 Analytical results of the two span continuous composite beam

	Mid-span deflection (mm)	Natural frequency (Hz)	Negative moment (kNm)
Owens *et al.*, 1994	25.2	4.1	136 (40%)
Beam model	19.9	5.22	159 (47%)

For the natural frequency of the continuous beam, the proposed beam model produced a higher value than Owens *et al.* (1994). In '*Steel Designer's Manual*', the natural frequency is also calculated by equation (6.1), but assuming the continuous beam as a simple support beam. This method will underestimate the natural frequency because the stiffness of the simple beam is less than the continuous beam. The finite element method is believed to be more accurate.

To conclude, good agreement is obtained for the prediction of the mid-span deflection of the simple supported beam between the proposed beam model and BS5950, Part 3 (1990). For the continuous beam, since the 'real' negative moment carried by the joint can be obtained from the beam model, the prediction of the deflection of the continuous beam is believed to be more accurate. The empirical equation (6.1) is coarse in predicting the natural frequencies of composite beams, while the finite element analysis is effective and accurate.

6.3.2 Beam model vs. continuous composite beam tests of Rakib

Two full-scale continuous composite beam tests were reported by Rakib (1991) to investigate the behaviour of composite beams with semi-rigid connections. The beams were designed to have one full span of 8m with a loaded cantilever of 2.5m. The

supporting columns were two 875mm high universal columns bolted on the strong floor of the laboratory. In order to observe the semi-rigid joint behaviour, two types of joint connection were used in the test. A web cleat connection was used in the first continuous beam (named as Beam1) and a flush end-plate connection for the second one (named as Beam2). Concrete slabs with profiled steel sheeting were used and the troughs are perpendicular to the main span. Fourteen stud shear connectors were used for the main span and five studs were used for the cantilever beam. The stud spacing was 600mm. For both beams a theoretical shear connection of 50% was provided. Five point loads were applied to the continuous beam. One was applied at the end of the cantilever beam, and four equal loads were applied on the main beam at a spacing of 2m. The main design data of the two beams are as follows:

Concrete slab

Total slab breadth 2.5m, effective slab width 1.6m, slab depth 110mm, trough depth 50mm and trough spacing 300mm

Shear connectors

19mm diameter and 95mm after welding, 7 studs at half span providing an actual degree of shear connection of 0.47.

Steel beam and Supporting column

Beam UB 305 × 102 × 33 grade 43; column UC 305 × 305 × 97 grade 43.

Main reinforcement

16mm diameter high tensile steel bars were used. The average yield stress was 538N/mm^2, the ultimate stress was 699N/mm^2, and the average Young's modulus is 203kN/mm^2.

The material properties of the test specimen are shown in Table 6.3.

Table 6.3 Material properties of steel beams and concrete slab

Steel beam	f_y (N/mm^2)	E (kN/mm^2)	Total No. of studs
1	272	206	19
2	276	206	19

Composite beam	f_{cu} (N/mm^2)	E_c (kN/mm^2)	f_t (N/mm^2)	Reinforcement ratio at support
1	33.0	20.0	2.2	0.15%
2	40.0	21.8	2.85	1.0%

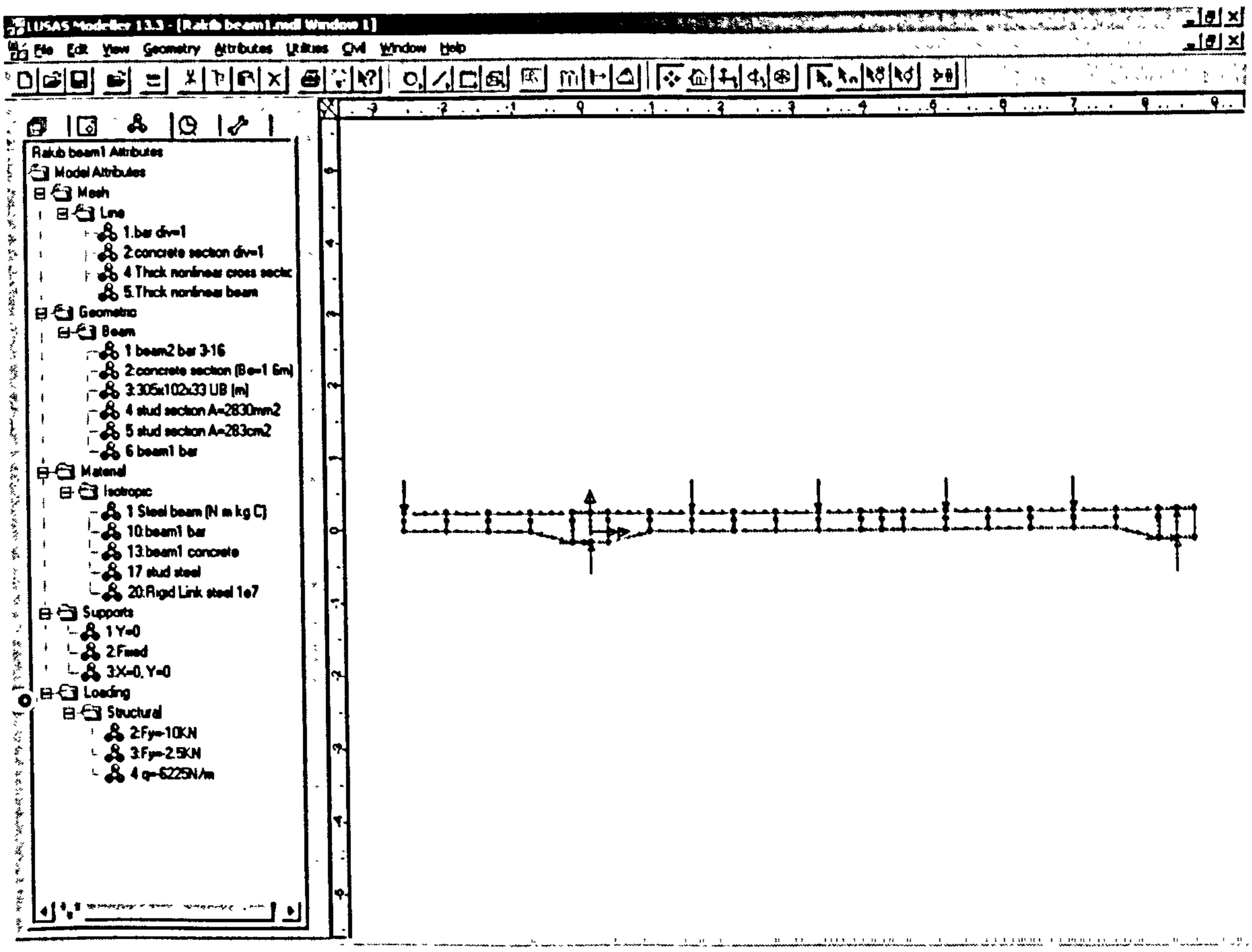

Figure 6.7 Continuous composite beam model of Rakib (1991) in LUSAS Modeller

- Modelling and analysis of Rakib's continuous beams

According to the provided design data these two continuous beams are modelled using the proposed composite beam model and analysed using the LUSAS program. The continuous beam model formed by LUSAS is shown in Figure 6.7. The steel beam is modelled as normal beam elements with elastic-perfect plastic stress-strain relationship. The concrete slab is modelled as nonlinear cross section elements with elastic-perfect plastic stress-strain relationship as well. The proposed stud element is used to model the shear studs. High stiffness rigid links are provided between the stud elements and the steel beam elements. In the joint areas bar elements are used to model the main reinforcement. Bi-linear stress-strain relationship is assumed to the bar elements according to the material properties. The geometries of the two beams are identical except that the beam depths at the supports are different. The beam depth at the support is determined by the steel joint configuration and the amount of slab reinforcement over the support. In the beam model it is taken as the equivalent lever arm of the reinforcement. For Beam1, the web cleat connection is regarded as pinned, the moment of resistance of the steel connection is consequently neglected. The equivalent lever arm of the reinforcement is therefore taken as the distance from the center of the reinforcement to the center of the bottom flange, i.e., D_{eq} = 402.3mm. For Beam2, the moment of resistance of the flush endplate connection must be calculated and from equation (5.8) the equivalent lever arm of the reinforcement is calculated as 562mm. The supporting columns within the beam depth are modelled as normal beam elements. Since the deformations of the columns were very limited during the tests, the supporting columns below the beam bottom flange are omitted to simplify the model and represented by support conditions of the beam model as shown in Figure 6.7. The beam model is loaded at four points within the main span and at the end of the cantilever beam according to the test arrangement.

Through model analysis, the mid-span deflections of the main span through the whole loading history are obtained. In Figure 6.8 the curves of the mid-span deflection versus

the total point loads are shown for both Beam1 and Beam2. The following is the observations of the model analysis from Figure 6.8.

- The load-deflection curves from beam model analysis are almost bi-linear. This is probably because of the assumed bi-linear or elastic-perfect plastic stress-strain relationships of the materials.
- The mid-span deflection of Beam2 is less than Beam1at the same load level. This is because the main reinforcement in the slab of Beam2 over the support is significantly increased compared to Beam1. Secondly, the steel joint is replaced from the web cleat connection of Beam1 to the flush endplate connection for Beam2. These two factors lead to the increase of the moment of resistance and the initial stiffness of the composite joint, and the deflection of the beam is consequently reduced.
- Beam2 model failed at a higher load level that Beam1 model. The reason for this is that the joint moment of resistance of Beam2 is higher than that of Beam1.
- The maximum deflections are close for Beam1 and Beam2. As load increases, the plastic hinges first appear at joint areas. As further increase of load will only increase the stress and strain of the beam span. As soon as the plastic hinge is formed at mid-span area, the beam will collapse. The deformation capacity of the composite beam is mainly determined by the beam span regardless of joint conditions. Because Beam1 and Beam2 are identical except that the joints are different, the maximum deflections of the two beams should be close when the beams fail.

From the analysis, it can be seen that the proposed model is capable of modelling such beams and the influence of slab reinforcement and steel joint conditions is satisfactorily captured.

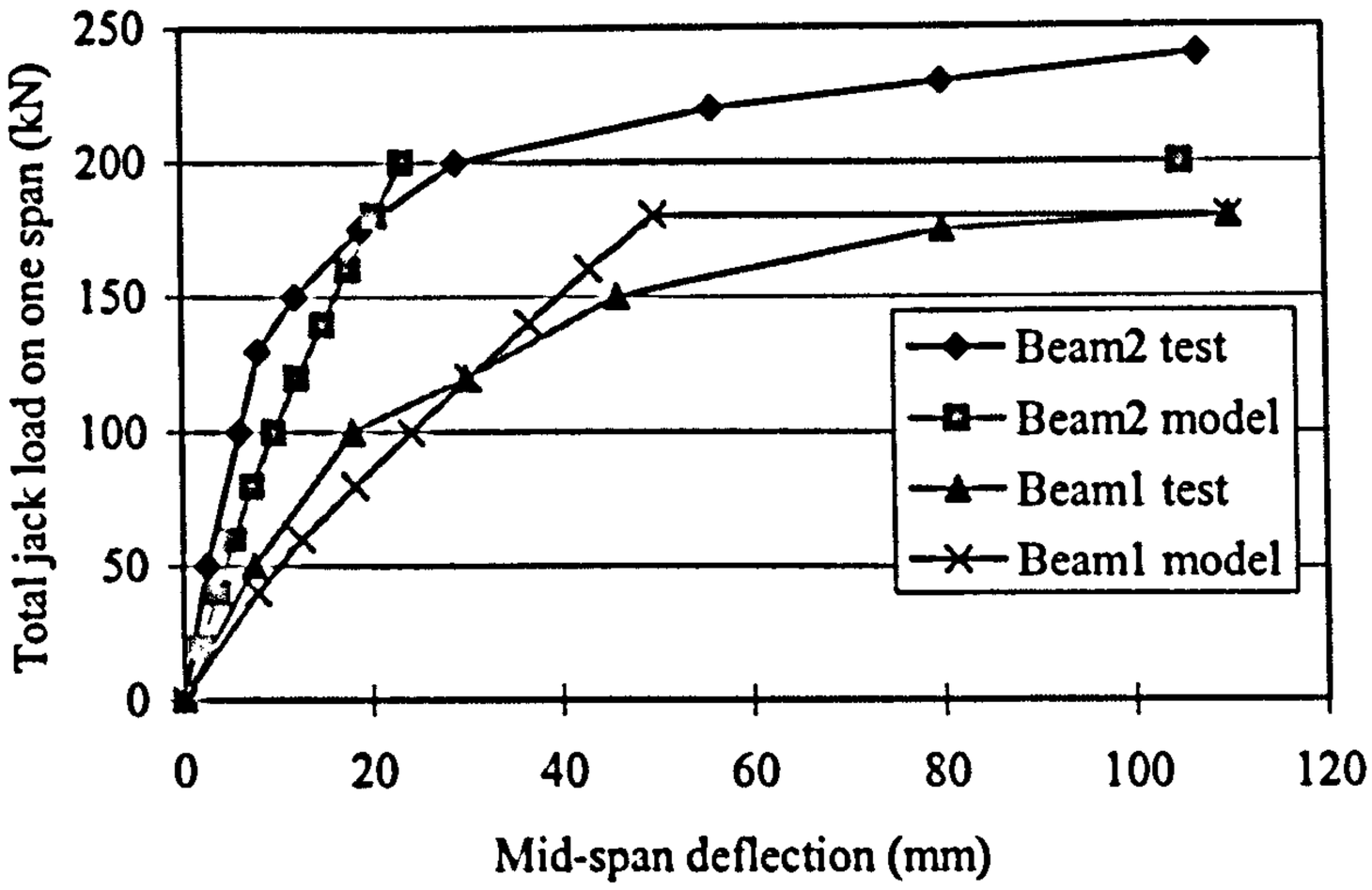

Figure 6.8 Mid-span deflection curves of Rakib (1991) composite beams

6.3.3 Beam model vs. composite beam tests of Wright

Four tests of simply supported composite beams with profiled steel sheeting were reported by Wright (1989). The beam span was 8m and welded stud shear connectors were used. In order to investigate the behaviour of composite beams with lower degrees of shear connection, the number of shear studs at half span was designed as 7, 4, 5 and 3, corresponding to the theoretical degrees of shear connection of 50%, 30%, 40% and 20%. Two types of simple support were designed: idealized roller support and conventional web cleat connection. The test specimens were supported by two short columns bolted on the strong floor of the laboratory. Four equal and symmetrical point loads were applied to the beams at a spacing of 2m. Dynamic tests were also performed on both support conditions, and the basic frequencies were obtained. These four beams were named BEAM 1, BEAM 2, BEAM 3, and BEAM 4. The design parameters of the four beams are as the following:

Concrete slab: Lightweight concrete with profile sheeting, 8m long, 2.5m wide,

$D_s = 115mm$, $D_p = 50mm$

Steel beam: UB $305 \times 102 \times 33$

Shear stud: 19mm diameter, 95mm after welding

Table 6.4 Material properties of composite beams of Wright (1989):

f - N/mm²; E - kN/mm²		BEAM1	BEAM2	BEAM3	BEAM4
Steel beam	f_y	297.5	281	312.5	317
	f_u	445	-	-	-
	E_s	205.5	204	198	200.8
Concrete slab	f_{cu}^-	40.5	45	39.8	39
	f_{cu}^+	4.05	3.96	3.2	2.69
	E_c	24.3	22	20.3	24
Steel mesh	f_y	386.5	386.5	36105	385.5
	f_u	491	491	530	490
	E	203	203	197.5	201
Shear stud	f_u	450	450	450	450

The main objective of the modelling of this group of composite beams is to evaluate the capability of the proposed beam model on composite beams with partial shear connection. The models of the four beams are established according the proposed procedure and the geometric and material properties of the beams provided by the test specimens. Since each stud (or a pair of studs if two studs are present within one trough) is modelled by a stud element, the degree of shear connection of the beam model is determined by the number of the stud elements. In the beam models, the number and position of the stud element comply with the studs in the composite beam specimens. Another objective of the modelling of this group of composite beams is to evaluate the dynamic analysis of the proposed model.

The beam model is loaded under the combination of self-weight and imposed loading. The self-weight is input as a uniformly distributed loading. The concrete slab, troughs, steel sheeting, and steel beam are included in the self-weight calculation. The weights of shear studs and rigid links are neglected. The imposed loading is four concentrated loads according to the tests. In the finite element analysis, the initial point load is set as 5kN, and the load increment is also 5kN for each load step. Simple supports are used for all the beams as the boundary conditions. The four beam models formed by LUSAS program are shown in Figure 6.8(a), (b), (c), (d).

From the LUSAS analysis, the relationship between the mid-span deflection and the imposed loading at one point can be obtained. In order to compare the results with the tests, the four imposed point loads are transformed to the uniformly distributed surface loading over the whole concrete slab. The relationships between the mid-span deflection and the transformed imposed surface loading of the four beams are shown in Figures 6.9a, b, c, d.

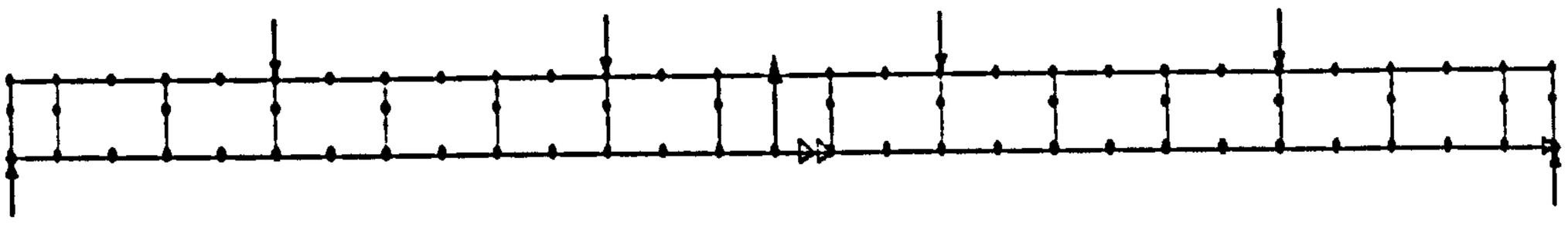

(a) BEAM 1 model (K = 0.5)

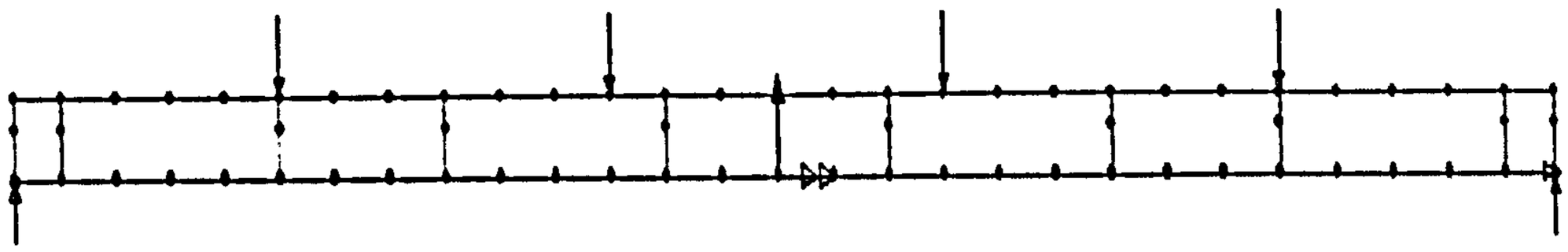

(b) BEAM 2 model (K = 0.3)

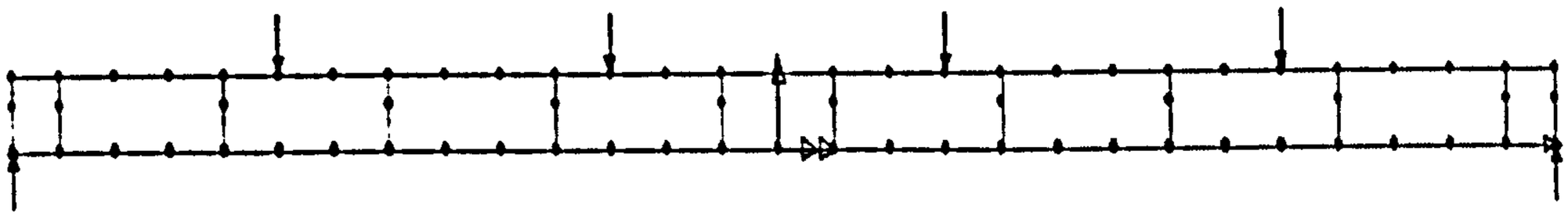

(c) BEAM 3 model (K = 0.4)

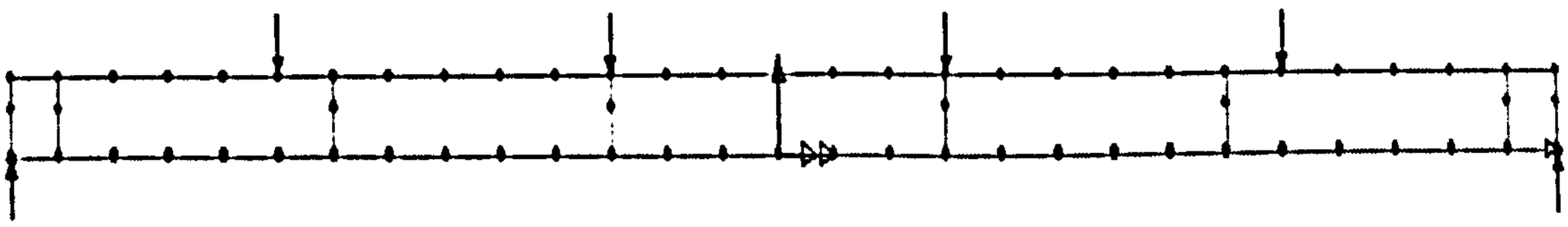

(d) BEAM 4 model (K = 0.2)

Boundary conditions

Support	x	y	θ
Right	R	R	F
Left	F	R	F

*R = Restrained; F = Free; K = degree of shear connection

Figure 6.8 Composite beam models of Wright (1989) beams

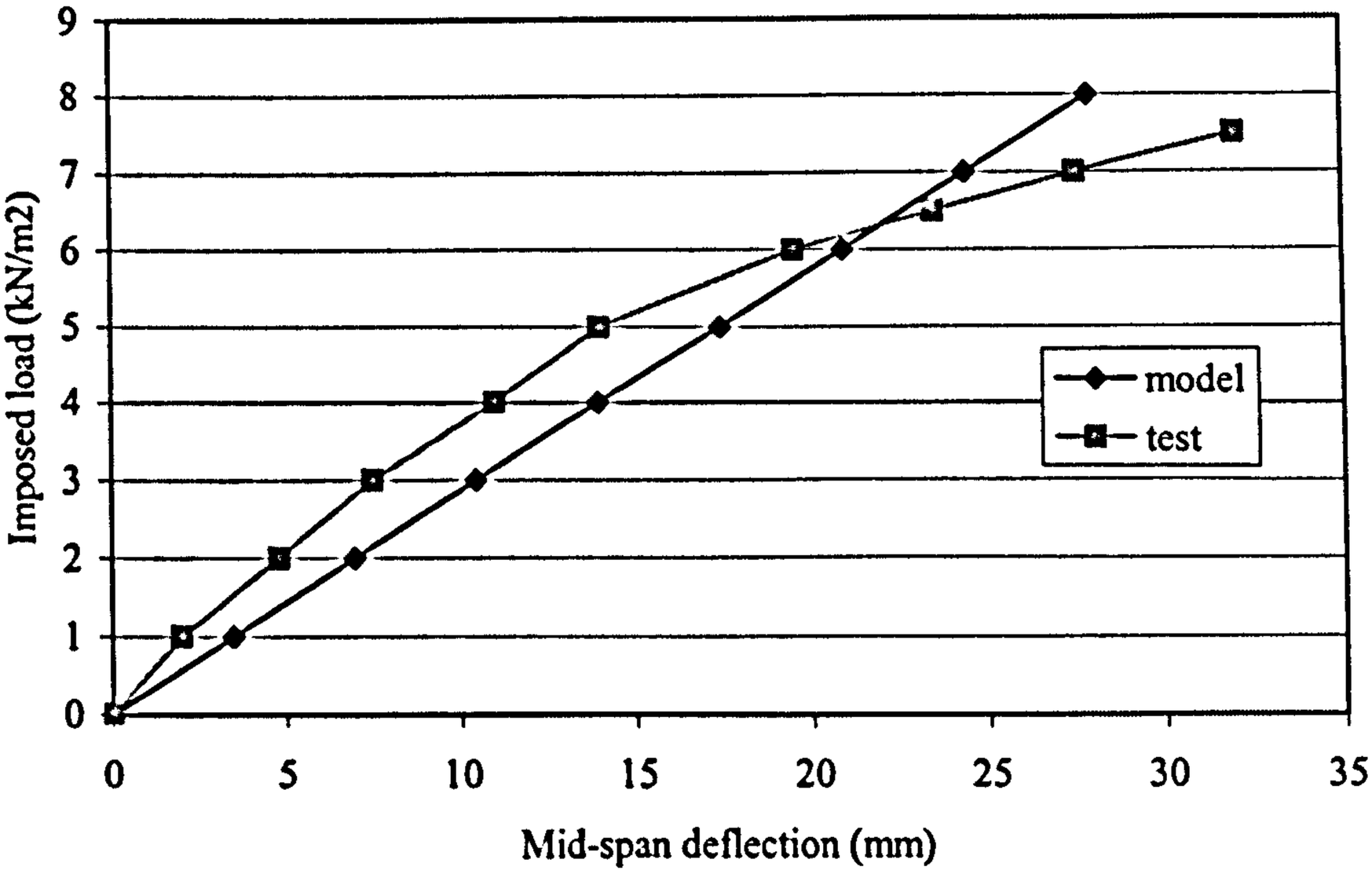

Figure 6.9a Load-Mid-span deflection curve of Beam 1

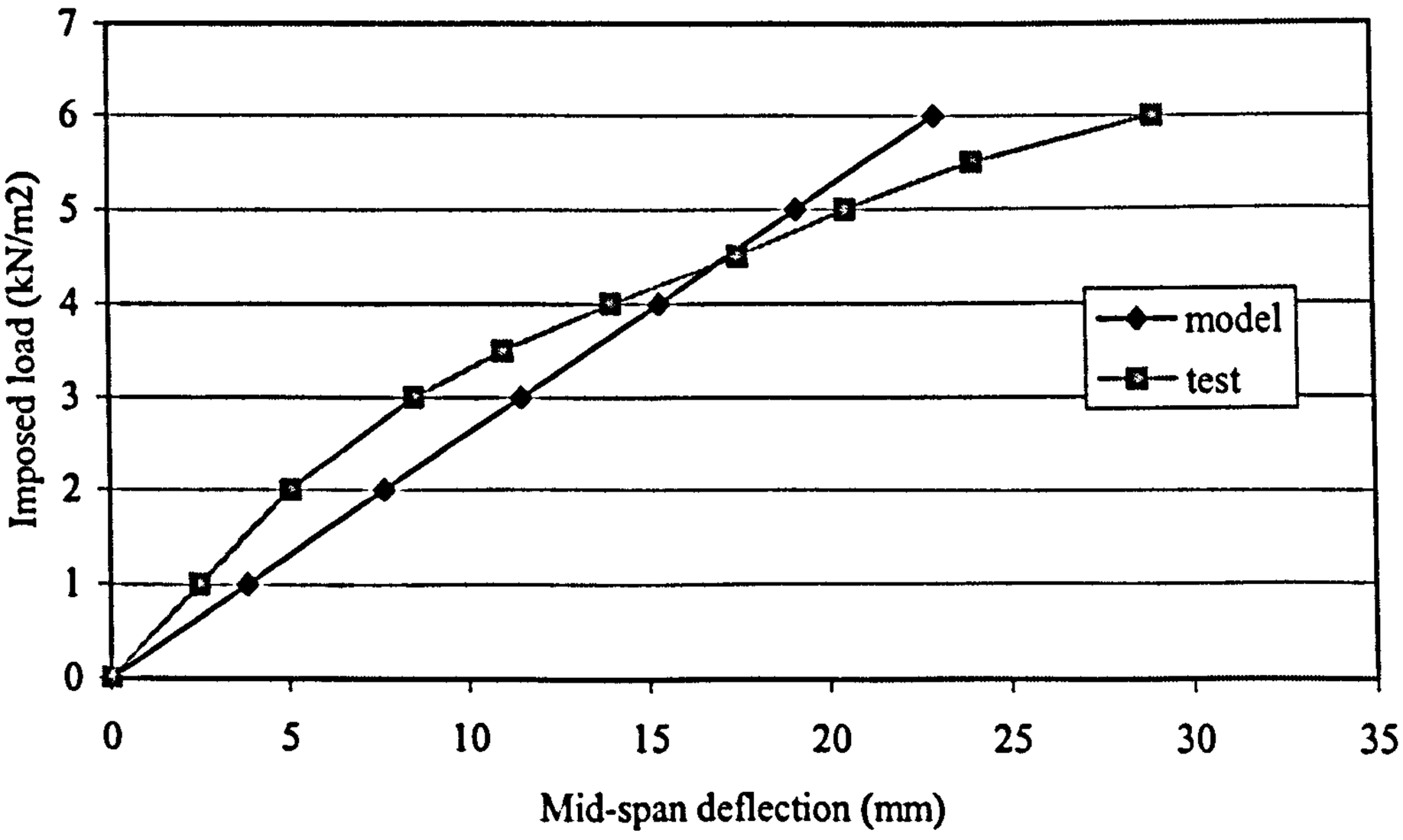

Figure 6.9b Load-Mid-span deflection curve of Beam 2

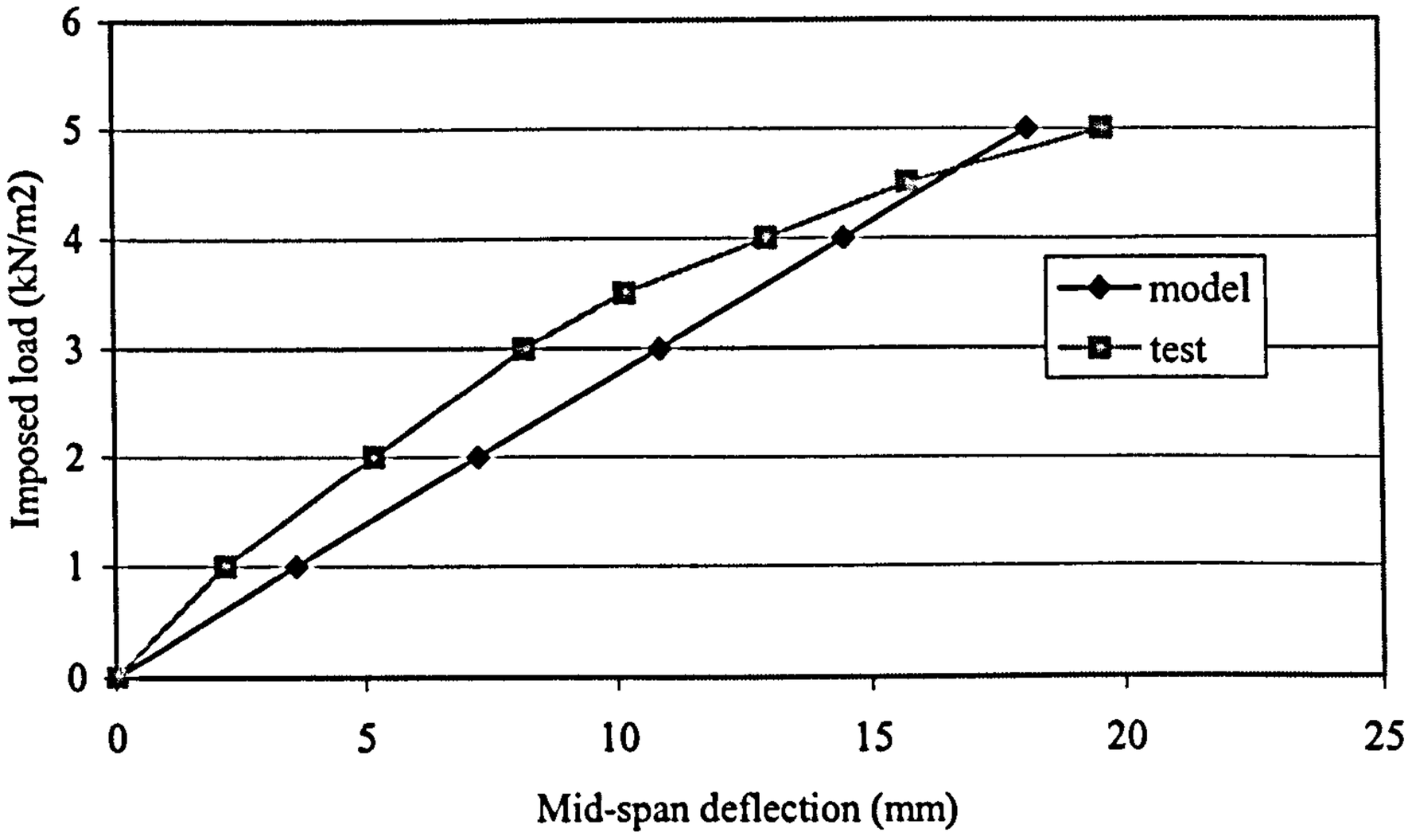

Figure 6.9c Load-Mid-span deflection curve of Beam 3

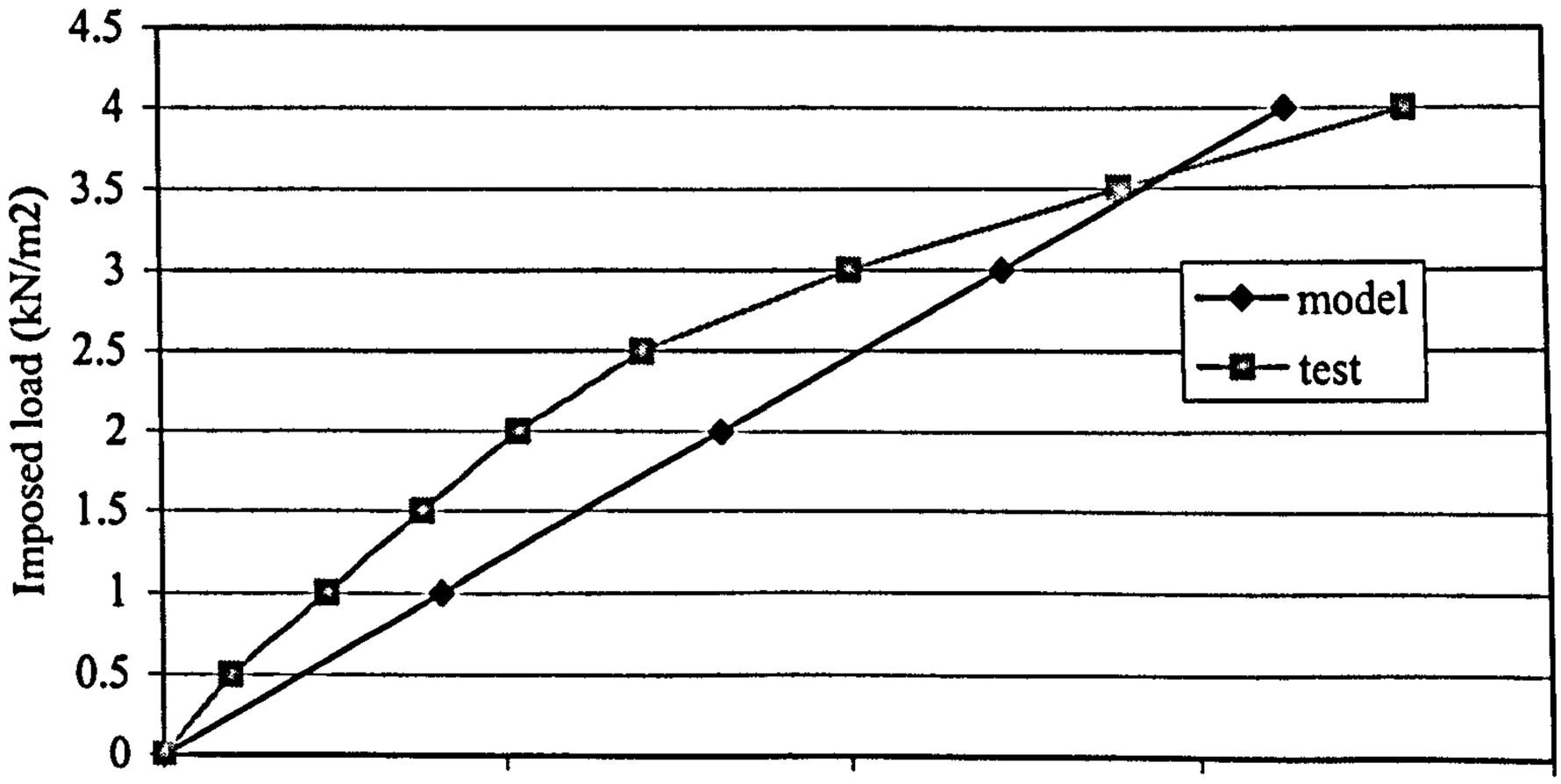

Figure 6.9d Load-Mid-span deflection curve of Beam 4

From Figures 6.9a, b, c, d, it can be seen that the predicted imposed load-mid-span deflection curves agree well with test curves although the predicted curves are nearly linear compared to the test curves. The linear relationship between the imposed loading and the mid-span deflection from the beam model analysis is mainly because of the assumed bi-linear or elastic perfect-plastic stress-strain relationship of the materials. The beam model therefore yields at a higher load level compared to the tests. It follows that if the predicted mid-span deflections are close to the tests at lower levels of imposed loading, it is quite possible that the beam model would under estimate the deflections of the composite beam at high load levels.

To investigate the beam model in the modelling of composite beams with different degrees of shear connection, the predicted mid-span deflections at different levels of surface loads are studied. From Table 6.5, it can be seen that at the same load level, the mid-span deflection increases with the decrease of the degree of shear connection. It proves that the beam model is capable of modelling beams with different degrees of shear connection.

Table 6.5 Mid-span deflections at different load levels (mm)

Surface load (kN/m^2)	1	2	3	4
BEAM1 (K=0.5)	3.48	6.97	10.44	13.93
BEAM3 (K=0.4)	3.63	7.26	10.88	14.52
BEAM2 (K=0.3)	3.83	7.65	11.48	15.31
BEAM4 (K=0.2)	4.07	8.14	12.21	19.29

Table 6.6 Frequencies of BEAM 1-BEAM 4 (Hz)

	Test	Model
BEAM 1	9.067	9.088
BEAM 2	8.317	8.490
BEAM 3	8.30	8.573
BEAM 4	8.179	8.322

Through the Eigenvalue analysis, the natural frequencies of the beams are easily obtained. As the program's default setting, the lump mass method is used in the Eigenvalue analysis. The mass of the rigid link elements is excluded. The predicted natural frequencies of the beams are listed in Table 6.6 along with the results from the tests. It can be seen that the predicted natural frequencies of the beams are very close to the test results. It is noticed that the predicted values are slightly higher than the tests. This is mostly because that the damping related to the mass and stiffness of the composite beam is neglected in the model analysis. It therefore may be concluded that the proposed model can accurately predict the natural frequencies of composite beams. Another advantage of the beam model in dynamic analysis is that the second mode frequency, even the third and higher mode frequencies can be easily obtained. As we know, the fundamental frequency is not always enough for the dynamic analysis of the structure. It is necessary to incorporate more mode shapes and frequencies to get better results of dynamic analysis.

6.4 Conclusions

In this chapter, the history of the modelling of composite beams is reviewed. Various beam models have been proposed for composite beams with different joint connections and beams with full or partial shear connections. But the available beam models are either too complicated for practical use or rely on data from composite joint tests. A simple composite beam model is therefore proposed. The proposed beam model is capable of analysing composite beams with different joint or support conditions, with

different degrees of shear connection, and with various loading conditions. The proposed beam model is validated against the current British Standard method and two groups of composite beam tests. The agreements are satisfactory.

The following conclusions may be drawn from the analysis of composite beams using the proposed composite beam model.

- The proposed model is simple to use and very little computer effort is needed.
- Both elastic and plastic analysis of composite beams can be performed using the proposed model.
- The behaviour of partial shear connection can be easily modelled.
- The modelling of composite beams with different degrees of shear connection is successful.
- The modelling of composite beams with semi-rigid joints is successful.
- For the analysis of continuous composite beams, the actual negative moment of resistance can be obtained without a presumed redistribution of the negative moment at the supports.
- A bi-linear relationship between the imposed loading and the mid-span deflection may be obtained from the beam model. The load level at yield is higher than the tests.
- The proposed model can accurately predict the natural frequencies of composite beams. And higher mode frequencies can be easily obtained.
- The empirical equation (6.1) is too coarse when it is used to predict the natural frequencies of composite beams.

Chapter 7 Modelling of composite frames with semi-rigid connections

7.1 Introduction

In conventional composite frame design, the composite beams are normally designed as simply supported beams between columns. There are no moments transferred to the columns through the beam-to-column connections. The connections are designed to transfer only the shear forces at beam ends. In semi-rigid construction, the beam-to-column connections are designed as semi-rigid or semi-continuous, which allow a certain amount of moment to be transferred to the columns. The benefits of semi-rigid construction are that the composite beam sizes maybe reduced which would lead to the savings on the overall construction costs. Secondly, the composite beams will provide additional lateral restraint to the columns, and hence increase the lateral stiffness of the structure. The slab steel also provides an excellent way to control the cracks on the concrete surfaces. It has been reported (Leon, 1990) that in braced frame construction, the semi-rigid composite system can be very economical if the design live loads exceed the dead loads by a factor of two or more. It can also be very advantageous in areas of moderate to high wind loads and low to moderate seismic loads. It is suggested that for unbraced frames such as those used for buildings stories should be limited to eight to ten, with the most economical range probably in the four to six-storey range.

In this chapter three semi-rigid composite frames are analysed and the influence of semi-rigid joints on the overall performance of composite frames is discussed. Recommendations for the design of semi-rigid composite frames are proposed.

7.1.1 Nethercot, 1995

Nethercot (1995) discussed the basic requirements for the application of the principles of the semi-continuous approach in nonsway composite frame design. Take a symmetrical

two-span uniformly loaded continuous beam for example. The ratio of support moment to mid-span moment is 1.8, but the sagging moment capacity of the composite beam cross-section is always greater than the hogging moment capacity according to the usual stress block method. It follows that the sagging moment capacity of the composite section may never be utilized if beam is designed elastically. If the full sagging moment capacity is to be developed in the mid-span region, a plastic hinge must form at the support and further loading is accommodated by redistribution of moment from the support. The composite joint is, however, required to sustain sufficient rotation capacity. Thus a satisfactory and economic design of a semi-continuous composite beam is determined by the joint moment capacity, the beam sagging moment capacity and the joint rotation capacity. The quasi-plastic collapse mechanism in Figure 7.1 was recommended as favourable, and the quasi-plastic design method was therefore proposed by the author for non-sway composite frames.

Through studying the moment redistribution of a single-span beam under different loading conditions, it is found that for the same level of beam loading weaker joints involve more rotation in order to redistribute greater proportions of moment into to the span. The rotations necessary to develop a required amount of moment redistribution increased remarkably once the load level was sufficient to cause yielding at midspan. So only in the case of higher level of available rotation capacity and stronger joints could the full sagging capacity of the cross-section be developed at midspan. However the author suggests that designing for 95% of M_u would significantly reduce the demands on the end connections without much loss of actual load carrying capacity.

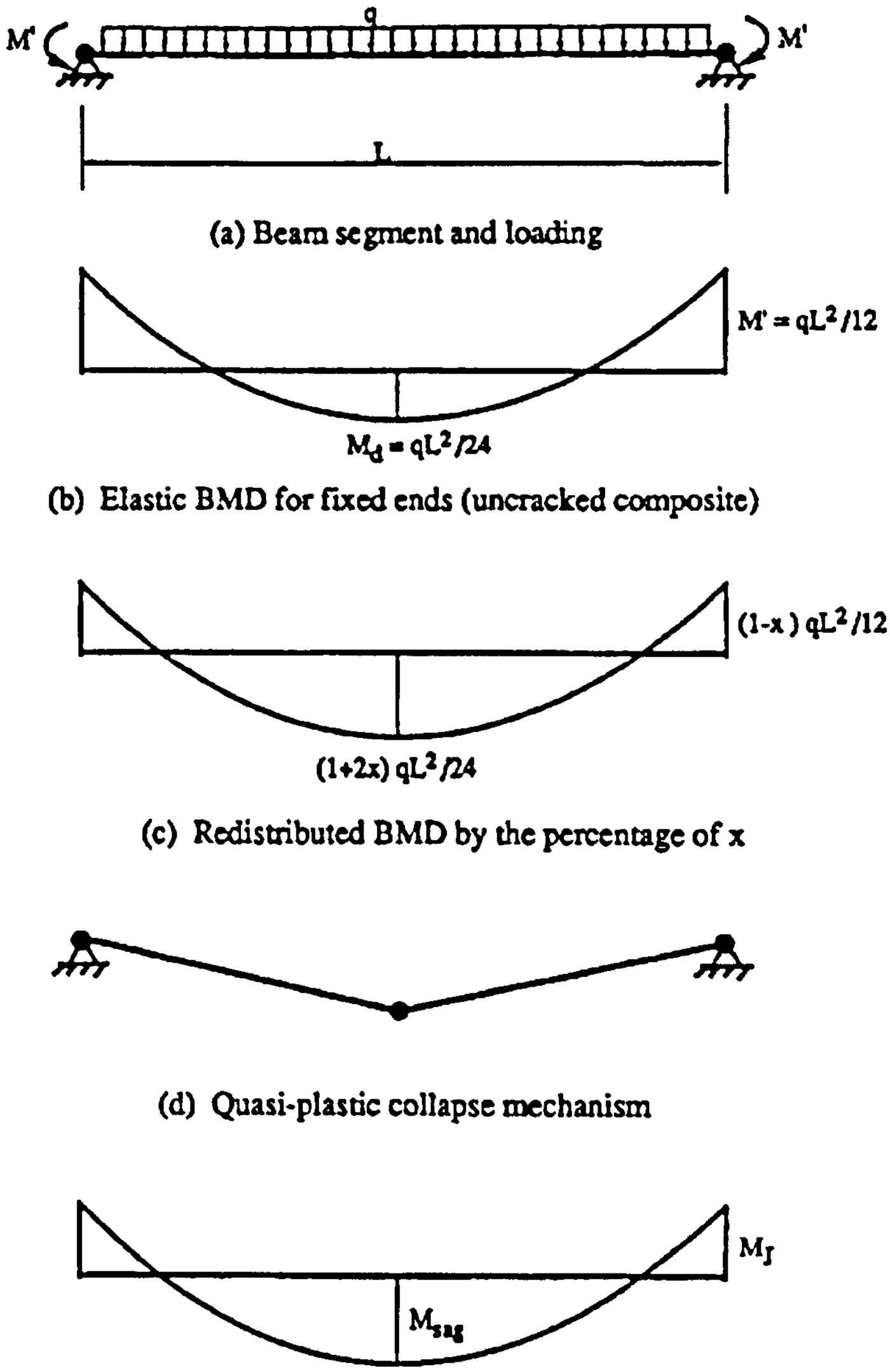

Figure 7.1 Quasi-plastic design method of Nethercot, 1995

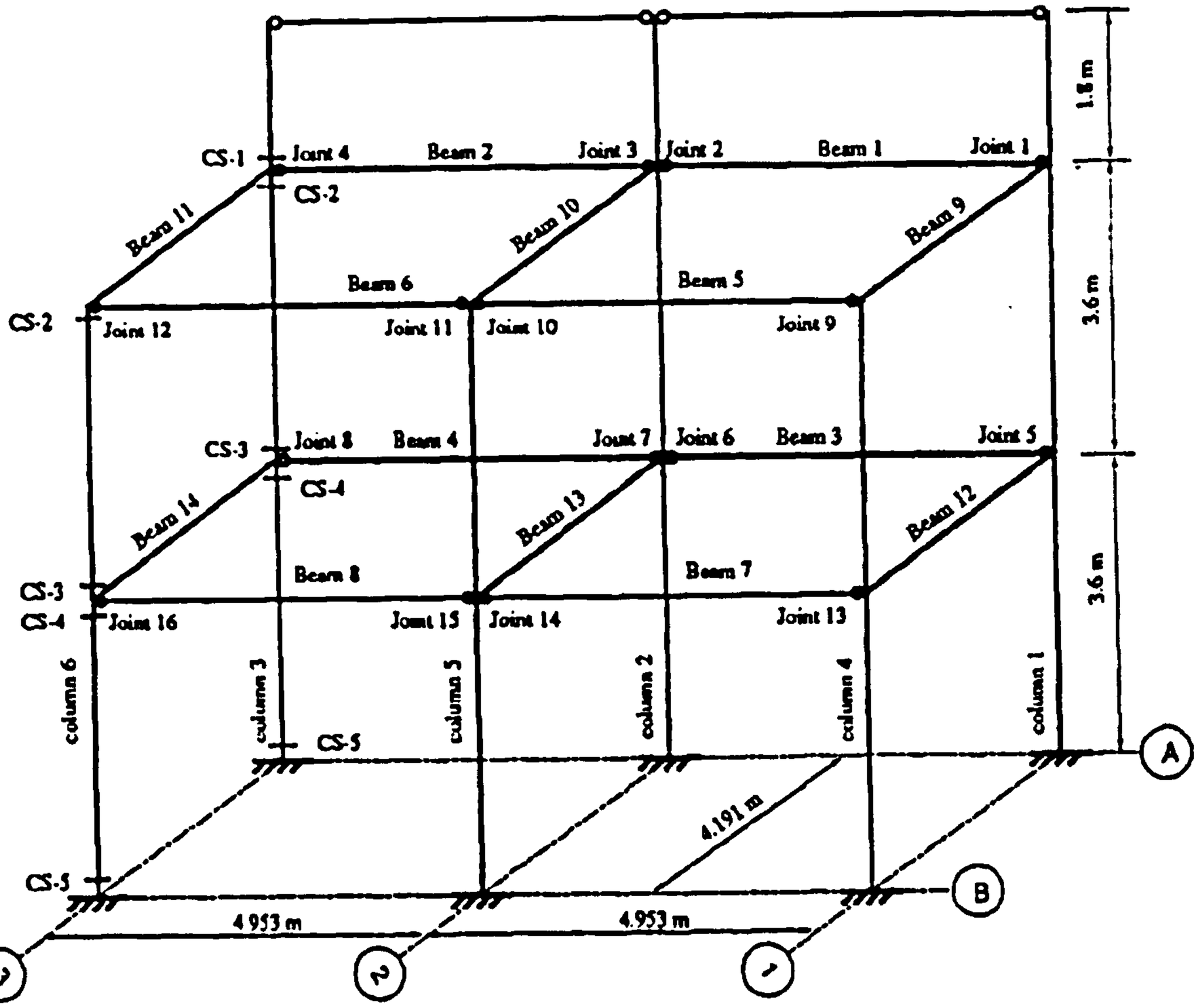

Figure 7.2 General layout of the frame specimen of Li et al., 1996[1], 1996[2]

7.1.2 Li et al., 1996

A full-scale test was reported on a two-span one bay two-storey composite frame (Figure 7.2) and the implications for the design of composite frames was provided (Li et al., 1996[1], 1996[2]). The main purpose of the frame tests was to investigate semi-rigid connection effects on overall frame behaviour. The three-dimensional frame was divided into two two-span plane frames, referred to as frame A and frame B. Frame A and frame B were loaded separately until failure. The moment diagrams of frame A and frame B showed that the rigid joint assumption largely overestimated the joint moments and

underestimated the span moments, while the pinned joint assumption significantly overestimated the span moments. By studying the connection behaviour, it was found that the joint moment capacities and rotational stiffness obtained from the frame test were smaller than those obtained from the isolated tests using identical specimens. By studying the beam deflections it was found that the mid-span deflections predicted by the design code method given in BS5950: Part 3.1 were systematically smaller than the test results. By examining the bottom flange strains it was found that the composite beams started to behave inelastically when the beam deflection was well within the serviceability limit specified by the code. By investigating the moment capacities of the beam sections, it was found that yield and ultimate moment capacities of composite beam predicted by BS5950: Part 3.1 were quite accurate. The quasi-plastic analysis gave the closest predictions of the joint moments compared to the test results. It was therefore recommended for the design of semi-rigid on-sway composite frames.

7.1.3 Dissanayake et al., 1998, 1999

Dissanayake et al. (1998, 1999) analysed five sub-frames from current UK commercial buildings, and one of them was selected for a case study. Twelve different sub-frame configurations were analysed by the computer programs developed by the authors. Two types of steel connections were used: seating cleat and flush end plate, featuring nominal pinned and semi-rigid connections, respectively. The reinforcement areas over the support were 0.2% and 1.0%. And three degrees of shear connection were assumed for composite beams, which were 49%, 86%, and 118%. For comparison, three simple support beams with the same degrees of shear connection were also analysed.

Three finite elements were used in the program to simulate the composite frames, namely the steel column element, the partial interaction composite beam element and the composite joint element. Partial interaction between the steel beam and the concrete slab is simulated by treating the composite beam as two parallel beam elements, one for the steel beam and one for the concrete slab, connected through a continuous shear medium

representing shear connectors. The shear-slip modulus and the internal force per unit length required were calculated from the load-slip behaviour of the stud and averaged the shear force per stud over the inter-stud spacing. A tri-linear load-slip relationship was assumed. The composite connections were modelled as the proposed 'macro-element' model (Dissanayake et al. (2000).

By comparing the load capacities with the composite beams, it wass found that the failure load increased 15% to 17% for beams with 0.2% of reinforcement over the support and pinned steel connections. An increase of 22% to 24% was observed for beams with semi-rigid steel connections and the same reinforcement. The failure load increased 20% to 44% for beams with 1.0% of reinforcement and pinned steel connections. An increase of 29% to 49% was observed for beams with semi-rigid steel connections and the same reinforcement. By comparing the deflections under service state and imposed load only with the corresponding calculations according to design code BS5950 (1990), it was found that the beam deflections reduced significantly (up to 51%) when the composite beams were considered as semi-continuous by adding a small amount of reinforcement over the supports. The reinforcement also increased the stiffness and the ductility of the composite connections.

7.1.4 Fang et al., 1999

Fang et al. (1999) proposed a single element per member method for geometric and material non-linear analysis of composite beams with semi-rigid connection. A composite beam model was established by assuming a deflection function of composite beams. The curvature of the beam could be obtained as the second derivative of the deflection. The stiffness matrix of a beam element could then be found. By using static condensation to eliminate the internal degrees of freedom, a simple beam element could be formed with the composite joints as the boundary conditions.

The semi-rigid beam-to-column joint was accounted for by approximating the moment-rotation curve of the composite joint as a simple exponential expression. The parameters of the expression could be obtained from steel joint test data or theoretical formula. For composite joints under sagging moment, because of limited experimental data on the monotonic behaviour of joints under sagging moment, three exponential equations were assumed. The first model, termed as model A, used the same expression as the hogging bending; the second model 'B' employed a lower ultimate moment of resistance; the third model 'C' was a simple linear model.

7.1.5 Liew et al., 2001

Liew et al. (2001) proposed a method for the inelastic analysis of the limit state behaviour of composite frames. The composite beam model was established by subdivided the beam along the length into a finite number of segments. The flexural stiffness of a segment was evaluated using the moment-curvature relationship of the composite beam section, which could approximately the partial interaction between the concrete slab and the steel beam. The static condensation method was then used to the segment model into a single beam-column element. The beam-to-column connections were supposed to be rigid. It is noticed that the moment-curvature relationships of all sections must be predetermined before a global analysis can be performed by using this approach.

To validate the proposed model, the behaviour of a simple supported composite beam, a two-span composite beam was studied and the results showed good agreements with the corresponding tests. And a steel portal frame was analysed to verify the proposed inelastic analysis method, and the results were compared with different approaches. The proposed analytical model was then used to study the limit behaviour of composite frames. A steel portal frame with composite beams was investigated, followed by the analysis of a three-dimensional 20-storey composite frame. The study indicated that the load limit of steel frames while considering the composite beam effect was about 30%

higher than that of the pure steel beams, and the lateral stiffness could be significantly enhanced by considering the composite action.

Although the economic and structural advantages of semi-rigid construction have been realized, the semi-rigid composite frame design is still not practical at present. A main reason is lack of a simple design approach to such complicated problems. In this chapter, a simple frame model is proposed in composite frame analysis. The proposed model is capable of analysing composite beams with semi-rigid connections. Three composite frames are modelled and results agree well with published papers. And finally design recommendations for composite frames are made.

7.2 Proposed model of composite frames

A composite frame is composed of three components: columns, composite beams, and composite beam-to-column connections. A successful composite frame model should be able to model these three components and predict the overall behaviour of the frame with acceptable accuracy. In order to acquire such a model, the behaviour of composite beam-to-column connections has been investigated and an effective analytical model has been proposed. A composite beam model has been proposed as well and has been validated for composite beam analysis. The type of column is normally a universal column section. Normal beam elements may be directly used to model the columns. For other types of column sections, such as columns formed by a universal column section encased by concrete, normal beam elements can also been used once the material properties are established. To clarify the frame model, each component model is described below:

- Columns

Columns are modelled as normal beam elements. Non-linear material properties are accommodated.

- Composite beam-to-column connections

The previous proposed composite joint model is used, in which the reinforcement in the concrete slab is modelled as bar elements; the steel beam is modelled as beam elements; the shear studs are modelled as stud elements developed by the author; rigid links are provided between the steel beam and the stud elements. The equivalent lever arm is calculated according to the composite joint configuration by equation (6.8).

- Composite beams

A composite beam is composed of three components: the concrete slab, shear connectors, and the steel beam. The previous proposed composite beam model is used in frame analysis, in which the concrete slab is modelled as non-linear cross-section elements; the steel beam is modelled as beam elements; the shear studs are modelled as stud elements (developed by the author); and rigid links are provided between the steel beam and the stud elements.

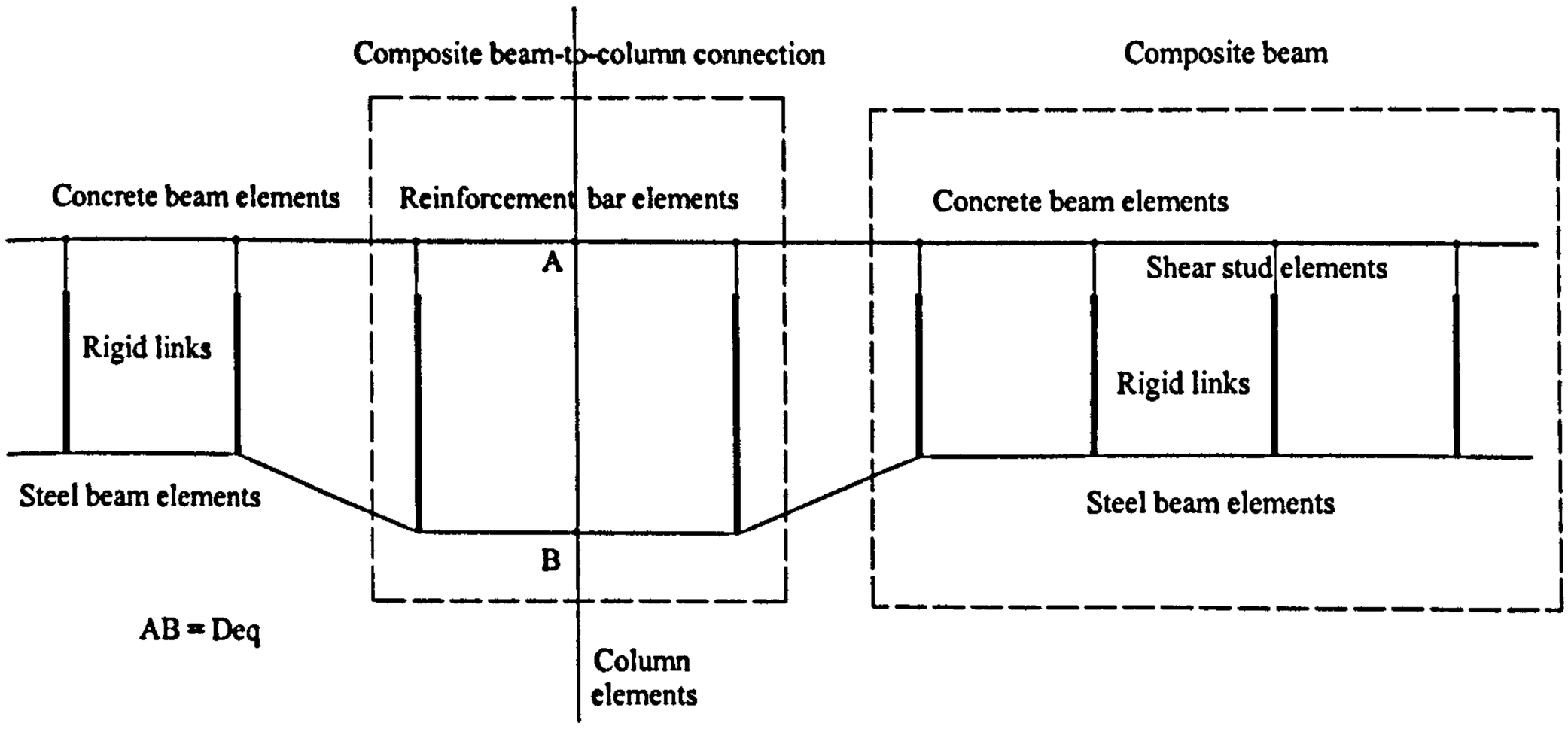

Figure 7.3 Assembly of the proposed semi-rigid connection and composite beam model in a composite frame

7.3 Validation of the proposed composite frame model

Due to lack of available design details of composite frames, only three composite frames were found in the literature and were chosen for the validation of the proposed composite frame model from published papers. They are: a portal frame, a six-storey plane frame, and a twenty-storey space frame. These three composite frames are analysed and the results are compared with corresponding papers. Satisfactory agreements are obtained.

7.3.1 Analysis of a steel portal frame with composite beam

Firstly, a steel portal frame with composite beams is analysed by the proposed composite frame model. The same composite portal frame was used by Liew et al. (2001) to investigate the limit state behaviour composite frames.

The portal frame consists a composite beam rigidly connected to two steel columns subjected to equal vertical and lateral loads. The geometry of the frame is shown in Figure 7.4. The frame is supported at both ends of the columns. The vertical and horizontal freedoms are restrained, but the rotational freedoms are free. The column section is W12 × 50. Other design parameters of the composite portal frame are:

Concrete slab:	B_e=1219mm, D_s=102mm, D_p=0, the cylinder strength of concrete f_c'=16N/mm^2.
Steel beam:	D=304mm, B_f=165mm, t_w=6.02mm, t_f=10.16mm, f_y=252.4N/mm^2, E=2 × 10^{11}N/mm^2
Shear connectors:	Assuming 19 mm diameter, 100 mm nominal height shear studs are used providing a shear degree of 90%.

The proposed analytical model of the portal frame generated by LUSAS 13 is shown in Figure 7.5. For the modelling of the portal frame, the steel columns are modelled as

nonlinear thick beam elements with four divisions. The steel beam is modelled as nonlinear thick beam elements. The concrete slab is modelled as nonlinear cross-section elements. The proposed shear stud model is used to model shear studs. The number of shear studs is 12 with the degree of shear connection of 90% according to BS5950, Part 3(1990). The rigid links are modelled as nonlinear thick beam elements, but with a high stiffness by assigning the Young's modulus as $2\times10^{14}N/m^2$ to ensure the transfer of forces between the shear connectors and the steel beam without seriously distortion of the original curvature of the composite beam. At both beam-to-column joints, bar elements are used to model the reinforcement bars. The length of the bar elements is determined from the first shear stud to the column center. Assuming that sufficient anchorage of the reinforcement bars is achieved outside the beam-to-column joint, and the steel beam-to-column connection is assumed to be pinned, the equivalent lever arm of the reinforcement bars is taken as the distance between the centre of the steel beam lower flange to the center of the reinforcement bars. For all elements, an elastic-perfect plastic stress-strain curve is assumed. In the analysis, the self-weight of the frame is neglected.

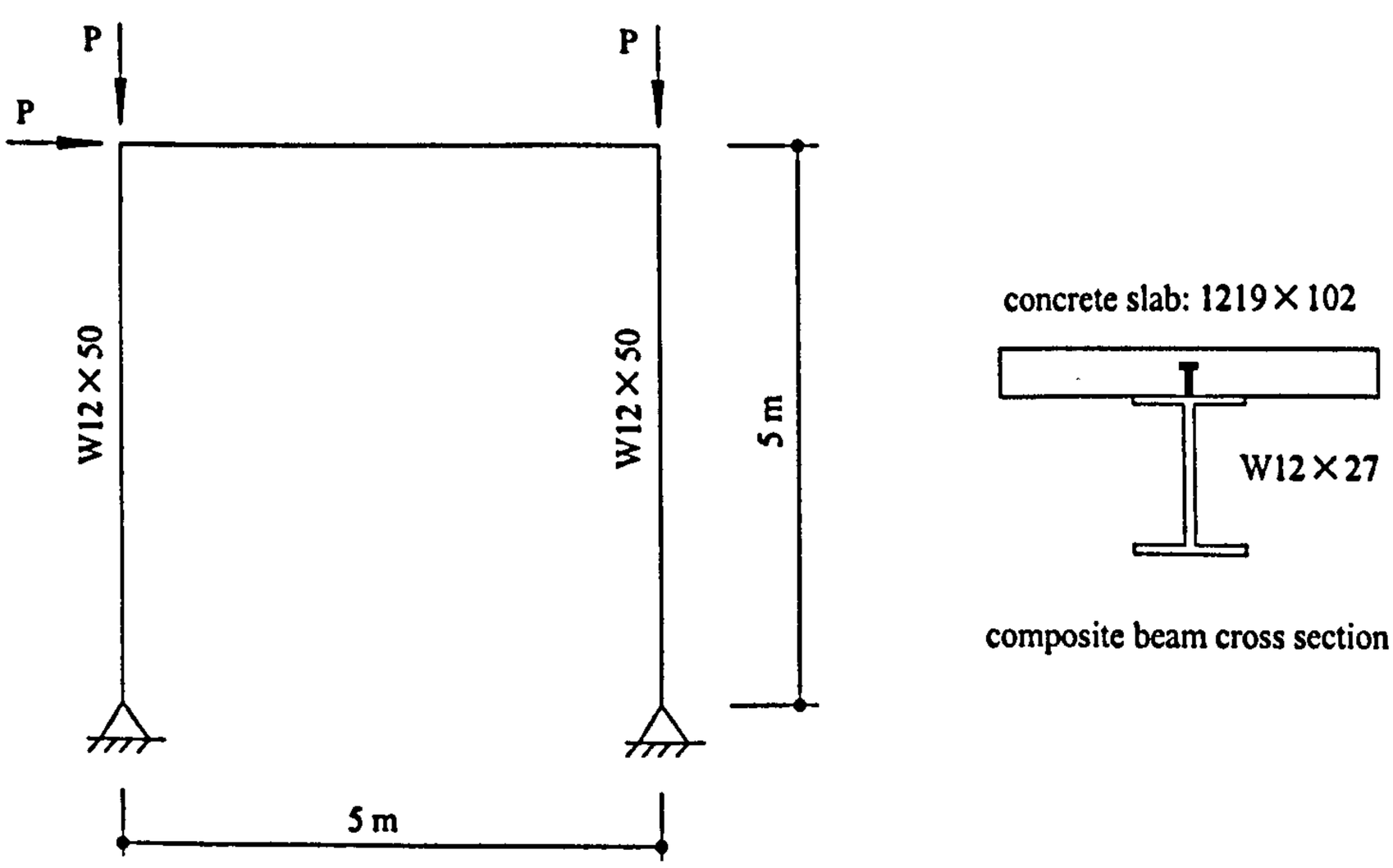

Figure 7.4 The portal frame from Liew et al. (2001)

In the analysis of Liew et al. (2001), the composite beam-to-column connections were assumed rigid. As we know the stiffness of a composite joint is determined by the steel joint configuration and the amount of reinforcement in the concrete slab over the support. In this analysis, the steel joint is assumed to be pinned. And the amount of the reinforcement is gradually increased from 0.1% to 0.5% of the effective concrete slab area. Thus the composite joints of the portal frame model would be semi-rigid rather than rigid. By changing the amount of reinforcement in the concrete slab, its influence on the lateral stiffness and the global behaviour of the portal frame can be studied. The curves of load (P) versus lateral displacement of the frame are illustrated in Figure 7.6. And the load limit of the composite portal frame is listed in Table 7.1. The load limit of pure steel frame is obtained from Liew et al. (2001).

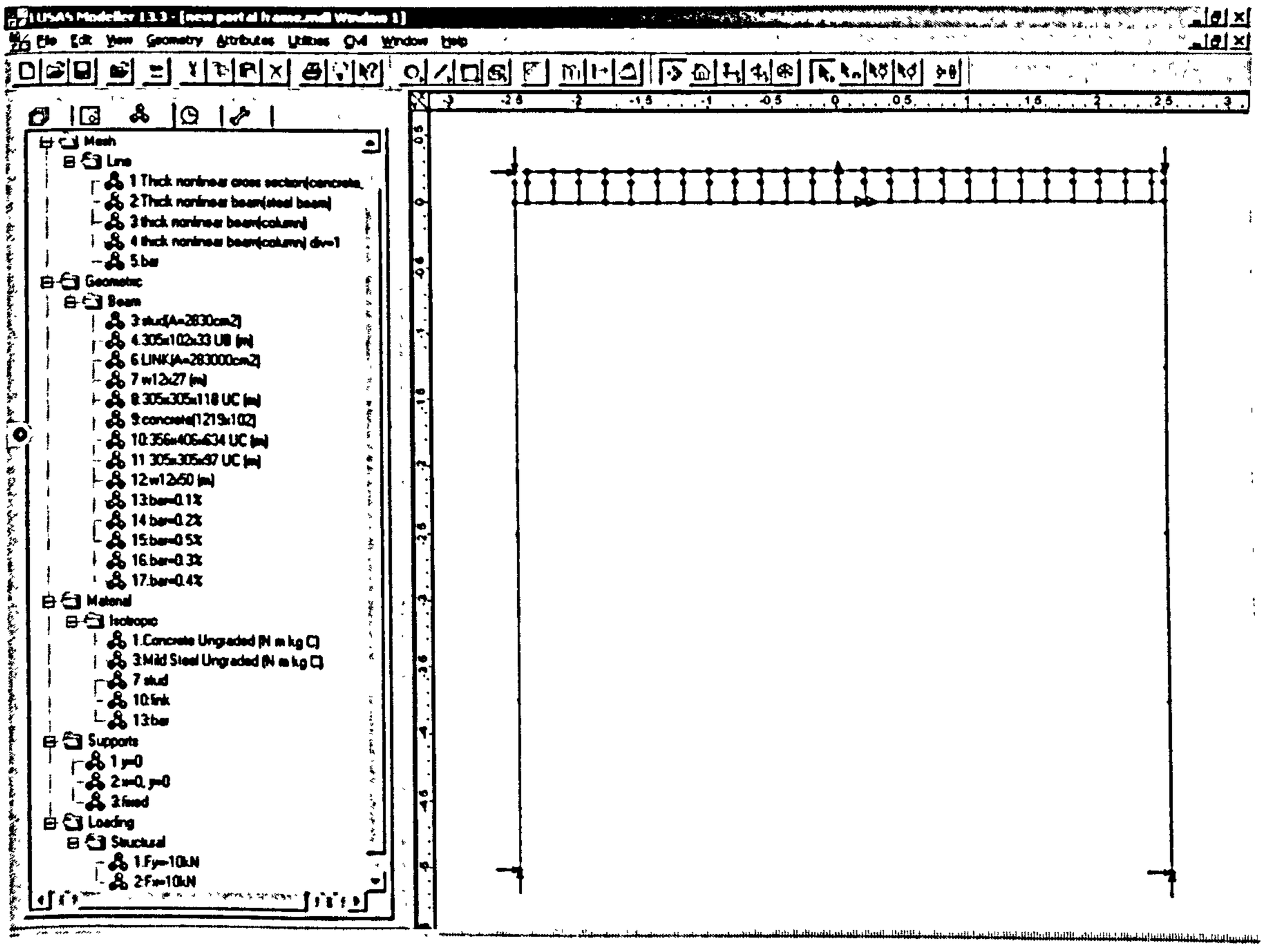

Figure 7.5 Screen shot of the portal frame model from LUSAS

In frame analysis, it is generally accepted that the amount of lateral displacement is closely related to the lateral stiffness of the frame. Frames with higher lateral stiffness will result in less lateral displacement, and vice versa. From Figure 7.5 it can be seen that with the increase of the reinforcement ratio, the lateral displacement of the portal frame decreased at the same load level. It follows that by increasing the reinforcement ratio, the initial stiffness and the lateral stiffness of the frame increased. Since we know from previous analysis of composite joints that the initial stiffness of composite joints will increase with the increase of the reinforcement ratio in the concrete slab, it follows that the initial stiffness and the lateral stiffness of composite frames will increase with the increase of the stiffness of composite joints. Consequently, by changing the amount of the slab reinforcement the lateral stiffness of composite frames can be adjusted. With the increase of the lateral stiffness, the load limit of the frame is also increased. This can be observed from both Table 7.1 and Figure 7.6.

By studying the load-lateral displacement curves in Figure 7.6, it can be seen that semi-rigid behaviour will develop with only a very small amount of reinforcement. Both the lateral stiffness and the load limit increased significantly. Since the rigid composite joint is very difficult to achieve, it is therefore recommended that a semi-rigid joint should be adopted in composite frame design. The semi-rigid composite joint can be easily achieved by adding a very small amount of reinforcement in the slab over the support. Furthermore, the rigidity of the composite joint can be adjusted by the reinforcement ratio.

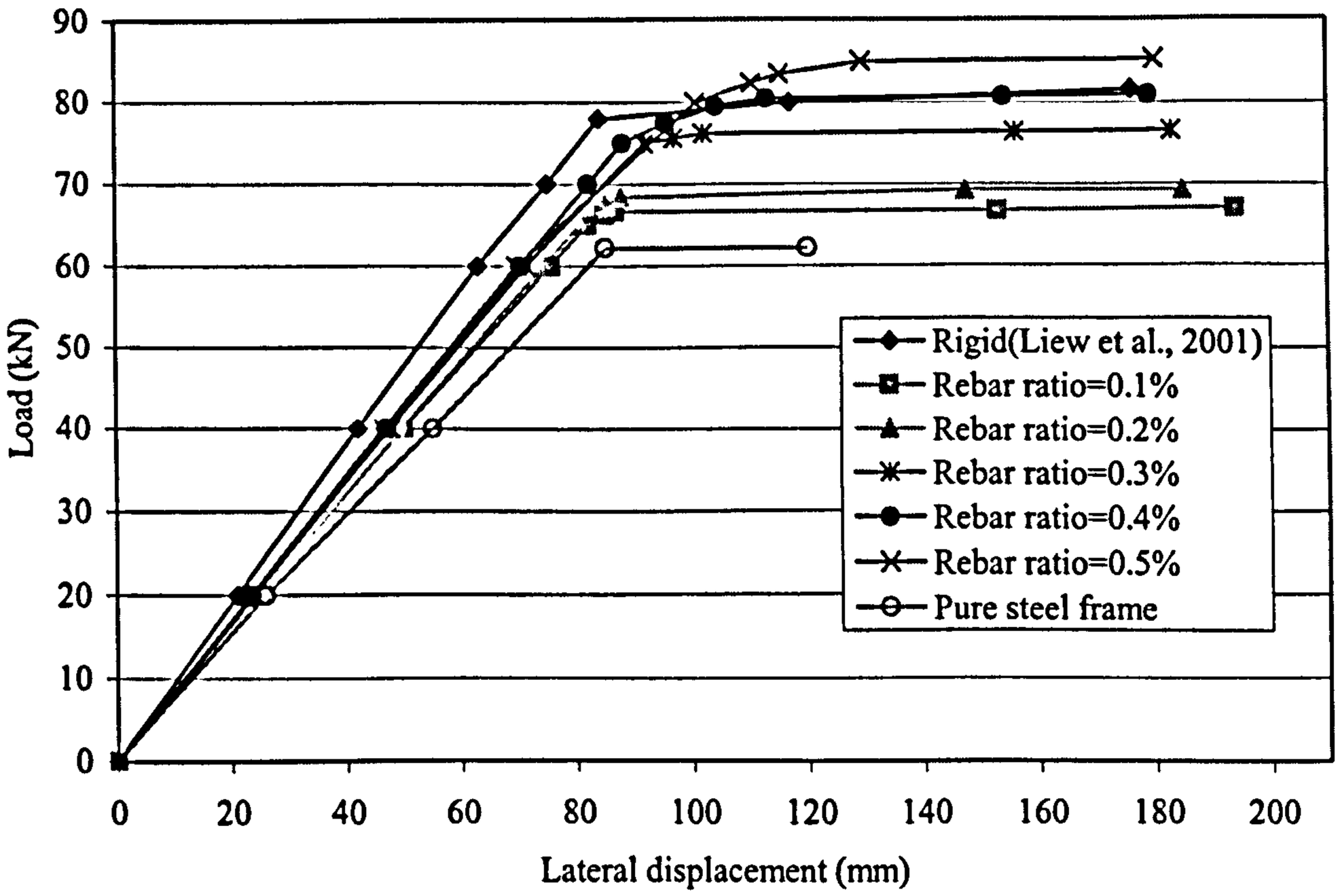

Figure 7.6 Load – lateral displacement curve of the portal frame

Table 7.1 Load limit of the composite portal frame

Reinforcement ratio	0.1%	0.2%	0.3%	0.4%	0.5%	Liew et al., 2001	Steel frame
Load limit (kN)	67	69.2	76.6	80.9	85.2	81.6	62.2

7.3.2 Analysis of a six-storey composite frame

As reviewed earlier, Fang et al. (1999) proposed an analytical method for the nonlinear analysis of composite frames. A six-storey composite frame with semi-rigid joint connections was one of the examples being analysed. The same frame is investigated by the proposed frame model in order that the results can be compared with the method of Fang et al. (1999). The section properties and loading conditions of the frame is illustrated are Figure 7.7. The material properties are as follows:

- Concrete design stress f_c=30N/mm^2
- Concrete strain at design stress ε_{c0}=0.002
- Young's modulus of steel E_s=2.0$\times 10^{11}$N/mm^2
- Yield stress of steel f_y=400N/mm^2

The members of the frames are modelled in the same way as the previous composite portal frame. For the modelling of composite joints, it is assumed that the steel beam-to-column joint is pinned, i.e., the moment of resistance of the steel joint is zero. Two circumstances are considered: joints located at outside columns and joints located at the middle column. For joints located at the middle column, the equivalent lever arm of the reinforcement bars is taken as the distance from the center of the bottom flange of the steel beam to the centre of the rebars, and the proposed joint model is applied. For the joints located at outside columns, assuming the reinforcement bars are not sufficiently anchored and the full moment of resistance of the composite joint cannot achieve, the equivalent lever arm of the reinforcement bars is taken as the distance between the elastic neutral axis of the steel beam to the center of the rebars. Since the degree of shear connection is not stated in the analysis of Fang et al. (1999), full shear connection is assumed in the beam model. In order to study the influence of the joint characteristics to the overall response of the composite frame, four levels of slab reinforcement are used: 0.15% (4T8), 0.34% (4T12), 0.61% (4T16), and 2%. The composite frame model generated by LUSAS 13 is shown in Figure 7.8.

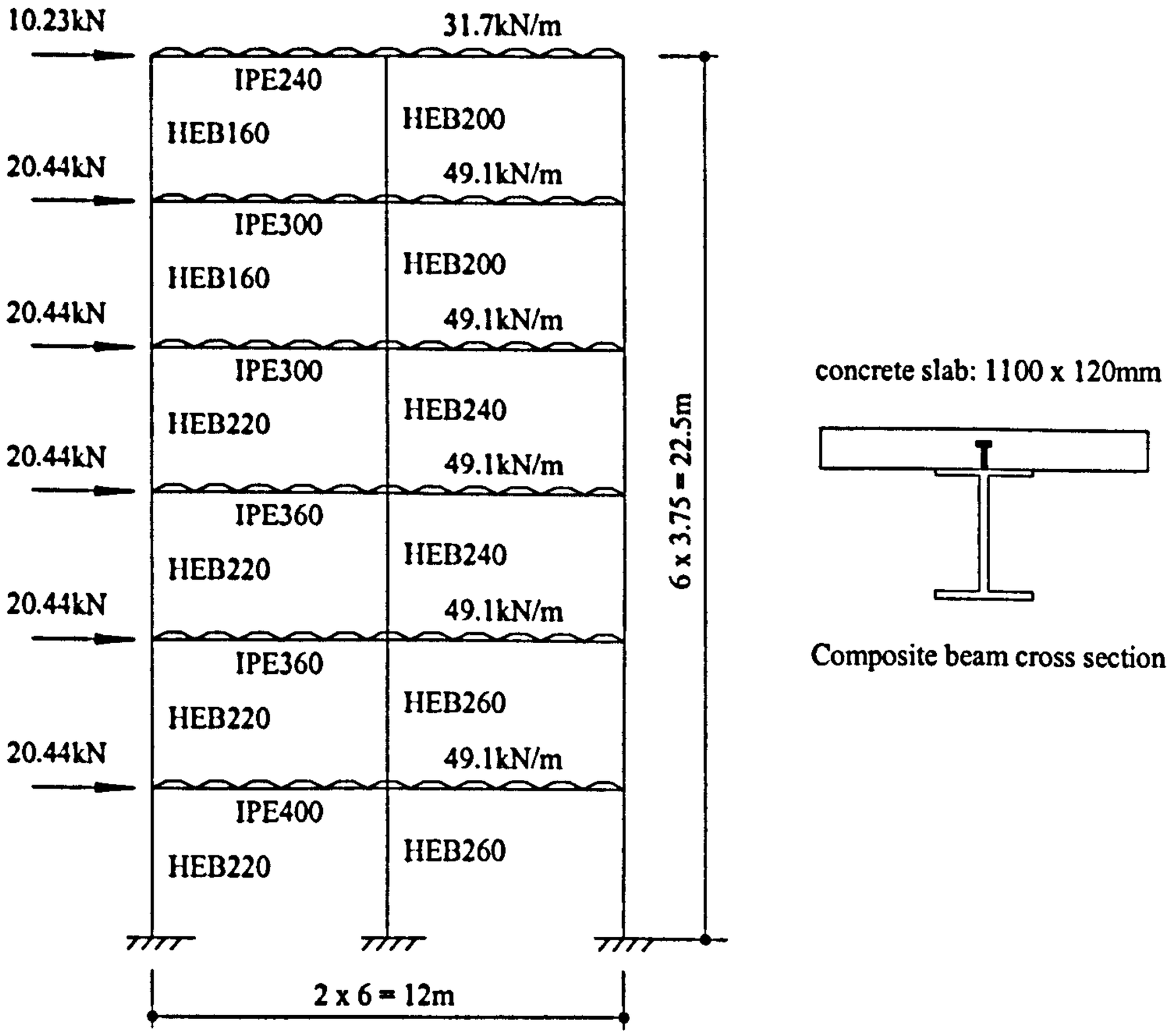

Figure 7.7 Lay-out of the six-storey composite frame from Fang, *et al.*, (1999)

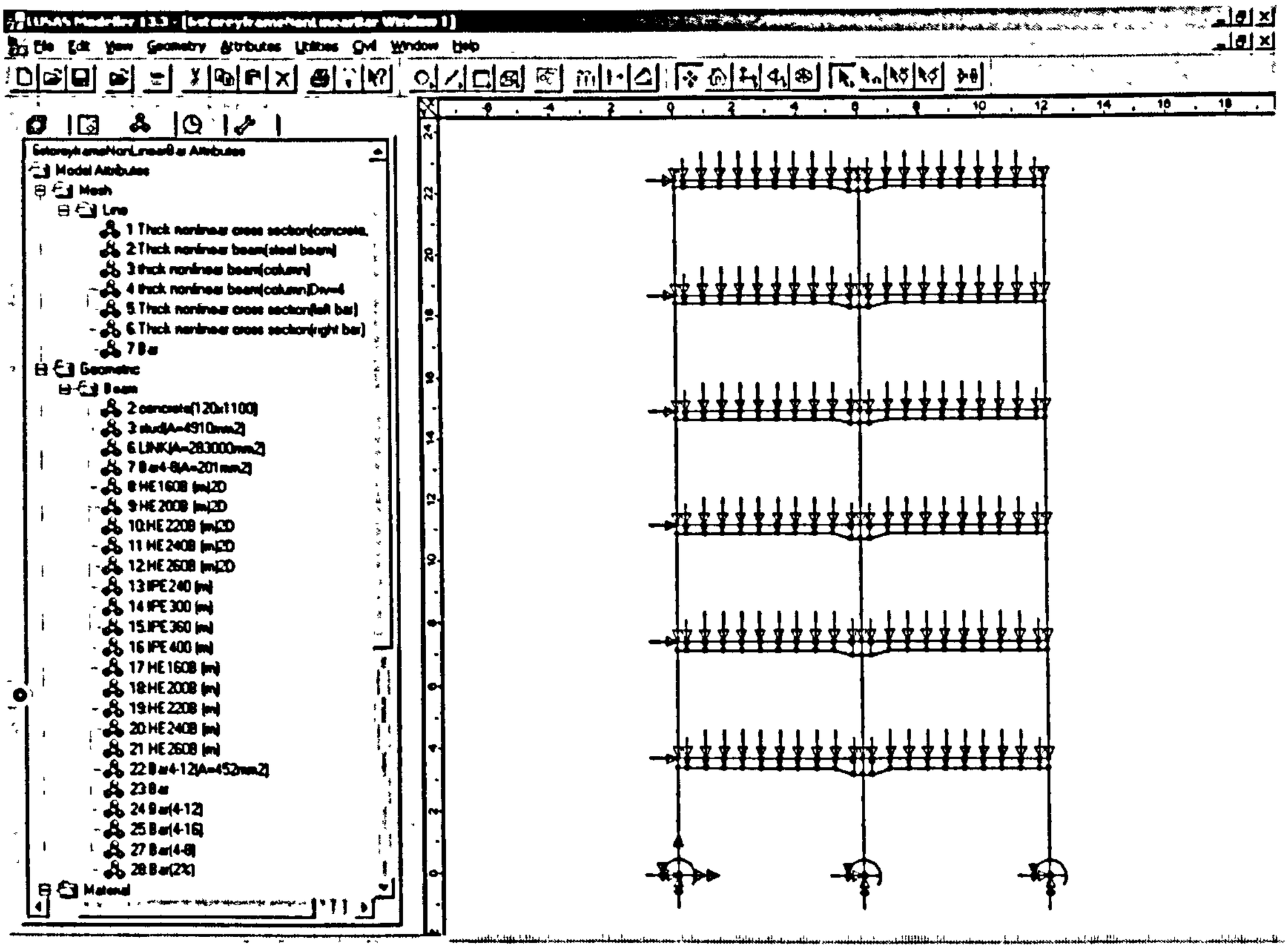

Figure 7.8 Analytical model of six-storey composite frame from LUSAS 13

Through the model analysis, the lateral displacements of the composite are obtained. The curves of the load factor versus the lateral displacement of the frame are shown in Figure 7.9. The results of frames with joint model A, model B, model C, and rigid joint are also shown in Figure 798 for comparison.

From Figure 7.9 it can be seen that the amount of slab reinforcement has significant influence on the overall behaviour of the composite frame. The observations are as the following:

- At the same load level the lateral displacement of the composite frame decreased with the increase of the reinforcement ratio. This is the same as the results analysed for the portal frame. It follows that the lateral stiffness of the composite frame increased with the increase of the reinforcement in the concrete slab.

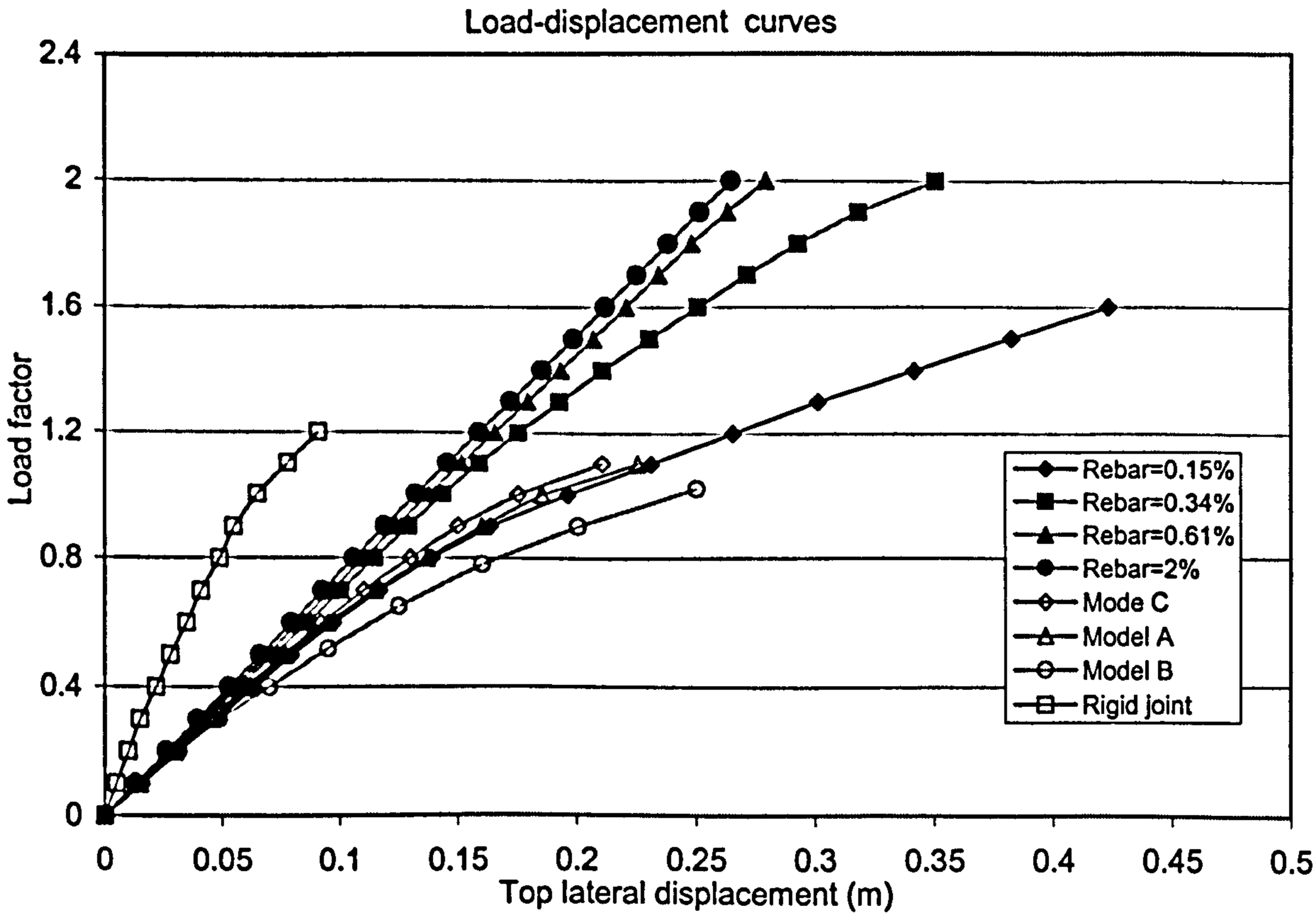

Figure 7.9 Lateral displacement curves of the six-storey composite frame

- By comparing the curve of rebar ratio 0.15% (4T8) to the curve of rebar ratio 0.34% (4T12), it can be observed that only a slight increase of the rebars reduced the lateral displacement significantly when the load factor exceeds 0.8.
- Continuing increase in the rebar ratio does not significantly reduce the lateral displacement, even when a very high rebar ratio (2%) is used. This is probably because that the lower flange of the steel beam in the joint area has yielded before the full strength of the rebar can be developed.
- The composite frames with higher reinforcement (0.34% and above) survived until a very high load level was applied (load factor=2).
- The lateral displacement curve of the frame with the rebar ratio of 0.15% is very close to the joint model B curve of Fang et al. (1999).

7.3.3 Analysis of a twenty-storey space frame with composite beams

A twenty-storey space frame with composite beams was analysed by Liew et al. (2001) in addition to the composite portal frame discussed before. The plan view and the elevation view are illustrated in Figure 7.10. The dimensions and section properties of the frame can be found in Table 7.2 and Figure 7.9. For all steel sections, the yield stress is taken as 344.8 N/mm^2 and the Young's modulus as 2×10^5 N/mm^2. The cylinder strength of concrete is taken as 27.3 N/mm^2. Full shear connection is assumed for all composite beams. The frame is analysed for the combination of gravity load 4.8 kN/m^2 and wind load 0.96 kN/m^2. A rigid floor diaphragm action is assumed in the global analysis.

Table 7.2 Properties of composite beams in 20-storey frame (Liew, 2001)

	B_e (mm)	D_s (mm)	D_p (mm)	Steel section
B1	1829	127	0	W21×57
B2	914	127	0	W16×36
B3	17314	127	0	W12×26
B4	1829	127	0	W12×26

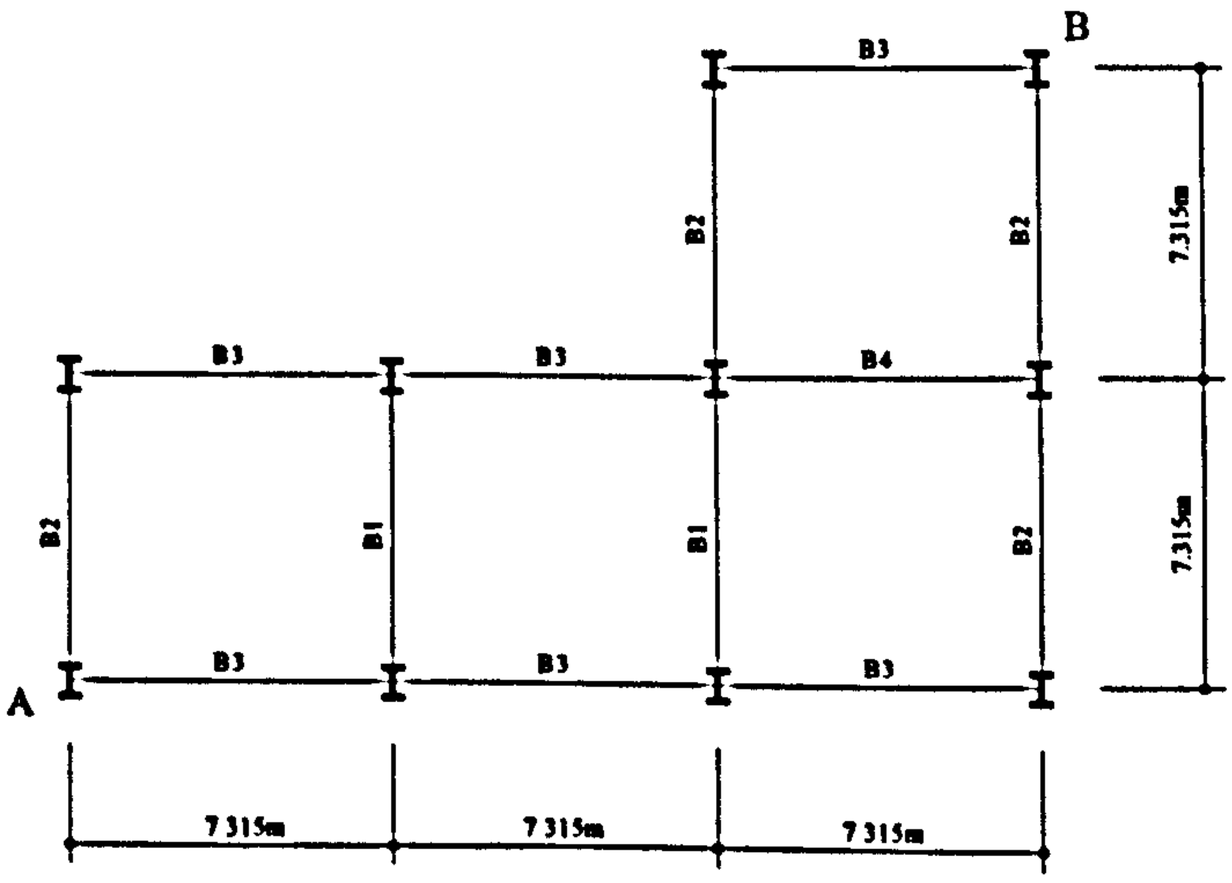

(a) Plan View

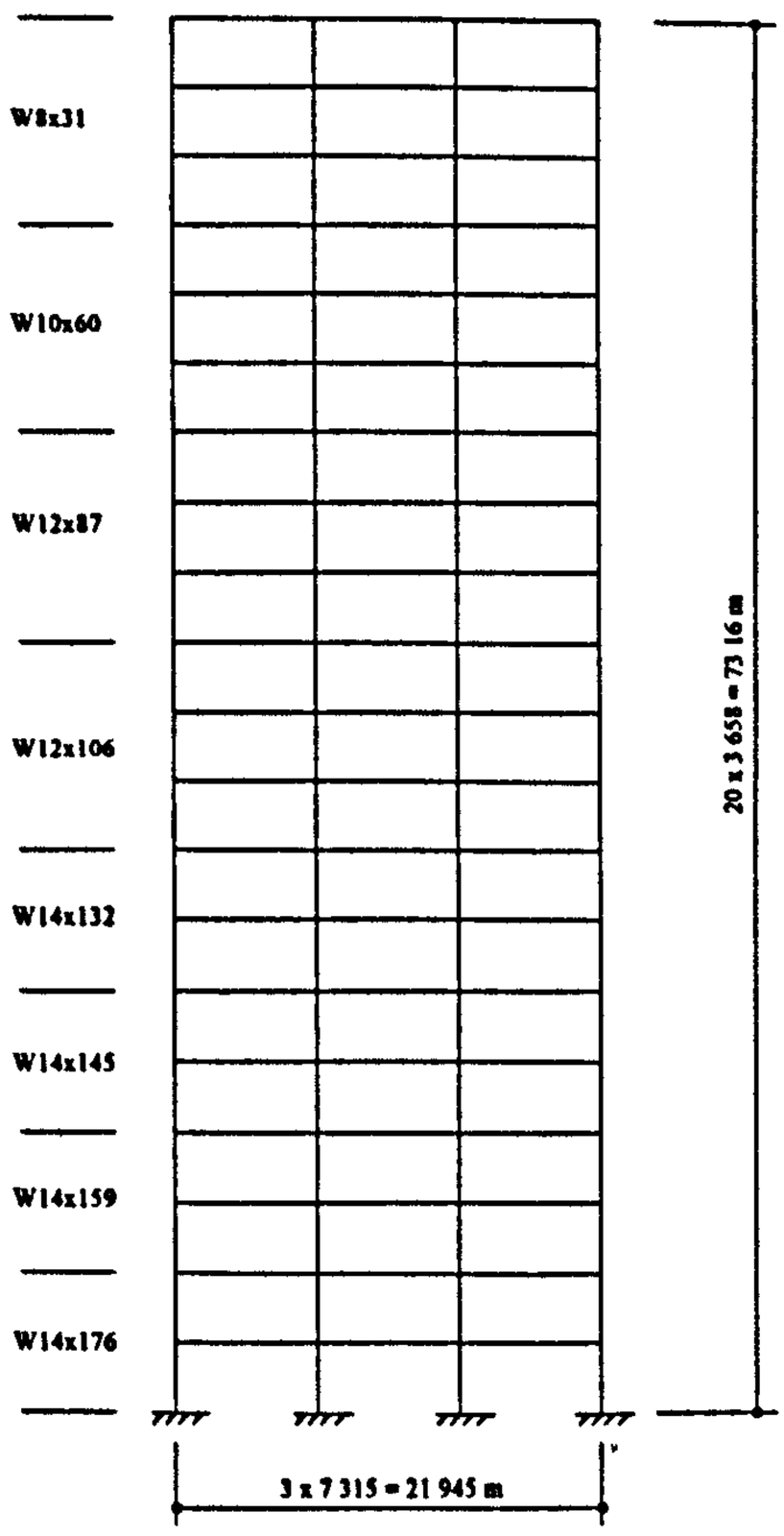

(b) Elevation View

Figure 7.10 20-storey composite frame from Liew et al., (2001)

In the assembly of the space frame model, the steel columns are modelled as normal beam elements. Composite beams are modelled as the proposed beam model, i.e., the concrete slab is modelled as nonlinear cross-section beam elements; the steel beam is modelled as normal beam elements; each shear stud is modelled as a stud element; and rigid links are provided between the stud elements and the steel beam elements. The number of shear studs is calculated on full shear connection condition.

Before the composite beam-to-column connections are modelled, two assumptions are made, they are

- Sufficient anchorage of slab reinforcement outside the columns is not achieved. This is possible because sufficient anchorage of slab reinforcement at such area is hard to achieve; and secondly the anchorage detail of slab reinforcement is not provided by the reference.
- The steel beam-to-column connections are assumed to be pinned. The purpose of this assumption is to investigate the influence of the amount of slab reinforcement to the overall behaviour of the space frame.

For joints located at outside columns, the joint model is established by taking the equivalent lever arm of the reinforcement bars as the distance between the center of the rebars to the elastic neutral axis of the steel beam. For continuous connections, the joint model is established by taking the equivalent lever arm of the reinforcement bars as the distance between the center of the rebars to the center of the steel beam lower flange. Three levels of reinforcement ratios over the connections are evaluated: 0.35%, 0.78% and 2%, representing low, medium and high reinforcement ratios, respectively. Since hardening parameters of the materials are not available, elastic-perfect plastic stress-strain relationship is assumed for all materials. The frame model in the LUSAS Modeller is shown in Figure 7.11. Figure 7.11(a) shows the global view of the frame model; and Figure 7.11(b) shows the top six storeys of the frame model.

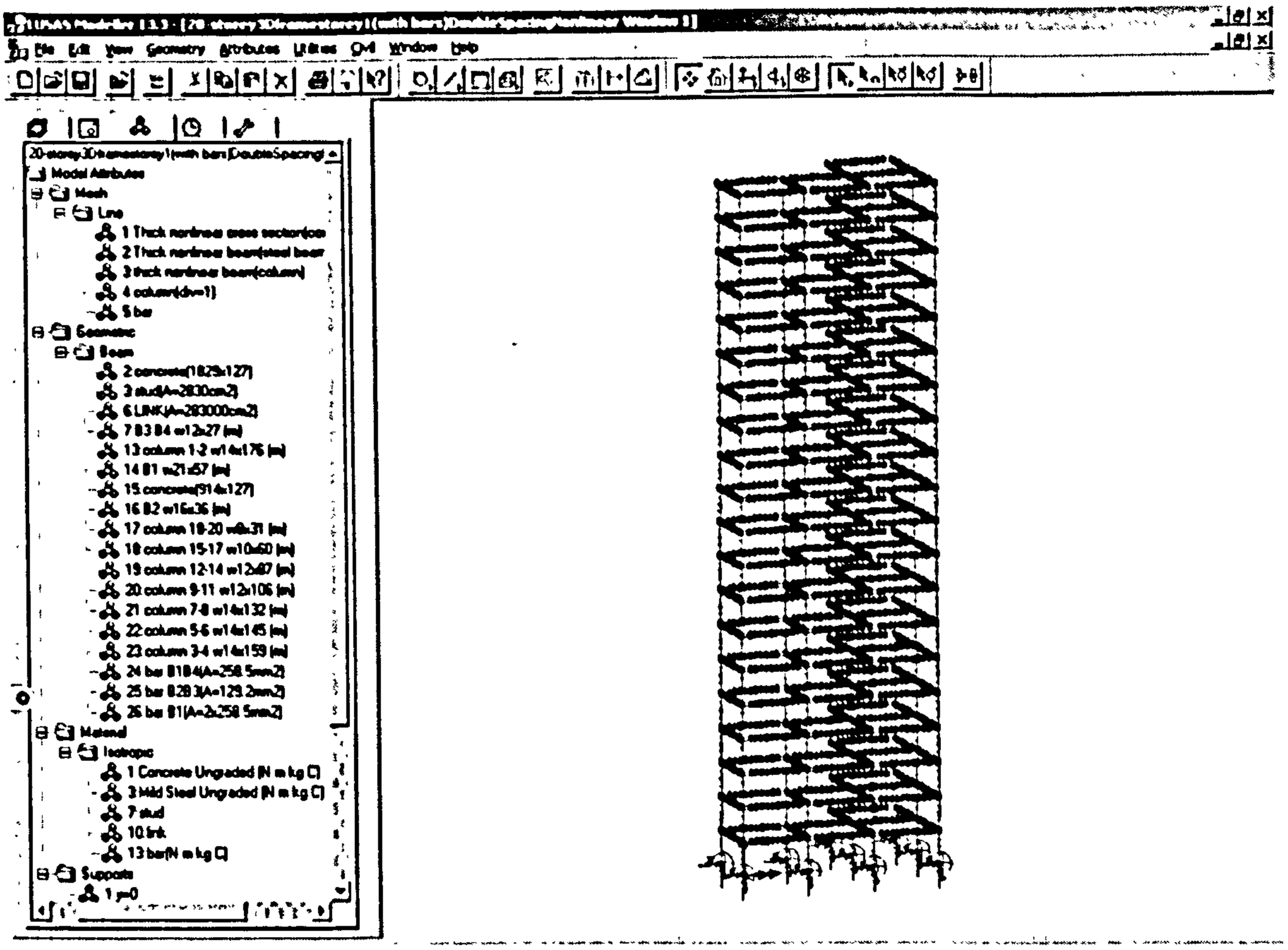

Figure 7.11 Screen shots of the 20-storey composite frame model from LUSAS (a): whole model.

The 20-storey space frame is analysed by increasing the load step at a load factor of 0.1. After yielding the load factor will automatically reduced until a convergence is reached. The iteration procedure stops when a failure mechanism is formed. The load limit ratios and the lateral displacements of the frame are obtained from the analysis. The displacements in the y-direction of two points, point A and B in Figure 7.10, at the top storey of the frame are studied. The load limit ratios obtained from the analysis are shown in Table 7.3. The top storey load-lateral displacement relationship at point A and point B is illustrated in Figure 7.12 and Figure 7.13.

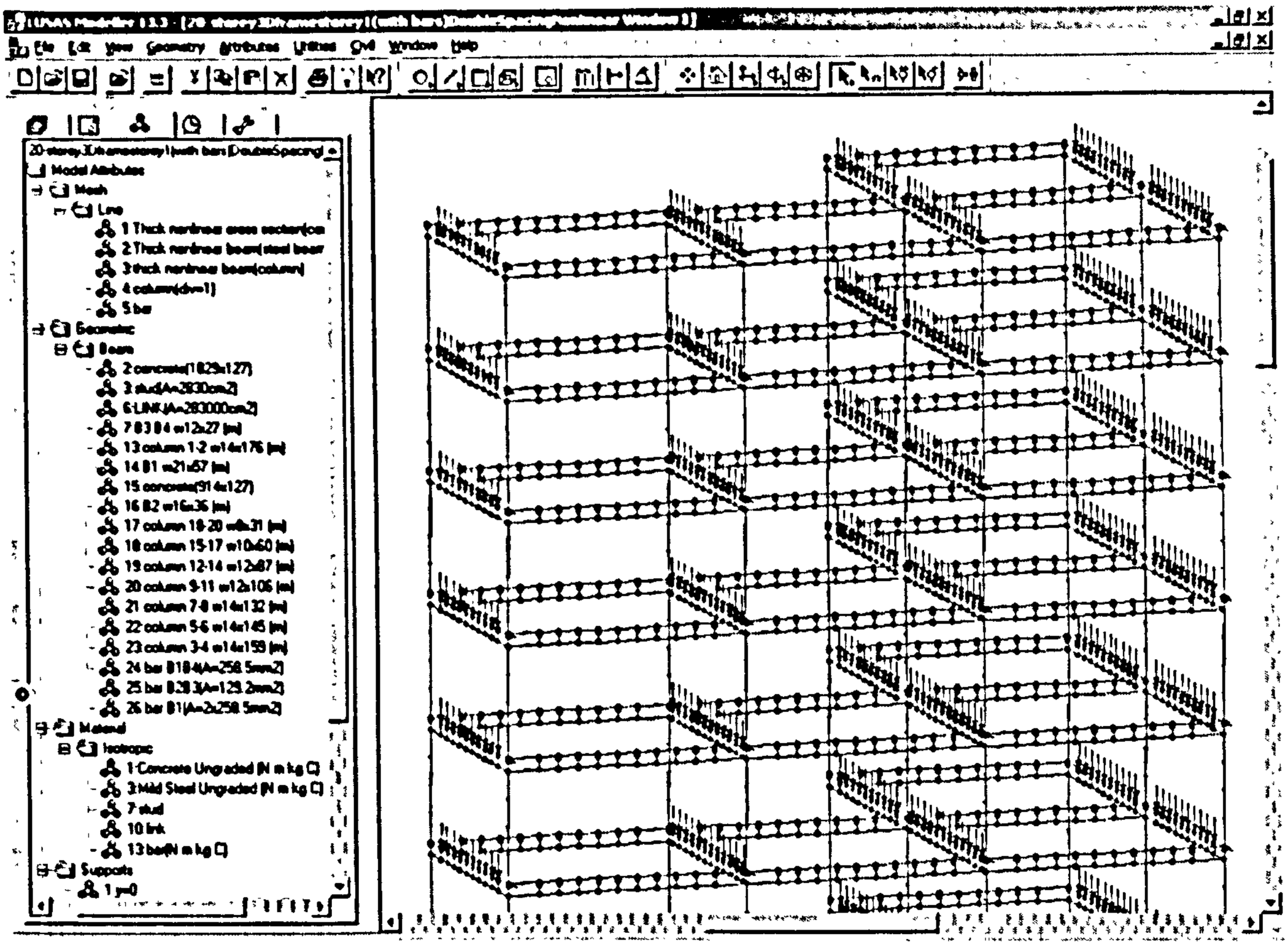

Figure 7.11 Screen shots of the 20-storey composite frame model from LUSAS(b): top six levels

Through studying the load limit of the space frame it can be seen that

- The load limit increased with the increase of the reinforcement ratio. This is probably because that the lateral stiffness of the frame increased with the increase of the reinforcement ratio, hence the frame is capable of resisting higher lateral loads.
- The predicted load limit of the composite frame is slightly lower than the prediction of Liew et al. (2001) even when the reinforcement ratio is as high as 2%. There are two main reasons. Firstly, the composite joints are assumed to be rigid in the model of Liew et al. (2001). Secondly the advantages of strain hardening are neglected for all materials in the proposed model.

- The load limit increased significantly after the reinforcement ratio is changed from 0.35% to 0.88%. But very limited further increase of the load limit (1.6%) is observed even when the amount of slab reinforcement reached a high level of 2%. This is probably because the moment of resistance of the composite joint is limited by the capacity of other joint components despite of the increase of the reinforcement.

Table 7.3 Load limit ratio of the 20-storey composite frame

Reinforcement ratio	0.35%	0.88%	2%	Liew et al., 2001
Load limit ratio	1.16	1.23	1.25	1.338

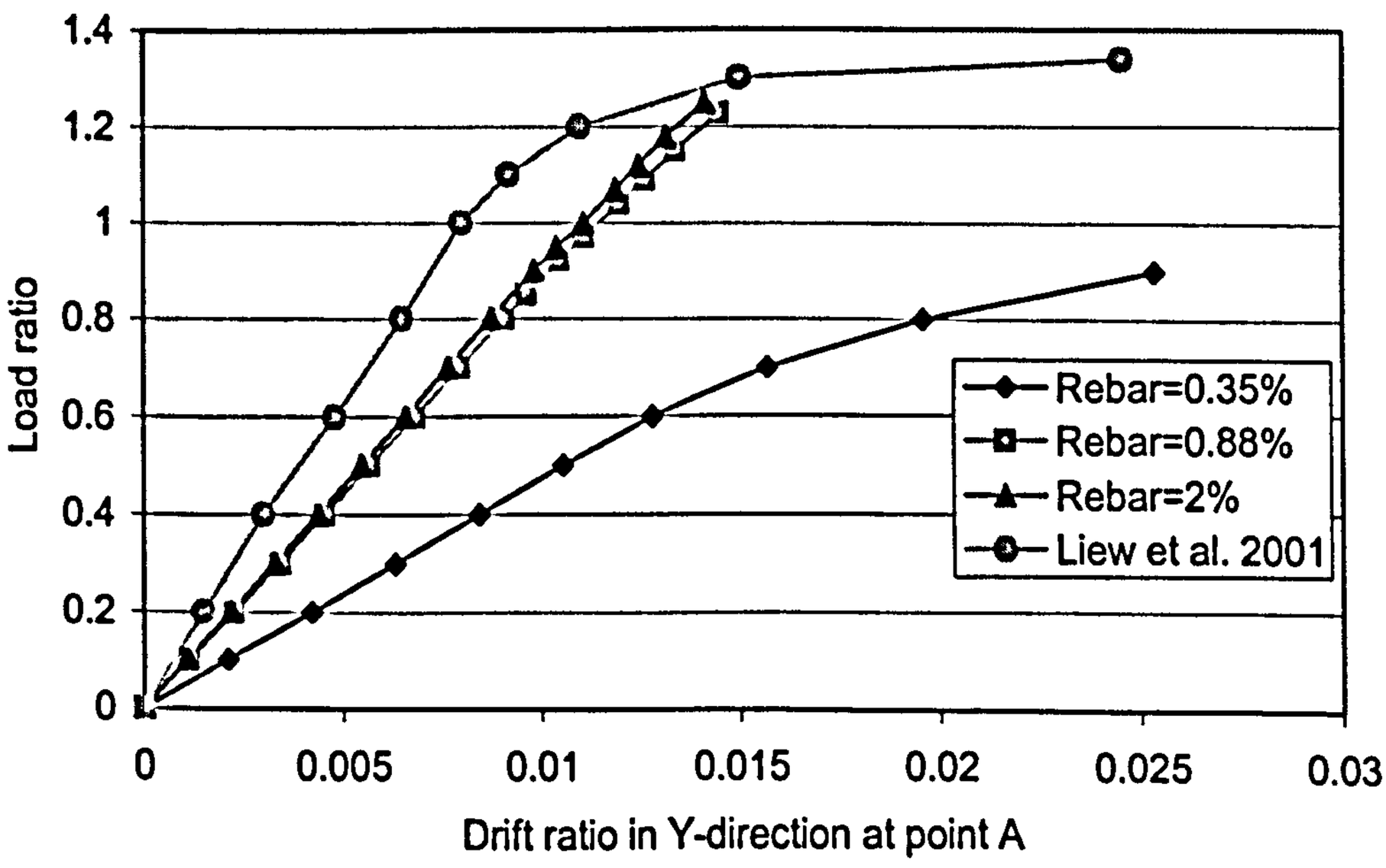

Figure 7.12 Top storey drift ratio in Y-direction at point A

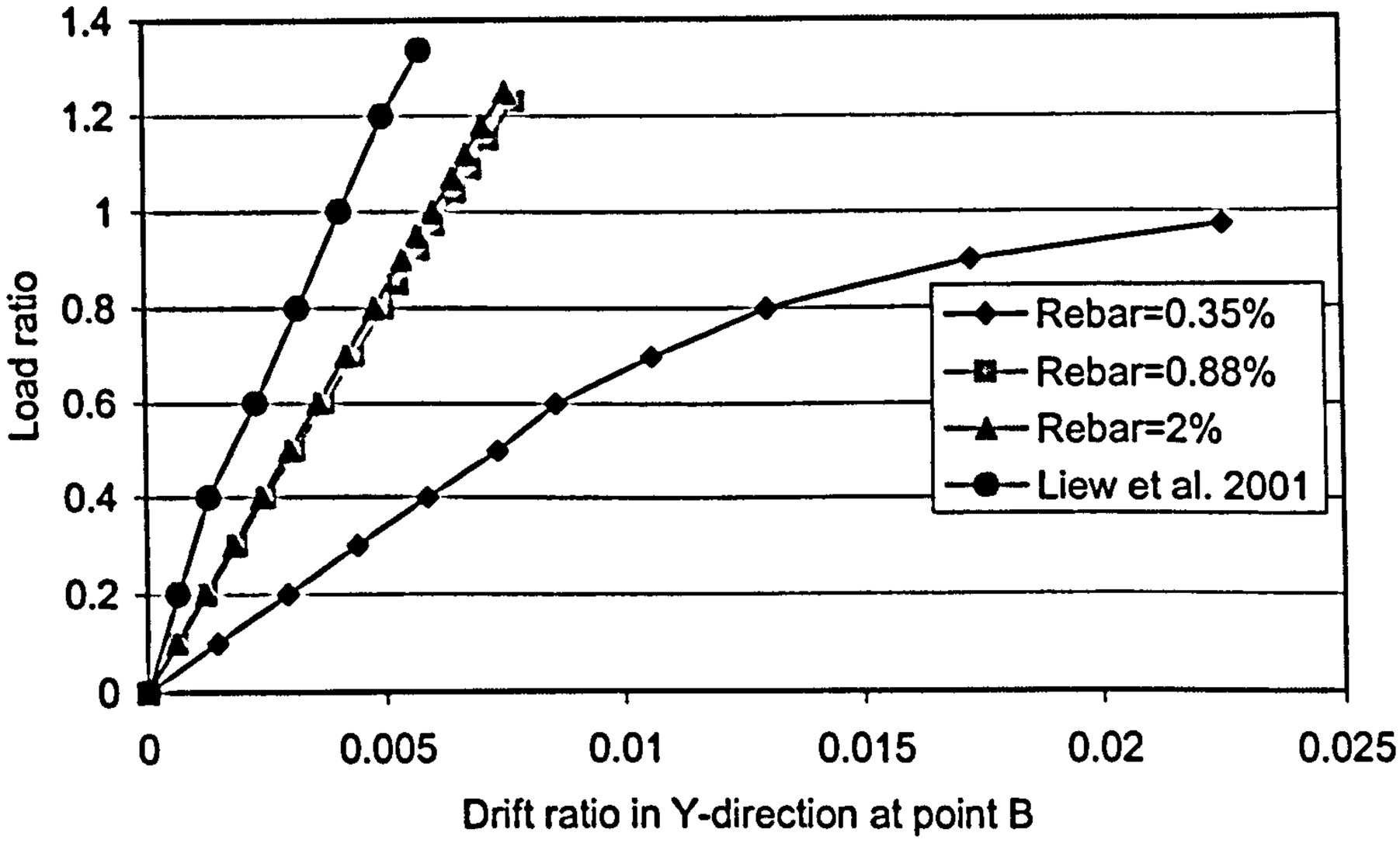

Figure 7.13 Top storey drift ratio in Y-direction at point B

Through studying the lateral displacements of the space frame it can be seen that

- The lateral displacements of the frame reduced with the increase of the slab reinforcement. Again this because the overall stiffness of the frame increased.
- The composite frame with a lower reinforcement ratio (0.35%) yield at a lower load factor (0.6), while the frame yields at the load factor of 0.8 when higher reinforcement ratios are present (0.88%, 2%).
- The lateral displacements of the composite frame reduced significantly when a higher reinforcement ratio (0.88%) is used, compared to a low reinforcement ratio of 0.35%.
- There is no significant reduction in the lateral displacements when the amount of slab reinforcement reached a certain level.
- The predicted lateral displacements of Liew et al. (2001) are smaller than the proposed frame model. This is true because rigid composite joints are assumed in the analysis of Liew et al. (2001).

7.4 Conclusions

An analytical model of composite frames is proposed. The frame model is established by incorporating the proposed composite joint and beam model, with the steel columns modelled as normal beam elements. To validate the proposed frame model, three composite frames are analysed: a composite portal frame, a six-storey composite frame, and a three-dimensional 20-storey composite frame. For all three frames, the amount of reinforcement in the concrete slab is varied to study the effect of the slab reinforcement on the overall performance of composite frames. And the following conclusions may be drawn from the composite frame analysis:

- Composite frames can be explicitly modelled and analysed by the proposed frame model. No extra programming is needed to establish the model.
- Since only line elements are used in the model, the total degrees of freedom of the composite frame model are greatly reduced. The proposed model is therefore very simple and computationally efficient.
- The analytical results agree well to other published approaches.
- The proposed model is effective in predicting the limit state behaviour of composite frames.
- The lateral stiffness of a steel frame will increase significantly if the composite action is taken into account at a very low cost.
- The amount of longitudinal reinforcement in the concrete slab at joint has great influence on the overall performance of composite frames.
- Increase in the amount of slab reinforcement will result in increase of the overall stiffness of composite frames; increase the load limit; and reduce the lateral displacements.
- Excessive slab reinforcement will make very little difference in the terms of the lateral stiffness and the load limit. The reinforcement ratio ranging from 0.6% to 1% seems to be sufficient for a satisfactory semi-rigid design.

- For the semi-rigid design of composite frames, it is also suggested that at composite joint the amount of longitudinal reinforcement in the concrete slab should be no less than 0.35%.
- Since the moment of resistance of composite joints is closely related to the slab reinforcement, the joint moments transformed to the columns can be easily controlled in order to comply the 'strong column, weak beam' design principle.
- Since the design of composite joints is non-symmetrical, the hysteric moment-rotation loops of composite joints are most likely non-symmetrical. For the analysis of composite frames, the behaviour of the composite joint model under sagging moment should be studied.

Chapter 8 Dynamic analysis of composite structures

8.1 Introduction

Since earthquakes occur frequently all year round over the globe and strong earthquakes can lead to great damage to modern society, it is necessary to investigate the nature of earthquakes and the dynamic response of structures, especially the earthquake resistance of structures. The importance of dynamic analysis lies in two points: firstly it can provide criteria to evaluate the capacity of existing structures under possible earthquake loading; and secondly it can provide design criteria for future structure design. In a word, the purpose of the research is to reduce the possible damage to the minimum through the optimal design method.

Composite construction has been widely used in the North America and most European countries in the past three decades. But the earthquake resistance of such structures is still a research topic. The research on semi-rigid design has shown that structures with semi-rigid connections have many advantages over conventional rigid or pinned connection designs. But with the introduction of semi-rigid composite beam-to-column connections, the complexity of the research is greatly increased. Reports on frame damage, after the 1994 Northridge earthquake, show that most damage started as cracking in the bottom beam flange weld but no damage was reported in steel moment frames designed with bolted or riveted connections (Nakashima, et al., 2000). Does that mean that semi-rigid composite construction is a better alternative in seismic design than the conventional fully welded connection design? This question can only be answered when the many aspects of the seismic performance and design problems of semi-rigid composite structures are fully investigated. In this chapter recent research on the seismic behaviour of composite structures is reviewed. Efforts on the modelling and analysis of composite frames under earthquake loading are reported. Future research on dynamic analysis of composite structures is outlined.

8.2 Literature review

Research on the dynamic analysis of composite structures started as soon as this type of construction was introduced to the industry. Due to the complexity of the composite joint and the response of the structures under dynamic loading, the research is still going on. Since a large number of failures were found in the fully welded connections after the 1994 Northridge earthquake, researchers have realized the advantages of moment-resisting frames with semi-rigid beam-to-column connections in the effort to find an alternative for the conventional rigid connection design. In this section, recent research reports on the investigation of the dynamic behaviour of semi-rigid joints and composite structures are reviewed.

8.2.1 Suarez, et al., 1996

Suarez, et al. (1996) studied the dynamic and seismic response of steel frames with flexible beam-to-column connections. A beam element was proposed for finite element analysis, in which the flexible connections were represented by rotational springs with linear moment-rotation relationships. A ten-storey plane steel frame was used to study the effect of the connection flexibility on the dynamic properties and seismic response. It was reported that the connection flexibility had the most effect on the lowest frequency and the partition factors and mode shapes were also affected. Those effects were also reflected in the seismic response. It was observed that the displacement responses were increased by the inclusion of the joint flexibility. Although the structure was more flexible by considering the joint flexibilities, the shear force and bending moments in the lower storey were increased. The peak amplitude of the floor response spectrum for the top floor was reduced. The authors finally concluded that the size and the eccentricity of the connection did affect the dynamic characteristics and response, however, this effect was not observed to be very large.

8.2.2 Broderick & Elnashai, 1996

In Eurocode 8 a structural behaviour factor is introduced in seismic design. The behaviour factor is employed to reduce the seismic design loads to a level which allows the benefits offered by the energy dissipation capacity of each structure to be developed, while still ensuring that the imposed ductility demand does not exceed the available supply. It is assumed that the total response, including both elastic and plastic deformations, is no greater than that implied by a linear plastic analysis under the reduced loads. Since the behaviour factors of composite frames are not available, Eurocode 8 employs the same values as the design of steel frames. In order to obtain more rational values of the behaviour factor, Broderick & Elnashai (1996) performed seismic analysis on 20 moment-resisting composite frames varying in dimension and member type using a nonlinear dynamic analysis program ADAPTIC. To include a realistically wide range of earthquakes, six different ground motion records were employed. Each frame was designed according to the requirements of the structural Eurocodes. For each frame the structural behaviour factors were identified by defining those ground motion intensities sufficient enough to cause yield and collapse. In this regard failure criteria were defined which reflect the response at both the local (member) and global (storey) levels.

Through a series of dynamic analyses it was found that the structural behaviour factors were significantly greater than those recommended by Eurocode 8. While the interstorey drift was the most severe response parameter, the inelastic rotation of composite beams under negative moment more usually determined the identified behaviour factors. Sufficient differences in the seismic behaviour of composite and steel frames have been identified to justify the use of separate behaviour factors, and hence the code provisions for composite structures should be amended to reflect the more accurate behaviour factors.

In the design of composite frames to resist gravity loading, a large portion of the negative beam moments are redistributed to the positive moment regions. However, as seismic design is normally based on elastic analysis, this is not possible when earthquake loads are to be resisted. To properly reflect the characteristics of composite frames, it was recommended that plastic design procedures should be employed. It was suggested that the use of local behaviour factors to reduce the design forces in selected locations might allow this to be achieved. It was observed that the enhanced rotation ductility capacities of composite members and the asymmetric behaviour of composite beams in particular, greatly improved the energy dissipation capacities of moment-resisting composite frames over that of their bare steel equivalents; leading directly to the identified higher behaviour factors.

8.2.3 Leon, et al., 1998

After the 1994 Northridge, California, earthquake, numerous unexpected fractures were found in welded connections of moment-resisting frames, mainly in the regions of the bottom girder flanges. In these frames, the steel beam flanges are connected to the column flanges using complete joint penetration (CJP) welds and details that were thought to provide excellent ductility and strength. Single plate shear tabs are usually bolted to the beam web and welded to the column flange, with some welding to the beam web being required if the steel beam flanges cannot transfer 75% of the plastic moment capacity of the steel cross section. Field reports indicated that 90-95% of the brittle failures initially documented in structures with rigid diaphragms were in the bottom flange connections, with many of the failures concentrated near the CJP weld of the beam flange to the column flange, and in the heat affected zone (HAZ) of the weld. The failure was observed in frames with a great variety of framing configurations, and often in frames that were built only a few years before the earthquake, indicating unexpected shortcomings in the design and detailing procedures.

In assessing the prevalence of bottom flange failures, the authors speculated that the presence of the floor slab might have played a major role in the local behaviour of the connection. In general, for seismic design it is assumed that the floor slab forms a rigid diaphragm and transfers only the in-plane loads to the moment-resisting frames. It is not customary to account for the presence of the slab in structure calculations of the beam and connection capacity. However, based upon a capacity design philosophy, the authors suggested that it might be unconservative to ignore the contribution of the concrete slab to the strength and stiffness of the structural system. It was possible to shift from a strong column/weak beam failure mechanism to a strong beam/weak column failure mechanism. Because the stiffness of the beam increases due to the presence of the slab, a larger portion of forces is attracted. This has to be transferred by the welds.

In order to investigate the effect of the composite floor slab, three full-scale specimens of interior pre-Northridge connections were tested, along with corroborating computational research, which included both continuum finite element analyses of the specimens and nonlinear analyses of an existing steel frame structure to assess demand during the Northridge earthquake. The tests included a bare steel specimen, a composite specimen with 55% composite interaction, and a composite specimen with 35% composite interaction. All six connections failed at the bottom flange by fracture. The three connections with a backup bar on the bottom flange failed prematurely at 1.5% drift by brittle failure at the interface between the complete joint penetration weld and the column flange, while the three connections without backup bars failed at 3% drift, but after only 1-3 cycles. The composite connections exceeded the plastic moment strength of their bare steel section, indicating the possible unexpected strong beam/weak column frame system if the concrete slab is neglected in the design. All six connections did not achieve their calculated moment strength in positive bending. And none of the connections exhibited adequate levels of ductility, especially when subjected to positive bending moment. The bottom region of the connections in the composite specimens generally sustained significantly more damage compared to the top region, featuring local flange buckling and extensive plastification at the bottom flange. This prevalence

of damage occurring to the bottom beam flange correlates well with the observed damage from the Northridge earthquake. The finite element analysis results verified that near the beam-to-column interface, the strains focused more substantially in the flanges, and especially in the bottom flange in the composite specimens.

Through the test investigation and finite element analysis, the authors concluded that it was prudent to establish an approach to connection design, which at a minimum, considered the inherent asymmetries in the connection region due to the presence of concrete floor slabs. It was suggested that an appropriate proportioning of beam-to-column connections be desired such that inelastic behaviour occurs at a location away from the column face, in which minimal use of the highly restrained column material and welded joints was recommended.

8.2.4 Leon, 1998

Since the basic code design accelerations in large areas of the U.S. and the rest of the world were upgraded to levels ranging from 0.10 to 0.20g, the author pointed out that fully restrained (FR) moment-resisting frames were unlikely to be economically built there. Partially restrained composite frames (PR-CFs) were an economic alternative since they could provide both energy dissipation and drift control. And PR-CFs could make use of the concrete floor slab to increase the strength, rigidity and redundancy of the structural system. Before the design method of PR-CFs is developed, the author stated several problems relating to the structure analysis:

- Determination of moment-rotation relationships;
- Incorporation of the slab effects into the member properties;
- Modelling of partial interaction in the beams;
- Frame stability;
- Effect of partial strength connections;
- Level of modelling required.

With particular reference to seismic considerations, the problems were:

- Determination of a natural period;
- Use of simplified modelling for preliminary design;
- Determination of force reduction and displacement amplification factors;
- Level of detailing required.

The author investigated and discussed the above problems arising from partial restrained composite frame design. By comparing the lateral drifts of FR and PR frames, it was found that a PR frame did not necessarily drift more than a FR one; in fact, in many cases it drifted less. Studies conducted on numerous PR frames utilising nonlinear dynamic analysis programs indicated that the envelopes of drift for PR and FR frames were very similar. The author suggested that there was no reason to believe that PR frames present a potential stability problem under seismic loads. Furthermore, studies showed that the rotational demands for PR frames subjected to seismic loads were well within the rotational capacities achieved in tests of PR connections. It was believed that PR frames could become an attractive structural alternative in areas of low to moderate seismic demand within a very short time.

8.2.5 Liu & Astaneh-Asl, 2000

Simple, or shear, steel beam-to-column connections are usually assumed to be pinned in frame design and no lateral resistance is considered for such connections. However, in composite construction these connections may act as partially rigid connections with the composite action of floor slab and they may possess certain lateral load resisting capacity. Liu & Astaneh-Asl (2000) performed six-teen full-scale cyclic tests on such composite connections to investigate the influence of concrete slabs on the performance of such connections.

The tests showed that the maximum lateral load resistance of composite connections were up to double that of bare steel connections. The composite action was lost due to damage to the concrete, along with severe buckling of the metal deck. And the composite connections reverted towards the behaviour of the bear steel connections. The maximum moment capacity of composite joints reached 30-45% of the plastic moment capacity of the composite beam sections. Additional reinforcement in the concrete slab did not significantly improve the cyclic performance of the composite connections. The negative moment capacities of the joints increased, but the lateral load resistance did not. By comparing the tests with and without concrete infill between the column webs, it was observed that the absence of concrete in the column web cavity reduced the maximum lateral load capacity of the joint. But the failure of the connection occurred later in such cases. It was therefore suggested that a slight increase in the ductility, but a decrease in the lateral capacity would result from the absence of the concrete in the column web cavity.

8.2.6 Bugaja et al., 2000

Bugeja et al. (2000) investigated the seismic performance of composite RCS moment frame systems, which consist of reinforced concrete (RC) columns and composite steel beam-reinforced concrete slab sections. Using RC, rather than steel columns can result in significant material cost savings, increased inherent structural damping, and significantly increased lateral stiffness of the building. Six tests were performed on two-thirds-scale subassemblage joint specimens with various beam-to-column joint detail arrangements. Test results showed that with appropriate joint detailing, the specimens exhibited a desirable beam plastic hinge mechanism with stable hysteretic response. Composite beam sections maintained near full composite behaviour beyond the drift limits suggested by the American design code with good energy dissipation characteristics and were able to undergo large plastic rotation magnitudes. For the purpose of composite beam design the authors gave recommendations on the effective flange width based on the test results. It was believed that composite RCS moment

frame systems were an alternative structural framing system for low-to-mid-rise structures in high seismic risk zones.

8.3 Seismic design criteria of composite structures

Current available European design provisions for seismic resistance of structures are Eurocode 8, Part 1.1 (1994). Future parts of Eurocode 8 include specific provisions for different kinds of structures. But seismic design provisions for composite structures are not among them. Since composite structures are the most popular type of construction for low to middle rise commercial and office buildings, it is necessary to produce seismic provisions for such buildings. To date a certain amount of research has been carried out on the seismic performance of composite frames and beam-to-column joints reported mainly in North America, Japan and some European countries. It is far from being enough to provide validation for the seismic design provisions. Extensive experimental and numerical research needs to be done on the seismic behaviour of composite joints, beams, columns and frames.

Despite the difficulties in the seismic design of composite structures, some basic principles and general rules can be applied to such structures. In order to evaluate the performance of composite frames under earthquake loading, the failure criteria of composite frames need to be studied. It is assumed that once one of these criteria is reached the composite frame will fail. Further increase in the loading will result in partial or overall collapse of the structure. For safety reasons these criteria should always be conservative in practical frame design. In general the following response criteria should be investigated.

8.3.1 Interstorey drift limit and storey stability

Under strong earthquake loading, large lateral displacements of the frame could occur. Excessive lateral displacement will lead to the P-Δ effects. To control the P-Δ effects,

the storey drift limit should be defined. The most common method of measuring the interstorey drift is by the interstorey drift index, Δ_i, defined as

$$\Delta_i = \frac{\delta_i - \delta_{i-1}}{h_i} \tag{8.1}$$

where δ_i is the instantaneous displacement at floor level i and h_i is the storey height under consideration. In some analysis (Broderic & Elnashai, 1996), a limit of 3% is suggested.

In Eurocode 8 an intersrotey drift sensitivity coefficient is defined to take into account the second order effects (P-Δ effects).

$$\theta = \frac{P_{tot} \cdot d_r}{V_{tot} \cdot h} \tag{8.2}$$

where θ is the interstorey drift sensitivity coefficient; P_{tot} is the total gravity load at and above the storey considered; d_r is the design interstorey drift; V_{tot} is the total seismic storey shear; h is the interstorey height. If $\theta \leq 0.1$, the P-Δ effects need not be considered. If $0.1 < \theta \leq 0.2$, the second order effects can approximately be taken into account by increasing the relevant seismic action effects by a factor of $1/(1 - \theta)$. the limit value of θ is set to 0.3.

8.3.2 Steel column response criteria

The column base at ground floor level is one of the critical zones in seismic design. It is demanded that sufficient rotation capacity be possessed by the column base to dissipate the large strain energy caused by earthquakes. It is therefore required that the critical

buckling strain of the compression flange should not exceed the plastic strain caused by earthquakes.

Apart from the critical buckling strain of the column flange, the plastic hinges on columns should also be monitored. A collapse mechanism will form if the simultaneous existence of plastic hinges at both the upper and lower ends of a steel column. The occurrence of a plastic hinge may be identified if strains in both tension and compression flanges of the column exceed the plastic strain.

8.3.3 Composite beam response criteria

In moment-resistance composite frames the lateral resistance is primarily provided by the flexural resistance of composite beams and steel columns. The composite beam-to-column connections may be subject to large negative moment and positive moment as well during an earthquake. In beam spans under positive bending the tensile failure of the steel beam section is unlikely to occur, while the failure of concrete slab under compression should be considered. The compression failure of concrete slab may be monitored by the critical compression strain of the concrete. A value of 0.0035 is suggested by (Broderic & Elnashai, 1996).

In composite joints under negative bending, if the rupture of the longitudinal reinforcement is unlikely to occur prior to the local buckling of the beam flange and web under compression, the critical local buckling stress and strain of the beam flange and web should be investigated, and the maximum stress and strain of the beam flange and web in compression should be monitored.

8.4 Seismic analysis of composite frames

In this section a six-storey composite frame is analysed under seismic loading and its performance is discussed. The same frame is used as previously described in Chapter 7

for static analysis. The elastic response spectrum is obtained from Eurocode 8. The proposed composite frame model is used and applied directly to the seismic analysis.

8.4.1 Elastic response spectrum

The earthquake motion at a given point of the surface may be represented by a ground acceleration response spectrum. For elastic seismic frame analysis, Eurocode 8 defines an elastic response spectrum, $S_e(T)$, by the following expressions:

$$0 \le T \le T_B: \quad S_d(T) = a_g \cdot S \cdot [1 + \frac{T}{T_b} \cdot (\eta \cdot \beta_0 - 1)] \tag{8.1a}$$

$$T_B \le T \le T_C: \quad S_d(T) = a_g \cdot S \cdot \eta \cdot \beta_0 \tag{8.1b}$$

$$T_C \le T \le T_D: \quad S_d(T) = a_g \cdot S \cdot \eta \cdot \beta_0 \cdot [\frac{T_C}{T}]^{k_1} \tag{8.1c}$$

$$T_D \le T: \quad S_d(T) = a_g \cdot S \cdot \eta \cdot \beta_0 \cdot [\frac{T_C}{T_D}]^{k_1} \cdot [\frac{T_D}{T}]^{k_2} \tag{8.1d}$$

Where

$S_e(T)$	the elastic response spectrum,
S	soil parameter,
T	vibration period of a linear single degree of freedom system,
T_B, T_C	limits of the constant spectral acceleration branch,
T_D	value defining the beginning of the constant displacement range of the spectrum,
a_g	design ground acceleration for the reference return period,
β_0	spectral acceleration amplification factor for 5% viscous damping,
η	damping correction factor with reference value $\eta = 1$ for 5% viscous damping,
k_1, k_2	exponents which influence the shape of the spectrum for a vibration period grater than T_C, T_D respectively.

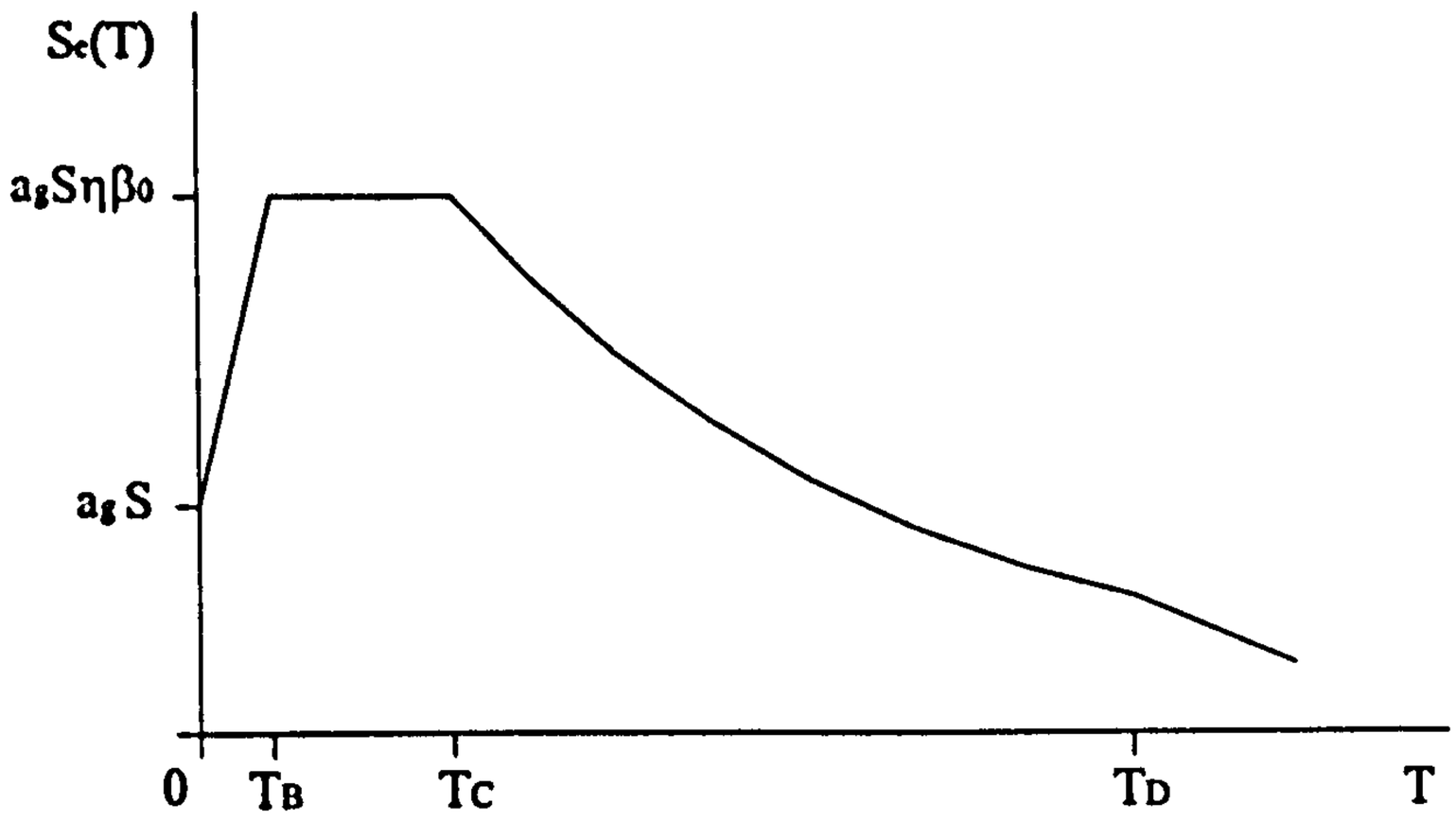

Figure 8.1 Elastic response spectrum of EC 8, Part 1.1 (1994)

8.4.2 Design response spectrum

For structural systems to resist seismic actions in the nonlinear range, the design capacity is generally smaller than that corresponding to a linear elastic response. To avoid explicit nonlinear structural analysis in design, Eurocode 8 recommends that a linear analysis be performed based on the design response spectrum, which is reduced with respect to the elastic response spectrum. This reduction is accomplished by introducing the behaviour factor q, which is defined in Eurocode 8, Part 1.1 (1994) as an approximation of the ratio of the seismic forces that the structure would experience if its response was completely elastic with 5% viscous damping, to the minimum seismic forces that may be used in design with a conventional linear model.

In Eurocode 8, Part 1.1 (1994) the design response spectrum as shown in Figure 8.1 is defined by the following expressions:

$$0 \le T \le T_B: \quad S_d(T) = \alpha \cdot S \cdot [1 + \frac{T}{T_b} \cdot (\frac{\beta_0}{q} - 1)] \tag{8.2a}$$

$$T_B \le T \le T_C: \quad S_d(T) = \alpha \cdot S \cdot \frac{\beta_0}{q} \tag{8.2b}$$

$$T_C \le T \le T_D: \quad S_d(T) = \alpha \cdot S \cdot \frac{\beta_0}{q} \cdot [\frac{T_C}{T}]^{k_{d1}} \quad , but \ge 0.20\ \alpha \tag{8.2c}$$

$$T_D \le T: \quad S_d(T) = \alpha \cdot S \cdot \frac{\beta_0}{q} \cdot [\frac{T_C}{T_D}]^{k_{d1}} \cdot [\frac{T_D}{T}]^{k_{d2}} \quad , but \ge 0.20\ \alpha \tag{8.2d}$$

Where

$S_d(T)$ the design response spectrum, normalised by g,

α ratio of the design ground acceleration a_g to the acceleration of gravity g ($\alpha = a_g/g$),

q behaviour factor,

k_{d1}, k_{d2} exponents which influence the shape of the design spectrum for a vibration period grater than T_C, T_D respectively.

8.4.3 Seismic analysis of a six-storey composite frame

A six-storey composite frame is chosen as a sample frame. The same frame was analysed by the proposed composite frame model to investigate the influence of semi-rigid composite joints on the global performance of the frame. The report can be found in section 7.3.2 of the thesis. This frame may be used to investigate the seismic performance of composite frames with semi-rigid joints though it may not have been designed according to seismic design codes. This is reasonable because the outcomes of the analysis may be used to evaluate those composite frames with no seismic designs under possible earthquake strikes. Secondly the results of the analysis may provide some indications on the seismic design of semi-rigid composite frames.

8.4.3.1 Design response spectrum

The design ground acceleration is assumed to be 0.1g, 0.2g, 0.3g, 0.4g, representing low to high seismic zones. Elastic response spectrums are used for the elastic seismic design method. If economical plastic seismic design is to be adopted, the behaviour factor is introduced to reduce the design ground acceleration. Since the behaviour factors for composite frames are not available, Eurocode 8 suggests the same value as the equivalent steel frames. Research by Broderick & Elnashai (1996) has shown that this assumption is conservative for composite frames, and a 40% increase of the value proposed by Eurocode 8 was suggested. Since the behaviour factors of composite frames are controversial at present, the commonly accepted conservative elastic response spectrums are used in this study. The design response spectrums are illustrated in Figure 8.2.

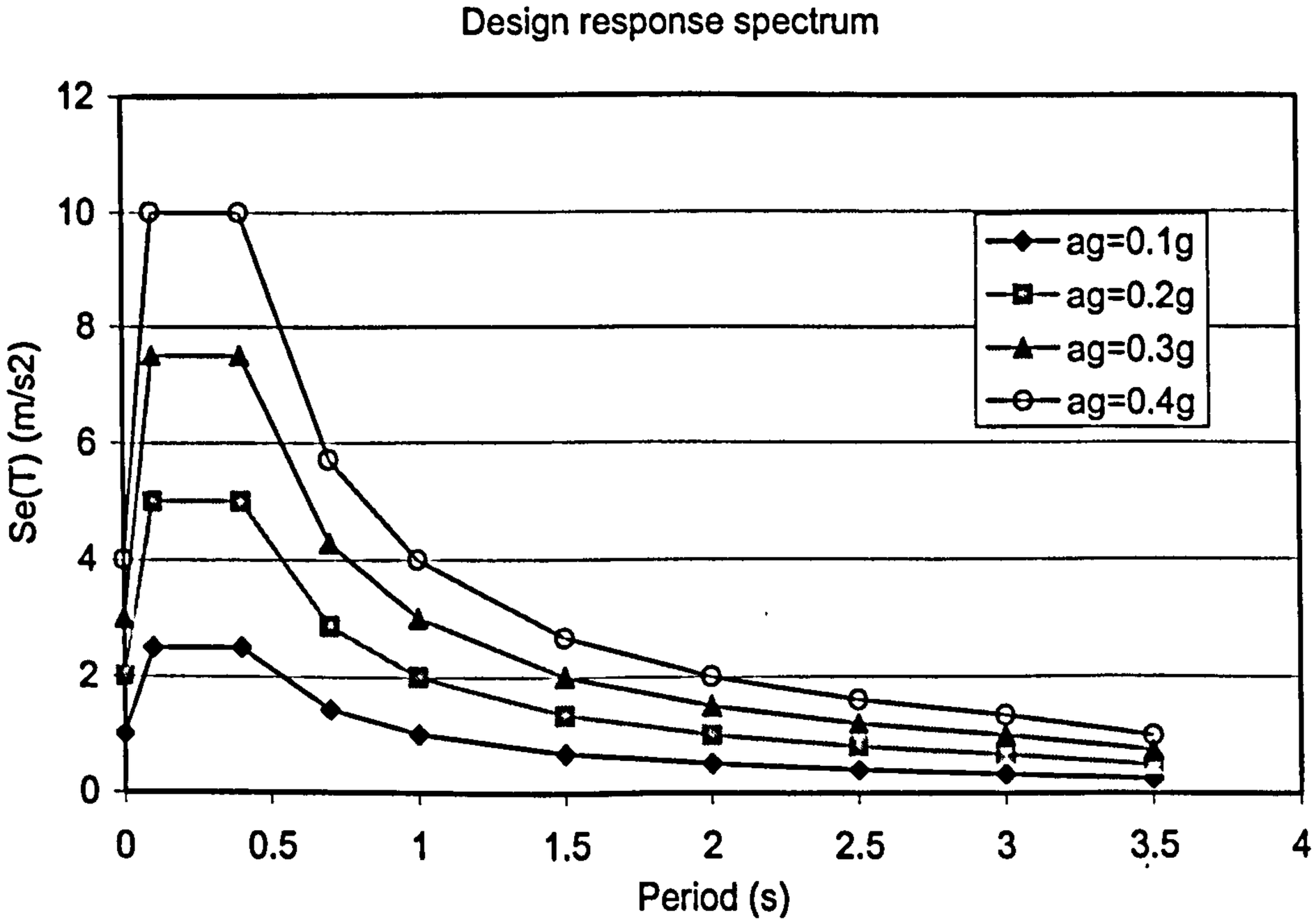

Figure 8.2 Design response spectrums

8.4.3.2 Eigenvalue analysis

The six-storey composite frame is modelled in exactly the same way as in the static analysis on Chapter 7. A brief review of the composite frame model is as following. The steel columns and beams are modelled as normal beam elements. The concrete slabs are modelled as non-linear cross-section elements. The steel beam elements and concrete slab elements are connected by shear stud elements through rigid link elements. The column elements are connected to the composite beams by the proposed composite joint models.

Prior to the seismic analysis, Eigenvalue analysis of the frame is performed to obtain the natural frequencies and the equivalent mode shapes of the frame. The analysis is performed through LUSAS 13 program by the lump mass method with 5% viscous damping. In the analysis the mass of the rigid link elements is neglected by entering a zero mass density because these elements do not exist in a real composite beam. In order to take into account the influence of high order frequencies and mode shapes, forty frequencies are obtained. The lowest five dominant frequencies and mode shapes are shown in Figure 8.3.

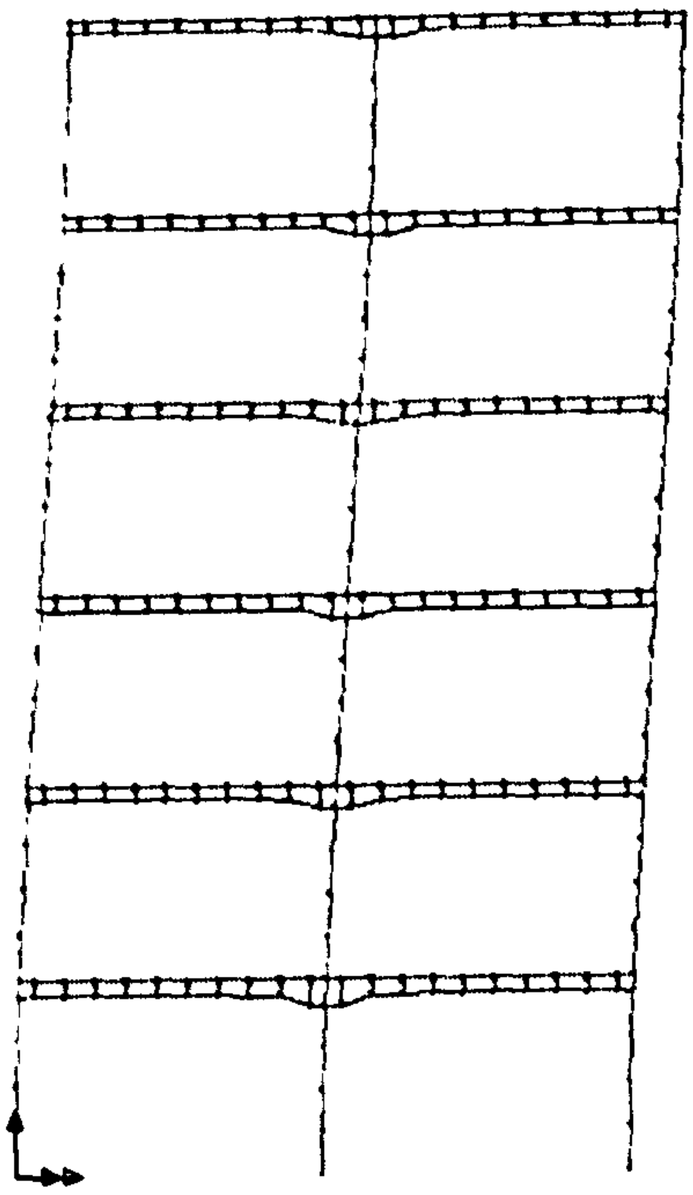

mode shape 1, $f_1 = 0.968s$

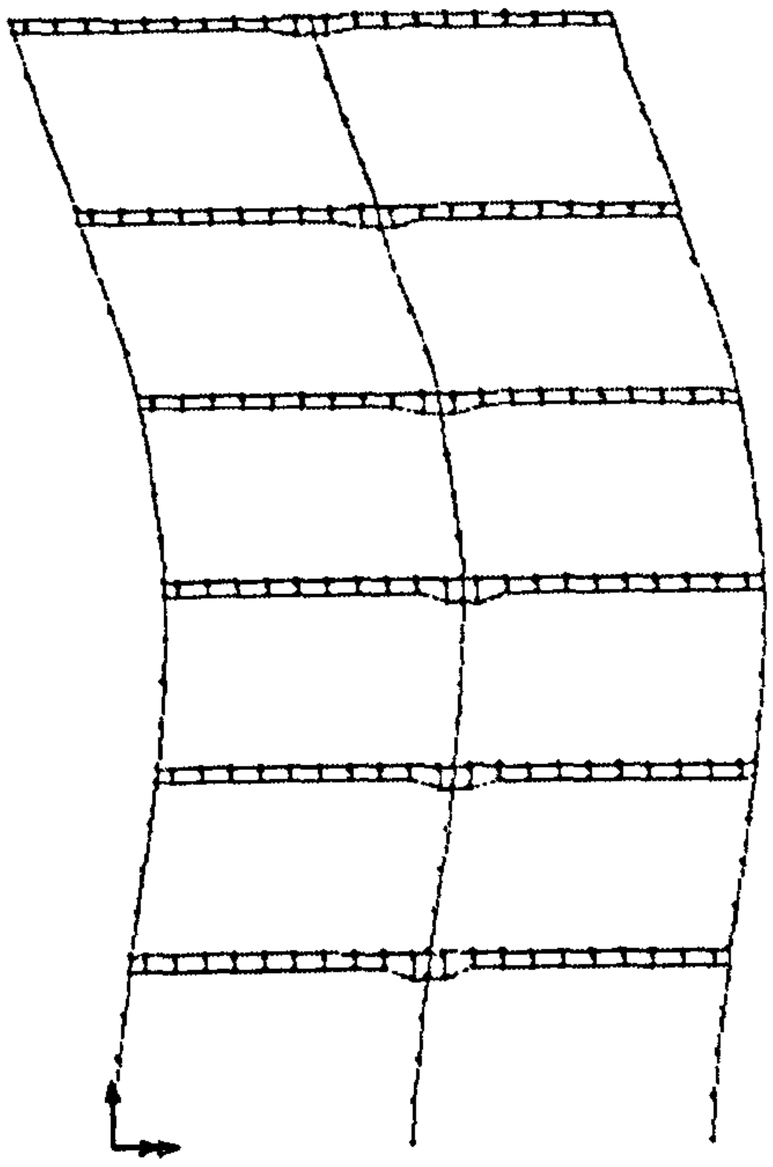

mode shape 2, $f_2 = 2.664s$

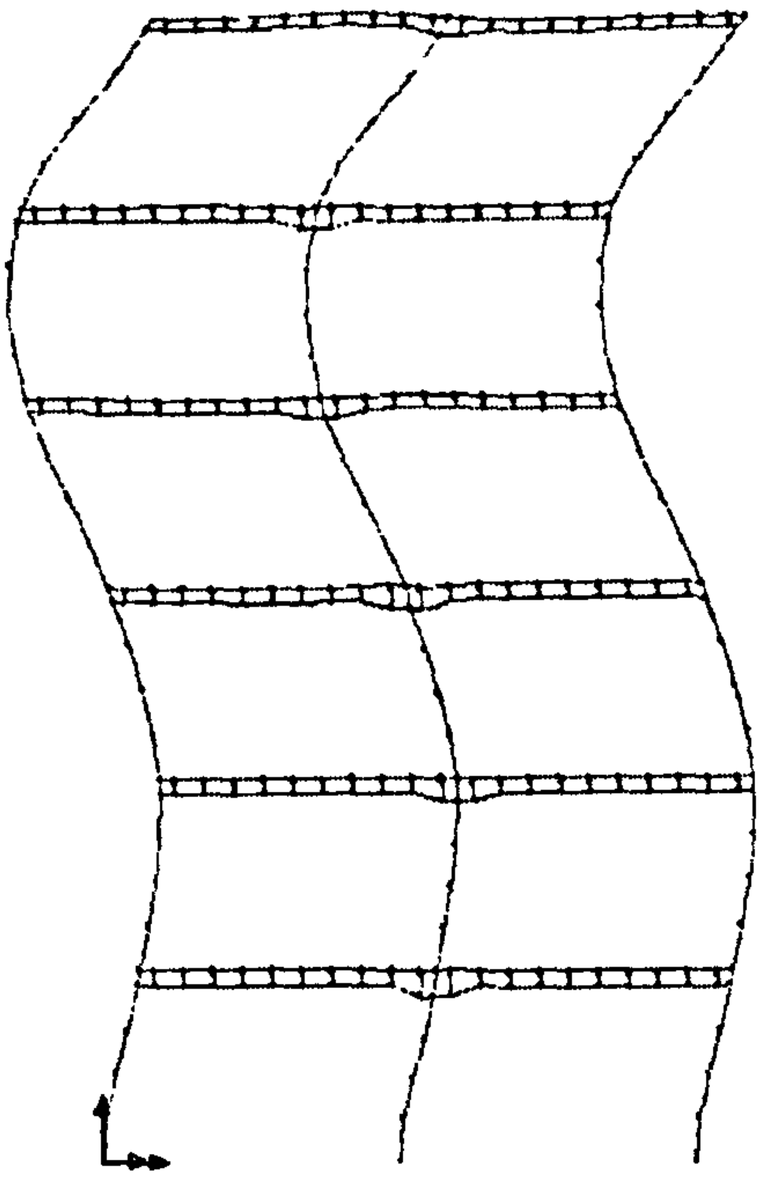

mode shape 3, $f_3 = 4.886s$

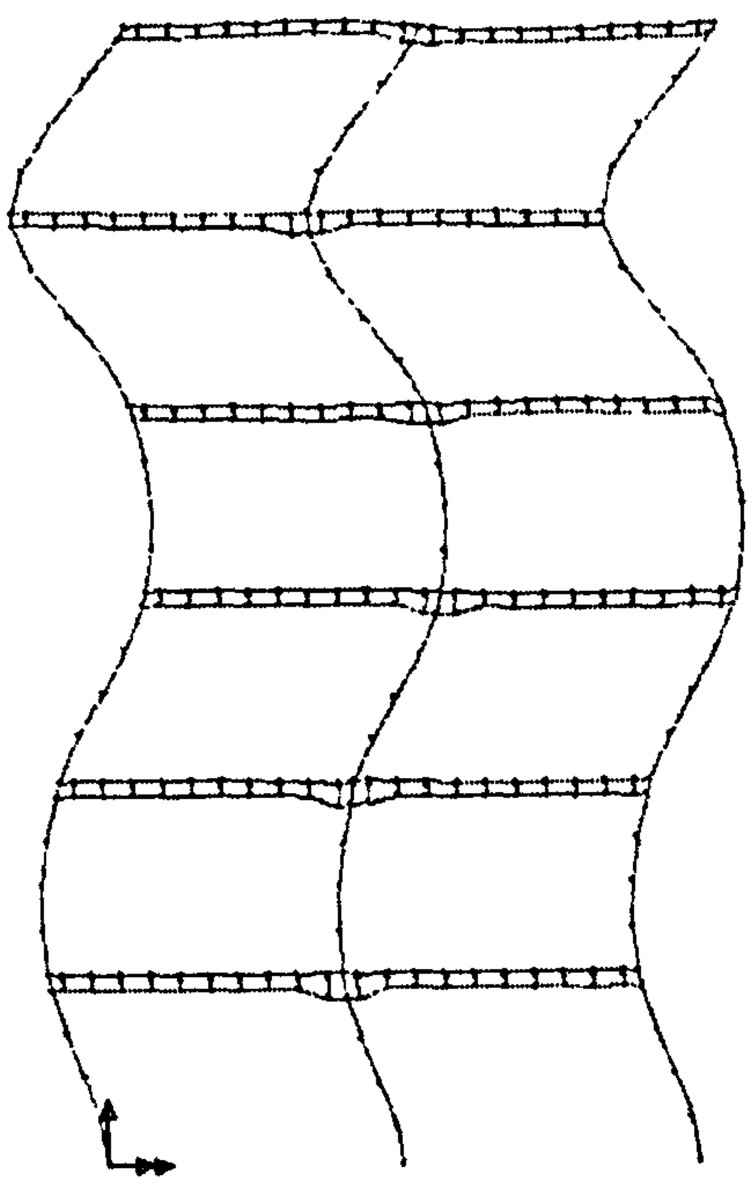

mode shape 4, $f_4 = 7.427s$

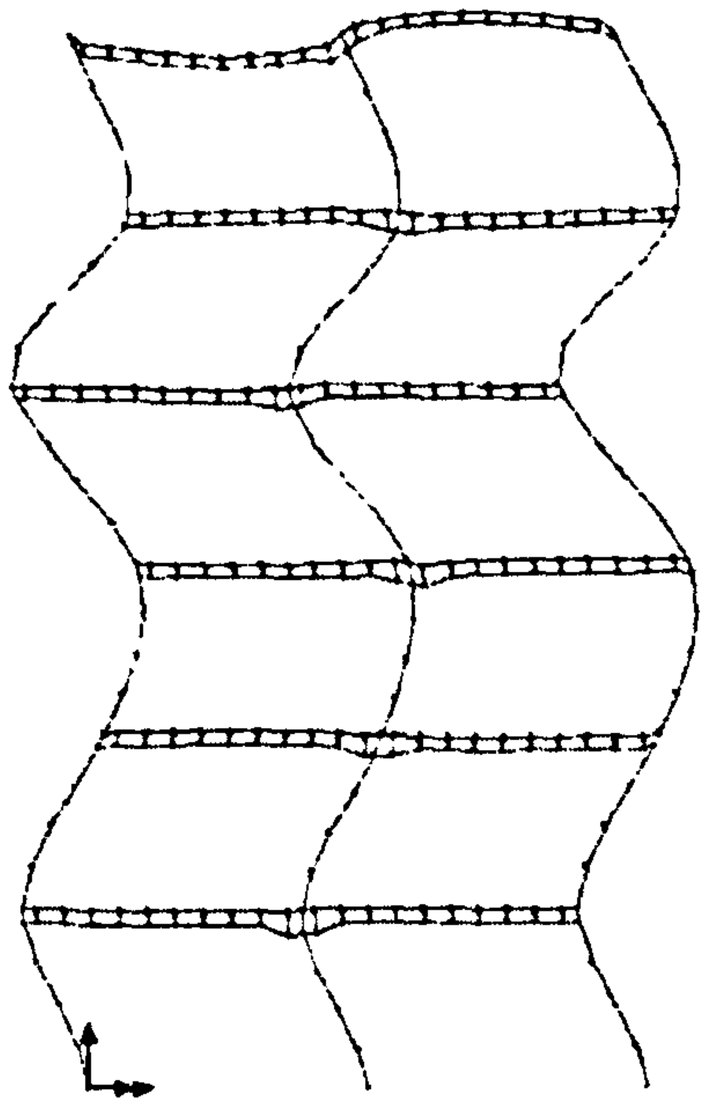

mode shape 5, f_5 = 10.655s

Figure 8.3 Natural frequencies and mode shapes of the six-storey composite frame

8.4.3.3 Seismic analysis

Since the response spectrums have been obtained, the seismic analysis can be performed based on the results of the Eigenvalue analysis of the composite frame, with 5% viscous damping assumed. During the analysis, the stiffness of the composite joint is changed by adjusting the main reinforcement of the slab over the joint. Four levels of reinforcement are adopted, i.e., 4T8, 4T12, 4T16, and 2% reinforcement ratio, representing low to high percentage of reinforcement ratios in the concrete slab. The corresponding four frames are named as Frame 1, Frame 2, Frame 3, and Frame 4, respectively. Through the analysis, the following results are obtained:

- The lateral displacements of the four composite frames, as listed in Table 8.1a, b, c, and d.

- The lateral drift ratios of the four frames, as shown in Table 8.2.
- The interstorey drift ratios of the four frames, as shown in Figure 8.4(a), (b), (c), and (d).

Table 8.1a Lateral displacements of Frame 1 (Rebar = 4T8, unit = meter)

Storey number	Ground acceleration			
	0.1g	0.2g	0.3g	0.4g
6	0.0412	0.0824	0.124	0.165
5	0.0353	0.0705	0.106	0.141
4	0.0273	0.0547	0.082	0.109
3	0.0195	0.0389	0.0584	0.0778
2	0.0115	0.023	0.0345	0.0459
1	0.004	0.008	0.012	0.016
Ground	0	0	0	0

Table 8.1b Lateral displacements of Frame 2 (Rebar = 4T12, unit = meter)

Storey number	Ground acceleration			
	0.1g	0.2g	0.3g	0.4g
6	0.0388	0.0776	0.116	0.155
5	0.0332	0.0664	0.0996	0.133
4	0.0257	0.0514	0.0771	0.103
3	0.0183	0.0366	0.0549	0.0733
2	0.0109	0.0217	0.0326	0.0435
1	0.00384	0.00767	0.0115	0.0153
Ground	0	0	0	0

Table 8.1c Lateral displacements of Frame 3 (Rebar = 4T16, unit = meter)

Storey number	Ground acceleration			
	0.1g	0.2g	0.3g	0.4g
6	0.0379	0.0758	0.114	0.152
5	0.0324	0.0648	0.0972	0.13
4	0.025	0.05	0.0751	0.1
3	0.0178	0.0357	0.0535	0.0714
2	0.0106	0.0212	0.0318	0.0424
1	0.00377	0.00753	0.0113	0.0151
Ground	0	0	0	0

Table 8.1d Lateral displacements of Frame 4 (Rebar ratio = 2%, unit = meter)

Storey number	Ground acceleration			
	0.1g	0.2g	0.3g	0.4g
6	0.037	0.0741	0.111	0.148
5	0.0317	0.0633	0.095	0.127
4	0.0244	0.0488	0.0732	0.0977
3	0.0174	0.0348	0.0523	0.0697
2	0.0104	0.0208	0.0311	0.0415
1	0.0037	0.00741	0.0111	0.0148
Ground	0	0	0	0

Table 8.2 Lateral drift ratios of Frame 1, Frame 2, Frame 3, and Frame 4

Frame number	Ground acceleration			
	0.1g	0.2g	0.3g	0.4g
Frame 1	0.183%	0.366%	0.551%	0.733%
Frame 2	0.172%	0.34%	0.516%	0.689%
Frame 3	0.168%	0.337%	0.506%	0.676%
Frame 4	0.164%	0.329%	0.493%	0.658%

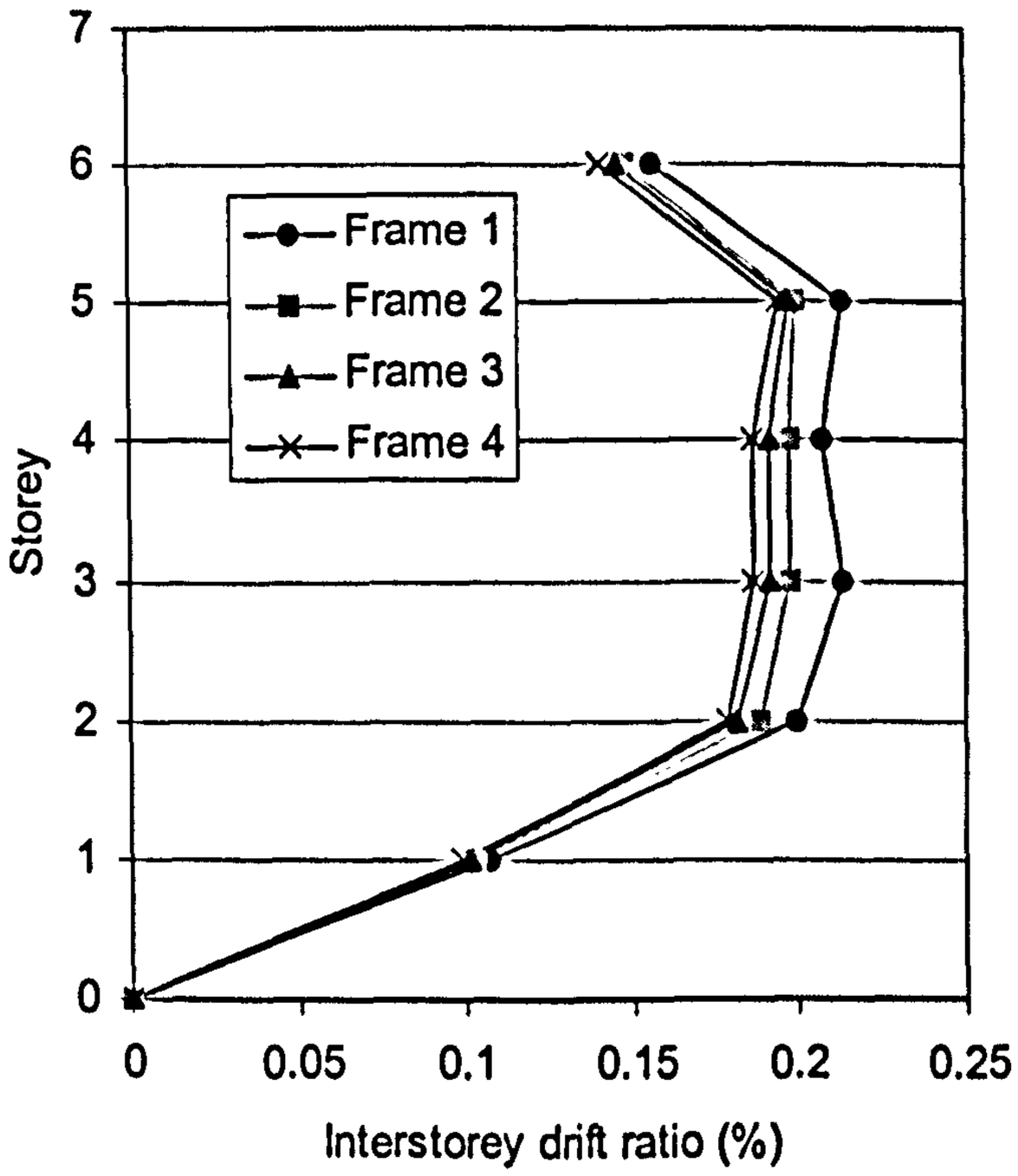

(a) Ground acceleration = 0.1g

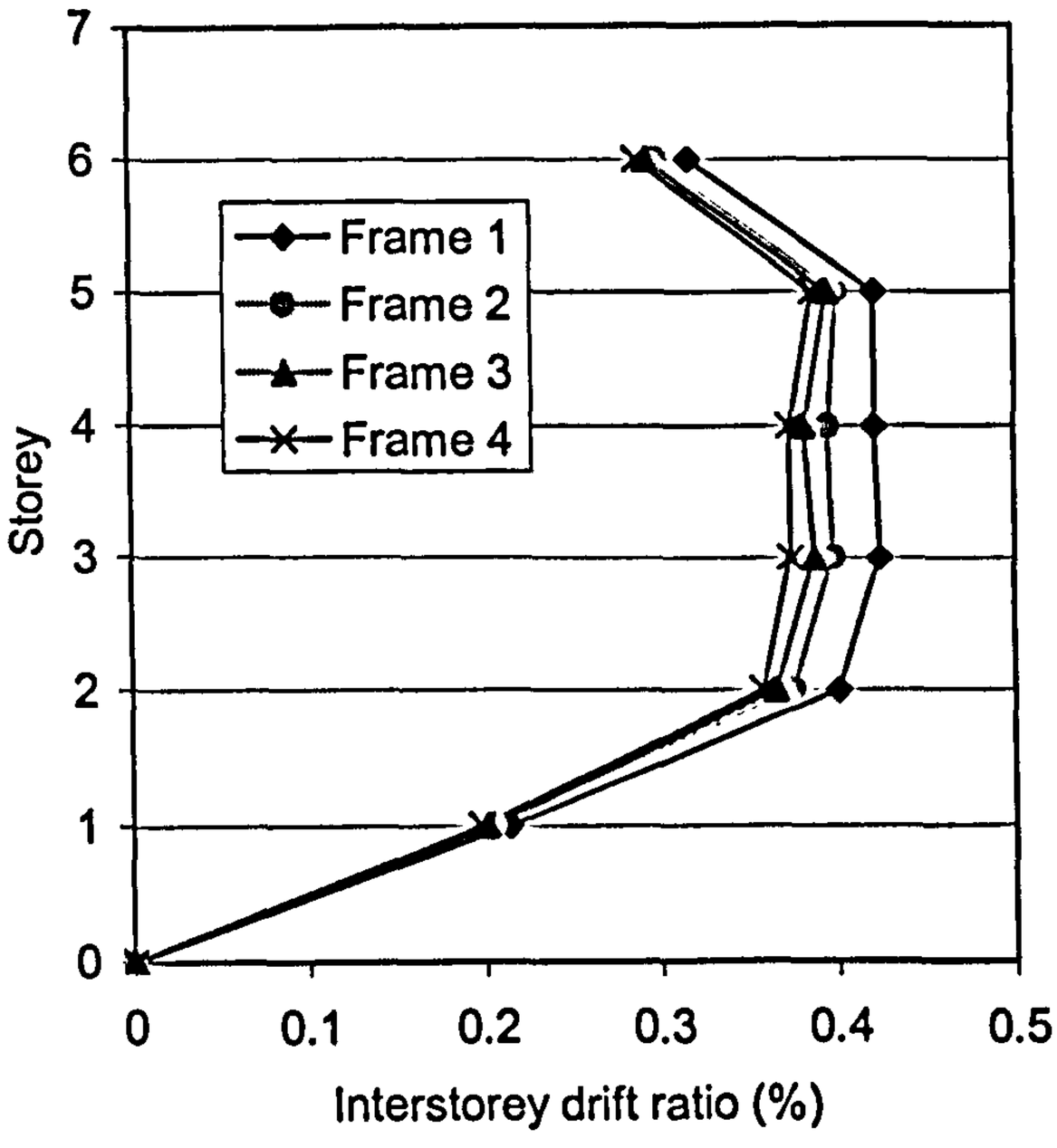

(b) Ground acceleration = 0.2g

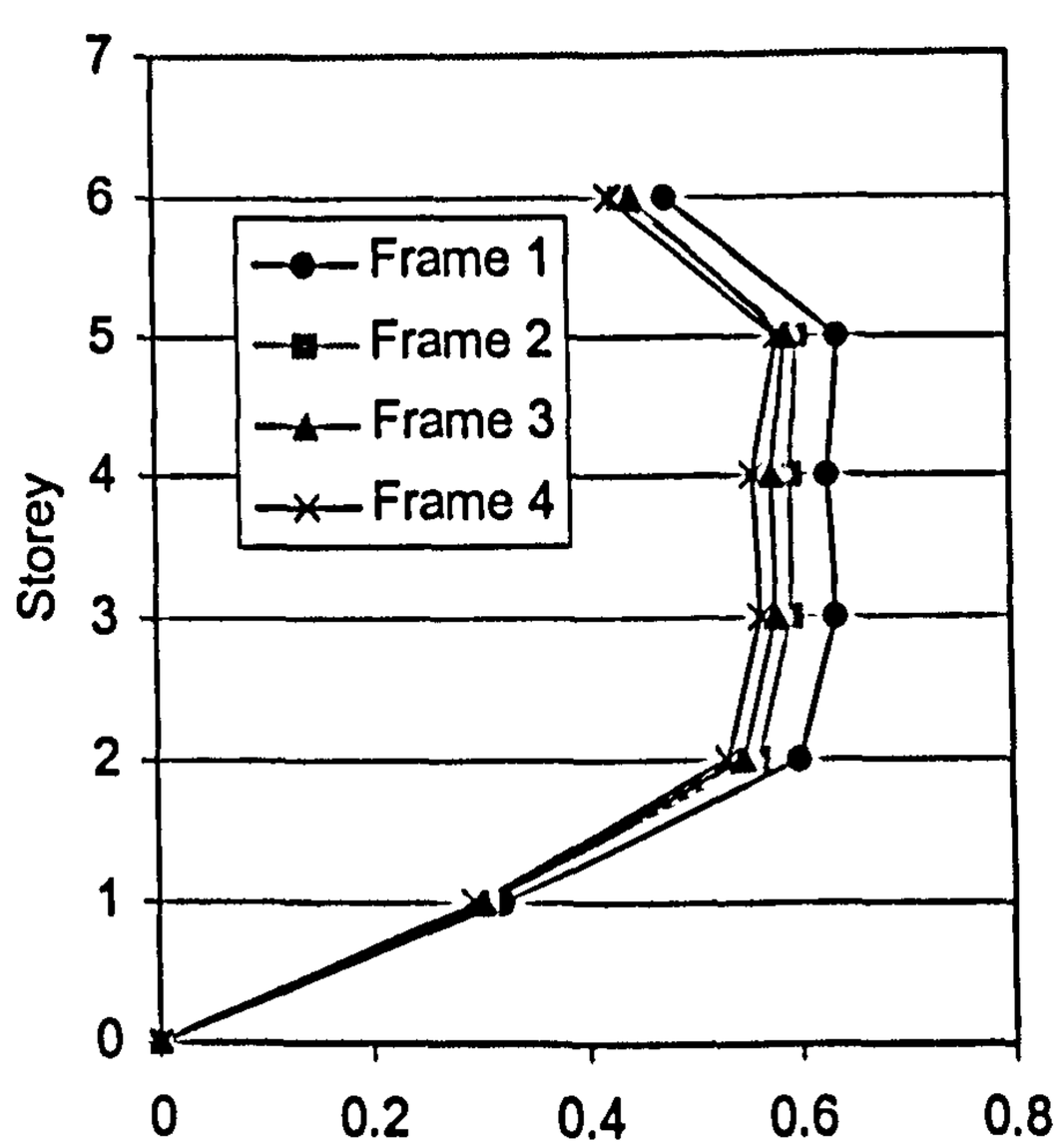

(c) Ground acceleration = 0.3g

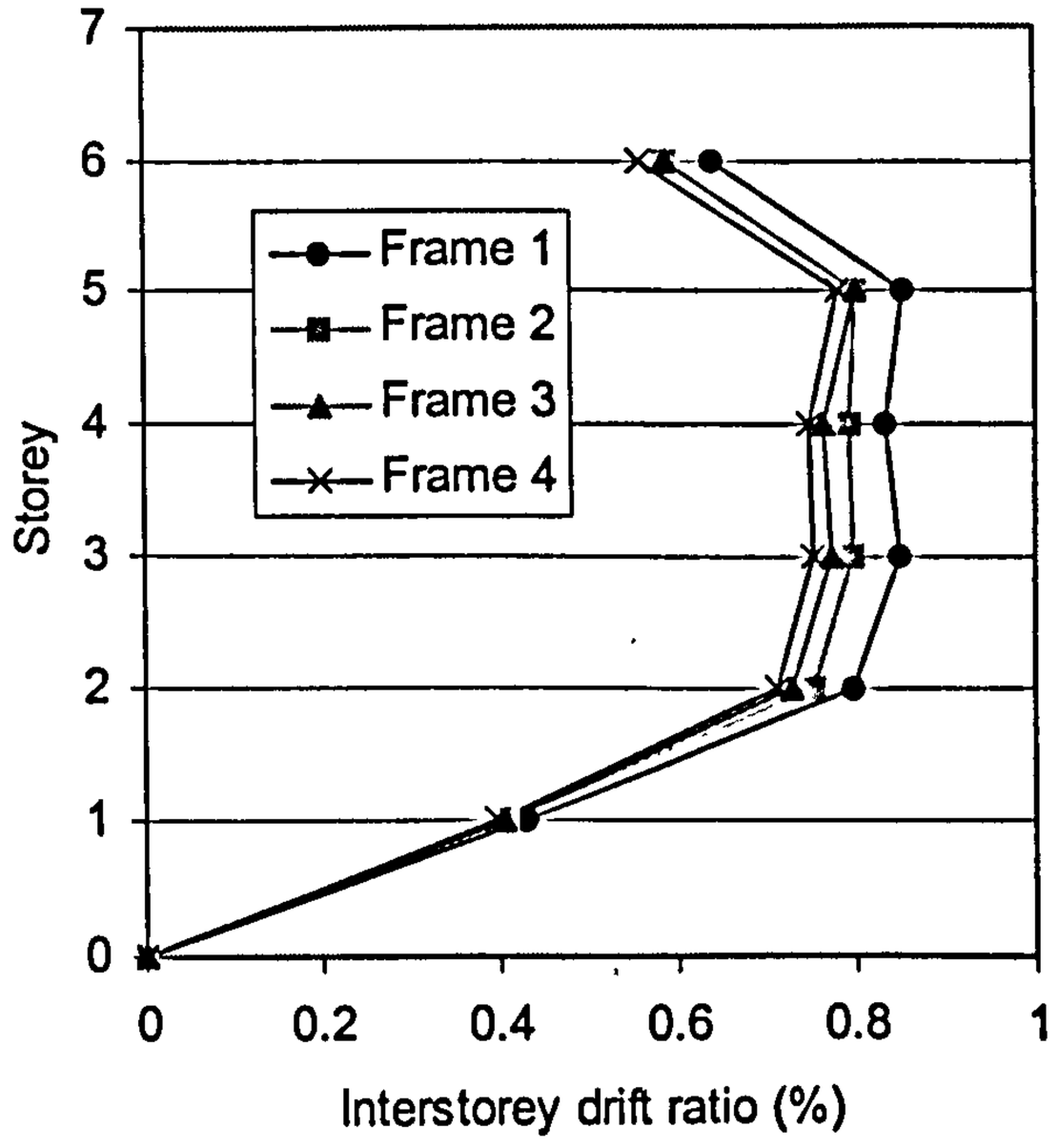

(d) Ground acceleration = 0.4g

Figure 8.4 Interstorey drift ratios of Frame 1, Frame 2, Frame 3, and Frame 4

8.4.3.4 Results analysis

The results of the lateral displacements of the four composite frames under different levels of earthquake loading are described here. Among the four frames, the amount of reinforcement in the composite joints is varied. Since the slab reinforcement within the composite joint is directly related to the stiffness of the joint, and hence the overall lateral stiffness of the composite frame, the overall performance of the composite frames with different lateral stiffness can be investigated through the seismic analysis of the four six-storey composite frames.

From Table 8.1, it can be seen that for each frame the lateral displacements increased with the increase of the ground acceleration. Furthermore the lateral displacements are

proportional to the ground accelerations. This means that all frames performed elastically during the analysis. By comparing the lateral displacements of the four frames under the same ground acceleration, it can be observed that the lateral displacements decreased with the increase of the amount of joint reinforcement. This can also be observed from Table 8.2 which shows the lateral drift ratios of the four frames. This indicates that frames with higher lateral stiffness may experience less lateral displacements under the same level of earthquake within elastic deformations.

From Figure 8.4, it can be observed that the interstory drift ratio decreased with the increase of the slab reinforcement and increased proportionally with the increase of the ground acceleration. The maximum interstorey drift occurred on the third floor with a maximum value of 0.85% well within the limit value of 3% suggested by Broderic & Elnashai (1996).

8.5 Conclusions

Seismic analysis is performed on a sample six-storey composite frame. The proposed composite joint model and beam model are used to compose an analytical composite frame model. Through the seismic analysis the following conclusions may be drawn regarding to the analytical frame model for dynamic analysis and the overall behaviour of composite frames under earthquake loading.

- The proposed composite frame model can give reasonable predictions of the overall behaviour of composite frames subjected to earthquake loading at least in the elastic analysis range, because the analysis gives reliable results of the frame lateral displacements on different levels of earthquake spectrums and frames with different lateral stiffness.
- The semirigid joint can be modelled and the influence on the overall frame performance can be obtained. The analysis shows that the lateral displacements

decrease with the increase of the joint stiffness in elastic deformation of the composite frame.

- Since the proposed composite joint model is composed of a series of bar/beam elements, the local failure within a composite joint, i.e., weld failure, local buckling of steel beam flange and web, cannot be accurately captured.
- For analysis of composite frames subjected to high ground accelerations with the proposed frame model, possible local failure within composite joints must be considered when using the analytical results.

Chapter 9 Conclusions and future work

9.1 Introduction

In this thesis a simple finite element method is proposed for the nonlinear analysis of semi-rigid composite structures. The finite element model is established on the basis of direct modelling of every component of the composite structure. Each component – steel column, steel beam, concrete slab, shear stud, reinforcement over connection – is modelled as one type of line element. The advantages of the proposed model are:

- The model can be used on both 2D and 3D analysis.
- Geometry and material nonlinearity can be accommodated.
- A finite element model can be established without relying on test data of composite joints.
- The total degrees of freedom of the analytical model are small and hence the computer resources required for the analysis are low.
- The model can be analysed by most structure analysis program and no extra programming is needed.

A finite element model for composite joint analysis is proposed in the first place. In order that the influence of the deformation of shear studs on the behaviour of composite joint can be accounted for, a shear stud model is also proposed according to the load-slip curve of the shear stud. Secondly, a composite beam model is proposed by introducing 'rigid link' elements. The semi-rigid joint behaviour can be accounted for by incorporating the composite joint model to the beam model. Finally, a composite frame model is obtained by introducing the composite joint and beam model with the steel column modelled as normal beam elements.

In this chapter, the main conclusions of the composite joint modelling, the composite beam modelling, and the composite frame modelling are summarised.

9.2 Conclusions of composite joint modelling

A simple analytical composite joint model is proposed along with a shear stud model. It gives satisfactory predictions of the characteristics of composite joints in general. The following assumptions are proposed in the process of establishing the composite joint model:

- The composite joint is subject to negative bending.
- The compression center coincides with the center of the bottom flange of the steel beam, and the whole composite joint rotates about the compression center.
- Failing or buckling of the column web and flange in compression does not occur, and the deformations of the column web and flange in compression are neglected.
- The shear deformation of column web in shear zone is neglected.
- The deformations of the column web and flange in tension zone are neglected.
- The reinforcement in the concrete slab is assumed to deform simultaneously regardless of their distance to the beam center.
- The full shear strength of the shear studs may develop before failing.

There are five types of elements in the composite joint model: a nonlinear beam element representing the steel beam, a nonlinear bar element representing the main slab reinforcement, a nonlinear cross-section beam element representing the uncracked concrete slab in tension, a shear stud element representing the shear studs, and a rigid link element. In order to establish a simple composite joint model, the moment of resistance of the steel joint is calculated according to Annex J of EC4 (1994). And then it is replaced by the moment of the reinforcement over a certain lever arm obtained from

equal moment principle. The total lever arm of the reinforcement, named as the equivalent lever arm (D_{eq}), is therefore obtained.

$$D_{eq} = \frac{R_r}{R_{yr}} D_r + \frac{\sum R_b D_b}{R_{yr}} \tag{5.8}$$

A simplified composite joint model is consequently established regardless of the type and configuration of the steel joint. A shear stud model is also proposed using beam element in order that the influence of the deformation of shear studs can be accounted for in the analysis of composite joints. The shear stud model is established according to its load-slip behaviour. For different shear studs, a different stud model should be established. Rigid links are elements with very high stiffness providing connections to the steel beam elements and the shear stud elements.

From the model analysis the following conclusions may be drawn:

- The proposed joint model can be easily established once the moment of resistance of the steel joint is calculated.
- The proposed model is simple to use and it can be analysed by any structural analysis program without extra programming.
- To account for the deformation of the shear studs, a shear model can be developed according to the load-slip curve.
- For composite joints failing by the fracture of the rebars, the predictions of the moment of resistance, rotation capacity, and initial stiffness are satisfactory.
- For composite joints failing by the local buckling of the bottom flange of the steel beam, the predictions of the moment of resistance and initial stiffness are satisfactory. But the proposed model tends to underestimate the rotation capacity.
- The proposed joint model tends to overestimate the yield moment of composite joints.

- According to the predicted bi-linear moment-rotation relationship, a tri-linear moment-rotation relationship is recommended for the design of composite joints.

To conclude, the proposed semi-rigid composite joint model shows good agreements with tests and can effectively predict the moment of resistance, rotation capacity and initial stiffness of semi-rigid composite joints. It can be applied for the further studies of composite beams and frames.

9.3 Conclusions of composite beam modelling

A simple composite beam model is proposed. The proposed beam model is capable of analysing composite beams with different joint or support conditions, with different degrees of shear connection, and with various loading conditions. The proposed beam model is validated against current British Standard method and two groups of composite beam tests. The agreements are satisfactory. The assumptions in the process of establishing the composite beam model are:

- The distribution of stress and strain through the whole steel beam cross-section is constant.
- The distribution of stress and strain through the whole concrete slab cross-section is constant.
- The full shear capacity of shear studs may develop before failing.

Four types of elements are used in the proposed composite beam model: nonlinear beam element representing the steel beam, nonlinear cross-section beam element representing the concrete slab, shear stud element representing the shear studs, and rigid link element. The shear stud elements and the rigid link elements are obtained in the same way as the proposed composite joint model. For composite beams with semi-rigid connections, the proposed composite joint model is used in the joint modelling.

The following conclusions may be drawn from the analysis of composite beams using the proposed composite beam model.

- A composite beam model can be quickly established through the proposed procedure. And very little computer efforts are needed for the analysis.
- Both elastic and plastic analysis of composite beams can be performed using the proposed model.
- The behaviour of partial shear connection can be easily modelled.
- The modelling of composite beams with different degrees of shear connection is successful.
- The modelling of composite beams with semi-rigid joints is successful.
- For the analysis of continuous composite beams, the actual negative moment of resistance can be obtained without a presumed moment redistribution of the negative moment at supports.
- A bi-linear relationship of the imposed loading and the mid-span deflection may be obtained from the beam model. The beam model tends to overestimate the beam yield load level.
- The proposed model can accurately predict the natural frequencies of composite beams. And higher mode frequencies can be easily obtained.
- The empirical equation (6.1) is coarse when it is used to predict the natural frequencies of composite beams.

9.4 Conclusions of composite frame modelling

A finite element model of composite frames is established by incorporating the proposed composite joint model and beam model, with the steel columns modelled as normal beam elements. To validate the proposed frame model, three composite frames are analysed: a composite portal frame, a six-storey composite frame, and a three-dimensional 20-storey composite frame. For all three frames, the amount of reinforcement in the concrete slab is varied to study the effect of the slab reinforcement

on the overall performance of composite frames. The limit state behaviour of the composite frames is discussed. The following conclusions may be drawn from the composite frame analysis:

- Composite frames can be explicitly modelled and analysed by the proposed frame model. No extra programming is needed to establish the model.
- Since only line elements are used in the model, the total degrees of freedom of the composite frame model are greatly reduced. The proposed model is therefore very simple and computationally efficient.
- The analytical results agree well to other published approaches.
- The proposed model is effective in predicting the limit state behaviour of composite frames.
- The lateral stiffness of a steel frame will increase significantly if the composite action is taken into account and this will be at a very low cost.
- The amount of longitudinal reinforcement in the concrete slab at joint has great influence on the overall performance of composite frames.
- Increase in the amount of slab reinforcement will result in increase of the overall stiffness of composite frames; increase the load limit; and reduce the lateral displacements.
- Excessive slab reinforcement will make very little difference in the terms of the lateral stiffness and the load limit. The reinforcement ratio of between 0.6% to 1% seems to be sufficient for a satisfactory semi-rigid design.
- For the semi-rigid design of composite frames, it is also suggested that at composite joint the amount of longitudinal reinforcement in the concrete slab should be no less than 0.35%.
- Since the moment of resistance of composite joints is closely related to the slab reinforcement, the joint moments transformed to the columns can be easily controlled in order to comply the 'strong column, weak beam' design principle.

9.5 Conclusions on seismic analysis of composite frames

The proposed composite joint model and beam model are used to form an analytical composite frame model. Seismic analysis is performed on a sample six-storey composite frame. The joint stiffness is varied and the overall performance of the sample frame is investigated. Through the seismic analysis the following conclusions may be drawn regarding to the analytical frame model for dynamic analysis and the overall behaviour of composite frames under earthquake loading.

- The proposed composite frame model can give reasonable predictions of the overall behaviour of composite frames subjected to earthquake loading at least in the elastic analysis range, because the analysis gives reliable results of the frame lateral displacements on different levels of earthquake spectrums and frames with different lateral stiffness.
- The semirigid joint can be modelled and the influence on the overall frame performance can be obtained. The analysis shows that the lateral displacements decrease with the increase of the joint stiffness in elastic deformation of the composite frame.
- Since the proposed composite joint model is composed of a series of bar/beam elements, the local failure within a composite joint, i.e., weld failure, local buckling of steel beam flange and web, cannot be accurately captured.
- For analysis of composite frames subjected to high ground accelerations with the proposed frame model, possible local failure within composite joints must be considered when using the analytical results.

9.6 Future work

In reviewing present proposed model of composite frames, further research efforts should be made on the following aspects:

- Since the design of a composite joint cross-section is non-symmetrical, the nonlinear hysteric moment-rotation loops of the composite joint are most likely non-symmetrical. The behaviour of the composite joint model under sagging moment should be studied. This is necessary because some joints may subject to positive bending when a composite frame is under lateral loading.
- The tri-linear moment-rotation relationship proposed in Chapter 5 may be introduced in the analysis of composite beams and frames. And more accurate predictions could be realized.
- The behaviour of composite joints under dynamic loading may be investigated by the proposed joint model.
- Seismic analysis of composite frames may be performed if the behaviour of composite joints under dynamic loading is investigated.

Future work on dynamic modelling and analysis of composite structures may be carried on the following:

- Since a bilinear moment-rotation relationship is used for composite joints, it is necessary to produce a composite joint model capable of modelling the nonlinear hysteric moment-rotation curves.
- The dynamic response of composite beams and the influence of the joint stiffness need to be studied. And the design criteria of composite beams under dynamic loading need to be investigated.
- Nonlinear behaviour of composite frames under earthquake loading should be studied.

References

Ahmed, B. & Nethercot, D. A. (1996) Effect of high shear on the moment capacity of composite cruciform endplate connections. Journal of Constructional Steel Research 40 129-163

Ahmed, B. & Nethercot, D. A. (1997) Prediction of initial stiffness and available rotation capacity of major axis composite flush endplate connections. Journal of Constructional Steel Research 41 31-60

Amadio, C. & Fragiacomo, M. (2002) Effective width evaluation for steel-concrete composite beams. Journal of Constructional Steel Research, 58, 373-388

Anderson, D. & Hughes, A. F (1997) Design of braced steel frames with ductile partial-strength connections. The Structure Engineer, Vol. 75, No. 3, 49-50

Anderson, D. & Najafi, A. A. (1994) Performance of composite connections: Major axis end plate joints. Journal of Constructional Steel Research 31 31-57

Ansourian, P. (1975) An application of the method of finite elements to the analysis of composite floor system. Proceedings of the Institution of Civil Engineers, Vol. 59, Part 2, 699-726

Ansourian & Roderick, (1978) Analysis of composite beams. Journal of the Structural Division, Vol. 104, No. ST10, 1631-1645

Arizumi, Y., Hamada, S., & Kajita, T. (1981) Elastic-plastic analysis of composite beams with incomplete interaction by finite element method. Composite structures, vol. 14 (5-6) 453-462

ASCE task committee on design criteria for composite structures in steel and concrete (1998) Design guide for partially restrained composite connections, Journal of Structural Engineering, Vol.124, No.10, 1099-1114

Baker, J. F. (1980) Early steel research, Journal of Constructional Steel Research 1(1), 3-9

Barnard, P. R. & Johnson, R. P., (1965[1]) Ultimate strength of composite beams. Proceedings of the institution of civil engineers, Vol. 32, 161-179

Barnard, P. R. & Johnson, R. P., (1965[2]) Plastic behaviour of *continuous composite* beams. Proceedings of the institution of civil engineers, Vol. 32, 180-197

British Standard Institution, BS5950-1: 2000. Structural use of steelwork in building, Part 1: Code of practice for design – Rolled and welded sections.

British Standard Institution, BS5950-3.1: 1990. Structural use of steelwork in building, Part 3: Design in composite construction.

British Standard Institution, BS6399: 1996. Loading for buildings, Part 1: Code of practice for dead and imposed loads.

British Standard Institution, BS 8110-1: 1997. Structural use of concrete, Part 1: Coe of practice for design and construction.

Broderick, B. M. & Elnashai, A. S., (1996[1]) Seismic response of composite frames – I. Response criteria and input motion. Engineering Structures, Vol. 18, No. 9, 696-706.

Broderick, B. M. & Elnashai, A. S., (1996[2]) Seismic response of composite frames – II. Calculation of behaviour factors. Engineering Structures, Vol. 18, No. 9, 707-723.

Brown, N. D. & Anderson, D. (2001). Structural properties of composite major axis end plate connections. Journal of Constructional Steel Research 57 327-349

Bugeja, M. N., Bracci, J. M. & Moore Jr., W. P. (2000) Seismic behaviour of composite RCS frame systems. Journal of Structural Engineering, ASCE, Vol. 126, No. 4, 429-436

Buchdoldt, H. (1997) Structural dynamics for engineers. Thomas Telford Publications. ISBN: 0 7277 2559 9

Chan, S. L. & Zhou Z. H. (1998) On the development of a robust element for second-order `non-linear integrated design and analysis (NIDA)'. Journal of Constructional Steel Research 47 169-190

Chapman, J. C. (1964) The behaviour of composite beams in steel and concrete. The Structural Engineer, 42, 115-125.

Chapman, J. C. & Balakrishnan, S. (1964) Experiments on composite beams. The Structural Engineer, 42, 369-383.

Chen, Y. F. & Kishi, N. (1987) Semi-rigid steel-to-column connections: database and modelling. Journal of Structural Engineering, ASCE, Vol. 113, No. 10, 2324-2327

Christopher, J. E. & Bjorhovde, R. (1998) Response characteristics of frames with semi-rigid connections, Journal of Constructional Steel Research 46:1-3 paper No.141

Clough, R. W. & Penzien, J. (1993) Dynamics of structures. Second edition. McGraw-Hill, Inc. ISBN: 0-07-011394-7

Dall'Asta, A. (2001) Composite beams with weak shear connection. International Journal of Solids and Structures, Vol. 38, pp. 5605-5624

Daniel, B. J. & Crisinel, M. (1993) Composite slab behaviour and strength analysis. Part I: Calculation procedure. Journal of Structural Engineering, Vol. 119, 16-35

Daniel, B. J. & Crisinel, M. (1993) Composite slab behaviour and strength analysis. Part II: Comparisons with Test Results and Parametric Analysis. Journal of Structural Engineering, Vol. 119, 36-49

DD ENV 1992-1-1: 1992. Eurocode 2: Design of concrete structures. Part1.1: General rules and rules for buildings.

DD ENV 1993-1-1: 1992. Eurocode 3: Design of steel structures. Part1.1: General rules and rules for buildings.

DD ENV 1993-1-1: 1992. Eurocode 3: Part1.1: General rules and rules for buildings.

Annex J (normative): Beam-to-column connections.

DD ENV 1994-1-1: 1994. Eurocode 4: Design of composite steel and concrete structures, Part 1.1: General rules and rules for buildings.

DD ENV 1998-1-1: 1996. Eurocode 8: Design provisions for earthquake resistance of structures, Part 1.1: General rules – Seismic actions and general requirements for structures.

DD ENV 1998-1-2: 1996. Eurocode 8: Design provisions for earthquake resistance of structures, Part 1.1: General rules – General rules for buildings.

DD ENV 1998-1-3: 1996. Eurocode 8: Design provisions for earthquake resistance of structures, Part 1.1: General rules – Specific rules for various materials and elements.

Dissanayake, U. I., Burgess, I. W., & Davison, J. B., (2000) Modelling of plane composite frames in unpropped construction. Engineering Structures, 22, 287-303

Dissanayake, U. I., Davison, J. B., & Burgess, I. W. (1999) Composite beam behaviour in braced frames. Journal of Constructional Steel Research, Vol. 49, 271-289

Dissanayake, U. I., Davison, J. B., & Burgess, I. W. (1998) Limit state behaviour of composite frames. Journal of Constructional Steel Research, Vol. 46, No. 1-3, Paper No. 71

Dowling, P.J. & Burgan, B.A. (1998) Steel structures in the new millennium, The 2nd world conference on steel in construction, Paper No.423, Journal of Constructional Steel Research, Vol.46 No.1-3.

Elnashai, A.S., Broderick, B. M., & Dowling P. J. (1995) Earthquake resistant composite steel/concrete structures. The Structure Engineer, 73(8), 121-132

Fabbrocino, G., Manfredi, G. & Cosenza, E. (2001) Ductility of composite beams under negative bending: an equivalence index for reinforcing steel classification. Journal of Constructional Steel Research 57 185-202

Fang, L. X., Chan, S. L., & Wong, Y. L. (1999) Strength analysis of semi-rigid steel-concrete composite frames, Journal of Constructional Steel Research, 52, 269-291.

Faella, C., Martinelli, E., & Nigro E. (2002) Steel and concrete composite beams with flexible shear connection: "exact" analytical expression of the stiffness matrix and applications. Computers & Structures, Vol. 80, pp. 1001-1009

Fisher, J. W. (1970) Design of composite beams with formed metal deck. American Institution of Steel Construction, Engineering Journal, Vol. 7, No. 2, 88-96

Galambos, T. V. (2000) Recent research and design developments in steel and composite steel-concrete structures in USA. Journal of Constructional Steel Research, 55, 289-303

Grant, J. A. Fisher, J. W. & Slutter, R. G. (1977) Institution of Steel Construction, Engineering Journal, Vol. 14, No. 1, 24-43

Hasan, R., Kishi, N., & Chen, W. F. (1998) A new nonlinear connection classification system. Journal of Constructional Steel Research, 47, 119-140

Hirst, M. J. S., & Yeo, M. F. (1980) The analysis of composite beams using standard element programs. Composite structures, Vol. 11, 233-237

Jayas, B. S. & Hosain, M. U. (1988) Behaviour of headed studs in composite beams: push-out tests. Canadian Journal of Civil Engineering, Vol. 15, 240-253

Johnson, R. P. (1975) Composite structures of steel and concrete, Volume1: Beams, columns, frames and application in building, Granada Publishing Ltd.

Johnson, R. P., Greenwood, R. D. & Van Dalen, K. (1969) Stud shear connectors in hogging moment regions of composite beams. Institution of Structural Engineers, September.

Johnson, R. P., Finlison, J. C. H. & Heyman, J. (1965) A plastic composite design. Proceedings of the institution of civil engineers, Vol. 32, 198-209

Johnson, R. P. & May, I. M. (1975) Partial-interaction design of composite beams. The Structure Engineer, 53(8), 305-311

Johnson, R. P. & Molenstra, I. N. (1991) Partial shear connection in composite beams for buildings. Proceedings of the Institution of Civil Engineers, Vol. 91, 679-704

Johnson, R. P. & Yuan, H. (1998[1]) Existing rules and new tests for stud shear connectors in troughs of profiled sheeting. Proceedings of the Institution of Civil Engineers, Structures & Buildings, Vol. 128, No. 3, 244-251

Johnson, R. P. & Yuan, H. (1998[2]) Models and design rules for stud shear connectors in troughs of profiled sheeting. Proceedings of the Institution of Civil Engineers, Structures & Buildings, Vol. 128, No. 3, 252-263

Kameshki, E. S. & Saka, M. P. (2001) Optimum design of nonlinear steel frames with semi-rigid connections using a generic algorithm, Computers & Structures 79 1593-1604

Kattner, M. & Crisinel, M. (2000) Finite element modelling of semi-rigid composite joints. Computers & Structures 78 341-353

Kemp, A. R. & Nethercot, D. A. (2001) Required and available rotations in continuous composite beams with semi-rigid connections. Journal of Constructional Steel Research 57 375-400

Kim, B. (1999) A study on a continuous stem girder system. PhD thesis, University of Strathclyde.

Kristek, V. & Studnicka, J. (1982) Analysis of composite girders with deformable connectors. Proceedings of the Institution of Civil Engineers, Vol. 73, Part 2, 699-712

Lawson, R. M. (1989) Design of composite slabs and beams with steel decking. The Steel Construction Institute, SCI Publication 055.

Lawson, R. M. (1989) Partial safety factors in composite beams. The Steel Construction Institute, SCI Publication 058.

Lawson, R. M. (1995) Moment connections in composite construction: Interim guidance for end-plate connections. Technical report. SCI publication 143.

Lawson, R. M. & Gibbons, C. (1995) Moment Connections in Composite Construction: Interim Guidance for End-plate Connections, Technical Report SCI Publication 143.

Leon, R. T. (1990) Semi-rigid composite comstruction. Journal of Constructional Steel Research, Vol. 15. 99-120

Leon, R. T. (1998) Analysis and design problems for PR composite frames subjected to seismic loads. Engineering Structures, Vol. 20, Nos 4-6, pp. 364-371

Leon, R. T., Hajjar, J. F. & Gustafson, M. A. (1998[1]) Seismic response of composite moment-resisting connections. I: Performance. Journal of Structural Engineering, ASCE, Vol. 124, No. 8, 868-876

Leon, R. T., Hajjar, J. F. & Gustafson, M. A. (1998[2]) Seismic response of composite moment-resisting connections. II: Behaviour. Journal of Structural Engineering, ASCE, Vol. 124, No. 8, 877-885

Li, G. Q. & Mativo, J. (2000) Approximate estimation of the maximum load of semi-rigid steel frames. Journal of Constructional Steel Research, Vol. 54, 213-225

Li, T. Q., Choo, B. S. & Nethercot, D. A. (1995[1]) Connection Element Method for the Analysis of Semi-rigid Frames. Journal of Constructional Steel Research, Vol. 32, 143-171

Li, T. Q., Choo, B. S. & Nethercot, D. A. (1995[2]) Determination of Rotation Capacity Requirements for Steel and Composite Beams. Journal of Constructional Steel Research, Vol. 32, 303-332

Li, T. Q., Moor, D. B., Nethercot, D. A. & Choo, B. S. (1996[1]) The Experimental Behaviour of a Full-scale, Semi-rigidly Connected Composite Frame: Overall Considerations. Journal of Constructional Steel Research, Vol. 39, 167-191

Li, T. Q., Moor, D. B., Nethercot, D. A. & Choo, B. S. (1996[2]) The Experimental Behaviour of a Full-scale, Semi-rigidly Connected Composite Frame: Detailed appraisal. Journal of Constructional Steel Research, Vol. 39, 193-220

Li, T. Q., Nethercot, D. A. & Choo, B. S. (1996[3]) Behaviour of Flush End-plate Composite Connections with Unbalanced Moment and Variable Shear/Moment Ratios--I. Experimental Behaviour. Journal of Constructional Steel Research, Vol. 38, 125-164

Li, T. Q., Nethercot, D. A. & Choo, B. S. (1996[4]) Behaviour of Flush End-plate Composite Connections with Unbalanced Moment and Variable Shear/Moment Ratios--II. Prediction of moment capacity. Journal of Constructional Steel Research, Vol. 38, 165-198

Li, T. Q., Nethercot, D. A. & Lawson, R. M. (2000) Required rotation of composite connections, Journal of Constructional Steel Research 56 151-173

Liew, J. Y. R., Chen, H., & Shanmugam, N. E., (2001) Inelastic analysis of steel frames with composite beams, Journal of Structural Engineering, Vol.127, No.6, 194-202

Liew, J. Y. R., Teo, T. H., Shanmugam, N. E. & Yu, C. H. (2000) Testing of steel-concrete composite connections and appraisal of results. Journal of Constructional Steel Research 56 117-150

Liu, E. M. & Chen, W. F. (1988) Behaviour of braced and unbraced semirigid frames. International Journal of Solids and Structures, Vol. 24(9), 893-913

Liu, J. & Astaneh-Asl, A. (2000) Cyclic testing of simple connections including effects of slab. Journal of Structural Engineering, ASCE, Vol. 126, No. 1, 32-39

Lloyd, R. M. & Wright, H. D. (1990) Shear connection between composite slabs and steel beams. Journal of Constructional Steel Research 15 255-285

LUSAS Version 13, 2000, Finite Element Analysis Ltd., UK.

Martin, L. H. & Purkiss, J. A. (1992) Structural Design of Steelwork to BS 5950. Edward Arnold, a division of Hodder & Sloughton Limited. ISBN 0-340-54443-0.

McGarraugh, J. B. & Baldwin, J. B. (1971) Light weight concrete on steel composite beams. American Institute of Steel Construction, Engineering Journal, Vol. 8, No. 3, 90-98

Menzies, J. B. (1971) CP 117 and shear connectors in steel-concrete composite beams made with normal-density and lightweight concrete. The Structure Engineer, Vol. 49, No. 3, 137-153.

Mohr, G. A. (1992) Finite elements for solids, fluids, and optimisation. Oxford University Press.

Najafi, A. A. & Anderson, D. (1997) Ductile steel-concrete composite joints. Composite Construction – Conventional and innovative, IABSE, Zurich, 427-432

Nakashima, M, Roeder, C. W., & Maruoka, Y. (2000) Steel moment frames for earthquakes in United States and Japan. Journal of Structural Engineering, Vol. 126, No. 8, 861-868

Nethercot, D. A. (1995) Semirigid joint action and the design of nonsway composite frames. Engineering Structures, Vol. 17, No. 8, 554-567

Nethercot, D. A. (1998) Towards a standardisation of the design and detailing of connections. Journal of Constructional Steel Research, Vol. 46, Nos. 1-3, pp. 3-4, paper number 58.

Nethercot, D. A. (2000) Frame structures: global performance, static and stability behaviour. General report. Journal of Constructional Steel Research 55 109-124

Nethercot, D. A. & Choo, B. S. (1996[1]) Behaviour of flush end-plate composite connections with unbalanced moment and variable shear/moment ratios I. Experimental behaviour. Journal of Constructional Steel Research 38 125-164

Nethercot, D. A. & Choo, B. S. (1996[2]) Behaviour of flush end-plate composite connections with unbalanced moment and variable shear/moment ratios II. Prediction of moment capacity. Journal of Constructional Steel Research 38 165-198

Nethercot, D. A. & Lawson, R. M. (2000) Required rotation of composite connection. Journal of Constructional Steel Research 56 151-173

Neuenhofer, A. & Filippou, F. C. (1997) Evaluation of nonlinear frame finite-element models. Journal of Structural Engineering, Vol. 123 (7), 958-966

Neuenhofer, A. & Filippou, F. C. (1998) Geometrically nonlinear flexibility-based frame finite element. Journal of Structural Engineering, Vol. 124 (6), 704-711

Oehlers, D. J. (1993) Composite Profiled Beams. Journal of Structural Engineering, Vol. 119, No. 4, pp. 1085-1100

Oehlers, D. J. & Coughlan, C. G. (1986) The shear stiffness of stud shear connections in composite beams. Journal of Constructional Steel Research, 6, 273-284

Oehlers, D. J. & Johnson, R. P. (1987) Strength of stud shear connections in composite beams. Structural Engineer, Vol. 65B, No. 2, 44-48

Ollgaard, J. G., Slutter, R. G. & Fisher, J. W. (1971) Shear strength of stud connectors in normal weight and lightweight concrete. American Institution of Steel Construction, Engineering Journal, Vol. 8, No. 2, 55-64.

Oven, V. A., Burgess, I. W., Plank, R. J. & Wali, A. A. A. (1997) An analytical model for the analysis of composite beams with partial interaction, Computers & Structures Vol. 62, No. 3, pp. 493-504

Owens, Graham W. & Knowles, P. R., (1994) Steel Designer's Manual, The Steel Construction Institute

Plum, D. R. & Horne, M. R. (1975) The analysis of continuous beams with partial connection. Proceedings of the institution of civil engineers, Vol. 59, 625-643

Porco, G., Spadea, G., & Zinno, R. (1994) Finite element analysis and parametric study of steel-concrete composite beams. Cement & Concrete composites, 16, 261-272

Puhali, R., Smotlak, I. & Zandonini, R. (1990) Semi-rigid composite action: Experimental analysis and a suitable model. Journal of Constructional Steel Research, Vol. 15, 121-151

Rakib, S. N., (1991) The behaviour of continuous composite beams. Ph.D. thesis, School of Engineering, University of Wales College of Cardiff.

Razaqpur, A. G. & Nofal, M. (1989) A finite element for modelling the nonlinear behaviour of shear connectors in composite structures. Composite Structures, Vol. 32 (1), 169-174

Razaqpur, A. G. & Nofal, M. (1990) Analytical modelling of nonlinear behaviour of composite bridges. Journal of Structural Engineering, Vol. 116, No. 6, 1715-1733

Rex, C. O. & Easterling, W. S. (2002) Partially restrained composite beam–girder connections. Journal of Constructional Steel Research, Vol. 58, 1033-1060

Report of the Subcommittee on the State-of-the-Art Survey of the Task Committee on Composite Construction, (1974) Composite steel-concrete construction. Journal of the Structural Division, ASCE, Vol. 100, No. ST5, 1085-1139

Robert, T. M. (1985) Finite difference of composite beams with partial interaction. Computers & Structures, 21, 469-473

Robinson, H. (1988) Multiple stud shear connections in deep ribbed metal deck. Canadian Journal of Civil Engineering, Vol. 15, 553-569

Salari, M. R. & Spacone, E. (2001) Analysis of steel-concrete composite frames with bond-slip. Journal of Structural Engineering, Vol. 127, No. 11, 1243-1250

Salari, M. R., Spacone, E., Shing, P. B. & Frangopol, D. M. (1998) Nonlinear analysis of composite beams with deformable shear connectors. Journal of Structural Engineering, Vol. 124, No. 10, 1148-1158

Sebastian, W. M. & McConnel, R. E. (2000) Nonlinear FE analysis of steel-concrete composite structures, Journal of Structural Engineering, Vol.126, No.6, 662-674

Sekulovic, M. & Salatic, R. (2001) Nonlinear analysis of frames with flexible connections, Computers & Structures 79 1097-1107

Shanmugam, N. E., Yu, C. H., Liew, J. Y. R. & Teo, T. H. (1998) Modelling of steel-concrete composite joints. Journal of Constructional Steel Research, Vol. 46, No. 1-3, Paper No. 138

Shi, Y. J., Chen, S. L. & Wong, Y. L. (1996) Ultimate strength analysis of composite plane frames. In: Proceedings of ICASS'96 International Conference of Advances in Steel Structure, Hong Kong, vol. 1. 221-226

Slutter, R. G. & Driscoll, G. C. (1965) Flexural strength of steel-concrete composite beams. Journal of the Structure Division. ASCE. Vol. 91, No. ST 2, 71-99

Subhash, C. G. & Medhat K. B. (1989) Analytical modelling of phase 2 steel structure. Journal of Structural Engineering, Vol.115, No.8, 1549-1559

The British Constructional Steelwork Association Limited and the Steel Construction Institute. (1990) Structural Steelwork Handbook: Properties & Safe Load Tables.

Tschemmernegg, F. (1998) Composite frames with slim floors. Journal of Constructional Steel Research Vol. 46, No. 1-3 Paper No. 107

Viest, I. M. (1955) Investigation of stud shear connectors for composite concrete and steel T-beams. American Concrete Institution, Vol. 52, No. 8, 875-891

Wang, Y. C. (1998) Deflection of steel-concrete composite beams with partial shear connection. Journal of Structural Engineering, Vol. 124, No. 10, 1159-1165

Weynand, K., Jaspart, J. P. & Steenhuis, M. (1998) Economy studies of steel building frames with Semirigid joints. Journal of Constructional Steel Research, Vol. 46, No. 1-3, Paper No. 63

Wegmuller, A. W. & Armer, H. N. (1977) Nonlinear response of composite steel-concrete bridges. Computers & Structures, 7(2), 161-169

Wright, H. D., (1989) Report on simply supported composite beam tests, School of Engineering, University of Wales College of Cardiff

Wright, H. D., (1990) The deformation of composite beams with discrete flexible connection. Journal of Constructional Steel Research, 15, 49-64

Wright, H. D., (1990) Shear connection between composite slabs and steel beams. Journal of Constructional Steel Research, 15, 255-285

Wright, H. D., Wang, Y. J. & Cairns, R. (2003) Modelling of semi-rigid composite joints. In: Proceedings of the international conference on advances in structures (ASSCCA '03), Sydney, Australia, June 2003. 745-750

Wyatt, T. A. (1989) Design guide on the vibration of floors. The Steel Construction Institute. SCI PUBLICATION 076. ISBN: 1 870004 34 5

Xiao, Y., Choo, B. S. & Nethercot, D. A. (1994) Composite connections in steel and concrete. I. Experimental behaviour of composite beam-column connections. Journal of Constructional Steel Research 31 3-30

Xiao, Y., Choo, B.S. & Nethercot, D. A. (1996) Composite connections in steel and concrete. Part 2: Moment capacity of endplate beam to column connections. Journal of Constructional Steel Research 37 63-90

Xu, L. (2002) Design and optimization of semi-rigid framed structures. Recent Advances in Optimal Structural Design, ASCE, 147-168

Yam, L. C. P. & Chapman, J. C. (1968) The inelastic behaviour of simply supported composite beams of steel and concrete. Proceedings of the institution of civil engineers, Vol. 41, 651-683

Yau, C. Y. & Chan, S. L. (1994) Inelastic and stability analysis of flexibly connected steel frames by spring-in-series model, Journal of Structural Engineering, Vol.120, No.10, 2803-2819

Yu, C. H., Liew, J. Y. R., Shanmugam, N. E. & Ng, Y. H. (1998) Collapse behaviour of sway frames with end-plate connections. Journal of Constructional Steel Research, Vol. 48, 169-188